

# **ROLE OF 14-3-3 $\sigma$ AND 14-3-3 $\gamma$ IN REGULATING CELL-CELL ADHESION**

*By*  
**KUMARKRISHNA RAYCHAUDHURI**  
**[LIFE09200904005]**

**TATA MEMORIAL CENTRE**  
**MUMBAI**

*A thesis submitted to the  
Board of Studies in Life Sciences  
In partial fulfillment of requirements  
for the Degree of*

**DOCTOR OF PHILOSOPHY**  
*of*  
**HOMI BHABHA NATIONAL INSTITUTE**



**January, 2016**



# Homi Bhabha National Institute

## Recommendations of the Viva Voce Committee

As members of the Viva Voce Committee, we certify that we have read the dissertation prepared by Kumarkrishna Raychaudhuri entitled "**Role of 14-3-3 $\sigma$  and 14-3-3 $\gamma$  in regulating cell-cell adhesion**" and recommend that it may be accepted as fulfilling the thesis requirement for the award of Degree of Doctor of Philosophy.

|   |                |
|---|----------------|
|    | 8/1/2016       |
| Chairperson – Dr. Subhada V. Chiplunkar   | Date:          |
|    | 8/1/2016       |
| Guide– Dr. Sorab N. Dalal   | Date: 8/1/2016 |
|    |                |
| Member - Dr. Milind Vaidya  | Date:          |
|   | 8/1/2016       |
| Member - Dr. Dibyendu Bhattacharyya   | Date:          |
|  | 8/1/2016       |
| External Examiner – Dr. Sagar Sengupta  | Date:          |

Final approval and acceptance of this thesis is contingent upon the candidate's submission of the final copies of the thesis to HBNI.

I hereby certify that I have read this thesis prepared under my direction and recommend that it may be accepted as fulfilling the thesis requirement.

Date: 8/1/2016

Place: Navi Mumbai

  
Dr. Sorab N. Dalal

Guide



## STATEMENT BY AUTHOR

This dissertation has been submitted in partial fulfilment of requirements for an advanced degree at Homi Bhabha National Institute (HBNI) and is deposited in the Library to be made available to borrowers under rules of the HBNI.

Brief quotations from this dissertation are allowable without special permission, provided that accurate acknowledgement of source is made. Requests for permission for extended quotation from or reproduction of this manuscript in whole or in part may be granted by the Competent Authority of HBNI when in his or her judgment the proposed use of the material is in the interests of scholarship. In all other instances, however, permission must be obtained from the author.



**Date: 12.01.16**

**Kumarkrishna Raychaudhuri**

**Place: Navi Mumbai**



## DECLARATION

I, hereby declare that the investigation presented in the thesis has been carried out by me.  
The work is original and has not been submitted earlier as a whole or in part for a degree /  
diploma at this or any other Institution / University.



**Date: 12.01.16**

**Kumarkrishna Raychaudhuri**

**Place: Navi Mumbai**



## List of Publications arising from the thesis

### PUBLICATIONS IN REFEREED JOURNAL:

a. Published:

1. K. Raychaudhuri, M. Gurjar, S. N. Dalal, Plakophilin3 and Plakoglobin recycling are differentially regulated during the disassembly of desmosomes. *J Biosci Tech* 6(1), 634-642 (Jan 2015).

b. Other Publications:

1. M. Gurjar, K. Raychaudhuri, S. N. Dalal, Loss of the desmosomal plaque protein plakophilin3 does not induce the epithelial mesenchymal transition. *J Biosci Tech* 6(1), 647-652 (Jan 2015).

c) Manuscript under preparation:

1. 14-3-3 $\sigma$  loss leads to epithelial mesenchymal transition through c-Jun Slug axis. Raychaudhuri K, Chaudhary N, Gurjar M, D'souza R, Maddika S and Dalal SN.

### CONFERENCES:

1. 14-3-3 $\sigma$  regulates Epithelial to Mesenchymal Transition through c-JUN-Slug axis. Kumarkrishna Raychaudhuri, Mansa Gurjar, Sorab N Dalal. The FEBS-EMBO Meeting 2014. Paris, France. August 30- September 4, 2014. Abstract for poster presentation.
2. 14-3-3 $\sigma$  loss leads to an Epithelial Mesenchymal Transition. Kumarkrishna Raychaudhuri, Mansa Gurjar, Sorab N Dalal. J Carcinogenesis, February 2015. Abstract for oral presentation.



**Kumarkrishna Raychaudhuri**



## **ACKNOWLEDGEMENTS**

*My Ph.D. tenure has been an exceptional journey and it gives me immense pleasure to take this opportunity to thank all the people without whose support and help I would not have made it to this day. The person who has been always with me in good, bad and in the ugly times is my Ph.D. mentor Sorab. I cannot thank him enough for providing me the opportunity to work in his laboratory. His strict role as a mentor and enthusiasm for teaching and science has played an important role in shaping my scientific and personal attributes. His constant care and guidance to develop presentation skills and communication skills has helped me to learn the art of communicating my work to my peers. I have enjoyed a great deal of freedom in terms of thinking and working in the laboratory with Sorab. I am grateful to the director, deputy director and administration of this institute to give me this excellent opportunity to work towards my Ph.D. program in ACTREC.*

*I would like to thank my doctoral committee chairperson Dr. Shubhada Chiplunkar for her constant support and motivation. I am indebted to her for supporting me during my extreme bad phase in Ph.D., which required change of Ph.D. project after 3 years of work and associated procedures with HBNI. I would have quit my Ph.D. program if she had not been there. She has always accommodated me within her extremely busy schedule as a Director of the Institute. I will never forget her care and love for students. Her criticism, appreciations and scientific inputs on my work have helped me to make my Ph.D. work better. I am also thankful to Dr. Rita Mulherkar, who is the ex-chairperson of my doctoral committee for her valuable scientific inputs. I would also like to thank my other doctoral committee members Dr. Milind Vaidya and Dr. Dibyendu Bhattacharyya for their timely and valuable scientific inputs. I am thankful to Dr. Maddika Subba Reddy and Neelam Chaudhary from CDFD to work with me in collaboration. I would like to*

*thank Dr. Jennifer Lippincott-Schwartz, Dr. Clare Waterman, Dr. Steve Pronovost, Dr. Markus Welcker, Dr. Sagar Sengupta, Dr. Sharmila Bapat, Dr. Vidita Vaidya, Dr. Randall Moon, Dr. Tanuja Teni, Dr. Venu Gopal Reddy, and Dr. Prasanna Venkatraman for helpful discussions and providing me constructs, reagents or instruments during my course of study. Thanks to Mansa, Dr. Rahul Thorat, Gehena, Jazeel, Roseline, Paloma, Akash and Ria who have worked with me and have contributed directly to my work. I am grateful to all my lab mates Prajakta, Amitabha, Lalit, Neelima, Pawar, Rashmi, Dipika, Rini, Mansa, Srikanta, Mugdha, Sonali, Abha, Akash, Sarika, Arun, and Vishal. They all have provided a wonderful environment for work. I have also been lucky to have excellent seniors and colleagues in ACTREC like Satya, A Srikant Alam, Ajit, Padma, Gaurav and Sameer.*

*I am immensely thankful to our ACTREC common facilities. I am thankful to Mr. Uday Dandkar for excellent maintenance of instruments in CIR. I am thankful to Ms. Vaishali, Ms. Tanuja, Ms. Mansi and Mr. Jayraj for their help in imaging facility and special to thanks to Ms. Vaishali for her great support to my work. I am thankful to Dr. Ingle and Dr. Rahul Thorat for their participation and help in my course of study. I would like to thank CSIR, TMH, HBNI and Welcome trust/DBT India alliance for providing fellowship during my Ph.D. tenure and for attending international conference. My deepest thanks to my mother, father and brother for their sacrifice, support and love. I would also like to thank Mansa for being with me throughout this journey.*

**Kumarkrishna Raychaudhuri**

## TABLE OF CONTENTS

|   |           |
|---|-----------|
| <b>SYNOPSIS OF Ph.D. THESIS.....</b>                          | <b>1</b>  |
| <b>LIST OF ABBREVIATIONS .....</b>                            | <b>15</b> |
| <b>LIST OF TABLES .....</b>                                   | <b>19</b> |
| <b>List of figures.....</b>                                   | <b>20</b> |
| <b>CHAPTER 1: INTRODUCTION .....</b>                          | <b>23</b> |
| 1.1. Cell - cell adhesion junctions in epithelial cells ..... | 26        |
| 1.2. Types of cell - cell junctions: .....                    | 27        |
| 1.2.1. Tight junctions: .....                                 | 27        |
| 1.2.1.1. Components of Tight junctions:.....                  | 29        |
| 1.2.1.1.1. Claudin: .....                                     | 29        |
| 1.2.1.1.2. Occludin: .....                                    | 30        |
| 1.2.1.1.3. Tricellulin:.....                                  | 30        |
| 1.2.1.1.4. JAM:.....  | 31        |
| 1.2.2. Gap junctions.....                                     | 31        |
| 1.2.3. Hemidesmosomes: .....                                  | 33        |
| 1.2.4. Adherens Junctions: .....                              | 34        |
| 1.2.4.1. Cadherin Catenin complex:.....                       | 35        |
| 1.2.4.2. Nectin Afadin complex .....                          | 35        |
| 1.2.4.3. Physiological relevance of adherens junctions: ..... | 37        |
| 1.2.5. Desmosomes.....  | 38        |
| 1.2.5.1. Desmosomal cadherins .....                           | 40        |
| 1.2.5.2. Armadillo repeat proteins .....                      | 42        |
| 1.2.5.2.1. Plakophilins .....                                 | 42        |
| 1.2.5.2.1.1. Plakophilin 1 .....                              | 43        |
| 1.2.5.2.1.2. Plakophilin 2.....                               | 44        |
| 1.2.5.2.1.3. Plakophilin 3 .....                              | 44        |
| 1.2.5.2.1.4. Plakophilin 4.....                               | 45        |
| 1.2.5.2.2. Plakoglobin.....                                   | 45        |
| 1.2.5.3. Desmoplakin .....                                    | 46        |
| 1.2.5.4. Role of Desmosomal proteins in cancer .....          | 47        |
| 1.3. Cytoskeleton .....                                       | 49        |
| 1.3.1. Microfilaments/ actin filaments .....                  | 49        |
| 1.3.2. Intermediate filaments.....                            | 50        |
| 1.3.3. Microtubules.....                                      | 50        |
| 1.4. Focal adhesions.....                                     | 51        |
| 1.4.1. Focal adhesion biogenesis during cell migration .....  | 52        |
| 1.4.2. Focal adhesion kinase .....                            | 54        |

|  |           |
|--|-----------|
| 1.4.3. Paxillin .....  | 56        |
| 1.4.4. Zyxin .....   | 56        |
| 1.5. Regulation of actin turnover during cell migration .....                                      | 57        |
| 1.5.1. Rho GTPases.....  | 58        |
| 1.5.2. RhoA.....   | 59        |
| 1.5.3. Cofilin .....   | 60        |
| 1.6. 14-3-3 proteins .....   | 61        |
| 1.6.1. 14-3-3 protein structure .....  | 62        |
| 1.6.2. Role of 14-3-3 $\sigma$ in regulating cell - cell adhesion and cancer.....                  | 64        |
| 1.6.3. Role of 14-3-3 $\gamma$ in regulating cell - cell adhesion and cancer .....                 | 65        |
| 1.7. Role of Kinesin motors and 14-3-3 proteins in transport of cell - cell junction proteins..... | 66        |
| 1.8. Epithelial to mesenchymal transition (EMT) .....  | 67        |
| 1.8.1. EMT specific transcription factors and their regulation during EMT ...                      | 69        |
| <b>CHAPTER 2: AIMS AND OBJECTIVES.....</b>   | <b>73</b> |
| <b>CHAPTER 3: MATERIALS AND METHODS.....</b>   | <b>77</b> |
| 3.1. Cell culture and transfections .....  | 79        |
| 3.2. Plasmids .....  | 80        |
| 3.3. Generation of stable cell lines.....  | 81        |
| 3.4. Lentivirus production and transduction.....   | 82        |
| 3.5. Immunofluorescence and confocal microscopy: .....   | 83        |
| 3.6. Calcium Switch and calcium chelation experiments.....   | 84        |
| 3.7. SDS PAGE and Western blotting:.....   | 84        |
| 3.8. Antibodies for Western blot.....  | 85        |
| 3.9. Reverse transcriptase PCR and Q-PCR .....   | 86        |
| 3.10. GST pull down experiments .....  | 88        |
| 3.10.1. Generation of bacterially purified GST proteins .....                                      | 88        |
| 3.10.2. In-vitro GST pulldown .....  | 89        |
| 3.11. Immunoprecipitation.....   | 91        |
| 3.12. In vivo ubiquitination Assays .....  | 93        |
| 3.13. In vitro ubiquitination Assays.....  | 93        |
| 3.15. Luciferase Assays .....  | 94        |
| 3.16. Growth curve assays .....  | 95        |
| 3.17. Hanging drop assays .....  | 95        |
| 3.18. Matrigel invasion assays.....  | 95        |
| 3.19. Soft agar assays.....  | 96        |
| 3.21. Fluorescence Recovery After Photo-beaching (FRAP) assay.....                                 | 97        |

|   |     |
|---|-----|
| 3.22. Nuclear cytoplasmic fractionation assay ..... | 98  |
| 3.23. Reagents:.....                                | 98  |
| 3.23.1. Calcium Phosphate transfection .....        | 98  |
| 3.23.2. SDS PAGE and Western Blotting.....          | 99  |
| 3.23.3. In vitro pull down experiments .....        | 100 |
| 3.23.4. Immunofluorescence .....                    | 102 |
| 3.23.5. Soft Agar assay .....                       | 103 |
| 3.23.6. Protein Estimation.....                     | 103 |

## **CHAPTER 4: RESULTS..... 105**

|  |     |
|--|-----|
| 4.1.: To determine if 14-3-3 $\sigma$ loss leads to deregulation of cell-cell adhesion and to neoplastic transformation. ....              | 107 |
| 4.1.1. Loss of 14-3-3 $\sigma$ leads to alterations in expression of multiple cell-cell junction proteins and cytoskeleton proteins.....   | 109 |
| 4.1.2. Alteration in expression of cell-cell junction and cytoskeleton proteins was due to decrease in mRNA levels.....                    | 112 |
| 4.1.3. 14-3-3 $\sigma$ knockout cells show EMT like phenotypic characteristics. ....   | 115 |
| 4.1.4. 14-3-3 $\sigma$ <sup>-/-</sup> cells did not show increased tumor formation and metastasis in immunocompromised mice.....           | 118 |
| 4.1.5. Ectopic expression of 14-3-3 $\sigma$ in 14-3-3 $\sigma$ <sup>-/-</sup> cells results in a reversal of the EMT phenotype.....       | 120 |
| 4.1.6. 14-3-3 $\sigma$ loss leads to increase in Slug and Zeb1.....  | 123 |
| 4.1.7. Inhibition of Slug expression leads to a reversal of EMT like characteristics in 14-3-3 $\sigma$ <sup>-/-</sup> cells.....          | 125 |
| 4.1.8. Ectopic expression of 14-3-3 $\sigma$ in 14-3-3 $\sigma$ <sup>-/-</sup> cells leads to decrease in expression of Slug and Zeb1..... | 126 |
| 4.1.9. c-Jun proteins levels are increased in 14-3-3 $\sigma$ <sup>-/-</sup> cells.....  | 127 |
| 4.1.10. Increased c-Jun proteins levels promote EMT in 14-3-3 $\sigma$ <sup>-/-</sup> cells.....   | 130 |
| 4.1.11. 14-3-3 $\sigma$ binds to c-Jun and induces the degradation of c-Jun.....   | 131 |
| 4.1.12. 14-3-3 $\sigma$ binds to c-Jun and induces its degradation by FBW7.....  | 132 |
| 4.1.13. Interaction of 14-3-3 $\sigma$ and c-Jun is necessary for ubiquitination of c-Jun. ....  | 134 |
| 4.1.14. Interaction of 14-3-3 $\sigma$ and c-Jun is required for ubiquitination and proteasome mediated degradation of c-Jun in vivo. .... | 137 |
| 4.1.15. 14-3-3 $\sigma$ is required for the nuclear export of c-Jun. ....  | 139 |
| 4.1.16. 14-3-3 $\sigma$ regulates activation of Focal adhesion kinase (FAK). ....  | 141 |
| 4.1.17. 14-3-3 $\sigma$ <sup>-/-</sup> cells show increased turnover of focal adhesions. ....  | 145 |
| 4.2.: To determine the role of 14-3-3 proteins in regulating transport of plakophilin3 and desmoplakin during desmosome assembly. ....     | 149 |

|  |            |
|--|------------|
| 4.2.1. PKP3 forms complex with 14-3-3 $\gamma$ and kinesin 1 family of motor proteins.....                             | 151        |
| 4.2.2. PKP3 is necessary for interaction of 14-3-3 $\gamma$ and other desmosomal proteins.....                         | 153        |
| 4.2.3. Anterograde transport of PKP3 and PG is microtubule dependent. ....   | 155        |
| 4.2.4. The retrograde transport of PKP3 and PG are differentially regulated. ....                                      | 157        |
| 4.2.5. Inhibition of retrograde transport of PKP3 does not inhibit desmosome disassembly.....                          | 159        |
| 4.2.6. Desmoplakin forms complex with KLC2 and 14-3-3 $\gamma$ . ....  | 160        |
| <b>CHAPTER 5: DISCUSSION .....</b>   | <b>163</b> |
| 5.1. 14-3-3 $\sigma$ loss leads to EMT.....  | 166        |
| 5.2. 14-3-3 $\sigma$ loss leads to altered actin dynamics and focal adhesion turnover to regulate cell migration. .... | 173        |
| 5.3. Role of 14-3-3 $\gamma$ in regulating transport of PKP3 and DP during desmosome assembly.....                     | 177        |
| 5.4. Conclusion and Future directions. ....  | 179        |
| <b>CHAPTER 6: BIBLIOGRAPHY.....</b>  | <b>181</b> |
| <b>REPRINTS OF PUBLISHED ARTICLES FROM THE THESIS.....</b>   | <b>235</b> |

# SYNOPSIS





**Homi Bhabha National Institute**

**Ph. D. PROGRAMME**

**SYNOPSIS OF Ph.D. THESIS**

- 1. Name of the Student: Kumarkrishna Raychaudhuri.**
- 2. Name of the Constituent Institution: Tata Memorial Centre, ACTREC.**
- 3. Enrolment No. : LIFE09200904005.**
- 4. Title of the Thesis: Role of 14-3-3 $\sigma$  and 14-3-3 $\gamma$  in regulating cell-cell adhesion.**
- 5. Board of Studies: Life Sciences.**

## **SYNOPSIS:**

### **1. Introduction:**

The 14-3-3 family is a group of highly conserved proteins that are expressed in all eukaryotic cells and regulate multiple cellular pathways (1, 2). Seven 14-3-3 isoforms namely,  $\beta$ ,  $\gamma$ ,  $\epsilon$ ,  $\eta$ ,  $\sigma$ ,  $\tau$ , and  $\zeta$ , have been identified in mammals (3). They generally bind to proteins containing one of two motifs [R(S/X)Xp(S/T)XP and RXXXp(S/T)XP (where 'X' denotes 'any amino acid residue' and p(S/T) denotes phosphorylated serine or threonine)] (4). Previous work from our lab suggested that 14-3-3 $\gamma$  and 14-3-3 $\sigma$  regulate cell-cell adhesion (5). Loss of cell-cell adhesion is a hallmark of the Epithelial Mesenchymal Transition (EMT), which is a key process encountered during progression of several epithelial cancers (6). During EMT, cells exhibit increased migration, increased invasive potential, loss of epithelial markers and gain of mesenchymal markers (7). EMT specific transcription factors e.g. Snail, Slug, Zeb and Twist are known to regulate expression of epithelial and mesenchymal markers during EMT (6). 14-3-3 $\sigma$  loss has been associated with progression of ovarian cancer, breast cancer, malignant transformation and epithelial mesenchymal transition (8-10). However, the mechanisms by which 14-3-3 $\sigma$  could regulate cell-cell adhesion and possibly EMT are not completely understood.

Loss of cell to extracellular matrix (ECM) adhesion is another important event during EMT and cancer progression (11). Focal adhesions (FA) which mediate cell to ECM adhesions are multi-protein complexes composed of transmembrane integrins and actin binding proteins (e.g. paxillin, zyxin, vinculin,  $\alpha$  actinin etc.) which connects actin filaments to focal complexes (12). Turnover, number and strength of focal adhesions are important regulators of cell to ECM adhesion and cell migration (12). Focal adhesion

kinase (FAK) is a non-receptor tyrosine kinase, which localizes to FA and plays a major role in regulating FA turnover and signalling from FA (13).

Previous results from our lab have shown deregulation of desmosomal proteins can also lead to increased cell migration and neoplastic progression (5, 14). Desmosomes are calcium dependent cell-cell junctions that anchor intermediate filaments (IF) to the cell membrane resulting in the formation of a tissue wide IF network and provide mechanical strength and rigidity to tissues (15). Desmosomes are composed of the plasma membrane spanning cadherins (desmogleins [DSGs] and desmocollins [DSCs]), the ARM family proteins (plakoglobin [PG] and plakophilins [PKPs]) and a Plakin family member such as desmoplakin (DP) (16). However, the mechanisms by which 14-3-3 proteins regulate desmosome assembly are not yet understood.

## **2. Aims and objectives:**

1. To determine if 14-3-3 $\sigma$  loss leads to deregulation of cell-cell adhesion and to neoplastic transformation.
2. To determine the role of 14-3-3 proteins in regulating transport of plakophilin3 and desmoplakin during desmosome assembly.

## **3. Results:**

**1. To determine if 14-3-3 $\sigma$  loss leads to deregulation of cell-cell adhesion and to neoplastic transformation.** Previous results from our laboratory have shown depletion of desmosomal proteins from the cell border on 14-3-3 $\gamma$  loss (5). Immunofluorescence (IF) and Western blotting performed on 14-3-3 $\sigma$ <sup>+/+</sup> and 14-3-3 $\sigma$ <sup>-/-</sup> cells for several junctional and cytoskeletal proteins showed that 14-3-3 $\sigma$  loss leads to a decrease in the levels of the junctional proteins e.g. PKP3, PG, DP, DSC2, DSG2, tight junction protein 1 (ZO1),  $\beta$ -catenin, E cadherin, P cadherin and a decrease in keratin levels. In contrast, 14-3-3 $\sigma$ <sup>-/-</sup>

cells showed an increase in the expression of mesenchymal markers such as vimentin and N cadherin. These results suggested that an EMT program (7) was induced upon loss of 14-3-3 $\sigma$ .

During EMT along with changes in expression of epithelial and mesenchymal markers, cells also exhibit functional changes such as the acquisition of migratory phenotype, decrease in cell to ECM adhesion, decrease in cell to cell adhesion, increase in invasion potential etc. (17). Wound healing assays showed that 14-3-3 $\sigma$ <sup>-/-</sup> cells are more migratory than 14-3-3 $\sigma$ <sup>+/+</sup> cells, disperse assays demonstrated that cell-cell adhesion was compromised in 14-3-3 $\sigma$ <sup>-/-</sup> cells as compared to 14-3-3 $\sigma$ <sup>+/+</sup> cells. 14-3-3 $\sigma$ <sup>-/-</sup> cells were more invasive and less adherent to ECM substrates (fibronectin, collagen IV laminin V and matrigel) as determined by Boyden chamber matrigel invasion assays and cell to ECM assays respectively. However, we did not observe a difference in the ability of 14-3-3 $\sigma$ <sup>-/-</sup> cells to form colonies in soft agar colony formation assays and to form tumors in mice when compared to the 14-3-3 $\sigma$ <sup>+/+</sup> cells.

To identify which EMT specific transcription factor is responsible for the EMT like phenotype observed in 14-3-3 $\sigma$ <sup>-/-</sup> cells, real-time PCR and Western blots were performed to compare the expression levels of different EMT specific transcription factors between 14-3-3 $\sigma$ <sup>+/+</sup> and 14-3-3 $\sigma$ <sup>-/-</sup> cells. We found that Slug and its downstream target effector Zeb1 (18) expression were upregulated in 14-3-3 $\sigma$ <sup>-/-</sup> cells. To determine how 14-3-3 $\sigma$  loss leads to up regulation of Slug we investigated different upstream regulators of Slug. We observed that c-Jun, which is reported to activate Slug expression (19), was increased at protein levels in 14-3-3 $\sigma$ <sup>-/-</sup> cells as compared to 14-3-3 $\sigma$ <sup>+/+</sup> cells. It was observed that treatment of 14-3-3 $\sigma$ <sup>+/+</sup> cells with MG132 (proteasomal inhibitor) lead to stabilization of c-Jun levels.

To determine how loss of 14-3-3 $\sigma$  leads to stabilization of c-Jun we asked if 14-3-3 $\sigma$  forms a complex with c-Jun. Bacterially produced GST-14-3-3 $\sigma$  formed a complex with c-Jun. Co-immunoprecipitation experiments were able to detect a complex between c-Jun and 14-3-3 $\sigma$  in cells treated with the proteasome inhibitor MG132, but not in cells treated with the vehicle control. These results suggested that c-Jun is degraded by the proteasome in 14-3-3 $\sigma$ <sup>+/+</sup> cells. A motif scan search identified the region around S267 in c-Jun as a potential 14-3-3 $\sigma$  binding site. Alteration of S267 to Alanine in c-Jun resulted in the generation of a mutant that does not form a complex with 14-3-3 $\sigma$ . Experiments performed in the laboratory of our collaborator Dr. Maddika Subba Reddy identified FBW7 as a potential E3 ligase for c-Jun in these cells and demonstrated that 14-3-3 $\sigma$  was required for the ubiquitination of c-Jun by FBW7.

To confirm that the changes in expression of epithelial and mesenchymal markers and EMT specific phenotypes in 14-3-3 $\sigma$ <sup>-/-</sup> cells are indeed due to loss of 14-3-3 $\sigma$ , we stably expressed 14-3-3 $\sigma$  in 14-3-3 $\sigma$ <sup>-/-</sup> cells. Western blotting and IF results confirmed that ectopic expression of 14-3-3 $\sigma$  in 14-3-3 $\sigma$ <sup>-/-</sup> cells resulted in an increase in E cadherin, plakoglobin protein levels while vimentin and N cadherin levels decreased. Notably, c-Jun and Slug protein levels decreased after ectopic expression of 14-3-3 $\sigma$  as compared to vector control cells in 14-3-3 $\sigma$ <sup>-/-</sup> cell. In addition, shRNA mediated knockdown of Slug and c-Jun also lead to increase in expression of epithelial markers and decrease in expression of mesenchymal markers in 14-3-3 $\sigma$ <sup>-/-</sup> cells. Interestingly, knockdown of c-Jun lead to decrease in Slug and Zeb1 protein levels. This corroborates our hypothesis that increase in c-Jun protein level is responsible for increase in transcription of Slug and Zeb1. We observed a decrease in Zeb1 upon knockdown of Slug. This suggests that increase in Zeb1 was a downstream effect of upregulation of Slug and could be reversed by down regulation of Slug. Wound healing assays and hanging drop assays suggested

that cell migration and cell to adhesion respectively were decreased in 14-3-3 $\sigma$ <sup>-/-</sup> cells expressing 14-3-3 $\sigma$  in comparison to cells expressing the vector control.

14-3-3 $\sigma$ <sup>-/-</sup> cells showed decreased cell to ECM adhesion and increased cell migration. Focal adhesions (FA) mediate cell to ECM adhesion and during cell migration FA turnover is increased (12). Autophosphorylation of FAK at Y397 leads to increased FA turnover, cell spreading and cell movement (20). 14-3-3 $\sigma$ <sup>-/-</sup> cells showed increased levels of FAK pY397 in as compared to 14-3-3 $\sigma$ <sup>+/+</sup> cells, whereas no appreciable difference was observed in total FAK. As FAK pY397 is known to promote cell spreading which also often associated with higher filopodia density, we performed cell spreading assays on matrigel and determined filopodia density in Phalloidin-FITC stained cells. Increased cell spreading and higher filopodia density were observed in 14-3-3 $\sigma$ <sup>-/-</sup> cells in comparison to 14-3-3 $\sigma$ <sup>+/+</sup> cells. To determine the mechanism for changes in actin organization which could lead to more filopodia formation in 14-3-3 $\sigma$ <sup>-/-</sup> cells we performed immunoblotting for proteins known to regulate actin dynamics. We observed a decrease in phospho cofilin levels in 14-3-3 $\sigma$ <sup>-/-</sup> cells as compared to 14-3-3 $\sigma$ <sup>+/+</sup> cells suggesting increased actin turnover in 14-3-3 $\sigma$ <sup>-/-</sup> cells (21). RhoA regulates cofilin phosphorylation through ROCK and LIMK (21). Decreased levels of active RhoA were observed in 14-3-3 $\sigma$ <sup>-/-</sup> cells as compared to 14-3-3 $\sigma$ <sup>+/+</sup> cells suggesting a possible mechanism of regulation of actin dynamics through cofilin in 14-3-3 $\sigma$ <sup>-/-</sup> cells. Fluorescence recovery after photobleaching (FRAP) performed on nascent (paxillin) and mature (zyxin) FA markers (22) showed that paxillin turnover was faster with shorter half-life in 14-3-3 $\sigma$ <sup>+/+</sup> cells in comparison to 14-3-3 $\sigma$ <sup>-/-</sup> cells whereas inverted turnover and half-life was observed for zyxin. 14-3-3 $\sigma$ <sup>-/-</sup> cells showed a decrease in focal adhesion strength as observed in our trypsin deadhesion assays (22). These results are consistent with the increase in cell migration observed in the 14-3-3 $\sigma$ <sup>-/-</sup> cells.

To determine how 14-3-3 $\sigma$  regulates FAK phosphorylation at Y397 we asked if 14-3-3 $\sigma$  interacts with FAK. In vitro GST pull down and in vivo endogenous IP data suggests that 14-3-3 $\sigma$  forms a complex with FAK, paxillin and  $\alpha$ -actinin. This suggests that 14-3-3 $\sigma$  forms a complex with multiple FA proteins raising a possibility of 14-3-3 $\sigma$  to localize at the FA. This interaction of 14-3-3 $\sigma$  and FAK might inhibit autophosphorylation of FAK at Y397.

## **2. To determine the role of 14-3-3 proteins in regulating transport of plakophilin3 and desmoplakin during desmosome assembly.**

During cell migration, wound healing and tissue remodeling the desmosome goes through cycles of assembly and disassembly. Desmosome assembly requires the localization of two armadillo (ARM) repeat containing proteins, plakophilin3 (PKP3) and plakoglobin (PG), at the cell border. Our results demonstrate that microtubule dependent anterograde transport is required for the localization of PKP3 and PG to the cell border. However, during desmosome disassembly, retrograde transport of PKP3 but not PG, was dependent on an intact microtubule network. PKP3 is retained at the cell border, unlike other desmosomal proteins, when microtubule organization was disrupted. These results suggest that PKP3 transport from the cell border to the cytoplasm occurs via a mechanism that is distinct from other desmosomal proteins and might reflect functions of PKP3 that are independent of its role in desmosome formation and maintenance.

## **4. Discussion:**

This study demonstrates that 14-3-3 $\sigma$  can interact with c-Jun and target it for degradation by the proteasome. c-Jun is an upstream regulator of Slug and elevated protein levels of c-Jun promote increased Slug transcription (19), which in turn can initiate an EMT program. c-Jun is known as an oncoprotein whose levels are kept low by different

mechanisms. Fbw7, Itch and Cop1 are three E3 ligases known to target c-Jun to proteasomal degradation (23-25). In our study it was observed that Fbw7 promoted c-Jun degradation in presence of 14-3-3 $\sigma$ . However, the role of other E3 ligases in regulation of c-Jun protein stability remains to be investigated. Fbw7 is known to be tumor suppressor and has been found to be deregulated in multiple cancer types (26). More interestingly, loss of Fbw7 has also been shown to initiate EMT like phenotype in HCC cells (27). Though, 14-3-3 $\sigma$ <sup>-/-</sup> cell showed higher invasion and cell migration they did not show appreciable difference in their ability to form tumors or metastasis in mice in comparison to 14-3-3 $\sigma$ <sup>+/+</sup> cells. This could be because of increased susceptibility of 14-3-3 $\sigma$ <sup>-/-</sup> cells to DNA damage, which ultimately results to apoptosis (28).

Reports correlate EMT with increased cell migration and decreased cell to ECM adhesion which involve alteration in regulation of actin cytoskeleton and focal adhesions (17). Our data suggests that 14-3-3 $\sigma$  can directly interact with FAK which is involved in regulation of FA dynamics and thus can directly regulate cell migration and ECM adhesion (20). Increase in FAKpY397 in 14-3-3 $\sigma$ <sup>-/-</sup> cells further supports the hypothesis that 14-3-3 $\sigma$  and FAK interaction might inhibit phosphorylation of FAK. In concert with increased FAKpY397, 14-3-3 $\sigma$ <sup>-/-</sup> cell also showed increase in turnover of mature FA and compromised FA strength in comparison to 14-3-3 $\sigma$ <sup>+/+</sup> cells. Active RhoA and subsequent decrease in phospho cofilin levels in 14-3-3 $\sigma$ <sup>-/-</sup> as compared to 14-3-3 $\sigma$ <sup>+/+</sup> cells alludes to a signaling cascade through ROCK and LIMK which explains altered actin dynamics and increased filopodia density in 14-3-3 $\sigma$ <sup>-/-</sup> cells (21).

The role of kinesin motor proteins in transport of desmosomal proteins to the cell border is well established (29). Results from our laboratory suggest that 14-3-3 $\gamma$  might play a role of an adapter protein between desmosomal proteins and kinesin motor proteins (5).

Studies carried out in this project further demonstrate that PKP3 binds to KIF5B and 14-3-3 $\gamma$ . We also observed that DP specifically binds to KLC2 and not KCL1.

Our work done on transport of PKP3 and PG during desmosome assembly and disassembly suggest that anterograde transport of PG and PKP3 is similarly regulated and depend on intact MT. However, retrograde transport of PG is not dependent on intact MT while transport of PKP3 requires MT. It is interesting to note that border retention of PKP3 post calcium chelation was not sufficient to retain DP and DSC2/3 at the cell border during retrograde transport (30).

### **5. References:**

1. Jin J, Smith FD, Stark C, Wells CD, Fawcett JP, et al. 2004. *Current biology* : CB 14: 1436-50
2. Storchova Z, Pellman D. 2004. *Nature reviews. Molecular cell biology* 5: 45-54
3. Wang W, Shakes DC. 1996. *J Mol Evol* 43: 384-98
4. Yaffe MB, Rittinger K, Volinia S, Caron PR, Aitken A, et al. 1997. *Cell* 91: 961-71
5. Sehgal L, Mukhopadhyay A, Rajan A, Khapare N, Sawant M, et al. 2014. *Journal of cell science* 127: 2174-88
6. Nieto MA. 2011. *Annual review of cell and developmental biology* 27: 347-76
7. Thiery JP, Acloque H, Huang RY, Nieto MA. 2009. *Cell* 139: 871-90
8. Ravi D, Chen Y, Karia B, Brown A, Gu TT, et al. 2011. *PloS one* 6: e15864
9. Du C, Zhang C, Hassan S, Biswas MH, Balaji KC. 2010. *Cancer research* 70: 7810-9
10. Hou Z, Peng H, White DE, Wang P, Lieberman PM, et al. 2010. *Cancer research* 70: 4385-93
11. Bijian K, Loughheed C, Su J, Xu B, Yu H, et al. 2013. *British journal of cancer* 109: 2810-8
12. Nagano M, Hoshino D, Koshikawa N, Akizawa T, Seiki M. 2012. *International journal of cell biology* 2012: 310616
13. Zhao J, Guan JL. 2009. *Cancer metastasis reviews* 28: 35-49

14. Kundu ST, Gosavi P, Khapare N, Patel R, Hosing AS, et al. 2008. *International journal of cancer. Journal international du cancer* 123: 2303-14
15. Desai BV, Harmon RM, Green KJ. 2009. *Journal of cell science* 122: 4401-7
16. Delva E, Tucker DK, Kowalczyk AP. 2009. *Cold Spring Harbor perspectives in biology* 1: a002543
17. Thiery JP. 2002. *Nature reviews. Cancer* 2: 442-54
18. Wels C, Joshi S, Koefinger P, Bergler H, Schaidler H. 2011. *The Journal of investigative dermatology* 131: 1877-85
19. Chen H, Zhu G, Li Y, Padia RN, Dong Z, et al. 2009. *Cancer research* 69: 9228-35
20. Parsons JT, Martin KH, Slack JK, Taylor JM, Weed SA. 2000. *Oncogene* 19: 5606-13
21. Sumi T, Matsumoto K, Takai Y, Nakamura T. 1999. *The Journal of cell biology* 147: 1519-32
22. Shah PP. 2014. *Role of 14-3-3 $\sigma$  and plakophilin3 in regulation of focal adhesion strength and turnover*. Sardar Patel University. 70 pp.
23. Wertz IE, O'Rourke KM, Zhang Z, Dornan D, Arnott D, et al. 2004. *Science* 303: 1371-4
24. Gao M, Labuda T, Xia Y, Gallagher E, Fang D, et al. 2004. *Science* 306: 271-5
25. Nateri AS, Riera-Sans L, Da Costa C, Behrens A. 2004. *Science* 303: 1374-8
26. Welcker M, Clurman BE. 2008. *Nature reviews. Cancer* 8: 83-93
27. Yu J, Zhang W, Gao F, Liu YX, Chen ZY, et al. 2014. *Hepatobiliary & pancreatic diseases international : HBPD INT* 13: 184-91
28. Meng S, Arbit T, Veeriah S, Mellinghoff IK, Fang F, et al. 2009. *Cell cycle* 8: 2238-46
29. Nekrasova OE, Amargo EV, Smith WO, Chen J, Kreitzer GE, Green KJ. 2011. *The Journal of cell biology* 195: 1185-203
30. Raychaudhuri K, Gurjar M, Dalal SN. 2015. *Journal of Bioscience And Technology* 6: 634-42

**Publication in Referred Journal:**

c. Published:

2. K. Raychaudhuri, M. Gurjar, S. N. Dalal, Plakophilin3 and Plakoglobin recycling are differentially regulated during the disassembly of desmosomes. *J Biosci Tech* 6(1), 634-642 (Jan 2015).

d. Other Publications:

2. M. Gurjar, K. Raychaudhuri, S. N. Dalal, Loss of the desmosomal plaque protein plakophilin 3 does not induce the epithelial mesenchymal transition. *J Biosci Tech* 6(1), 647-652 (Jan 2015).

e. Presentations at conferences:

3. 14-3-3 $\sigma$  regulates Epithelial to Mesenchymal Transition through c-JUN-Slug axis. Kumarkrishna Raychaudhuri, Mansa Gurjar, Sorab N Dalal. The FEBS-EMBO Meeting 2014. Paris, France. August 30- September 4, 2014. Abstract for poster presentation.
4. 14-3-3 $\sigma$  loss leads to an Epithelial Mesenchymal Transition. Kumarkrishna Raychaudhuri, Mansa Gurjar, Sorab N Dalal. *J Carcinogenesis*, February 2015. Abstract for oral presentation.

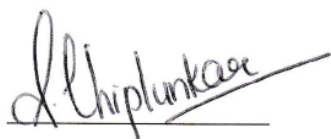
Signature of Student: *Kumarkrishna Raychaudhuri*

Date: 25/3/2015.

**Doctoral Committee members:**

| S. No. | Name                            | Designation      | Signature               | Date    |
|--------|---------------------------------|------------------|-------------------------|---------|
| 1.     | Dr. Prof. S. V. Chiplunkar.     | Chairperson      | <i>S. V. Chiplunkar</i> |         |
| 2.     | Dr. Dr. Sorab N. Dalal.         | Guide & Convener | <i>S. N. Dalal</i>      |         |
| 3.     | Dr. Dr. Milind Vaidya.          | Member           | <i>M. Vaidya</i>        | 27/3/15 |
| 4.     | Dr. Dr. Dibyendu Bhattacharyya. | Member           | <i>D. Bhattacharyya</i> | 27/3/15 |

Forwarded through:

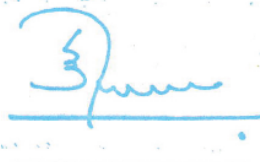


Prof. Shubhada Chiplunkar

Director,

ACTREC-TMC

**Dr. S. V. Chiplunkar**  
Director  
Advanced Centre for Treatment, Research &  
Education in Cancer (ACTREC)  
Tata Memorial Centre  
Kharghar, Navi Mumbai 410210.



Dr. Kailash S. Sharma

Director-Academics,

**PROF. T.M.C. SHARMA**  
DIRECTOR (ACADEMICS)  
TATA MEMORIAL CENTRE,  
PAREL, MUMBAI

## **LIST OF ABBREVIATIONS**

ADP = Adenosine diphosphate

AF6 = ALL-1 fused gene from chromosome 6, also called as afadin

Arp = Actin related protein

ATP = Adenosine triphosphate

cAMP = Adenosine 3'5' cyclic monophosphate

CAR = coxsackie and adenovirus receptor

CC = Coiled coil

Cdc = Cell division control protein

CpG = A C (cytosine) base followed immediately by a G (guanine) base (a CpG).

DP = Desmoplakin

DSC = Desmocollin

DSG = Desmoglein

EDTA = Ethylene diamine tetraacetic acid

EGTA = Ethylene glycol tetraacetic acid

EMT = Epithelial mesenchymal transition

EPLIN = epithelial protein lost in neoplasm; also known as Lima-1

ERK = extracellular signal-regulated kinases

ERK = extracellular signal-regulated kinases

FAK = focal adhesion kinase

FGF = Fibroblast growth factor

FXR1 = fragile-X-related protein

G3BP = ras-GAP-SH3-binding protein

Grb2 = Growth factor receptor-bound protein 2

GST = Glutathione S transferase

JAM = junctional adhesion molecule

LEF = lymphoid enhancer factor

LIMK = LIM kinase

LMB = Leptomycin B

MAGI-1 = membrane associated guanylate kinase

MDCK = Marine Darby Canine Kidney epithelial cells

MET = Mesenchymal epithelial transition

MMP = Matrix metallo protease

MT = microtubule

MUPP1 = multi-PDZ (post-synaptic density protein, Drosophila disc large tumor suppressor and zona occludens-1 protein) domain protein 1

NES = Nuclear export signal

PAGE = Polyacrylamide gel electrophoresis

PAK = p21 activated kinase

PALS1 = protein associated with lin-7

PATJ = Pals1-associated tight junction protein

PCR = polymerase chain reaction

PDZ = Acronym combining the first letters of three proteins — post synaptic density protein (PSD95), Drosophila disc large tumor suppressor (Dlg1), and zonula occludens-1 protein (Zo-1)

PG = Plakoglobin

PKC- $\alpha$  = protein kinase C- $\alpha$

PKC- $\alpha$  = protein kinase C- $\alpha$

PKP1/2/3/4 = Plakophilin1/2/3/4

PLEKHA7 = pleckstrin homology domain containing, family A member 7

PV = Pemphigus Vulgaris

Q-PCR = Quantitative PCR

ROCK = Rho-associated protein kinase

RT-PCR = reverse transcriptase PCR

SAGE = Serial analysis of gene expression

SDS = sodium dodecyl sulphate

SH2 = Src homology 2

Src = Rous Sarcoma

TCF = T-cell specific, HMG-box transcription factor

TJ = Tight junction

TPR = Tetratricopeptide Repeat

VASP = Vasodilator-stimulated phosphoprotein.

WASP = Wiskott–Aldrich Syndrome protein

Wnt = identified as ‘wingless’ in *Drosophila* and ‘int1’ in mice - the int/ Wingless family was renamed the Wnt family and int1 became Wnt1

ZEB = Zinc finger E-box-binding homeobox

ZO1 = zonula occludens 1

---

## LIST OF TABLES

|  |    |
|--|----|
| Table 3.1. Amount of reagents required for specific tissue culture dishes for transfection using PEI.....                    | 79 |
| Table 3.2. Amount of reagents required for specific tissue culture dishes for calcium phosphate method of transfection. .... | 80 |
| Table 3.2. Reverse transcriptase and Q-PCR primers for EMT specific transcription factors.....                               | 86 |
| Table 3.3. Reverse transcriptase and Q-PCR primers for cell- cell junction proteins. ....                                    | 87 |

## LIST OF FIGURES

|   |     |
|---|-----|
| Figure 1.1. Different cell - cell junctions present in epithelial cells.....  | 26  |
| Figure 1.2. Schematic representation of different components of Tight Junction.....   | 28  |
| Figure 1.3. Multiple levels of structure of gap junction .....  | 33  |
| Figure 1.4. Molecular architecture of adherens junction .....   | 37  |
| Figure 1.5. Molecular architecture of desmosome.....  | 39  |
| Figure 1.6. Domain organization and splice variants of desmosomal cadherins.....  | 40  |
| Figure 1.7. Domain organization and splice variants of desmosomal armadillo repeat<br>containing proteins.....  | 42  |
| Figure 1.8. Domain organisation and splice variants of desmoplakin.....   | 47  |
| Figure 1.9. Molecular components of cell to extracellular matrix adhesion .....   | 51  |
| Figure 1.10. Formation and turnover of focal adhesion during cell migration.....  | 52  |
| Figure 1.11. Molecular components associated with formation and turnover for focal<br>adhesion .....  | 53  |
| Figure 1.12. Domain structure of focal adhesion kinase .....  | 55  |
| Figure 1.13. Regulation of actin dynamics by RhoGTPases and its downstream effectors.<br>.....  | 60  |
| Figure 1.14. Structure of 14-3-3 dimer .....  | 63  |
| Figure 4.1.1. Loss of 14-3-3 $\sigma$ leads to alterations in expression of multiple cell-cell<br>junction proteins and cytoskeleton proteins.....                | 110 |
| Figure 4.1.2. Loss of 14-3-3 $\sigma$ leads to alterations in expression of multiple cell-cell<br>junction proteins and cytoskeleton proteins at mRNA level. .... | 114 |
| Figure 4.1.3. 14-3-3 $\sigma$ knockout cells show EMT like phenotypic characteristics. ....   | 116 |
| Figure 4.1.4. 14-3-3 $\sigma$ <sup>-/-</sup> cells did not show increased tumor formation and metastasis in<br>immunocompromised mice.....                        | 119 |
| Figure 4.1.5. Ectopic expression of 14-3-3 $\sigma$ in 14-3-3 $\sigma$ <sup>-/-</sup> cells can rescue EMT like<br>characteristics.....                           | 121 |
| Figure 4.1.6. 14-3-3 $\sigma$ loss leads to increase in Slug and Zeb1. ....   | 124 |
| Figure 4.1.7. Down-regulation of Slug leads to reversal of EMT like characteristics in 14-<br>3-3 $\sigma$ <sup>-/-</sup> cells.....                              | 126 |
| Figure 4.1.8. Ectopic expression of 14-3-3 $\sigma$ in 14-3-3 $\sigma$ <sup>-/-</sup> cells leads to decrease in<br>expression of Slug and Zeb1 .....             | 127 |
| Figure 4.1.9. c-Jun proteins levels are increased in 14-3-3 $\sigma$ <sup>-/-</sup> cells. ....   | 128 |
| Figure 4.1.10. Increased c-Jun proteins levels promote EMT in 14-3-3 $\sigma$ <sup>-/-</sup> cells. ....  | 130 |
| Figure 4.1.11. 14-3-3 $\sigma$ binds to c-Jun and might target the later to proteasomal<br>degradation.....   | 131 |
| Figure 4.1.12. 14-3-3 $\sigma$ targets to c-Jun and might to proteasomal degradation in FBW7<br>dependent manner. ....  | 133 |
| Figure 4.1.13. Interaction of 14-3-3 $\sigma$ and c-Jun is necessary for ubiquitination of c-Jun.<br>.....  | 136 |

---

|   |     |
|---|-----|
| Figure 4.1.14. Abrogation of interaction of c-Jun and 14-3-3 $\sigma$ leads to inhibition of ubiquitination and proteasomal degradation of c-Jun in vivo.....                                     | 138 |
| Figure 4.1.15. 14-3-3 $\sigma$ can induce the nuclear export of c-Jun. A. 14-3-3 $\sigma^{+/+}$ cells were transfected with HA-c-JunWT, HA c-JunS58A and HA-c-JunS267A along with GFP vector..... | 140 |
| Figure 4.1.16. 14-3-3 $\sigma$ interacts with multiple focal adhesion proteins including Focal adhesion kinase (FAK) and regulates activation of FAK. ....  | 143 |
| Figure 4.1.17. 14-3-3 $\sigma^{-/-}$ cells show faster recovery of mature focal adhesion protein zyxin.....   | 146 |
| Figure 4.2.1. PKP3 forms complex with 14-3-3 $\gamma$ and kinesin 1 family of motor proteins. ....  | 152 |
| Figure 4.2.2. Depletion of PKP3 expression leads to compromised interaction of 14-3-3 $\gamma$ and other desmosomal proteins.....   | 154 |
| Figure 4.2.3. Anterograde transport of PKP3 and PG is dependent on an intact microtubule network. ....  | 156 |
| Figure 4.2.4. Disruption of the microtubule network blocks retrograde transport of PKP3 but does not inhibit desmosome disassembly. ....  | 159 |
| Figure 4.2.5. Desmoplakin forms complex with 14-3-3 $\gamma$ and KLC2. ....   | 161 |
| Figure 5.1. 14-3-3 $\sigma$ loss leads to epithelial to mesenchymal transition by stabilizing c-Jun protein levels.....   | 171 |
| Figure 5.2. Turnover of nascent and mature focal adhesions are differentially regulated during rapid cell migration.....  | 175 |
| Figure 5.3. 14-3-3 $\sigma$ regulates focal adhesion turnover and actin dynamics.....   | 176 |



# CHAPTER 1: INTRODUCTION



Multi-cellularity can be considered as one of the most significant advancements in the evolution of life. Unlike acellular organisms, multicellular organisms are obligated to develop various cellular processes required for maintenance of cell - cell communication. Cell - cell adhesion is one such process, which allows neighboring cells to adhere to, communicate with, and to exchange solutes with each other [1-3]. An assembly of cells that are connected to each other and dedicated to perform a specific function in a multicellular organism is a tissue. A number of tissues can be grouped together into a system performing a specific physiological function called an organ. The integrity of an organ or a tissue is primarily dependent on cell - cell adhesion (reviewed in [4]). However, cell - cell junctions should not be considered as static and rigid structures. On the contrary, cell - cell junctions are very dynamic in nature and undergo continuous reorganization and biogenesis. Such dynamic regulation of cell - cell junctions is particularly evident during embryonic development, morphogenesis and wound healing (reviewed in [5]). All these cellular and developmental processes require extensive cell migration and reshuffling of cell positioning which takes place in conjunction with dramatic reorganization of cell - cell adhesion junctions [6, 7].

It is easy to apprehend that abrogation of cell - cell adhesion could lead to various abnormalities and diseases. Indeed, it has been reported that loss of cell - cell junction proteins in many instances gives rise to embryonic lethality due to failure of different cellular or organ functions [8-15]. During metastasis cell - cell adhesions are compromised which facilitates migration and dissemination of cancer cells to other organs [16, 17]. In addition to the vast amount of literature which suggest important role of cell - cell adhesion in various cellular processes and cancer progression, results from our lab has also shown that compromised cell - cell adhesion junction like desmosome leads to cancer progression and metastasis [17].

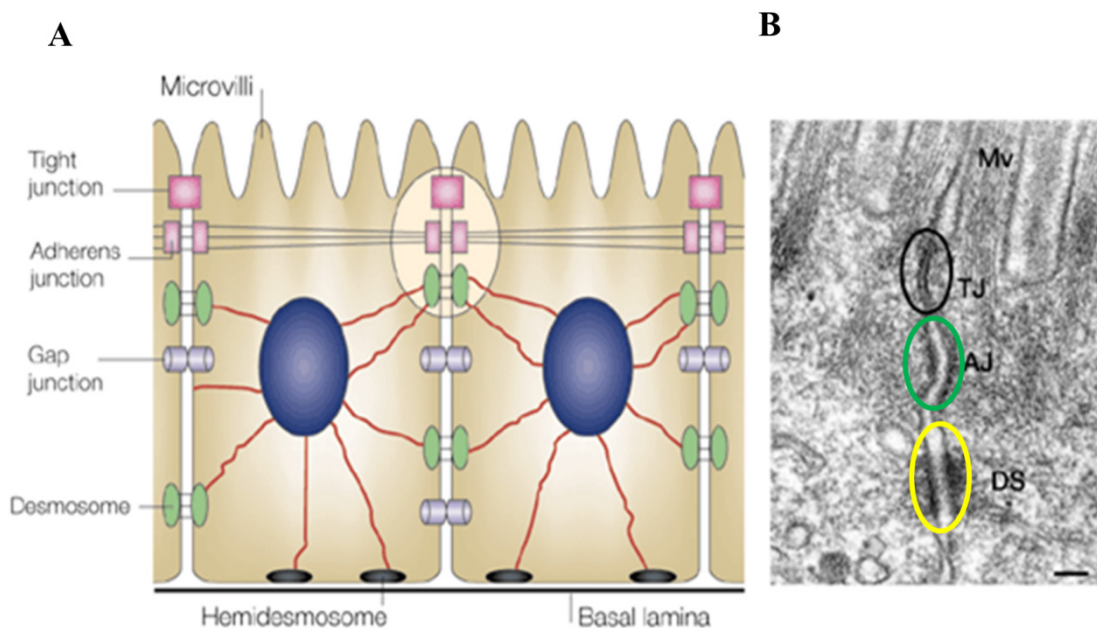


**Figure 1.1. Different cell - cell junctions present in epithelial cells.** Adapted and modified from [18] (A) A cartoon depicting different cell - cell junctions present in intestinal epithelial cells. (B) An electron micrograph of two mouse intestinal epithelial cells apposed to each other. The electron dense junctional complexes between the two cells are circled. (Mv, microvilli; TJ, tight junction; AJ, adherens junction; DS, desmosome). Scale bar, 200nm.

### 1.1. Cell - cell adhesion junctions in epithelial cells

Epithelial tissues form the lining of all organs and their primary role is to function as a barrier to insulate the interior of the organ from toxic compounds present either in the environment or the luminal space. Epithelial tissues contain cells that are closely packed in a single or multiple layers. Epithelial cells exhibit extremely specialized cell - cell communication and cell - cell junction systems. Epithelial tissues undergo continuous cell reshuffling and self-renewal (reviewed in [19]). To support all these functions epithelial

cells have developed a variety of specialized cell - cell junctions each of which have unique biological functions (0).

The different cell - cell junctions that will be discussed here are

1. Tight junctions
2. Gap junctions
3. Hemidesmosomes
4. Adherens junctions
5. Desmosomes

## **1.2. Types of cell - cell junctions:**

### **1.2.1. Tight junctions:**

Farquhar and Palade in 1963 first described the fine structure of Tight Junctions (TJ) at the most luminal side of the lateral plasma membrane [20]. Scanning electron microscopic studies followed by freeze fracture reveals TJ as electron dense flat band encircling the entire cell at the uppermost region of the lateral intercellular space. This electron dense band is composed of many anastomosing meshwork of fibrils called “strands” [21]. TJ, also known as zonula occludens, are mostly found in epithelial cells, however, they are also present in myelin sheaths formed by oligodendrocytes and Schwann cells [22, 23] and reviewed in [21]. TJ are prevalent in cells of blood brain barrier and blood testis barrier (reviewed in [24, 25]).

Over a 100 proteins have been identified to be associated with TJ, which are broadly divided into four classes (0). These include multi-pass trans-membrane proteins - occludin, claudin and tricellulin; single-pass transmembrane proteins e.g. coxsackie and adenovirus receptor (CAR) and junctional adhesion molecule (JAM); cytoplasmic

scaffolding proteins e.g. zonula occludens 1 (ZO1), membrane associated guanylate kinase (MAGI-1) and multi-PDZ (post-synaptic density protein, Drosophila disc large tumor suppressor and zona occludens-1 protein) domain protein 1 (MUPP1); signaling molecules e.g. protein kinase C- $\alpha$  (PKC- $\alpha$ ), protein associated with lin-7 (PALS1), focal adhesion kinase (FAK) and several transcription factors associated with TJ e.g. Jun, Fos and CCAAT/enhancer binding protein (C/EBP) (reviewed in [24]).

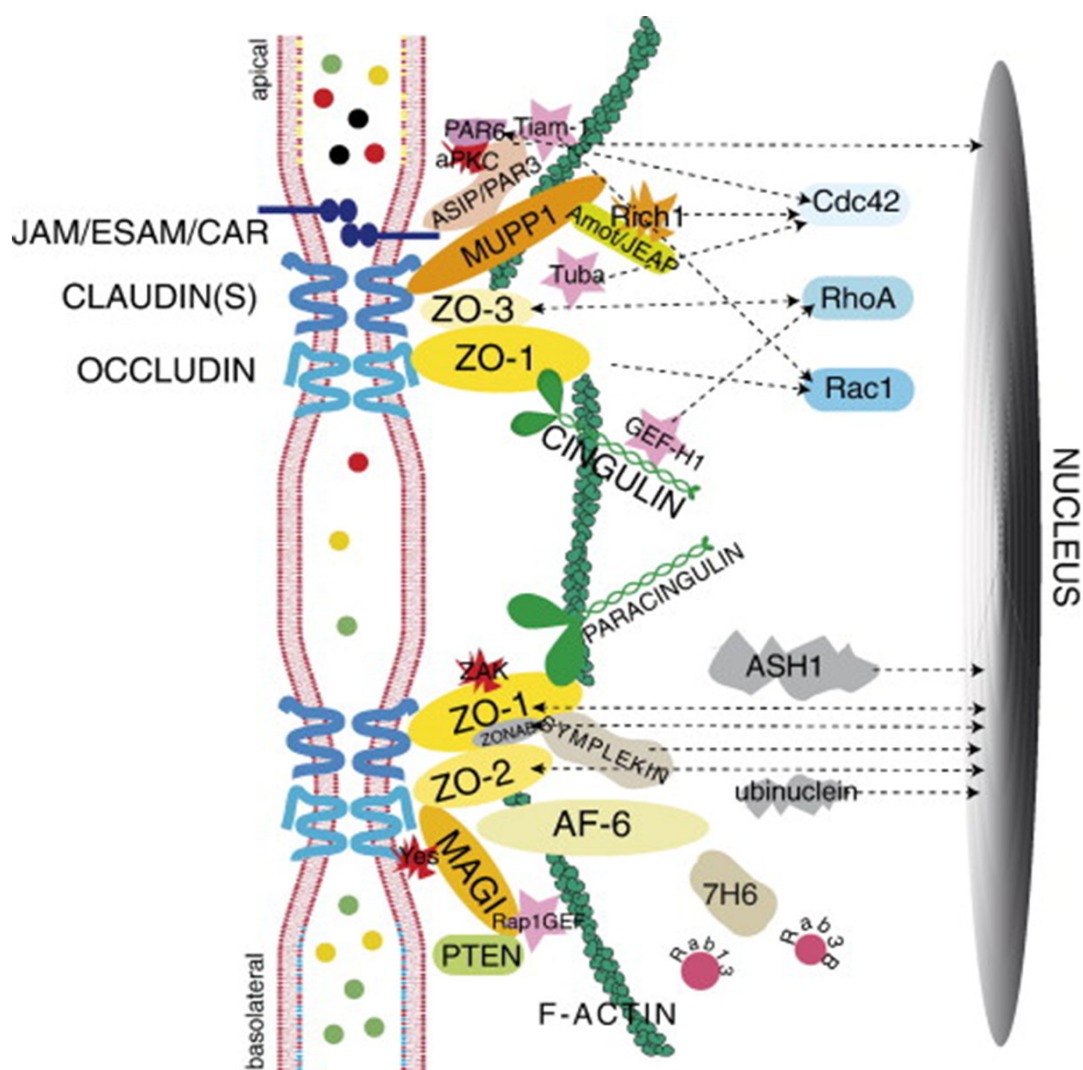


**Figure 1.2. Schematic representation of different components of Tight Junction** (Reproduced from [26]). See text for details. Transmembrane proteins e.g. JAM, claudin

*and occludin cross the lipid bilayer. Major PDZ containing proteins shown here are ZO proteins, PAR proteins, MUPP, MAGI and AF6. Kinases associated with cellular signaling e.g. FAK aPKC and c-YES are in red. GEFs are represented by pink stars. Membrane traffic regulators e.g. Rab3 and Rab13 are represented as circles. Functional regulation and structural interaction of tight junction proteins and signaling proteins are indicated by dotted arrows between them. Arrows directed to nucleus from few tight junction proteins indicate their dual localization i.e. both junctional and nuclear (See text for further details).*

### **1.2.1.1. Components of Tight junctions:**

#### **1.2.1.1.1. Claudin:**

There are approximately 24 distinct members identified in claudin family of proteins in mammals. Claudin 1-10, 14,15,17 and 19 share a considerable sequence homology and are defined as classical claudins whereas, the rest of the members in claudin family are known as non-classical claudins (reviewed in [27]). They are 21-28 kDa tetraspan membrane proteins with two extracellular loops and cytoplasmic N- terminal and C terminal ends. Claudins from neighboring cells engage in homophilic and heterophilic interactions and these are termed as trans interactions. in However, claudins on the same cell membrane also exhibit homophilic and heterophilic cis interactions leading to thickening of TJ stands [28, 29]. Most of the claudin family members share a conserved motif (GLWxxC[8-10 aa]C) in the first extracellular loop (reviewed in [30]). The first extracellular loop of claudins is believed to be involved with charge selective barrier function of TJ [31], whereas the 2<sup>nd</sup> extracellular loop mediates cell - cell adhesion [29]. The C terminal domain of claudins contain a PDZ domain binding motif which is

essential for association of claudin with PDZ domain containing plaque proteins e.g. ZO proteins, MUPP1, PATJ etc. [32-34].

#### **1.2.1.1.2. Occludin:**

Occludin is a tetraspan membrane protein with two extracellular loops, an intracellular turn, and N-terminal and C-terminal cytoplasmic domains. Almost 60% of the amino acids in the N-terminus of occludin are glycine and tyrosine residues, however no function has been associated with this stretch of amino acids (reviewed in [21]). Occludin contains multiple serine and threonine residues in the C-terminal end, which are phosphorylated when occludin is concentrated at the TJ, suggesting a possible role of these phosphorylation events in recruitment of occludin to the TJ. Occludin is shown to be associated with multiple protein kinases e.g. Src, FAK, c-YES etc. and protein phosphatases e.g. PP2A and PP1, which might regulate the phosphorylation status of the C-terminus of occludin [24, 35-39]. The C-terminus of occludin is also responsible for the association between occludin and ZO proteins. Therefore, occludin plays an important role in maintaining interactions between different TJ proteins [32].

#### **1.2.1.1.3. Tricellulin:**

Tricellulin is a multi-pass transmembrane protein with four integral membrane domains. There is considerable sequence similarity between tricellulin and the claudins in the C-terminal domain, which is required for the interaction of these transmembrane proteins of TJ with the ZO proteins. In L cells expressing TJ components, tricellulin co-localized with claudin 1 and induced crosslinking of claudin 1 leading to an increase in the length of the TJ [40]. Down-regulation of expression of tricellulin leads to compromised barrier function of TJ and abnormal organization of TJ present in tricellular and bicellular contacts [21, 41]. Expression of tricellulin was found to be regulated by Snail

transcription repressor, which is known to promote epithelial to mesenchymal transition [41].

#### **1.2.1.1.4. JAM:**

JAM and CAR are single pass transmembrane proteins. There are five members in the JAM family of immunoglobulin like proteins, namely JAM-A, JAM-B, JAM-C, JAM4 and JAM like proteins. JAMs are known to form both homotypic and heterotypic complexes and interact with integrins, (reviewed in [24]). are required for the internalization of integrins during cell migration and regulate cell morphology [42, 43]. Down-regulation of JAMs results in the mis-localization of TJ proteins such as occludin, claudin 1 and ZO-1. Reports have suggested that loss of JAMs leads to loss of cell polarity and disruption of junction assembly [44].

Recent reports suggest that TJ associated proteins are also involved in regulation of other cellular pathways as well such as cell motility, cell proliferation and regulation of gene expression. TJ also play a crucial role in regulation of cell polarity (reviewed in [24, 45]). Disruption of TJ formation has been associated with numerous diseased conditions like cancer, diabetic retinopathy, pulmonary disorders, and inflammatory bowel disease (reviewed in [46-48]).

All these TJ associated proteins play very important role in maintaining TJ function. Loss of TJ function has been shown to cause multiple diseases as well including cancer progression (reviewed in [26, 46]).

#### **1.2.2. Gap junctions**

Gap junctions are communicating junctions and are expressed in most metazoan cell types (reviewed in [49]). They play a major role in tissue homeostasis, regulation of

developmental processes, propagation of electrical signals, and transport of ions and exchange of metabolites [50-52] (also reviewed in [49, 53]). There are three types of gap junctions reported i.e. connexin, innexin, and pannexin protein family based gap junctions [54-56]. The connexin based gap junctions have been extensively studied. Connexins (Cx) are the basic structural constituent of gap junctions and participate in homotypic and heterotypic interactions across the junction (reviewed in [49]). There are >20 connexin members that are expressed in a tissue and cell type specific manner [57, 58]. Connexins are tetraspan trans membrane proteins with four  $\alpha$  helical domains, two extracellular loops and one cytoplasmic loop [59]. Six connexin molecules on adjacent cells communicate to give rise to a cylindrical structure called the connexon [60]. Docking of connexons during formation of gap junctions requires close apposition of the plasma membranes with a very narrow extracellular gap of about 2-3 nm in-between the two membranes (figure 1.3) reviewed in [49]). A connexon can be thought of having 3 domains: an extracellular domain where two connexons dock, a trans-membrane domain that forms the channel and a cytoplasmic domain that regulates the gating of the channel [61]. Passage of ions, solutes and metabolites through gap junctions is stringently regulated. Multiple connexins are expressed by majority of cell types and they can oligomerize in homomeric or heteromeric manner to form functional hemichannels between adjacent communicating cells [62, 63]. A rapid regulation of transport of solutes or ions is achieved by changing the voltage dependent conductance of connexons, whereas, a slower mode of regulation exists which involves alteration of number of channels in the plasma membrane, synthesis and degradation rate of connexins and even post translational modification of connexins (reviewed in [49]). Mutations in connexin genes have been associated with several disease conditions like X-linked Charcot-Marie-

Tooth syndrome [64], skin disease [65], cataracts [66], ODDD (Oculodentodigital or oculodentoosseous dysplasia) [67].

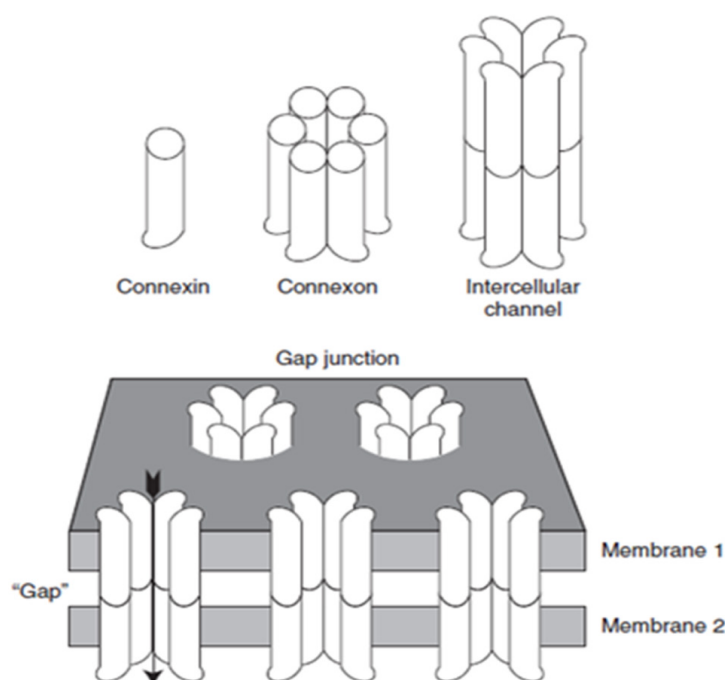


**Figure 1.3. Multiple levels of structure of gap junction** (reproduced from [49]). Individual connexins assemble into hexameric complex called connexon. Two connexons from neighboring cells can dock on each other to form an axial membrane channel.

### 1.2.3. Hemidesmosomes:

Hemidesmosomes are specialized junctions which mediate cell to extracellular matrix and basement membrane attachment in stratified and other complex epithelia such as skin, cornea, respiratory tract (reviewed in [68]). Hemidesmosomes are found in the ventral surface of basal epithelial cells where they associate with sub basal dense plate of lamina lucida and are connected via thread like filaments to the lamina densa. In electron micrographs they appear as electron dense areas of less than  $0.5\mu\text{m}$  (reviewed in [68]). Hemidesmosomes have been classified into two types. Type I or the classical

hemidesmosomes are found in stratified or pseudo-stratified epithelium and contain multiple proteins including  $\alpha 6\beta 4$  integrins, plectins, tetraspanin CD15, Bullous Pemphigoid Antigen 180 and 230 (BPAG 180 and 230 respectively).  $\alpha 6\beta 4$  integrin and BPAG 180 are strong and weak receptors respectively for laminin 332 in the extracellular matrix [69-71]. On the intracellular face, hemidesmosomes connect to keratin intermediate filaments through the plectin family members and BP 180, thus stabilizing the adhesion complex [72]. Type II hemidesmosomes are found in simple epithelia like the inner lining of the intestine and are composed of  $\alpha 6\beta 4$  integrin and plectins (reviewed in [68]). Signaling from hemidesmosome associated integrins have been shown to regulate various cellular processes and their aberrant regulation has been shown to promote cell migration and cancer progression (reviewed in [73, 74]). Mutation or loss of other hemidesmosomal proteins also lead to various pathophysiological conditions e.g. hand BP230 null mice manifests severe blistering and plectin knockout mice show phenotypes of epidermolysis bullosa [75, 76].

#### **1.2.4. Adherens Junctions:**

Adherens junctions also known as zonula adherens are calcium dependent cell - cell junctions that mediate homotypic cell - cell adhesion [4, 77]. In polarized epithelial cells adherens junctions are found at the luminal side of the lateral plasma membrane [20]. They are found in a variety of cell types and can be identified in electron micrograph images as electron dense structures where the plasma membranes from neighboring cells are apposed at a distance of 10-20 nm and the intercellular space is bridged by rod shaped electron dense molecules (reviewed in [78]). Adherens junctions are composed of transmembrane cadherins which associate with cytoplasmic plaque proteins which in turn anchor actin filaments (reviewed in [79]). There are two kinds of adhesion cores observed

in adhesion junction, the calcium independent nectin-afadin complex and calcium dependent cadherin catenin complex [80].

#### **1.2.4.1. Cadherin Catenin complex:**

Twenty members are there in classical cadherin family all of which share a similar domain organization [81]. The classical cadherins have a short N terminal domain, five extracellular EC domains which contain  $\text{Ca}^{2+}$  binding sequences; a single trans membrane domain and a cytoplasmic domain (figure 1.4) [82]. Cadherins are expressed in tissue specific manner e.g. epithelial cells express E cadherin (Cdh1), neuronal cells express N cadherin (Cdh2) and P cadherin is predominantly found in placental tissue (reviewed in [83]).

The cytoplasmic domain of the cadherins associate with the armadillo repeat family of proteins such as p120 catenin,  $\alpha$  catenin,  $\beta$  catenin and  $\gamma$  catenin (also known as plakoglobin) (figure 1.4) [84-90]. These catenins in turn associate with actin cytoskeletal components and other associated components such as vinculin and EPLIN [91, 92]. Adherens junctions can also interact with microtubules via the PLEKHA-Nehza complex (figure 1.4). The PLEKHA -Nehza complex interacts with signaling molecules such as aPKC and also regulates other cellular processes such as morphogenesis [93-95]. The adherens junction is also associated with polarity determining proteins such as PATJ, Pals1, CRB3, PAR3, PAR6 etc. thus linking AJ to polarity determination and morphogenesis [96-98].

#### **1.2.4.2. Nectin Afadin complex**

Nectins belong to the immunoglobulin super-family of adhesion molecules and there are four members in the family, Nectin 1-4, which are encoded by the pvr1 1-4 genes

respectively (reviewed in [99, 100]). Nectins contain an extracellular domain comprising of three IgG loops, a single transmembrane domain and a C-terminal domain, which also contains a PDZ binding motif (reviewed in [101]). During AJ assembly Nectins accumulate first at the cell - cell contacts and subsequently cadherins colocalize with nectin afadin complex (figure 1.4) (reviewed in [102]). They accumulate at the AJ and bind to afadin on their cytoplasmic side [103]. Nectins and afadins are calcium independent adhesion molecules show both heterophilic and homophilic interactions with each other. However, there is preference for heterotypic interactions, which are

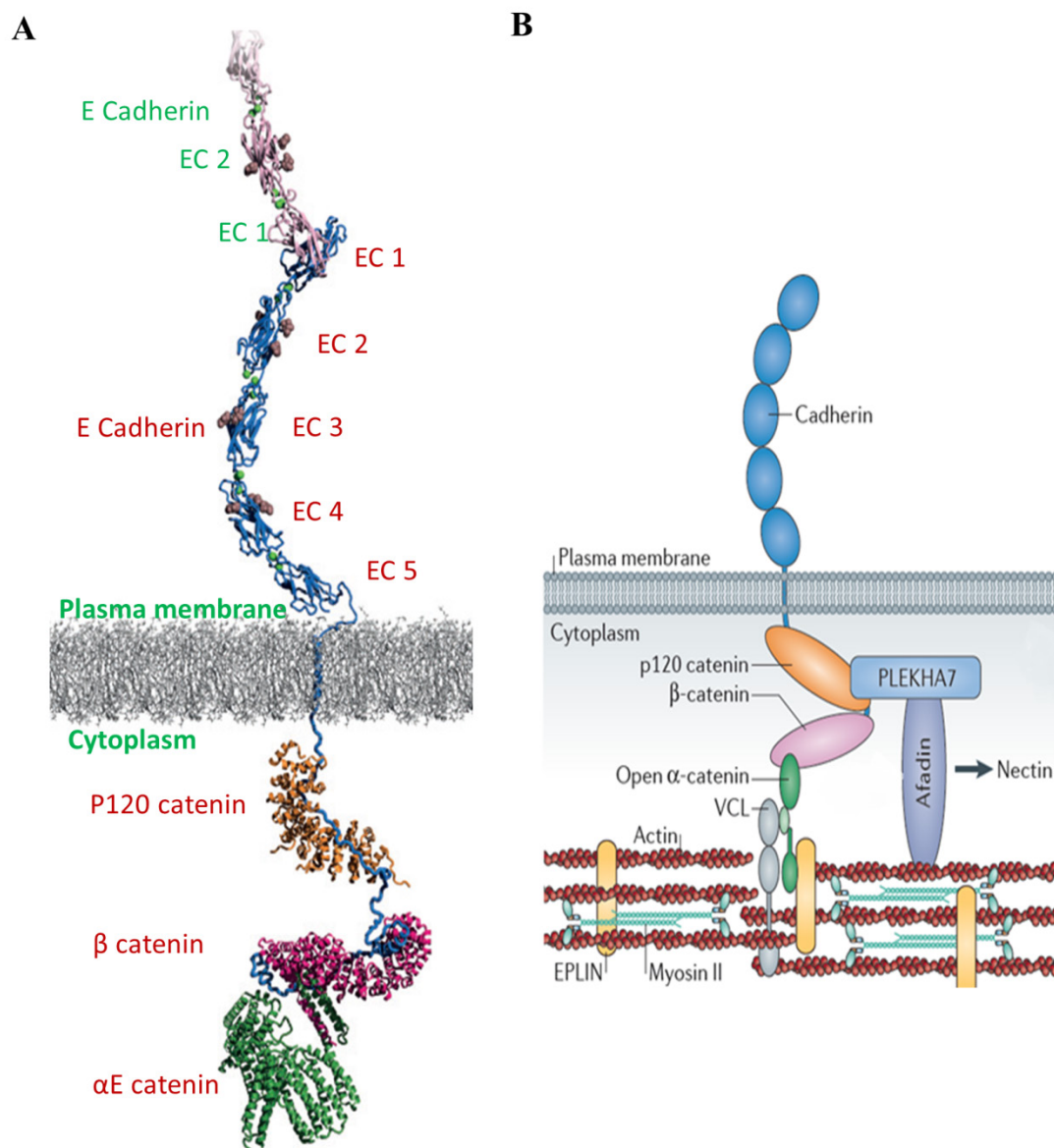


**Figure 1.4. Molecular architecture of adherens junction** (adapted from [79]). A. A cartoon representing cadherin catenin complex based on the crystal structure of strand swapped trans dimer of E cadherin (light pink and blue), p120 catenin (orange) bound to juxtamembrane domain of E cadherin.  $\beta$ -catenin (dark pink) in complex with catenin binding domain of E cadherin (blue) and  $\alpha$ E catenin (green) in complex with  $\beta$ -catenin.  $Ca^{2+}$  ions (green spheres) and O-linked glycans (brown sphere) are shown bound to extracellular domains (EC) of E cadherin. B. Cytoplasmic components of adherens junction. Dashed line represents interaction of cadherin catenin complex and nectin afadin complex.

comparatively stronger than homophilic interactions (reviewed in [78]). The cytoplasmic domain of Afadin interacts with  $\alpha$  catenin, Ras/Rap family of GTPase and ZO1 [104]. Loss of AJ function as well as mutations in different AJ component proteins has been shown to cause multiple human diseases (discussed in detail in the following sections). Reports from literature suggest a strong correlation of cancer progression and loss of AJ proteins (also discussed in the following sections).

#### **1.2.4.3. Physiological relevance of adherens junctions:**

The primary function associated with adherens junction is to provide adhesive contacts between neighboring cells. However, apart from cell - cell adhesion there is a growing list of other cellular functions that has been linked to adherens junction proteins such as cell proliferation, regulation of cell polarity, morphogenesis, cell sorting during embryonic development, regulation of cell signaling pathways [4, 77, 78, 105, 106]. Other reports suggest that adherens junctions regulate desmosome formation [107]. Deregulation of expression and localization of different adherens junction proteins have also been associated with cancer progression and metastasis (reviewed in [78]). A decrease in E

cadherin expression has been observed in multiple cancer types (reviewed in [106]). E cadherin is considered as a tumor suppressor gene and loss of heterozygosity and mutation in E cadherin gene is observed in multiple different cancer types such as cancers of the breast, ovary, thyroid, endometrium and stomach [108, 109]. Aberrant expression and localization of other adherens junction proteins like  $\beta$  catenin,  $\alpha$  catenin and p120 catenin is also reported to be associated with multiple human cancers (reviewed in [106]). These catenin family of proteins also regulate WNT signaling by interacting with TCF-LEF transcription factors (reviewed in [110]). The role of adherens junctions and particularly the role of catenin family of proteins in regulation of cellular signaling pathways and cancer progression have been described in detail later in the introduction.

### **1.2.5. Desmosomes**

Desmosomes are also known as ‘maculae adhaerentes’ and were first identified as small dense nodules in the spinous layer of epidermis by Italian pathologist Giulio Bizzozero. They are adherens like calcium dependent junctions present in the basolateral membrane domains between adjacent cells of tissues that experience mechanical stress such as myocardial cells, dendritic cells of lymph nodes, meningeal cells and Purkinje cells (reviewed in [111, 112]). Desmosomes link intermediate filaments to the site of intercellular junctions and help to distribute and withstand mechanical stress [113]. Desmosomes are composed of three different families of proteins and appear as a tripartite electron dense zipper like appearance in electron micrographs. Desmosomal cadherins are trans membrane proteins, which are required for  $\text{Ca}^{2+}$  dependent adhesive interactions in the extracellular region between two adjacent cells to bring about the adhesion and this interaction results in the formation of the electron dense region called the dense midline (DM) [114, 115]. On the cytoplasmic side of the plasma membrane desmosomal cadherins interact with another family of proteins called the armadillo repeat

containing proteins (e.g. plakophilins and plakoglobin) forming an electron dense plaque known as outer dense plaque (ODP) [116, 117]. This complex of junctional proteins associates with the plakin family member, desmoplakin, which tethers intermediate filaments to the desmosomal junction. The region where DP associates with the Ifs is electron dense and is called the inner dense plaque (IDP) (figure 1.5.) [111, 118].

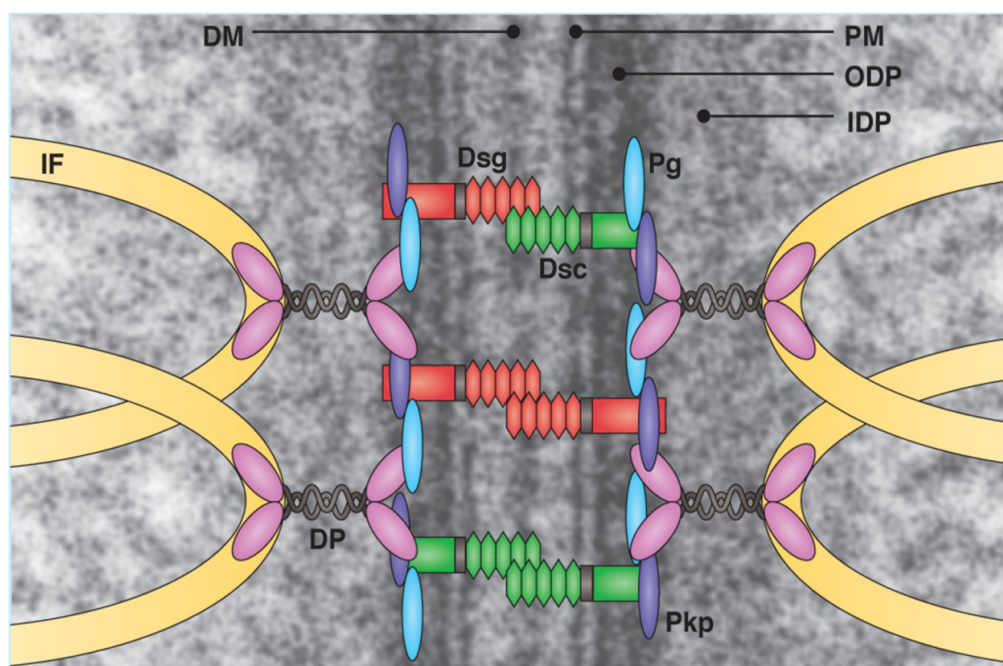


**Figure 1.5. Molecular architecture of desmosome** (reproduced from [119]). Electron micrograph of desmosome superimposed with a cartoon representing the molecular architecture of desmosome. Desmosomal cadherins (DSG and DSC) interact in homophilic and heterophilic manner in intercellular space. This region forms an electron dense midline (DM) which can be seen in the electron micrograph. On the cytoplasmic face of the plasma membrane these desmosomal cadherins interact with armadillo repeat containing proteins (PKP and PG). PKP and PG again associates with plakin family protein desmoplakin (DP). This region can be seen as an electron dense layer which forms the outer dense plaque (ODP) and lastly another electron dense

region can be seen, the inner dense plaque (IDP), where desmoplakin links the desmosome to intermediate filaments (IF)

Though desmosomes are known to be Ca<sup>2+</sup> dependent structures, they become Ca<sup>2+</sup> independent in confluent cultured cells and in intact tissue. Ca<sup>2+</sup> dependency of desmosome is regulated by Protein Kinase C  $\alpha$  (PKC $\alpha$ ) [120].

### 1.2.5.1. Desmosomal cadherins

The genes encoding the single pass trans membrane desmosomal cadherins namely desmogleins and the desmocollins are clustered on chromosome number 18 in human cells [121]. Four isoforms of desmoglein (DSG 1-4) and three isoforms of desmocollin (DSC 1-3) are present in mammalian cells. The DSCs are often expressed as two splice variants “a” and “b” (figure 1.6.). DSG2 and DSC2 are ubiquitously expressed in all tissues and all epithelial cell layers [122, 123], however the other cadherins show variable expression in different tissues and are differentially expressed in the different layers of stratified epithelium.

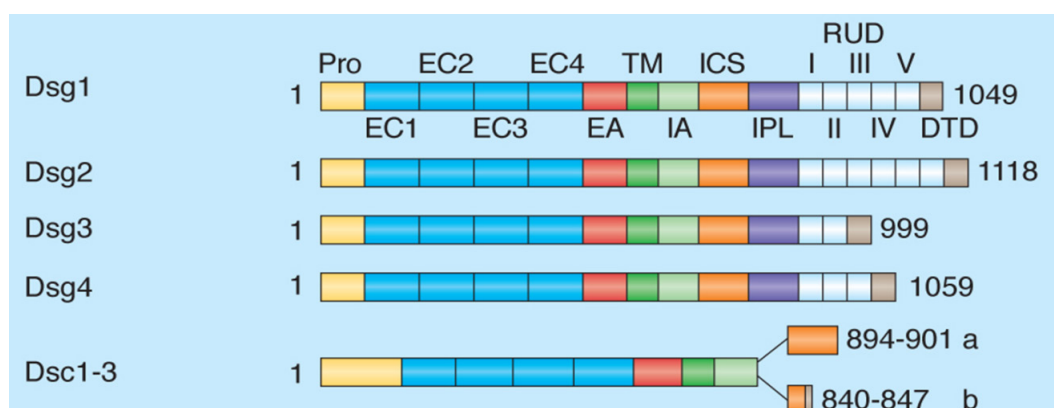


**Figure 1.6. Domain organization and splice variants of desmosomal cadherins** (reproduced from [119]). Pro = pro domain, EC = extracellular domain, TM =

*transmembrane domain, ICS = internal catenin binding site, RUD = repeat unit domain, DTD = distal terminal domain.*

Genes encoding desmosomal cadherins are differentially expressed in keratinocytes and in cells that undergo terminal differentiation (reviewed in [124]). DSG1 expression is higher in upper layers of epidermis, while DSG4 is mostly expressed in the hair follicle and granular layers. DSC2 and 3 are expressed primarily in the basal and spinous layers while, DSC1 expression is restricted to the granular layer only (reviewed in [111]). The desmosomal cadherins interact in homophilic and heterophilic manner via their extracellular domains [125-127]. All the members of desmosomal cadherin family of proteins contain four extracellular repeat domains (EC 1-4) of 110 amino acids, which also contain a  $\text{Ca}^{2+}$  binding motif. The  $\text{Ca}^{2+}$  binding site when bound to  $\text{Ca}^{2+}$  promotes conformational changes, which trigger cadherin oligomerization [128]. They also contain extracellular anchoring region (EA), a single trans-membrane domain (TM), Intracellular anchoring region (IA) and internal catenin binding site (ICS). DSG have additional domain like distal terminal domain (DTD), intracellular prolin rich linker domain (IPL) and repeat unit domain (RUD) (figure 1.6.) (reviewed in [129, 130]). The ICS region is essential for their association with the armadillo repeat containing proteins like plakophilins and plakoglobin on the cytoplasmic face of the plasma membrane. The EC1 domain mediates heterophilic interaction of cadherins through cell adhesion region (CAR domain) (reviewed in [111]).

Loss of expression and deregulate expression of desmosomal cadherins can lead to multiple cellular defects. Mis-expression of DSG3 in in suprabasal epidermal layer resulted in hyperproliferation and abnormal differentiation [131]. Ectopic expression of DSG2 in the differentiated layers of epidermis results in hyperproliferation. This leads to vulnerability to chemically induced carcinogenesis [132]. Ablation of DSG3 in mice

causes decreased cell - cell adhesion, separation of keratinocytes and compromised cell - cell adhesion. Loss of DSG2 leads to embryonic lethality shortly after implantation [133, 134]. Similarly loss of DSC1 and DSC3 in mice have led to epidermal fragility, decreased cell - cell adhesion, hyperproliferation, abnormal differentiation and embryonic lethality due to miss-implantation [11, 12, 135].

### 1.2.5.2. Armadillo repeat proteins

Four plakophilin family members (plakophilin 1-4) and plakoglobin represent the armadillo family of proteins in the desmosome. They all contain the characteristic 42 amino acid ARM repeats originally identified in *Drosophila* armadillo protein [136]. They associate with desmoplakin which links the intermediate filaments to the desmosome (reviewed in [137]). Apart from their role in forming cell junctions these proteins play important roles in gene regulation, signal transduction and their deregulation is associated with various disease conditions such as cancer (reviewed in [111, 137]).

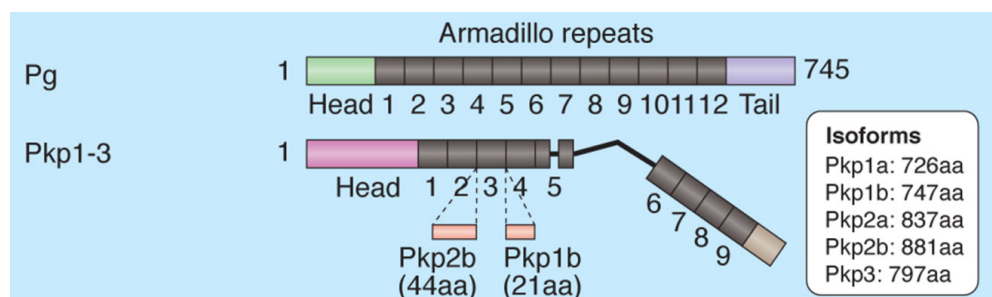


**Figure 1.7. Domain organization and splice variants of desmosomal armadillo repeat containing proteins** (reproduced from [119]). See text for details.

#### 1.2.5.2.1. Plakophilins

Plakophilins belong to the p120<sup>CTN</sup> family of armadillo proteins. They share common domain organization, which has a non-homologous N-terminal domain; a variable number of ARM repeats which share 50-80% homology followed by a C terminal

domain. The N terminus also contains a homology region 2 (HR2) which show considerable sequence similarity between PKP family members (reviewed in [138]). There is a short flexible stretch of linker sequence present between repeat 4 and 5, which could produce a bend in the molecular structure of plakophilins. There are splice variants reported for plakophilin 1 and 2 among the four family members. Plakophilins show considerable variation in their expression pattern. However, plakophilin 2 and 3 are the most ubiquitously expressed proteins in this family and have different functions with respect to desmosome formation and cell-cell adhesion (reviewed in [111]).

#### **1.2.5.2.1.1. Plakophilin 1**

The plakophilin1 (PKP1) gene has been mapped to chromosome 1q32 [139]. There are two splice variants reported 'a' and 'b'. The 'a' isoform contains an insertion of 21 amino acids (aa) between ARM repeat 3 and 4. The isoform 'a' is a 747 amino acid long protein and comprises a 275 aa long N terminal domain, a short C terminal domain and 10 arm repeats (figure 1.7.) [139, 140]. The 'b' isoforms is localized exclusively in the nucleus whereas the 'a' isoform is present in both nucleus and desmosome [140, 141]. It is mostly expressed in the suprabasal layer of stratified and complex epithelia [142]. The N terminal domain of PKP1 recruits DSG1, DSC1, and desmoplakin to the desmosome and helps to tether intermediate filaments. The C-terminal domain of PKP1 is responsible for its targeting to the desmosome [143-145]. PKP1 over-expression leads to transition of desmosomes from Ca<sup>2+</sup> dependent to Ca<sup>2+</sup> independent state [146]. Mutation in PKP1 gene leads to ectodermal dysplasia and skin fragility syndrome [147]. PKP1 is also known to bind to mRNA binding proteins and thus could regulate mRNA stability and translation and other functions [148].

#### **1.2.5.2.1.2. Plakophilin 2**

The gene encoding plakophilin2 (PKP2) is located in chromosome 12p13 [149]. It is quite similar to PKP1 in domain organization and only differs in the N terminal region. There are two splice variants 'a' and 'b' reported for PKP2 which differ by 44 amino acids insertion between repeat 3 and 4 (figure 1.7. [150]). It is ubiquitously expressed in all layers of epithelial cells with strong expression in basal layers of stratified and complex epithelia [150]. PKP2 interacts with wide range of desmosomal proteins such as DSG1/2, DSC1/2, DP, keratin filaments and other plakophilin family members (reviewed in [138]. PKP2 can regulate recruitment of other desmosomal proteins to the desmosome e.g. PKP2 recruits DP to the desmosome in a PKC $\alpha$  dependent manner. Plakophilin 2 is speculated to play a role in regulation of transcription as PKP2 is reported to interact with RPC115 (largest subunit of RNA PolIII) and  $\beta$  catenin [151, 152]. It interacts with  $\beta$  catenin and thus can regulate WNT signaling pathway [153]. Ablation of PKP2 results in mid gestational embryonic lethality due to cardiac patterning defects and fragility in myocardium. Epidermal cells of mice lacking PKP2 show retraction of intermediate filaments (IF) from the plasma membrane indicating its role in tethering DP-IF complex to the desmosome [14].

#### **1.2.5.2.1.3. Plakophilin 3**

The gene expressing plakophilin 3 (PKP3) is located on chromosome 11p15 [141]. It is ubiquitously expressed in simple and stratified epithelia [141]. PKP3 interacts with DP, DSG1-3, DSC 1, PG, keratin 18 and other plakophilin members as well. Mostly it interacts with the N terminal and arm repeat domain [154] and reviewed in [111, 119]. PKP3 may compete with  $\beta$  catenin and regulate WNT pathway. PKP3 has been also shown to interact with ETV1 transcription factor to regulate gene expression [155] and

reviewed in [138]. PKP3 associates with stress granules and bind to stalled translation initiation complex proteins viz. Poly (A) binding protein (PABPC1), fragile-X-related protein (FXR1), ras-GAP-SH3-binding protein (G3BP), eIF-4E and the ribosomal protein S6 kinase [156, 157]. Conditional ablation of PKP3 in mouse epidermis resulted in defective hair follicle morphogenesis and hyperproliferation. Reports from our laboratory as well as other laboratory have shown that loss of PKP3 leads to mis-localization of other desmosomal proteins [158, 159]. Down-regulation of PKP3 results in acquisition of neoplastic properties both in vitro and in vivo [17].

#### **1.2.5.2.1.4. Plakophilin 4**

Plakophilin4 (PKP4) is the most recently identified member of PKP family and the gene encoding this protein is located on chromosome 2q24 [160]. A 135 kDa protein consisting of a 509 amino acid long N- terminal domain, 10 ARM repeats and 170 amino acid long C terminal domain [160]. PKP4 is expressed in all epithelial tissues and colocalize with classical cadherins and adherens junction (reviewed in [86]). It interacts with PG and PKP2 through its ARM domains and associates with DP through its N-terminal domain [161]. Its overexpression leads to desmosomal instability [162].

#### **1.2.5.2.2. Plakoglobin**

Plakoglobin (PG) is expressed in all cell types containing desmosomes. Plakoglobin interacts with desmosomal cadherins and classical cadherins as well so is a part of both desmosomes and adherens junctions [163]. It is a 746 amino acid, 87kDa molecule with a short N terminus and C terminus which flank the 12 arm repeats (figure 1.7.). There is spacer sequence between ARM 9 and 10. Plakoglobin associates with desmosomal cadherins and classical cadherins through its ARM domain while the N terminal domain is important for its interaction with desmoplakin [164]. Truncation of the C terminal

domain of PG leads to formation of extremely long desmosomes [165]. There are reports of various posttranslational modifications of plakoglobin, which contribute to its different functions. Phosphorylation of Tyr133 and Tyr643 leads to decreased interaction of plakoglobin with E cadherin and  $\alpha$  catenin with subsequent increase in its association with DP, however, phosphorylation of Tyr 693, 724, 729 as a consequence of activation of EGFR leads to decrease in interaction of plakoglobin with DP [166, 167]. Knockout of plakoglobin is embryonic lethal due to failure in cardiac function [168]. Mutations of plakoglobin results in Naxos disease with arrhythmogenic right ventricular cardiomyopathy, palmoplantar keratoderma, and woolly hair [169].

Plakoglobin share significant homology with  $\beta$  catenin and can functionally replace the later from AJ and also compete it for degradation. That leads to increased accumulation of  $\beta$  catenin in nucleus leading LEF/TCF mediated gene transcription. However, it is reported that PG can also activate WNT signalling by directly binding and recruiting LEF/TCF transcription factors [170-172].

### **1.2.5.3. Desmoplakin**

Desmoplakin is ubiquitously expressed plakin family protein found in epithelial tissue and has two splice variants. Desmoplakin is a dumbbell shaped molecule with three distinct domains, an N terminal domain which mediates its association with desmosomal cadherins and armadillo proteins, a central rod domain which is essential for dimerization and a C terminal domain containing three plakin domain repeats i.e. A, B and C (PDRs). The B and C PDRs contain an intermediate filament binding site (figure 1.8). Desmoplakin associates with intermediate filament proteins such as vimentin, keratin and desmin and tethers desmosome to the cytoskeletal elements [111, 173]. Desmoplakin is also reported recruit centrosomal proteins to desmosome and may contribute to MT

assembly at the cortex [174]. Knockout of desmoplakin is embryonic lethal whereas, haploinsufficiency and mutations of desmoplakin lead to different diseased conditions like striate palmoplantar keratoderma, skin fragility and woolly hair, acantholytic epidermolysis bullosa [175-178].

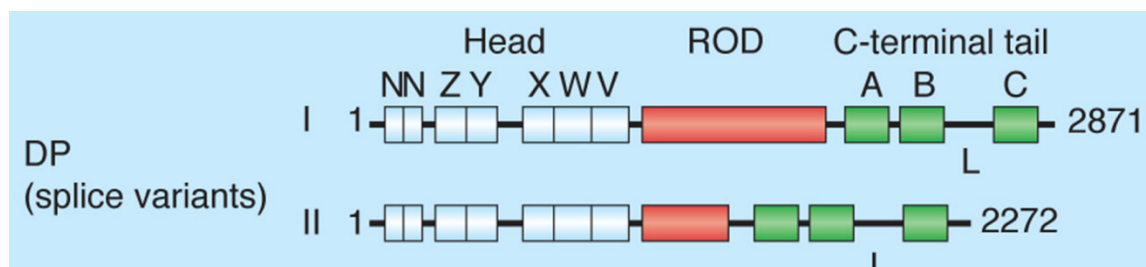


**Figure 1.8. Domain organization and splice variants of desmoplakin** (reproduced from [119]). See text for details.

#### 1.2.5.4. Role of Desmosomal proteins in cancer

One of prerequisites for metastasis in epithelial tumors is dissolution of cell - cell adhesion. This process is associated with dynamic regulation of cell - cell junctions. Deregulation of desmosome function has been associated with myriad types of cancers. However, more and more reports are suggesting role of desmosomal proteins in other cellular functions like signaling, regulation of gene expression, cytoskeletal dynamics, cell migration and cell proliferation and programmed cell death [111, 119, 138, 152, 174, 179-181].

Deregulation of desmosomal cadherins have been reported in many cancers. Loss of heterozygosity (LOH) has been reported for the locus of chromosome 18 harboring the genes of desmosomal cadherins in esophageal and head and neck cancers (reviewed in [181]). DSG3 loss is associated with poor prognosis in lung cancer patients [182]. DSC3 expression has been shown to be repressed in breast cancer by hyper methylation of its

promoter at chromosome 18. siRNA mediated knockdown of DSG3 in human head and neck cancer (HNC) cell lines leads to a decrease in cell proliferation and significant reduction of colony formation potential and reduced tumor volumes when injected in mouse models [183]. Loss of desmosomal cadherin expression often leads to an increase in the cytoplasmic pool of PG which in turn leads to increased nuclear translocation of  $\beta$ -catenin thereby activating the WNT signaling pathway and expression of genes like bcl2, c-myc and cyclin D1 thus leading to cell proliferation and cell survival (reviewed in [184]). DSG3 down regulation and upregulation of DSG2 has been recently reported for head and neck squamous cell carcinoma [185]. Several studies have shown loss of DP to be associated with uterine adenocarcinoma, oral squamous cell carcinoma and increased metastasis and poor prognosis [186, 187].

LOH of PG and suppression of PG expression through various mechanisms like deacetylation and hyper-methylation of its promoter have been found to be associated with progression of different types of cancers in vivo. These results have later been recapitulated in in-vitro model systems [188-190]. LOH and promoter methylation of PG has been reported to be associated with human prostate carcinoma, ovarian carcinoma, breast cancer and renal carcinoma [191, 192]. Reduced expression of plakoglobin has been observed in poorly differentiated tumors. Several types of cancers such as bladder cancer, lung cancer, kidney cancer and neuroblastomas show loss of expression of PG [193, 194]. PG has been reported to be associated with decreased cell-cell adhesion, increased invasion and dissemination of breast cancer cells in vivo [195]. Repression of PG leads to alteration in cell-cell adhesion and motility in triple negative breast cancer and prostate cancer cells [196, 197].

Expression PKP1-3 has been found to be inversely correlated with tumor differentiation and poor prognosis. A reduced level of expression has been reported for PKP3, PKP2 and

PKP1 in several types of cancers such as oropharyngeal carcinoma, colorectal adenocarcinoma, pancreatic, prostate and hepatocellular carcinoma [198]. Also their loss has been correlated with acquisition of neoplastic properties in vitro and in vivo. However, a contradicting report shows that in lung cancer PKP3 levels increases [199]. Reports from our laboratory have shown that loss of PKP3 leads to abrogation of desmosome assembly which leads to decreased cell - cell adhesion and increased cell migration in vitro. Loss of PKP3 has also been shown to result in tumor progression and metastasis in vivo [17, 159]

### **1.3. Cytoskeleton**

All these junctional complexes described above connect to one or the other cytoskeletal components. Dynamic regulation of these cytoskeletal components also affects various aspects of cell behavior like migration, motility, proliferation, signaling etc. In animal cells majorly three types of cytoskeletal components are found, these are microfilaments (actin filaments), intermediate filaments and microtubules.

#### **1.3.1. Microfilaments/ actin filaments**

Actin filaments connect to adherens junctions and focal adhesions. They also form tracks for myosin motors and thus play a role in cell motility and cytokinesis (reviewed in [200]). Globular monomers of G actin polymerize to form linear single stranded polymers with distinct polarity, which are known as F actin. Actin filaments are dynamic polymers that exhibit tread milling activity i.e. actin filaments polymerize at one end and depolymerization occurs at the other end [201].

At the initial E cadherin contacts Arp2/3, Ena/ VASP and cortactin mediated actin polymerization link adherens junctions to actin filaments [202]. However, N-WASP

antagonizes this polymerization [203]. The adherens junction component,  $\alpha$ -catenin can associate with different actin binding proteins viz. vinculin, eplin, ZO-1, FMN1, or AF6 which in turn can associate with actin filaments thus linking the actin cables to the AJ [204, 205].

### **1.3.2. Intermediate filaments**

Intermediate filaments connect (IF) desmosomes and tight junctions. They are more rigid and the fibers are about 10 nm in width. Vimentin and keratin filaments are most common IF (reviewed in [206]). In desmosomes plakin family protein desmoplakin connects the intermediate filaments to the desmosomal plaque [207] whereas, in hemidesmosomes plectins and BP180 link the junctional complex to intermediate filaments (reviewed in [71]). Keratin 5 and keratin 14 bind to type I hemidesmosomes and keratin 8 & 18 bind type II hemidesmosomes (reviewed in [71]).

### **1.3.3. Microtubules**

Microtubules (MT) are bundles of protofilaments and are hollow cylindrical structure with outer diameter of 25 nm and inner diameter of 12 nm. Thirteen protofilaments formed by polymerization of  $\alpha$  tubulin and  $\beta$  tubulin associate laterally to give rise to an imperfect helix (reviewed in [208]). MT polymerization generally is nucleated from a microtubule organizing center such as centrosome or basal body in cilia and flagella (reviewed in [209]). Polymerization of  $\alpha$  tubulin and  $\beta$  tubulin is a dynamic process and requires optimal concentration of the monomers and this process is positively powered by GTP hydrolysis [210]. MT filaments can grow as long as 25 micrometers in length and they form tracks for the transport of proteins, vesicles and organelles in the cell [211]. MT have distinct polarity and dedicated + end & - end motor proteins (kinesin and dynein

respectively) can transport cargo in the respective polarity in MT track (reviewed in [212-214]).

#### 1.4. Focal adhesions

Focal adhesions are sites of cell to ECM junctions, which contain multiple proteins such as trans-membrane proteins, actin binding proteins, linker proteins and signaling molecules. Integrins and proteoglycans are transmembrane proteins at the focal adhesion, which mediate cell to ECM adhesion. Attachment of cells to ECM induces integrin clustering.

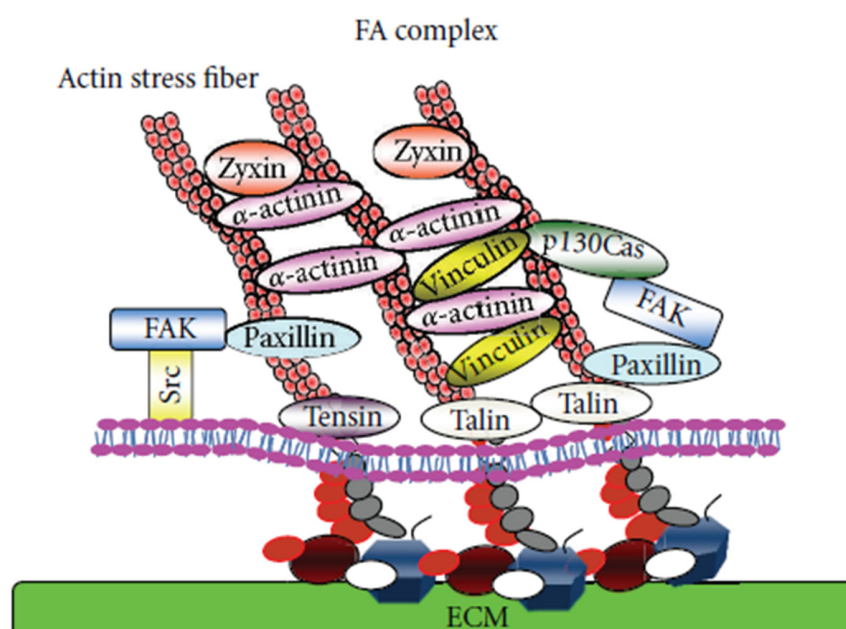


**Figure 1.9. Molecular components of cell to extracellular matrix adhesion** (reproduced from [215] . see text for details.

Integrins are presented at the cell surface as heterodimers of non-covalently associated  $\alpha$  and  $\beta$  subunits. There are 18 different  $\alpha$  and 8 different  $\beta$  subunits reported in mammals. A particular heterodimer of integrins associates with a specific ECM substrate thus allowing cells to sense the ECM environment (reviewed in [216, 217]. On the

cytoplasmic domain of these integrin molecules a large number of actin binding scaffolding proteins such as talin, paxillin, zyxin, vinculin, and  $\alpha$ -actinin are assembled. These actin-binding proteins link actin filaments to focal adhesion complexes. A large number of signaling molecules also have been reported to localize to focal adhesions such as the Ras family GTPases Rho, Rac and Cdc42, Focal adhesion kinase, Src, calpain and the phosphatase PTP-PEST (figure 1.9.). Signaling from focal adhesion is known to regulate different cellular behavior such as cell proliferation, cell migration, cell morphology, survival and differentiation (reviewed in [215, 218]).

#### 1.4.1. Focal adhesion biogenesis during cell migration

Focal adhesions play a crucial role during cell migration. Focal adhesions provide anchorage and necessary traction forces to enable the leading edge of the cell to crawl over ECM as the cell moves forward. These adhesions are rapidly turned over at the posterior trailing edge of the cell. New focal adhesions continuously keep emerging at the anterior tip of the lamellipodia and as the lamella moves forward these junctions also turnover at the posterior part of the lamella (figure 1.10.) [219, 220]. Such anterior flow of focal adhesions coincides with the forward movement of a lamellipodia in a migrating cell (reviewed in [221]).

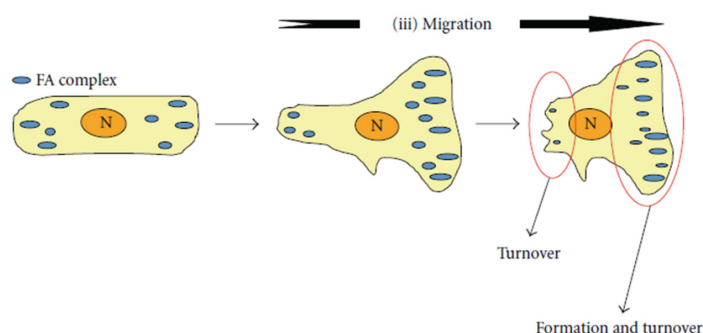


**Figure 1.10. Formation and turnover of focal adhesion during cell migration**

*(reproduced from [215]). See text for details.*

The rate of focal adhesion turnover is a limiting factor for rate of cell migration. Focal adhesion kinase associated with focal adhesions has been found to be a regulator of focal adhesion turnover [222]. Focal adhesions go through different phases of maturation during cell migration. Initially at the leading edge of migrating cell, integrin engagement is induced upon contact of the lamellipodia with the ECM substrate [223]. These are known as adhesive foci or focal points that contain paxillin. These focal points are nascent focal adhesions, which are not connected to actin stress fibers. These nascent focal adhesions are localized just posterior to the actin network continue to recruit other focal adhesion proteins e.g.  $\alpha$ -actinin, zyxin etc. to grow into mature focal adhesions or focal complexes and establish attachment to actin stress fibers to provide the necessary traction force as the cell extends its protrusion leading to cell migration (figure 1.11.) [215, 218, 224, 225].

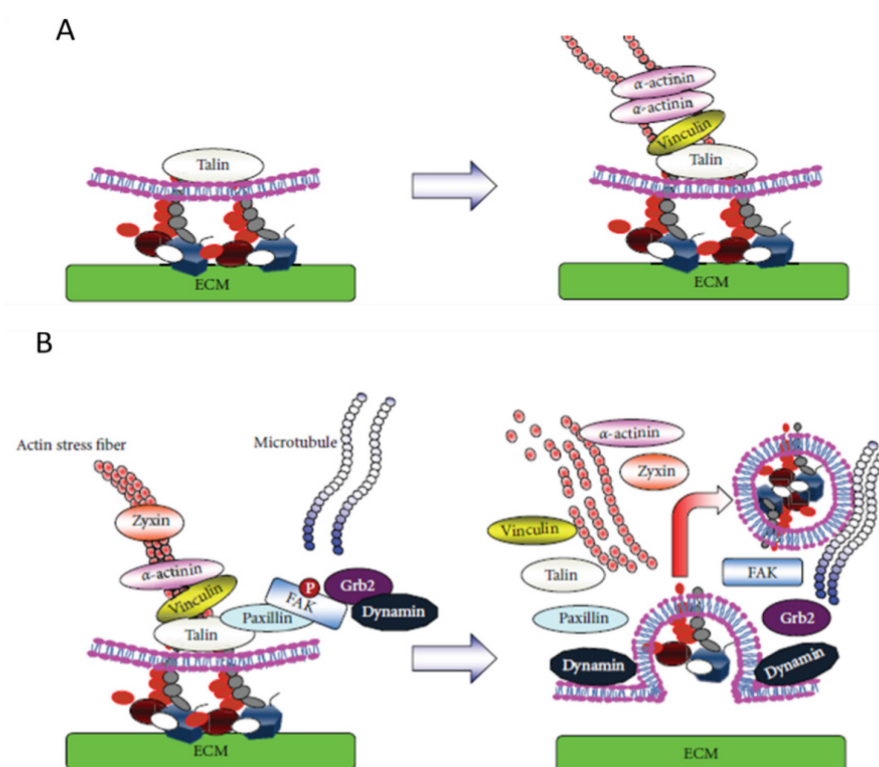


**Figure 1.11. Molecular components associated with formation and turnover for focal adhesion** (reproduced from [215]). A. At the early phase of focal adhesion formation

*integrin clustering is seen. As the focal adhesion mature actin binding proteins such as talin,  $\alpha$ -actinin, and vinculin, are recruited and tethers the focal adhesion to actin filaments. B. During focal adhesion disassembly FAK is phosphorylated at Y397 (shown in red sphere). This lead to recruitment of SH2 homology containing proteins such as Grb2. Subsequently dynamin which is a microtubule associate protein involved in endocytosis is recruited. At this step microtubules can be seen extending to focal adhesion. Grb2 and dynamin complex is believed to cause dissolution of focal adhesion by some yet unidentified mechanism. Integrins are internalized in endosomal vesicles and are transported along the microtubule track to the cytoplasm.*

Paxillin is localized to the focal contacts very early during maturation of focal adhesions. Paxillin is considered as a nascent focal adhesion marker whereas zyxin, which is associated mature focal adhesion, connected with actin stress fibers are considered as a late or mature focal adhesion marker [226, 227].

#### **1.4.2. Focal adhesion kinase**

Focal adhesion kinase (FAK) is a focal adhesion associated non-receptor tyrosine kinase of about 125kDa molecular weight. It was first identified as a protein phosphorylated in response to Src mediated transformation recruitment to focal adhesions through [226]. FAK contains a short N-terminus a FERM (4.1 protein Ezrin Radixin Moesin) domain, a kinase domain, three proline rich motifs, a FAT (focal adhesion targeting) domain which is responsible for targeting it focal adhesion, and a short C-terminal domain (figure 1.12). The FERM domain acts as an auto-inhibitory domain and this inhibition is relieved on interaction with cytoplasmic tail of  $\beta$ 1 integrin [227]. The proline rich motifs have been shown to be important for interaction of FAK and other signaling proteins e.g. p130Cas, paxillin etc. [218, 228]. FAK is well established as a major signaling protein in the focal

adhesion, which could regulate cell proliferation, mechanosensing, turnover of focal adhesions and integrin activity [218, 229, 230].

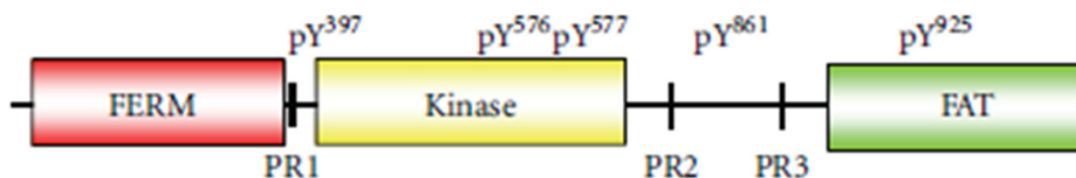


**Figure 1.12. Domain structure of focal adhesion kinase** (Reproduced from [215]).

*FERM* (protein 4.1, ezrin, radixin, and moesin homology), *PR* (proline-rich motif), *FAT* (focal adhesion targeting), *pY* (phosphorylated tyrosine).

FAK contains multiple phosphorylation sites, which are important determinants of cell function (figure 1.12). Phosphorylation of Tyrosine 397 (Y397) results in activation of FAK and this phosphorylation event is induced upon integrin engagement [231]. Further clustering of FAK at focal adhesion enhances Y397 phosphorylation generating a binding site for Src. Src phosphorylates FAK at Y576 and Y577 in the kinase domain leading to the activation of FAK kinase activity [232]. Additional phosphorylation of FAK at Y861 and Y925 by Src creates docking sites for SH2 domain containing proteins such as Grb2, which leads to activation of Ras and MAPK pathway [233, 234]. Interaction of FAK with talin and paxillin is induced upon phosphorylation of FAK at Y861 (reviewed in [235]). Phosphorylation of FAK at Y925 at the FAK domain by Src is known to induce depletion of FAK from focal adhesions [236]. These reports suggest presence of a negative feedback loop, which limits the half-life of a focal adhesion complex. Phosphorylation of FAK at Y397 is known to induce focal adhesion turnover by mechanisms that are currently not understood. During focal adhesion disassembly microtubules extend to the focal adhesion followed by internalization of integrin by endosomes. This coincides with

the recruitment of Grb2 followed by dynamin (reviewed in [215, 218]). Dynamin is a microtubule binding protein and is assumed to mediate transport of endocytic vesicles containing internalized integrin from the disassembled focal adhesion (reviewed in [215]).

### **1.4.3. Paxillin**

Paxillin is one of the important scaffolding proteins at the focal adhesion. Paxillin can be recruited to the early adhesive contacts through its interaction with the cytoplasmic tails of  $\alpha4 \beta1$  integrin and is associated with early steps in the formation of focal adhesions [218, 237, 238]. Phosphorylation of Y31 and Y118 in paxillin by FAK/Src complex promotes interaction between paxillin and Crk, which is important for localization of paxillin at focal adhesion (reviewed in [218]). Y118 phosphorylation of paxillin is also considered as marker for mature focal adhesion complexes as paxillin associated with mature adhesions only exhibit this phosphorylation [239, 240]. Crk can also recruit a complex of proteins including  $\beta$ -PIX, GIT2/PKL to paxillin and this multiprotein complex can lead to activation of small GTPases such as Rac thereby promoting cell migration [241]. Paxillin has five LD motifs which are responsible for its interaction with FAK and PKL, a proline rich motif which enables mediates its interaction with the SH3 domain in Src and four C-terminal LIM domains which are essential for the interaction of paxillin with the phosphatase PTP-PEST. The LIM domains of paxillin are also important for its attachment to the cell membrane (reviewed in [218]).

### **1.4.4. Zyxin**

Zyxin exhibits considerable domain similarity with paxillin and also belongs to the LIM domain containing family of proteins. It has an N-terminal domain, which contains proline rich sequences. These prolin rich sequences are important for its interaction with

SH3 domain containing proteins such as Src. The C-terminus contains the LIM domains which function as scaffolding sites for other focal adhesion proteins and direct the attachment of Zyxin to the cell membrane (reviewed in [242]). Zyxin is a mature focal adhesion marker as it is targeted to focal adhesions during the later phase of focal adhesion assembly when actin stress fibers are attached to the focal adhesion leading to formation of focal complexes which provide traction forces during cell migration [215, 218, 243]. Zyxin is required for the thickening of actin stress fibers associated with focal adhesions as loss of zyxin results in disruption of this process. Zyxin interacts with stretch sensitive proteins such as p130Cas suggesting that zyxin has a role in mechanosensing through focal adhesions [244, 245]. Other reports also suggest that zyxin is required for actin polymerization at the focal adhesion and also regulates actin fiber reorganization [246-248]. The N-terminus of zyxin interacts with other focal adhesion proteins and actin dynamics associated proteins such as  $\alpha$ -actinin and VSAP [248, 249].

### **1.5. Regulation of actin turnover during cell migration**

Cell migration is an important process during embryogenesis, morphogenesis, and wound healing. [250-252]. Deregulation of cell migration is often observed during the process of metastasis (reviewed in [253]). Cell migration is a complicated cellular process which requires stringent regulation of actin dynamics and focal adhesion complexes (reviewed in [221]). During cell migration, cell shape is continuously altered to support formation of different structures such as filopodia, lamellipodia and invadopodia in invasive cancer cells. These morphological changes are accompanied by a drastic remodeling of the actin cytoskeleton [254, 255]. In addition, actomyosin based contractile forces are required to regulate the rate of cell migration and provide the mechanical force required for cell migration [255]. Such dynamic regulation of actin cytoskeleton, polymerization and depolymerization of actin filaments at the leading edge cell during cell migration, and Kumarkrishna Raychaudhuri

modulation of actomyosin based traction forces are regulated by RhoGTPases such as RhoA/B/C, Rac1/2/3 and Cdc42. These small RhoGTPases regulate the activity of a number of actin related proteins, kinases and phosphatases which are involved in actin filament nucleation, actin filament severing function and actin bundling. The activity of these actin regulatory proteins such as WASP, VASP, Arp2/3, Cofilin, Profilin, Myosin II, ROCK, LIMK and PAK (p21 activated kinase) are regulated by a number of activating and inhibitory phosphorylation events (figure 1.13) (reviewed in [254, 256, 257]). These are described in detail in the following sections.

### 1.5.1. Rho GTPases

The Rho family of small GTPases belongs to Ras superfamily of proteins and is known to regulate a variety of cellular functions such as cell motility, cell proliferation, apoptosis (reviewed in [258-260]). They are about 20-30 kDa proteins and contain an effector domain that changes conformation between GTP and GDP bound states. This effector domain is responsible for binding to its downstream targets. There is a hypervariable region and CAAX box in the C-terminus of RhoGTPases which are sites for palmitoylation and farnesylation which are required for the sub-cellular localization of RhoGTPases (reviewed in [257]). Like other GTPases, they act as molecular switches and are active in GTP bound state and inactive in GDP bound state. Transition between these active and inactive states are regulated by GTPases activating protein (GAP) which mediates switch from GTP to GDP bound state and guanine nucleotide exchange factor (GEF) which mediate switch from GDP to GTP bound state [261, 262]. Rho guanine nucleotide dissociation inhibitors (RhoGDIs) can interact with a number of RhoGTPases and can regulate their localization and function by masking the prenyl group in the GTPases and also by inhibiting GTPases from interacting with their effector proteins (reviewed in [263]). GDIs can also target RhoGTPases to specific compartment or to

specific protein complexes in the cell e.g. RhoGDI $\alpha$  is required for targeting Cdc42 to the plasma membrane [263, 264].

The Rho family of GTPases includes Rho, Rac and Cdc42. These Rho GTPases have different and overlapping roles in regulating actin filament organization during cell migration. Rac induces lamellipodia formation and extension, whereas as Cdc42 is involved in filopodia formation [256, 265]. RhoA is associated with formation of stress fibers, regulation of adhesion complex and contractile phenotype (reviewed in [260]). Rac1 and Cdc42 function are mediated by Wiskott-Aldrich Syndrome family of proteins which include WASP, N-WASP and WAVE. They can interact with Rac1 and Cdc42 GTPases through their CRIB (Cdc42-Rac-interactive binding) domains, which are recognized by Cdc42 and Rac1. Both WASP and WAVE proteins are known to drive actin polymerization through Arp2/3 complex (figure 1.13.) (reviewed in [266]).

### **1.5.2. RhoA**

Rho subgroup of RhoGTPases contains three RhoGTPases namely RhoA, RhoB and RhoC. They share about 85% amino acid sequence similarity, however, there is a hypervariable region found at the C-terminal end of these proteins (reviewed in [267]). RhoA is required for reorganization of the actin cytoskeleton and focal adhesion turnover in migrating cells. Their expression and activation has also been associated with multiple types of human cancer such as breast cancer, head and neck cancer, lung cancer, prostate cancer etc. (reviewed in [260]). Recent reports with FRET biosensors suggest that RhoA activation precedes activation of Rac and Cdc42 at the leading edge of migrating cells [268]. RhoA is implicated in stress fiber formation, actin polymerization, actomyosin contractility and membrane ruffling at the leading edge of migrating cells (reviewed in [260]). RhoA has been shown to stimulate membrane ruffling and lamellae formation in

carcinoma cells through  $\alpha 6\beta 4$  integrin signaling [269, 270]. ROCK and mDia are the downstream mediators of RhoA function. ROCK phosphorylates myosin-binding subunit of myosin phosphatases thus inactivating their inhibitory function. ROCK can also directly activate myosin by phosphorylating its light chain and thus positively regulating actomyosin contractility. Activation of ROCK further leads to bundling of actin fibers and integrin clustering at focal adhesions [270]. Activated ROCK can also phosphorylate and activate LIMK, which in turn inhibits cofilin (actin severing protein) leading to stabilization of actin filament [271] (figure 1.13.) (reviewed in [260]).

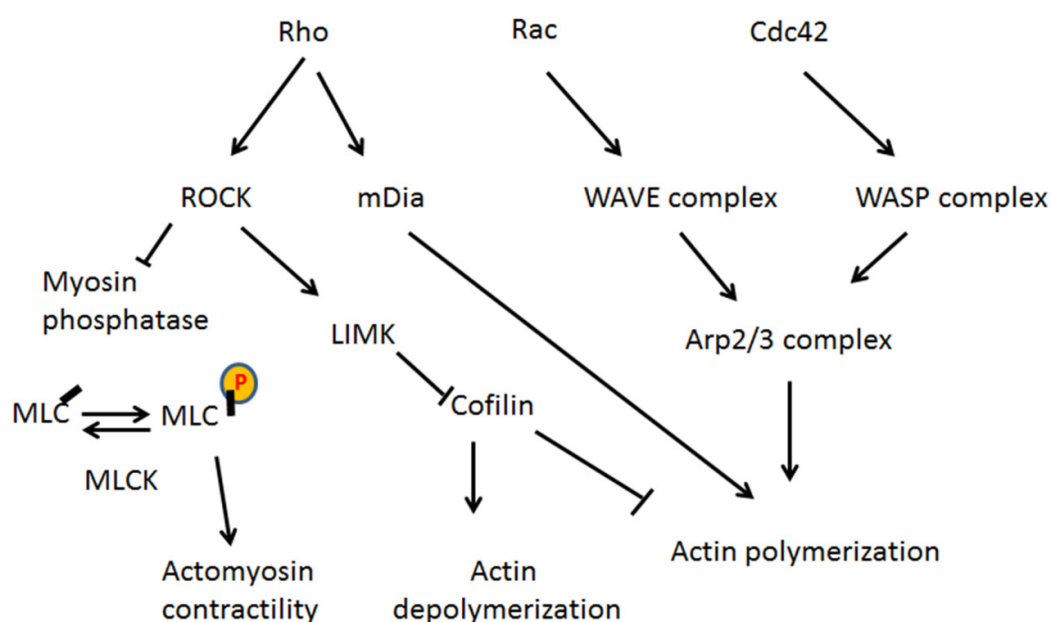


**Figure 1.13. Regulation of actin dynamics by RhoGTPases and its downstream effectors.** See text for details.

### 1.5.3. Cofilin

Cofilin is a small ubiquitous protein of around 19kDa, which can bind to both monomeric and filamentous actin. It functions as an actin severing protein and is regulated by a number of upstream effectors as reviewed in [272]. Cofilin activity can be observed very

early during extension of lamellipodia. Its actin severing activity depolymerizes existing actin filament and generates new barbed ends that can be used by Arp2/3 complex to construct an actin network which leads to extension of lamellipodia. [273, 274]. Recent studies have shown that cofilin induces lamellipodia formation and is important for defining the direction of cell migration [275]. One of the most commonly observed mode of regulation of cofilin function in migratory cells is mediated by LIM kinase proteins. LIMK can phosphorylate cofilin at a Serine (S) residue at position 3 (S3) which inhibits cofilin binding to actin filaments and thus negatively regulates the actin severing function of cofilin [260, 276]. Down regulation of cofilin expression or expression of constitutively active LIMK negatively regulates cell motility [277, 278]. Cofilin promotes *in vivo* invasion by inducing invadopodial membrane recycling and also has been associated with invasion and metastasis in human cancer [279, 280].

### **1.6. 14-3-3 proteins**

14-3-3 proteins are acidic, small (~30 kDa) and ubiquitously expressed proteins present in all eukaryotic cells. Each species has a varying number of isoforms ranging from two in budding yeast to seven in mammals. They are highly conserved group of proteins and share similar tertiary structure, however the N-terminal domain which is required for dimerization and the C-terminal hypervariable region show less sequence homology across different 14-3-3 isoforms [281, 282]. They generally bind to proteins containing one of two motifs [R(S/X)Xp(S/T)XP and RXXXp(S/T)XP (where 'X' denotes 'any amino acid residue' and p(S/T) denotes phosphorylated serine or threonine)] [283, 284]. However a considerable number of ligands for 14-3-3 have been identified which can interact with 14-3-3 proteins in a phosphorylation dependent manner but do not contain a sequence that closely matches with the above mentioned conserved motifs [285].

In mammals seven different 14-3-3 isoforms have been identified 14-3-3 $\beta$ ,  $\gamma$ ,  $\epsilon$ ,  $\eta$ ,  $\sigma$ ,  $\tau$ , and  $\zeta$  [286]. As many as 300 binding partners of 14-3-3 proteins have been identified and current models suggest that 14-3-3 proteins act as adapter proteins by binding to their target motifs thereby, causing allosteric change in proteins shape. Thus they may facilitate or block protein-protein interactions by steric interference [287]. 14-3-3 proteins affect diverse cellular functions such as cell cycle progression, gene expression, signal transduction, programmed cell death, cellular transport and trafficking and are dysregulated in various disease conditions such as cancer [288-293].

### 1.6.1. 14-3-3 protein structure

Crystal structure of 14-3-3 $\tau$  and 14-3-3 $\zeta$  isoforms revealed important information about the mode of functions of 14-3-3 proteins. 14-3-3 proteins function as a homodimer or heterodimer and distinct isoforms also show preferential homodimerization or heterodimerization. E.g. 14-3-3 $\gamma$  forms heterodimer with 14-3-3 $\epsilon$  isoforms whereas, 14-3-3 $\epsilon$  does not form homodimers [294, 295] unlike 14-3-3 $\sigma$ , which preferentially forms homodimers [296, 297] (also reviewed in [298, 299]). Each monomer in the U shaped dimer contains nine  $\alpha$  helices of which four directly participate in dimer formation. 14-3-3 binding to conserved phosphoserine / phosphothreonine containing motifs is mediated by direct interactions of L49 and R56 in helix $\alpha$ C, and R127 and Y128 in helix  $\alpha$ E with phosphate of group of the ligand (figure 1.14.) [300].

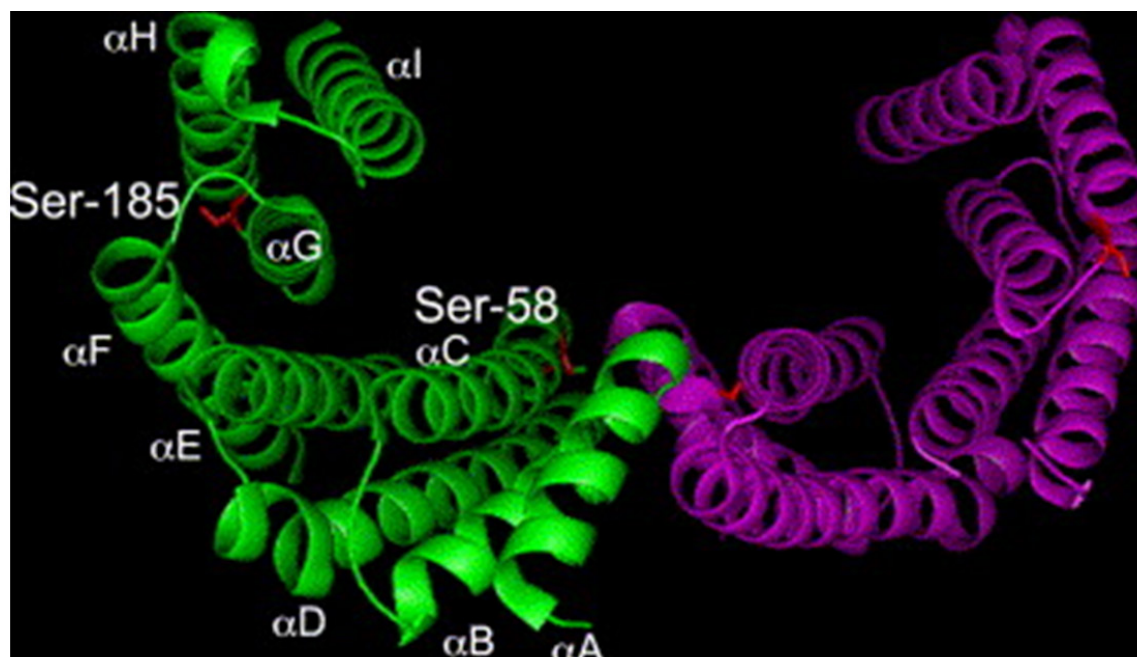


*Figure 1.14. Structure of 14-3-3 dimer (Reproduced from [282]). Each monomer is shown in different color (green and purple). All  $\alpha$  helices are indicated. Ligand binding occurs in the central cavity. S58 and S185 phosphorylation positions have also been indicated. S58 regulates dimerization, whereas, S185 is responsible for ligand binding.*

Multiple post translational modifications e.g. phosphorylation have been reported for multiple 14-3-3 isoforms such as 14-3-3 $\beta$  and 14-3-3 $\zeta$ . Phosphorylation of 14-3-3 proteins can lead to conformational changes which can inhibit dimerization or ligand binding affinity of 14-3-3 proteins. Phosphorylation of Serine 58 (S58) inhibits dimerization in 14-3-3 $\zeta$  and phosphorylation of Serine 185 (S185) is required for ligand binding as demonstrated with 14-3-3 $\zeta$ ,  $\alpha$  and  $\beta$  isoforms (figure 1.14.) [301-303] (also reviewed in [282]). The S185 and T233 sites on 14-3-3 $\zeta$  have been identified as target of proline targeted kinases or other kinases respectively [301]. It was observed that phosphorylation of 14-3-3 $\zeta$  on T233 by casein kinase 1 leads to conformational change which resulted in compromised phosphorylation dependent ligand binding [304].

### **1.6.2. Role of 14-3-3 $\sigma$ in regulating cell - cell adhesion and cancer**

14-3-3 $\sigma$  is also known as stratifin because it was first discovered in human stratified epithelia and is expressed in all epithelial cells [282, 305]. An aberrant expression of 14-3-3 $\sigma$  has perhaps shown the strongest association with cancer progression among the other 14-3-3 isoforms. Initially MALDI-TOF and MS/MS after trypsin digestion showed that 14-3-3 $\sigma$  was lost in breast cancer patient samples whereas, 2D analysis showed that breast epithelial cells expressed 14-3-3 $\sigma$  [306]. Later SAGE analysis revealed that mRNA levels of 14-3-3 $\sigma$  were undetectable in more than 90% of primary breast carcinomas that were tested. High frequency of hypermethylation at the promoter region and CpG islands at the 14-3-3 $\sigma$  gene locus was identified as the prevalent mechanism of down-regulation of 14-3-3 $\sigma$  in breast cancer [307, 308]. 14-3-3 $\sigma$  expression has been found to be down-regulated in multiple other human cancers as well such as oral squamous cell carcinoma, urinary and bladder carcinoma, lung carcinoma, vulva squamous neoplasia, head and neck squamous cell carcinoma, hepatocellular carcinoma etc. [309-315]. Other mechanisms might also exist which could lead to compromised 14-3-3 $\sigma$  expression during cancer progression such as upregulation of E3 ubiquitin ligase which targets 14-3-3 $\sigma$  to ubiquitin mediated degradation. Indeed down-regulation of E3 has reduced tumor burden in vivo [316]. However, there is also a large number of reports which suggest that increased expression of 14-3-3 $\sigma$  can be correlated with multiple human cancer types such as ovarian cancer metastasis, oral squamous cell carcinoma, human scirrhous-type gastric carcinoma cells, endometrial carcinoma etc. [317-320]. Such contradicting reports raise the possibility of variable function of 14-3-3 $\sigma$  at different stages of cancer progression and would require more controlled experiments to delineate the mechanism of 14-3-3 $\sigma$  function during cancer progression.

14-3-3 $\sigma$  was shown to be a p53 responsive gene and is required to enforce the G2/M DNA damage checkpoint in epithelial cell lines. Loss of 14-3-3 $\sigma$  in HCT116 cells resulted in failure of G2/M checkpoint following DNA damage induced by Adriamycin and subsequently cells undergone mitotic catastrophe and cell death. It was observed that 14-3-3 $\sigma$ <sup>-/-</sup> HCT116 cells failed to requester Cdc2/ CyclinB1 complex to the cytoplasm after DNA damage leading to G2/M checkpoint override [321]. DNA damage dependent interaction between 14-3-3 $\sigma$  and p53 has also been observed which may result in stabilization and optimal transcriptional activity of p53. Serine 378 residue in p53 was found to be important for its interaction with 14-3-3 $\sigma$ . Mutant p53 unable to interact with 14-3-3 $\sigma$  had a lower transcriptional activity [322].

There is not much known about role of 14-3-3 $\sigma$  in regulation of cell - cell adhesion. However, few studies have shown that 14-3-3 $\sigma$  in regulation of desmosome and cell polarity. 14-3-3 $\sigma$  loss lead to compromised plakophilin3 exchange with the desmosomal plaque and increases cell migration [323]. In a recent report 14-3-3 $\sigma$  has been shown to stabilize a complex of soluble actin and intermediate filaments which can be used a pool for polarized assembly of cytoskeletal network during cell migration [324]. Ectopic expression of 14-3-3 $\sigma$  in ErbB2 transformed mammary tumor cells resulted in restoration of epithelial polarity whereas, loss of 14-3-3 $\sigma$  expression lead to loss of cell polarity in MCH10A cells [325].

### **1.6.3. Role of 14-3-3 $\gamma$ in regulating cell - cell adhesion and cancer**

Results from our laboratory have shown that loss of 14-3-3 $\gamma$  results in compromised cell - cell adhesion. 14-3-3 $\gamma$  is required for transport of PG to the cell border during desmosome assembly in a KIF5B dependent manner and thus loss of 14-3-3 $\gamma$  leads to abrogation of desmosome function [326]. 14-3-3 $\gamma$  has been shown to form complex with multiple

desmosomal proteins such as PG, PKP3 and DP and might regulate their transport to the cell border [326]. Severe adhesion defects were observed in the testis of mice injected with 14-3-3 $\gamma$  shRNA suggesting its role in regulation of cell - cell adhesion [327]. 14-3-3 $\gamma$  interacts with Cdc25C and is required for maintenance of S phase and G2/M checkpoint upon DNA damage [328, 329]. Unpublished data from our lab also suggest role of 14-3-3 $\gamma$  in regulation of centrosome duplication. Loss of 14-3-3 $\gamma$  resulted in multipolar spindle and multiple centrosome phenotypes resulting in aneuploidy and tumor formation in mice [330]. However, reports also suggest that 14-3-3 $\gamma$  over-expression can promote polyploidy in lung cancer cells and it can also inhibit transcriptional activity of p53 [331, 332].

### **1.7. Role of Kinesin motors and 14-3-3 proteins in transport of cell - cell junction proteins**

Kinesins are molecular motors involved in directed transport of intracellular cargo on MT tracks. Kinesin superfamily proteins (also known as KIF) use ATP as energy source to generate motor force to pull cargo along MT track (reviewed in [333]). Forty five mammalian KIF genes have been identified and alternative splicing leads to the presence of twice as many proteins [334]. There are 15 families in KIF (kinesin 1 to 14B) which can be broadly classified in three groups i.e. N kinesin, M kinesin and C kinesin (they contain the motor domain in N terminal, middle and C terminal region respectively) [334, 335] (also reviewed in [336]). Kinesin family proteins share homology only at the motor domain responsible for ATP binding while other domains show considerable variation however, the position of the motor domain is again variable which has allowed categorisation of kinesin family proteins. Kinesin 1 motor proteins represent the conventional kinesin and are a heterotetrameric structure composed of homodimer of two kinesin heavy chains (120-kDa) and homodimer of two kinesin light chains (KLC) of

about 64 kDa which are responsible for motor activity and cargo binding respectively [335, 337, 338].

There are reports, which have shown accumulation of minus end directed kinesin motor proteins KIFC3 at the AJ. AJ associated protein and Nezha, which interacts with PLEKHA, binds to MT minus end and tethers them to AJ. Depletion of any one of this complex has results to disorganization of AJ [339]. Kinesin driven MT based transport has also been shown to regulate N cadherin dependent cell-cell contact biogenesis [340]. AJ protein p120 catenin forms a complex with kinesin heavy chain with its N- terminal head and vesicles containing p120 catenin has been shown to be transported to the cell membrane along microtubule track [341]. Desmosomal cadherins, desmoglein2 (Dsg2) and desmocollin2 (Dsc2) are transported to the membrane through MT dependent kinesin 1 and kinesin 2 dependent manner respectively [342]. Results from our lab have also shown that KIF5B mediates transport of PG to the cell border during desmosome assembly in a 14-3-3 $\gamma$  dependent manner [326].

14-3-3 proteins have also been found to regulate kinesin motor based cell trafficking. In PC12 cultured cells 14-3-3  $\eta$  has been found to interact with kinesin 1 in vivo by immunoprecipitation studies. KLC2 binds to 14-3-3  $\eta$  in a phosphorylation dependent manner [343]. Other kinesin 1 superfamily proteins like KLC1C and KIF3 has also been reported to interact with 14-3-3 proteins [344, 345]. KLC1 has picked up 14-3-3  $\beta$ ,  $\gamma$ ,  $\epsilon$  and  $\zeta$  isoforms when used as bait in a two-hybrid screen [344, 346].

### **1.8. Epithelial to mesenchymal transition (EMT)**

Epithelial and mesenchymal cells are the two major cell types that constitute most tissue types in multicellular organisms. These two cell types have unique characteristics and are specialized to perform different functions. Epithelial cells are mostly non migratory,

cohesive, show highly polarized distribution of cell - cell junctions and cytoskeletal elements, show apico basal polarity of membrane domains and forms continuous cell layers. On the contrary mesenchymal cells are highly motile, show very loose interaction with neighboring cells and do not form continuous cell layers, do not show any polarized distribution of membrane domain or cytoskeletal elements and junctions (reviewed in [347, 348]). Mesenchymal cells are invasive in nature and secrete a number of ECM degrading enzymes called matrix metallo proteases (MMPs). During development of higher multicellular animals epithelial cells often undergo transition to mesenchymal cells through a process which is stringently regulated by various inducers or growth factors such as TGF $\beta$ , EGF, HGF etc., EMT effectors such as E cadherin,  $\beta$ -catenin etc. and a number of transcriptional regulators such as Snail, Slug, Zeb and Twist family of transcription factors. The process of EMT involves loss of epithelial markers such as E cadherin, PG, keratin filaments etc. and gain of mesenchymal markers such as N cadherin and vimentin. Loss of cell - cell adhesion and cell to ECM adhesion is one of the hallmarks of EMT (reviewed in [349-354]). EMT is a normal biological process but often exhibited by neoplastic cell that has undergone genetic and epigenetic changes. During metastasis cancer cells of epithelial origin often acquire mesenchymal characteristics which enable them to invade through ECM and basement membrane to local blood vessels and lymphatic channels and disseminate to distant target organs (reviewed in [353]). In literature three different types of EMT has been characterized such as type 1, which includes EMT involved in embryo development, reorganization of germ layers, organ development etc.; type 2 EMT is associated with repair events such as wound healing, tissue regeneration and organ fibrosis which mostly follows trauma or inflammatory injury, type 3 EMT is exhibited by neoplastic cells which acquire invasive characteristics and leads metastasis (reviewed in [352]). EMT is not an irreversible

process. Epithelial cells that have undergone an EMT often go through a reverse program called MET to continue their epithelial differentiation path (reviewed in [347, 348]). The general scientific notion about metastasis is cancer cells undergo EMT during the process of metastasis. Indeed several studies indicate presence of EMT like features in clinical samples of human cancer and in in vivo models of EMT.

There are multiple reports which suggest EMT like process during the progression of during multiple human cancers [355, 356] and reviewed in [354]. In another study injection of SCID mice with vimentin negative MDA-MB-468 breast cancer cells resulted in formation of primary tumors with regions of vimentin positivity. These vimentin positive cells also showed enrichment for other mesenchymal markers. In addition circulating tumor cells also showed enrichment of mesenchymal markers. These results suggest that spontaneous EMT events promote invasion and metastasis [357]. However, there are also reports which undermine the importance of EMT in cancer progression such as results from our laboratory have shown that loss of PKP3 leads to lung metastasis in vivo without initiating an EMT like program [17, 358, 359].

### **1.8.1. EMT specific transcription factors and their regulation during EMT**

There are four classic EMT specific transcription factors Snail (SNAI1), Slug (SNAI2), ZEB1 and Twist. These transcription factors generally belong to zinc finger family such as Snail and Slug, zinc finger E box-binding homeobox family such as ZEB1 and basic helix-loop-helix (bHLH) family of transcription factors such as Twist. They are involved in repressing expression of epithelial markers such as E cadherin where both Snail and Slug can bind to E boxes in E cadherin promoter to inhibit its transcription [360, 361]. At the same time EMT specific transcription factors upregulate expression of mesenchymal markers such as N cadherin, vimentin, MMPs, etc. (reviewed in [348]). Stable

transfection of Sail lead to gain of expression in mesenchymal markers such vimentin and fibronectin in MDCK cells [362]. Down-regulation of E cadherin can lead to increase in the cytosolic pool of  $\beta$ -catenin which can shuttle to the nucleus and form complex with LEF-TCF family of transcription factor and initiate EMT through WNT signaling [363]. ZEB1 is also reported repress E cadherin expression by suppressing miRNA200. miR-141 and miR-200c belongs to miRNA200 family and are negative regulators of TGF $\beta$  and ZEB1 [364, 365]. Expression of other cell - cell junction proteins such as ZO-1 and claudin is also regulated by Sail, Slug and ZEB family of proteins [366, 367]. These transcription factors are induced by upstream growth factors or transcription factors and perform overlapping and redundant functions. They also show positive regulation by each other such as Sail and Slug can bind to their own and each other's E2 boxes in the promoter region to positively regulate gene expression [368] Sail and Slug is also known to promote ZEB1 expression [369] (also reviewed in [353]). TGF $\beta$  has been shown to induce expression of Sail, SNI2, ZEB and Twist family of EMT specific transcription factors [348, 370]. Slug plays an important role during the initial phase of growth factor induced EMT where it promotes desmosome dissociation, cell spreading and initiation of cell separation [371]. AP1 transcription factor c-Jun is reported to activate Slug expression [372], c-Jun is known as an oncoprotein whose levels are kept low by different mechanisms of which proteasomal degradation is one of the prevalent mechanism. Fbw7, Itch and Cop1 are three E3 ligases known to target c-Jun to proteasomal degradation [373-375]. More interestingly, loss of Fbw7 has also been shown to initiate EMT like phenotype in HCC cells [376].

Though role of 14-3-3 $\sigma$  has been well established in regulation during cancer progression, there remains a considerable ambiguity in terms of its role in promotion or inhibition of neoplastic progression. Also there is not enough clarity about the role of 14-3-3 $\sigma$  in

regulation of cell - cell adhesion and processes like EMT. In this thesis work we have tried to delineate the role of 14-3-3 $\sigma$  in regulating cell - cell adhesion. During our course of study we observed that loss of 14-3-3 $\sigma$  is just not responsible for loss of cell - cell adhesion but also leads to a type 3 EMT. Role of 14-3-3 $\gamma$  in regulating cell - cell adhesion has been studied in great detail in our laboratory. Here in this study we have tried to extend our present findings to understand the role of 14-3-3 $\gamma$  in transport of desmosomal proteins to the cell border.



## **CHAPTER 2: AIMS AND OBJECTIVES**



**Aims and objectives:**

1. To determine if 14-3-3 $\sigma$  loss leads to deregulation of cell-cell adhesion and to neoplastic transformation.
2. To determine the role of 14-3-3 proteins in regulating transport of plakophilin3 and desmoplakin during desmosome assembly.



## **CHAPTER 3: MATERIALS AND METHODS**



### 3.1. Cell culture and transfections

HCT116 (ATCC), HCT116 derived 14-3-3 $\sigma$ <sup>+/+</sup> and 14-3-3 $\sigma$ <sup>-/-</sup> cells [321], HEK293, and HCT116 derived stable cell lines were cultured in Dulbecco's modified Eagles medium (DMEM) (Gibco) supplemented with 10% Fetal Bovine Serum (Sigma/Gibco), 100U of penicillin (Nicholas Piramal), 100 $\mu$ g/ml of streptomycin (Nicholas Piramal) and 2  $\mu$ g/ml of amphotericin B (Hi Media). HEK293FT cells were maintained in Dulbecco's modified Eagles medium (DMEM) (Gibco) supplemented with 10% Fetal bovine Serum (Sigma/Gibco), 100U of penicillin (Nicholas Piramal), 100 $\mu$ g/ml of streptomycin (Nicholas Piramal) and 2  $\mu$ g/ml of amphotericin B (Hi Media and 5mg/ml G418 (Sigma). Stable clones expressing HA tagged 14-3-3 $\sigma$  namely SP4 and SP4 and the respective vector control (VP1) clones were generated in HCT116 14-3-3 $\sigma$ <sup>-/-</sup> cells and maintained in DMEM medium with 10% FBS containing 1 $\mu$ g/ml of puromycin (Sigma). Stable knockdown clones of Slug (S1 and S2) or c-Jun (J1 and J2) and the corresponding vector control cells (Vec) were generated in HCT116 derived 14-3-3 $\sigma$ <sup>-/-</sup> cells using published shRNA sequences to down regulate Slug and c-Jun expression [377-379] and were maintained in DMEM medium with 10% FBS containing 1 $\mu$ g/ml of puromycin (Sigma).

| Diameter of culture dish | Amount of DNA | Amount PEI  | Amount of DMEM | Total Volume |
|--------------------------|---------------|-------------|----------------|--------------|
| 35mm                     | 3 $\mu$ g     | 18 $\mu$ l  | 182 $\mu$ l    | 200 $\mu$ l  |
| 60mm                     | 5 $\mu$ g     | 30 $\mu$ l  | 470 $\mu$ l    | 500 $\mu$ l  |
| 100mm                    | 20 $\mu$ g    | 120 $\mu$ l | 880 $\mu$ l    | 1000 $\mu$ l |

**Table 3.1. Amount of reagents required for specific tissue culture dishes for transfection using PEI.**

Transfections were performed by either of the following methods; calcium phosphate precipitation method as described in [380] or Lipofectamine LTX (Invitrogen; 15338-100), PEI according to the manufacturer’s protocol (Polysciences Inc.) and Fugene xtremegene HP Transfection Reagent (Roche Applied Science) as per manufactures protocol. The amount of DNA and corresponding reagents for specific culture dish area are tabulated below for calcium phosphate precipitation method of transfection. The reagents are described separately.

| Diameter of culture dish | Amount of DNA | Amount of distilled water (D/W) | Amount of 0.5 M CaCl <sub>2</sub> | Amount of 2X BBS | Total Volume |
|--------------------------|---------------|---------------------------------|-----------------------------------|------------------|--------------|
| 35mm                     | 5 $\mu$ g     | 45 $\mu$ l                      | 50 $\mu$ l                        | 100 $\mu$ l      | 200 $\mu$ l  |
| 60mm                     | 10 $\mu$ g    | 90 $\mu$ l                      | 100 $\mu$ l                       | 200 $\mu$ l      | 400 $\mu$ l  |
| 100mm                    | 25 $\mu$ g    | 225 $\mu$ l                     | 250 $\mu$ l                       | 500 $\mu$ l      | 1000 $\mu$ l |

**Table 3.2. Amount of reagents required for specific tissue culture dishes for calcium phosphate method of transfection.**

Sterile D/W and a working aliquot of Calcium chloride for transfection were stored at 4°C and were used for not more than a month. BES buffered saline (BBS) was stored at -20°C. Calcium chloride and D/W were prewarmed to 37°C about half an hour prior to use, and BBS was thawed at room temperature just before use.

### 3.2. Plasmids

Published shRNA sequences for Slug and c-Jun were used to generate stable knock down clones derived from 14-3-3 $\sigma$ <sup>-/-</sup> cells [377, 378]. These shRNAs for Slug and c-Jun were cloned in pLKO.1 vector previously in the laboratory [379]. shRNAs were cloned in pLKO.1 vector as described in (<http://www.addgene.org/tools/protocols/plko/>). HA 14-3-

3 $\sigma$  was cloned in pCDNA3 puro vector, HA c-Jun WT, HA c-JunS58A and HA c-Jun S267A were generated by site directed mutagenesis and cloned in pCDNA3 vector as described using BamHI and XhoI sites [379].

FBW7 $\alpha$ , c-Jun WT, c-Jun S267A and 14-3-3 $\sigma$  were cloned into a mammalian expression vector expressing an S-protein/Flag/streptavidin binding protein (SBP) triple-epitope tag (SFB) and a Myc-tagged destination vector described previously described in [381] using a Gateway cloning system (Invitrogen). Bacterially expressing glutathione S-transferase (GST)-c-Jun WT, GST-c-Jun S267A, and maltose binding protein (MBP)-FBW7 $\alpha$ , MBP-14-3-3 sigma vectors were generated by transferring their coding sequences into destination vectors previously described in [381] in Dr. Maddika Subba Reddy's laboratory by Neelam Chaudhary.

GFP Paxillin and GFP Zyxin were kind gifts from Dr. Clare Waterman (NIH, USA.) and Dr. Steve Pronovost (University of Utah, USA.) pRL-TK was a kind gift from Dr. Shubha Tole (TIFR, India). FBW7 constructs were a kind gift from Dr. Sagar Sengupta (NII, India) and Dr. Markus Welcker (Fred Hutchinson Cancer Research Centre, USA). DPI GFP and V5 tagged deletion mutants of DP were kind gift from Dr. Terry Lechler (Duke University Medical Centre, Durham.) TOP Flash plasmid used to measure  $\beta$  catenin response promoter activity was a kind gift from Dr. Randall Moon's laboratory (Washington University, USA.), GFP 14-3-3 $\sigma$ , HA 14-3-3 $\sigma$ , GST PKP3, GST PKP3 $\Delta$ ARM, GST PKP3  $\Delta$ NH3, GST 14-3-3 $\gamma$ , GST 14-3-3 $\sigma$ , GST KLC1, GST TPR, GST CC and GST KLC2 were previously described [326, 327, 382, 383].

### 3.3. Generation of stable cell lines

To generate 14-3-3 $\sigma$ <sup>-/-</sup> cells stably expressing 14-3-3 $\sigma$ , 3 $\mu$ g DNA of pCDNA3 puro containing HA 14-3-3 $\sigma$  was transfected in 14-3-3 $\sigma$ <sup>-/-</sup> cells. Forty-eight hour post

transfection cells were grown in presence of 1 $\mu$ g/ml puromycin (Sigma) selection. Two individual clones stably expressing 14-3-3 $\sigma$ , namely SP4 and SP4 were generated through selection in puromycin and screening for expression of 14-3-3 $\sigma$  using 14-3-3 $\sigma$  antibodies. Vector control cells (VP1) were generated by transfecting pCDNA3 puro in 14-3-3 $\sigma$ <sup>-/-</sup> cells followed by selection in puromycin under similar conditions.

Stable knock down clones of Slug (S1 and S2) and c-Jun (J1 and J2) were generated by transducing 14-3-3 $\sigma$ <sup>-/-</sup> cells with viral particles containing pLKO.1 lentiviral vector with desired shRNAs. Twenty-four hours post transduction cells were grown in presence of 1 $\mu$ g/ml puromycin. Individual clones for knockdown of Slug (S1 and S2) and c-Jun (J1 and J2) were generated by selection in puromycin followed by screening for knockdown of Slug and c-Jun respectively. Vector control cells (Vec) were generated by transducing 14-3-3 $\sigma$ <sup>-/-</sup> cells with viral particles containing pLKO.1 lentiviral vector without shRNAs followed by selection in 1 $\mu$ g/ml puromycin containing media under similar conditions.

#### **3.4. Lentivirus production and transduction**

293FT cells were maintained and used as per guidelines lines provided by Invitrogen and were used as virus packaging cell line. These were transformed at a confluency of 60% by calcium phosphate precipitation method as described [380]. pLKO.1 lentiviral vectors were used and were transfected along with pPAX2 and pMD2.G packaging constructs (for 100mm culture dish 6 $\mu$ g +4.5  $\mu$ g+ 1.5  $\mu$ g respectively). Post transfection cells were kept in DMEM supplemented with 10% FBS and antibiotics, without any other supplement or selection. Virus supernatants were collected 60 hours post transfection and were filtered using filters with 0.45 $\mu$  pore size (MDI). Filtered supernatants were collected in screw capped 50ml conical tubes (Tarson) and were kept in 4 $^{\circ}$ C until further use.

HCT 116 derived 14-3-3 $\sigma$ -/- cells were used for transduction. 3000 cells were seeded in 35mm culture dishes and 1ml of filtered supernatants were used for transduction and the final volume of media was made up to 2ml and supplemented with 8 $\mu$ g/ml polybrene in a 35mm culture dish (Sigma). Two similar transductions were performed after removing the previous media from the 35mm culture dish after a 12-hour interval. Forty-eight hours post transduction cells were grown in presence of 1 $\mu$ g/ml puromycin for selecting clones with positive integration for lentivirus.

### **3.5. Immunofluorescence and confocal microscopy:**

To determine the cellular localization of different proteins primary antibodies against the respective endogenous proteins or fluorophore tagged expression constructs were used to detect these proteins in their cellular locale after different fixation and staining procedure. Cells were cultured at the desired confluency (as per experimental requirement) on glass cover slips treated with chromic acid with or without poly L lysine coating. Cells were washed with 1X PBS twice before fixation. Cells were fixed in absolute methanol for 10min at - 20<sup>0</sup>C to detect N cadherin, Vimentin and 14-3-3 $\sigma$  cells. Immunofluorescence with antibodies against PG, DSC2/3, DSG2, HA antibody, PKP3, DP, ZO1, E cadherin,  $\beta$  catenin,  $\alpha$  tubulin and CK8 were used as described previously [16, 17, 159, 326]. Cells were permeabilized using 0.3% triton-X100 in 1X PBS for 10 minutes at room temperature followed by two washes of 1X PBS. Primary antibodies were prepared in 3% BSA in 1X PBS + 0.1% NP-40 solution. The fixed and permeabilized cells were incubated with primary antibodies against either Vimentin (Sigma, dilution 1:500) or N cadherin (BD transduction laboratories, dilution 1:10) overnight at 4<sup>0</sup>C in a humidified chamber on a piece of parafilm. The coverslips were then transferred to a fresh parafilm with the help of beaked forceps. The coverslips were washed with thrice with 1X PBS + 0.1% NP-40 and 1X PBS with the two solutions being used alternately. After completing

the washes the coverslips were incubated with secondary antibodies. The secondary antibodies, either Alexa 568 or Alexa 488 conjugated anti mouse IgG or anti rabbit IgG, (Molecular Probes) were prepared in 3% BSA in 1X PBS + 0.1% NP-40 solution and used at dilution of 1:100. After half an hour incubation cells were transferred to a fresh piece of parafilm followed by four alternate washes of 1X PBS and 1X PBS + 0.1% NP-40. DAPI was used at a concentration of 5 $\mu$ g/ml to stain the nuclei. The coverslips were then mounted on chromic acid treated, clean glass slides using 10-20  $\mu$ l of Vectashield (Vectastain) mounting agent. Images were obtained by using a LSM 510 Meta Carl Zeiss Confocal system with an Argon 488 nm and Helium/Neon 543 nm lasers at 40 X or 63 X magnifications with or without 2X optical zoom.

### **3.6. Calcium Switch and calcium chelation experiments**

To determine the role of microtubule in desmosome disassembly and de novo desmosome assembly, HCT116 cells were grown on poly L-Lysine coated glass coverslips to a confluency of 90 %. EGTA was used at a concentration of 0.4mM to chelate Ca<sup>2+</sup> in the media to promote desmosome disassembly and subsequently cells were washed and fed with normal calcium containing medium to promote desmosome assembly as described in [384]. Cells were fixed and immunofluorescence staining was performed to determine the localization of the different desmosomal proteins.

### **3.7. SDS PAGE and Western blotting:**

EBC lysis buffer or 1X laemmli's buffer or 3X laemmli's buffers were used for making cell lysates as per experimental requirement. These protein samples were resolved on a SDS-PAGE gel and transferred onto a nitrocellulose membrane (Micro devices Inc.) at 55 constant volts for 3 hrs. at 16 °C for proteins with a molecular weight < 100 KD or the transfer was set up at 16<sup>0</sup>C for 60 minutes at 100 constant volts (Biorad transfer

apparatus) for smaller proteins. The membrane was stained with Ponceau stain (Sigma) with subsequent three washes of 1X PBS to destain the membrane. Membranes were blocked with 5% milk prepared in TBS-T for 1 hr. at room temperature followed by three washes of PBS, 3 minutes each to remove excess blocking solution. The membranes were then incubated with primary antibody at 4<sup>0</sup>C, overnight. Membranes were washed thrice with TBS-T for 5 minutes each and then incubated with secondary anti-mouse/ anti rabbit HRP (Pierce) antibody for 1 hour at room temperature.. Membranes were washed thrice with TBS-T for 10 minutes each before incubating with substrate. The blots were developed with PicoWest (Pierce) Western blot chemiluminiscent substrates as per the manufacturer's instructions and the signal captured onto X-ray films (Kodak).

### **3.8. Antibodies for Western blot**

Primary antibodies for PKP3 (clone 23E3-4, Zymed, dilution 1:2000), desmoglein2 (mouse monoclonal, Zymed, dilution 1:500), desmocollin2/3 (mouse monoclonal, Zymed, dilution 1:500), DP-200 (mouse monoclonal, Abexome, dilution 1:1000), plakoglobin (mouse monoclonal, Abcam, dilution 1:500; mouse monoclonal, abexome, dilution 1:1000), Vimentin (Sigma, dilution 1:5000), N cadherin (BD transduction laboratories, dilution 1:100), cytokeratin 8 (Sigma, dilution 1:5000), cytokeratin 18 (Sigma, dilution 1:5000), 14-3-3 $\gamma$  (CG31; abcam ab76525; dilution 1:2500), FAK (cell signaling, dilution 1:1000), FAK pY397 (cell signaling, dilution 1:1000), Paxillin (BD transduction laboratories, dilution 1:1000),  $\alpha$ -actinin (Cell signaling, dilution 1:500), Sail (Santa Cruz, dilution 1:100), Slug (Santa Cruz Biotechnologies, dilution 1:100), ZEB1 (Santa Cruz Biotechnologies, dilution 1:100), c-Jun (Abcam, dilution 1:100), c-Jun pS63 (Cell signaling, dilution 1:1000), Laminin A (Abcam, dilution 1:2000),  $\alpha$  tubulin (Abcam, dilution 1:1500), Flag (Sigma, dilution 1:2000), GST (Sigma, dilution 1:1000), Ubiquitin (Millipore, dilution 1:1000) and anti-Myc clone 9E10 (Santa Cruz

Biotechnology, dilution 1:2000),  $\beta$ -actin (Sigma A5316; dilution 1:5000), 14-3-3 $\sigma$  (hybridoma supernatant CS112; dilution 1:50), HA (12CA5 hybridoma supernatant; dilution 1:50) were used for Western blot experiments. Primary antibodies for ZO1, E cadherin, KIF5B and  $\beta$  catenin were used as described in [159, 326]. The secondary goat anti-mouse HRP (Pierce) and goat anti-rabbit HRP (Pierce) antibodies were used at a dilution of 1:5000 for Western blot analysis.

### 3.9. Reverse transcriptase PCR and Q-PCR

RNA was prepared using RNeasy Plus kit (Qiagen). 2 $\mu$ g of RNA was converted to cDNA using High-Capacity cDNA Reverse Transcription Kit (Applied Biosystems). Reverse transcriptase assays were performed as described in [326]. Quantitative real time PCR (Q-PCR) was performed using SYBR® Green PCR Master Mix (Applied Biosystems) using GAPDH as a control.

| Sl. No. | Oligo        | Sequence               |
|---------|--------------|------------------------|
| 1       | Slug RT5'    | AGACCCCCA TGCCA TTGAAG |
| 2       | Slug RT3'    | GGCCAGCCCAGAAAAAGTTG   |
| 3       | Snail RT5'   | TAGCGAGTGGTTCTTCTGCG   |
| 4       | Snail RT3'   | AGGGCTGCTGGAAGGTAAAC   |
| 5       | Twist 1 RT5' | AGCTGAGCAAGATTCAGACCC  |
| 6       | Twist 1 RT3' | GCAGCTTGCCATCTTGGAGT   |
| 7       | Zeb 1 RT5'   | AGGA TGACCTGCCAACAGAC  |
| 8       | Zeb 1 RT3'   | CTTCAGGCCCCAGGATTTCTT  |

**Table 3.2. Reverse transcriptase and Q-PCR primers for EMT specific transcription factors.**

Fold change was determined by relative quantitation method by determining  $2^{-\Delta\Delta Ct}$  values. The significance was determined using the Student's t-test as described previously [385]. Primers used for both RT PCR and Q-PCR for PKP3, CK8, CK18, and Vimentin and c-Jun are previously described [326, 377, 386]. Primer sequences are listed in the table 3.2 and 3.3.

| Sl. No. | Oligo        | Sequence              |
|---------|--------------|-----------------------|
| 1       | CDH1 RT 5'   | GCAGGTCTCCTCTTGGCTCTG |
| 2       | CDH1 RT 3'   | TGTGCCCACTTTGAATCGG   |
| 3       | DSP I RT 5'  | GCTGATTAATGATTACAG    |
| 4       | DSP I RT 3'  | CACCAGAAGGCTCTCTCTTTC |
| 5       | DSP II RT 5' | AAGGTTGAGGGTTCTACTGC  |
| 6       | DSP II RT 3' | TTGTCTTGCTCCAGGACTT   |
| 7       | DSC2 RT 5'   | GTTTTACTCAGCCCCGTCTTG |
| 8       | DSC2 RT 3'   | GCCCATCTTCTTCTTGTCGT  |
| 9       | DSG2 RT 5'   | TACGCCCTGCTGCTTCTCC   |
| 10      | DSG2 RT 3'   | TCTCCCTCCCGAAGAGCCACG |
| 11      | TJP1 RT 5'   | CAAGAGCACAGCAATGGAGGA |
| 12      | TJP1 RT 3'   | TCCCCACTCTGAAAATGAGGA |
| 13      | CTNNB1 RT 5' | AGTGCTGAAGGTGCTATCTGT |
| 14      | CTNNB1 RT 3' | GAACAAGAGTCCCAAGGAGAC |
| 15      | JUP RT 5'    | CTACGGCAACCAGGAGAGC   |
| 16      | JUP RT 3'    | GGGACACACGGATAGCACCT  |

**Table 3.3. Reverse transcriptase and Q-PCR primers for cell- cell junction proteins.**

### 3.10. GST pull down experiments

#### 3.10.1. Generation of bacterially purified GST proteins

To generate bacterially purified GST tagged proteins, BL21, a protease negative strain of *E.coli* was transformed separately with plasmids expressing GST alone, GST 14-3-3 $\sigma$ , GST-14-3-3 $\gamma$ , GST PKP3, GST PKP3  $\Delta$ ARM, GST PKP3 $\Delta$ NH3, GST- KLC1, GST-TPR and GST-CC. The transformants were used to inoculate a 5ml LB Amp culture in a 50ml conical tube (Tarson). The culture was incubated for 16-18 hours at 37 °C with shaking (200rpm). This culture was subsequently used as a starter culture for 100ml LB Amp broth in 1.5L flask (Tarson) and was incubated for 1 hour as described above. After 1 hour the flasks were kept in cold room (4°C) for 30 minutes and then were induced for protein production with 11 $\mu$ l of 1M IPTG (final concentration 0.1mM) or 44 $\mu$ l of 1M IPTG was added to each flask (to achieve a final concentration of 0.4 mM) for GST tagged PKP3 wild type and deletion constructs. The flasks were then incubated in shaker incubator for 3 hours as described above. After 3 hours the culture was transferred to a 50 ml round bottom tube (HS-50, Laxbro) on ice. The cells were pelleted by centrifugation at 5000 rpm (SS-34 rotor, Sorvall) for 10 minutes at 4°C. The supernatant was discarded and the cell pellets were re-suspended gently in 10 ml of 0.1% Triton X-100 in PBS. These uniform cell suspensions were sonicated (Branson) at 50 duty cycles for 10 seconds and placed on ice for 10 sec. This step was repeated 3 times. The suspension was centrifuged at 5000 rpm for 10 minutes at 4°C. The supernatant was carefully collected in a fresh 15 ml screw cap conical tube (Tarsons) and 150 $\mu$ l of 50% slurry of glutathione sepharose beads (Amersham) was added to each tube. These tubes were placed on a rocker for 1 hour at 4°C. The beads were pelleted down by centrifuging at 3000 rpm (Rotor number 8, Rota 6R-V/Fm PlastoCrafts) for 1 minute at 4°C. The supernatants were

discarded and beads were collected in a fresh 1.5 ml eppendorf tube on ice. The conical tubes were rinsed with ice-cold NET-N buffer to collect the additional beads present there on the surface of the tubes. After collecting all the beads bound to GST or GST conjugated proteins they were given 3 washes with ice cold NET N buffer by repeated centrifugation at 3000 rpm for 1 minute at 4°C and discarding the supernatant after that. Finally the beads were re-suspended in ice-cold NET N buffer in 1.5 ml eppendorf tubes final volume 1ml. These beads were stored at 4°C and were used up to 1-2 weeks period. To check the quality of proteins expressed and immobilized to the beads, 5µl of the slurry of glutathione sepharose beads were mixed with 10 µl of 1X Laemmli's buffer β-mercaptoethanol and bromophenol blue and boiled for 10 minutes in a boiling water bath. The samples were loaded on a 10% SDS-PAGE gel. The gel was stained for 1 hour with coomassie blue followed by destaining using destaining solution containing methanol: acetic acid: water in the ratio 4:1:5.

### **3.10.2. In-vitro GST pulldown**

HCT 116 derived 14-3-3σ<sup>+/+</sup>, HCT 116 derived 14-3-3σ<sup>-/-</sup> cells or HEK293 cells were grown in 100 mm culture dishes. To determine if 14-3-3σ binds to ZEB1 14-3-3σ<sup>-/-</sup> cell lysates from three 100mm culture dishes were made in EBC lysis buffer and incubated with GST or GST14-3-3σ.

To determine in vitro binding GST14-3-3σ and c-Jun wild type (WT) or point mutants (S58A and S267A) HEK293 cells were transfected with HA c-Jun WT, HA c-JunS58A and HA c-JunS267A. Cell lysates from two 100 mm tissue culture dishes were made in EBC lysis buffer and incubated with GST or GST14-3-3σ.

To determine in vitro interaction of 14-3-3σ with FAK and paxillin cell lysates of 14-3-3σ<sup>+/+</sup> cells from one 100 mm culture dish was prepared in EBC lysis buffer and

incubated with GST or GST14-3-3 $\sigma$ . Appropriate antibodies were used to detect interaction of 14-3-3 $\sigma$  with FAK and paxillin.

To determine in vitro interaction of PKP3 or deletion mutants of PKP3 such as PKP3  $\Delta$ ARM and PKP3 $\Delta$ NH<sub>2</sub> with KLC1 and KIF5B or the interaction between 14-3-3 $\gamma$  and PKP3 or deletion mutants of PKP3 such as PKP3  $\Delta$ ARM and PKP3 $\Delta$ NH<sub>2</sub>, cell lysates of HCT116 cells were prepared in EBC lysis buffer and incubated with GST, GST14-3-3 $\gamma$ , GST KLC1, GST PKP3, GST PKP3  $\Delta$ ARM, GST PKP3 $\Delta$ NH<sub>2</sub>, GST TPR and GST CC. Appropriate antibodies were used to detect interactions.

To determine interaction of DP with KLC motor proteins and deletion mutants of KLC1 such as TPR and CC or interaction of DP with 14-3-3 $\gamma$  cell lysates of HCT116 cells were prepared in EBC lysis buffer and incubated with GST, GST14-3-3 $\gamma$ , GST KLC1, GST KLC2, GST TPR and GST CC. Appropriate antibodies were used to detect interactions.

To determine interaction of 14-3-3 $\gamma$  with DP or deletion mutants of DP such as DP 1-1790 and DP 1-1380, HEK293 cells were transfected with DP GFP, DP 1-1790 and DP 1-1380. Cell lysates from four 100 mm tissue culture dishes were made in EBC lysis buffer and incubated with GST or GST14-3-3 $\gamma$ . Appropriate antibodies were used to detect interactions.

To determine interaction of 14-3-3 $\gamma$  and desmosomal proteins in PKP3 knockdown cells, pTU6, S9 and S10 cells were collected from one 100 mm culture dish followed by lysis in EBC lysis buffer. Cell lysates were subjected to protein estimation. Equivalent amount of cell lysates for pTU6, S9 and S10 containing 1mg of protein for pTU6, S9 and S10 were incubated with either GST or GST14-3-3 $\gamma$  for each GST pulldown. Appropriate antibodies were used to detect interactions.

In each of the above experiments cells were first collected in 1 ml PBS per 100mm culture dish in a 15ml conical tube (Tarson). Cells were pelleted down by centrifugation at 2500 rpm (Rotor number 8, Rota 6R-V/Fm PlastoCrafts), 4°C for 2 minutes and using same parameter pellets were washed after resuspending in 3 ml of PBS once. The supernatants were discarded and the final pellets were re-suspended in 500µl ice-cold EBC lysis buffer containing protease inhibitors, per 100mm culture dish on ice and were incubated for 15 minutes. The tubes were centrifuged at 7,000rpm (Rotor number 8, Rota 6R-V/Fm PlastoCrafts) for 20 minutes at 4°C. The supernatant was carefully transferred to a fresh 1.5 ml eppendorf tube on ice. The volume in each of the tubes was made up to 750µl using EBC lysis buffer containing protease inhibitors. 5% of the total cell lysates were taken as whole cell extract (WCE) and appropriate volume of 3X Laemmli's buffer containing β- mercaptoethanol and bromophenol blue was added and the tubes were boiled for 10 min in a boiling water bath. This was stored at -20°C until further use. Equivalent amount of GST or GST fusion proteins were added and incubated at 4°C for overnight binding on a rocker. Beads were then pelleted by centrifugation at 3000 rpm (Rotor number 1, Rota 6R-V/Fm PlastoCrafts) for 1 minute at 4°C. The beads were washed 3 times with NET- N buffer. After the final wash 50 µl of 1X Laemmli's buffer containing β- mercaptoethanol and bromophenol blue was added to the beads and boiled for 5 minutes in a boiling water bath. The samples were then resolved on a 6% and 10% step SDS-PAGE gel and Western blots were performed using the appropriate antibodies.

### **3.11. Immunoprecipitation**

Immunoprecipitation experiments were performed to detect in vivo endogenous interactions of 14-3-3σ with c-Jun. 14-3-3σ<sup>+/+</sup> cells were treated with MG132 (10M) for 6 hours and cell lysates were prepared with EBC lysis buffer. 120µl of 14-3-3σ antibody (hybridoma supernatant CS112) was used to immunoprecipitated 14-3-3σ. Myc antibody

(9E10, mouse monoclonal) was used as isotype control. This was followed by Western blotting with c-Jun and PKP3 antibodies.

To determine in endogenous interaction of 14-3-3 $\sigma$  with FAK and  $\alpha$  actinin cell lysates of 14-3-3 $\sigma$ <sup>+/+</sup> cells were incubated with 120 $\mu$ l of 14-3-3 $\sigma$  antibody (hybridoma supernatant CS112) to immunoprecipitated 14-3-3 $\sigma$ . Myc antibody (9E10, mouse monoclonal) was used as isotype control. This was followed by Western blotting with FAK and  $\alpha$ -actinin antibodies.

To determine in endogenous interaction of FAK with 14-3-3 $\sigma$  cell lysates of 14-3-3 $\sigma$ <sup>+/+</sup> cells were incubated with 4 $\mu$ g of FAK antibody to immunoprecipitated FAK. HA-rabbit antibody (Santa Cruz biotechnology) was used as isotype control. This was followed by Western blotting with 14-3-3 $\sigma$  antibody.

To determine in endogenous interaction of PKP3 with KIF5B cell lysates of 14-3-3 $\sigma$ <sup>+/+</sup> cells were incubated with 5 $\mu$ g of PKP3 antibody to immunoprecipitated PKP3. HA-antibody (12CA5, hybridoma supernatant) was used as isotype control. This was followed by Western blotting with KIF5B antibody.

In each experiment cells were first collected in 1 ml PBS per 100mm culture dish in a 15ml conical tube (Tarson). Cells were pelleted down by centrifugation at 2500 rpm (Rotor number 8, Rota 6R-V/Fm PlastoCrafts), 4°C for 2 minutes and using same parameter pellets were washed after resuspending in 3 ml of PBS once. The supernatants were discarded and the final pellets were re-suspended in 500 $\mu$ l ice-cold EBC lysis buffer containing protease inhibitors, per 100mm culture dish on ice and were incubated for 15 minutes. The tubes were centrifuged at 7,000rpm (Rotor number 8, Rota 6R-V/Fm PlastoCrafts) for 20 minutes at 4°C. The supernatant was carefully transferred to a fresh 1.5 ml eppendorf tube on ice. 5% of the total cell lysates were taken as whole cell extract (WCE) and appropriate volume of 3X Laemmli's buffer containing  $\beta$ - mercaptoethanol

and bromophenol blue was added and the tubes were boiled for 10 min in a boiling water bath. This was stored at -20°C until further use. The remaining lysate was incubated with specific antibody or respective IgG controls. Total of 5µg of PKP3 antibody, 200µl of 12CA5 antibody supernatant, 4µg of FAK antibody was used for each IP. The tubes were rocked for 2 hours at 4°C. The tubes were allowed to rock for another 1 hour after adding 40µl of Protein G Sepharose (GE Healthcare). The Immunocomplexes were washed thrice with NET-N, boiled in 3X sample buffer and resolved on a SDS-PAGE gel. Western blotting was performed with appropriate antibodies to detect different proteins.

### **3.12. In vivo ubiquitination Assays**

Cells were transfected with various combinations of plasmids. At 24 h posttransfection, cells were treated with MG132 (10 M) for 6 h, and whole-cell extracts were prepared by NET-N lysis or denaturing lysis and subjected to immunoprecipitation of the substrate protein. The analysis of ubiquitination was carried out by immunoblotting with substrate antibodies or antiubiquitin antibodies.

### **3.13. In vitro ubiquitination Assays**

The reactions were carried out at 30°C for 15 min in 25 ul of ubiquitylation reaction buffer (40mM Tris-HCl at pH7.6, 2mM dithiothreitol [DTT], 5mM MgCl<sub>2</sub>, 0.1M NaCl, 2mM ATP) containing the following components: 100M ubiquitin, 20nME1 (UBE1), and 100 nM UbcH5b (all from Boston Biochem); bacterially purified MBP-FBW7 alpha and MBP-14-3-3 sigma were added to the reaction mixture. Bacterially purified GST, GST-c-Jun, and GST c-JunS267A bound to glutathione-Sepharose beads (Amersham) were used as substrates in the reaction mixture. After the reaction, beads were washed three times with NETN buffer and boiled with SDS-PAGE loading buffer; ubiquitination of substrates was detected by Western blotting with anti-GST antibody.

### 3.14. Wound healing Assays

To determine if loss of 14-3-3 $\sigma$  leads to an increase in cell migration in vitro, a monolayer wounding assays alternatively also known as scratch wound assays were performed. The 14-3-3 $\sigma$ <sup>+/+</sup> cells and 14-3-3 $\sigma$ <sup>-/-</sup> cells were grown to form uniform confluent uniform monolayers in 35mm culture dishes and were treated with 10  $\mu$ g/ml of mitomycin C (Sigma) for 3 hours, to inhibit proliferation. Post mitomycin C treatment the cells were washed and multiple linear scratch wound was made on the plate with the help of 2 $\mu$ l white tips. The cells were fed with complete medium and time lapse video and images were acquired with an Axiovert 200 M Inverted Carl Zeiss microscope. The stage was maintained at 37 $^{\circ}$ C and 5% CO<sub>2</sub>. Images were taken every 5 minutes for 20 hours using an AxioCam MRm camera with a 10 X phase 1 objective. Migration was measured using Axiovision software. Mean was plotted in the bar graph and non-parametric t test was applied to calculate the p value using Graph pad prism software.

### 3.15. Luciferase Assays

Luciferase assays were performed using TOP Flash reporter system containing multiple TCF binding sites. 14-3-3 $\sigma$ <sup>+/+</sup> and 14-3-3 $\sigma$ <sup>-/-</sup> cells were co-transfected with TOP Flash construct or with pRL-TK (Renilla luciferase) as control. Cells were harvested after 48 h and assayed for luciferase activity using a dual luciferase assay system (Promega) as per manufacturer's instruction. Firefly luciferase and renilla luciferase values were determined using Berthold microplate luminometer. All experiments were performed at least three times. Bar graphs were made and non parametric t test was performed to calculate p value using GraphPad Prism software.

### 3.16. Growth curve assays

To determine if loss of 14-3-3 $\sigma$  leads to alteration in cellular properties such as growth to high density or alteration in growth rate, growth curve assays were performed with 14-3-3 $\sigma^{+/+}$  and 14-3-3 $\sigma^{-/-}$  cells.  $2 \times 10^5$  cells were plated in 35mm dishes and fed every two days during the course of the experiment. At various intervals, the cells were harvested by trypsinization and counted in triplicate using a haemocytometer. Non parametric t test was performed to calculate p value using Microsoft Excel program.

### 3.17. Hanging drop assays

To determine if ectopic expression of 14-3-3 $\sigma$  in 14-3-3 $\sigma^{-/-}$  cells could lead to increase in cell – cell adhesion a hanging drop assays were performed to compare the cell-cell adhesive properties of vector control and the stable clones expressing 14-3-3 $\sigma$  such as SP4 and SP4.  $2 \times 10^4$  cells were suspended in 35 $\mu$ l drops of complete medium from the lid of 60 mm culture dish for 16 h. The dish contained PBS to maintain humidity. After the incubation, the drops were pipetted five times with a 200 $\mu$ l standard tip, fixed with 3% glutaraldehyde. The aliquots were spread on coverslips and was allowed to dry followed by mounting with DPX. Images of five random fields from three independent suspensions were taken with a Axiovert 200 M Inverted Carl Zeiss microscope using an AxioCam MRm camera with a 10 X phase 1 objective. The area of individual cell clusters was determined using the Image J software using free line tool. Corresponding area were tabulated for different sizes of aggregates.

### 3.18. Matrigel invasion assays

Matrigel invasion assays were performed with Boyden chamber inserts from BD Biosciences. Inserts were placed in 24 well plates. Inner side of the chamber was washed

2-3 times with 1X PBS and then once with DMEM without FBS. 100 $\mu$ l of 300 $\mu$ g/ml working solution of matrigel (BD Biosciences) was used to coat the inner surface of the insert and was allowed to dry in the 37°C incubator for 1 hour. Un-polymerised matrigel was removed from the top. 50000 cells were re-suspended in 200 $\mu$ l of DMEM without FBS and was seeded in the insert. 700 $\mu$ l DMEM with FBS was added in lower chamber to act as chemoattractant. 36 hour post incubation at 37°C incubator with 5% CO<sub>2</sub>, inserts were cleaned with cotton swab and fixed in 100% chilled methanol. The inserts were stained with 1% crystal violet and the membranes were cut out and mounted on slides with DPX. Images of 20 random fields were taken with Axiovert 200 M Inverted Carl Zeiss microscope using an AxioCam MRm camera with a 10 X phase 1 objective. Experiments were performed in triplicate. Number of cells, which invaded through the matrigel, was counted. Mean was plotted in the bar graph and non-parametric t test was applied to calculate the p value using Graph pad prism software.

### **3.19. Soft agar assays**

HCT116 14-3-3 $\sigma$ <sup>+/+</sup> and 14-3-3 $\sigma$ <sup>-/-</sup> cells were trypsinised and 2.500 cells were counted, The lower base was made of 0.8% agarose (Sigma tissue culture grade) in DMEM with 10% FBS, which was poured and solidified prior to pouring the upper base containing 0.4% agarose mixed with single suspension of cells in DMEM with 10% FBS. These plates were supplemented with 200ul of DMEM with 10% FBS. Three plates were seeded for each cell lines. After about 3 weeks numbers of colonies were counted in 20 random fields for each plate and the average was taken. The plates were stained with 0.1% crystal violet (Sigma) and distained using 2 PBS (1X) washes. Images of colonies were taken on 10X under Carl Ziess inverted microscope. Images of full plate were taken with regular digital camera. The experiments were performed in triplicate. Standard deviation was

plotted in the bar graph and non-parametric t test was applied to calculate the p value using Graph pad prism software.

### **3.20. Tumor formation in Nude mice**

To determine if loss of 14-3-3 $\sigma$  leads to neoplastic progression in vivo,  $1 \times 10^6$  cells of the HCT116 derived 14-3-3 $\sigma^{+/+}$  and 14-3-3 $\sigma^{-/-}$  cells were counted and re-suspended in DMEM media without serum and injected subcutaneously in the dorsal flank of 6-8 weeks old Nude mice (obtained from ACTREC animal house facility). Tumor formation was monitored at intervals of 2-3 days for 5-6 weeks and tumor size was measured by a Vernier calipers. Tumor volume ( $\text{mm}^3$ ) was calculated with the formula  $\frac{1}{2} LV^2$  where L is the largest dimension and V its perpendicular dimension. The tumor bearing animals were sacrificed after 6 weeks. Sections of tumor, liver, lungs, kidney, and spleen were prepared for Haematoxylin and eosin staining to determine if these organs contained metastatic colonies.

### **3.21. Fluorescence Recovery After Photo-bleaching (FRAP) assay**

FRAP assays were performed to determine if loss of 14-3-3 $\sigma$  loss leads to an alteration in the turnover of focal adhesions. GFP tagged Zyxin was used to monitor the turnover of mature focal adhesions as described [243]. 35mm glass bottom culture dishes were with 10mg/ml Matrigel solution (BD Bioscience) as described in [387]. 14-3-3 $\sigma^{+/+}$  and 14-3-3 $\sigma^{-/-}$  cells were sparsely seeded in these plates. Twenty-four hour post seeding 0.5 $\mu\text{g}$  of GFP Zyxin was used for transfection with Lipofectamine LTX (Invitrogen) as per manufacturer's protocol. Twenty-four hour post transfection FRAP was performed using 3i Spinning Disc Imaging System with Slidebook 6 imaging software. Approximately 10 pre-bleach images were taken followed by photo-bleaching with a 488nm argon laser at 100% power for 10seconds. Fluorescence recovery was recorded by acquiring images at regular intervals of 5ms for a period of 3mins. Fluorescence intensity values were

normalized against an unbleached region to obtain photo bleach corrected normalized fluorescence intensity values. All calculations for the above mentioned values were performed using Slidebook 6 imaging software. Corrected intensities were plotted against time using GraphPad to compare the fluorescence recovery rates in 14-3-3 $\sigma$  +/+ and 14-3-3 $\sigma$  -/- cells (n=15). The half-life and mobile fraction values for the protein in both the cell lines were obtained after curve fitting using GraphPad by nonlinear regression analysis. Total fluorescence or whole cell GFP intensities of each cell was also calculated using Slidebook6 and were plotted using GraphPad to compare expression level of our construct in 14-3-3 $\sigma$  +/+ and 14-3-3 $\sigma$  -/- cells.as described in [387]. Statistical analysis was done using GraphPad Prism software.

### 3.22. Nuclear cytoplasmic fractionation assay

14-3-3 $\sigma$ +/+ cells were transfected with plasmids expressing either HA c-Jun WT, HA c-JunS58A and HA c-JunS267A or the vector control. Forty-eight hour post transfection cells were harvested by trypsinization and nuclear and cytoplasmic fractions were prepared as per the manufacturer’s instructions using the NE-PER kit from Promega. Protein lysates were separated on an SDS-PAGE gel.  $\alpha$ -tubulin and lamin A antibodies were used as controls for cytoplasmic and nuclear fractions respectively.

### 3.23. Reagents:

#### 3.23.1. Calcium Phosphate transfection

##### 2X BBS (BES buffered solution), pH 6.95

| Component   | Final concentration | Amount  |
|---|---------------------|---------|
| BES   | 50mM                | 1.066g  |
| NaCl  | 250mM               | 1.636g  |
| Na <sub>2</sub> HPO <sub>4</sub> .2H <sub>2</sub> O | 1.5mM               | 0.0267g |
| D/W   |                     | 100ml   |

pH adjusted to exact 6.95 with 5N NaOH. Filtered using 0.22  $\mu\text{m}$  membrane and stored at  $-20^{\circ}\text{C}$ .

**0.5 M  $\text{CaCl}_2$ :** 18.375g of  $\text{CaCl}_2$  was dissolved in 250 ml of D/W. Filter sterilized in a sterile conical 50 ml tube and stored at  $-20^{\circ}\text{C}$ . In use vial was stored at  $4^{\circ}\text{C}$ .

### 3.23.2. SDS PAGE and Western Blotting

#### 10X running buffer (10X Electrode buffer)

| Component         | Final concentration | Volume |
|-------------------|---------------------|--------|
| Tris base (Sigma) | 250mM               | 30g    |
| Glycine (Sigma)   | 2.5M                | 187.7g |
| SDS               | 10%                 | 10g    |

Dissolve in 750ml of distilled water. Make up the volume to 1000ml with distilled water.

#### Transfer buffer

| Component         | Final amount |
|-------------------|--------------|
| Tris base (Sigma) | 12.1g        |
| Glycine (Sigma)   | 57.6g        |
| 10%SDS            | 4ml          |
| Methanol          | 800ml        |

Make up volume to 4L with distilled water and store at  $4^{\circ}\text{C}$ . It can be reused thrice.

#### TBS-T (Tris buffered saline with Tween-20)

| Component     | Final concentration | Volume |
|---------------|---------------------|--------|
| 1M Tris pH8.0 | 10mM                | 10ml   |
| 2.5M NaCl     | 150mM               | 60ml   |

Make up the volume to 1000ml with distilled water.

### 30% Acrylamide

Dissolve 29.2g of acrylamide (Sigma) and 0.8g of Bis-acrylamide (Sigma) in 100ml of D/W. Ascertain that the pH of the solution is less than 7.0. Filter and store in a dark bottle at room temperature.

### Coomassie Blue stain

Dissolve 50mg of R250 Brilliant Blue in 100 ml of destainer. Stored in a dark bottle.

### Destainer/Fixative

| Component           | Volume |
|---------------------|--------|
| Methanol            | 100ml  |
| Acetic acid glacial | 500ml  |
| D/W                 | 500ml  |

### 3.23.3. In vitro pull down experiments

#### EBC lysis buffer

| Component                 | Final concentration | Volume |
|---------------------------|---------------------|--------|
| 1M Tris pH8.0             | 50mM                | 50ml   |
| 2.5M NaCl                 | 125mM               | 50ml   |
| NP-40 (or Igepal) (Sigma) | 0.5%                | 5ml    |

Make up volume to 1L with distilled water. Store at 40C. Before use add the following protease inhibitors.

#### Protease Inhibitors (per 10 ml EBC lysis buffer)

| Inhibitor | Final concentration | Volume      |
|-----------|---------------------|-------------|
| Leupeptin | 10 $\mu$ g/ml       | 100 $\mu$ l |

|                       |               |             |
|-----------------------|---------------|-------------|
| 2mg/ml Aprotinin      | 20 $\mu$ g/ml | 100 $\mu$ l |
| 500mM PMSF            | 1mM           | 20 $\mu$ l  |
| 1M NaF                | 50mM          | 500 $\mu$ l |
| 0.2M Na orthovanadate | 1mM           | 50 $\mu$ l  |
| 0.5M EDTA             | 1mM           | 20 $\mu$ l  |
| 10mg/ml pepstatin     | 10 $\mu$ g/ml | 10 $\mu$ l  |

**NET-N**

| Component                | Final concentration | Volume |
|--------------------------|---------------------|--------|
| 1M Tris pH8.0            | 20mM                | 20ml   |
| 2.5M NaCl                | 100mM               | 40ml   |
| 0.5M EDTA pH 8.0         | 1mM                 | 2ml    |
| NP-40 (or Igpal) (Sigma) | 0.5%                | 5ml    |

Make up volume to 1L with distilled water. Store at 40C. Use 360ml of 2.5M NaCl to prepare NET-N 900mM.

**1X Laemmli's buffer**

| Component                | Final concentration |
|--------------------------|---------------------|
| 1M Tris pH 6.8           | 50m                 |
| Glycerol (SD fine)       | 10%                 |
| 10% SDS                  | 2%                  |
| Bromophenol blue (Sigma) | 0.1%                |

Make up the volume to 95ml with distilled water. Before use, add 50 $\mu$ l of  $\beta$ -mercaptoethanol to 950 $\mu$ l of 1X buffer.

### 3X Laemmli's buffer

| Component                | Final concentration | Volume |
|--------------------------|---------------------|--------|
| 1M Tris pH 6.8           | 150mM               | 15ml   |
| Glycerol (SD fine)       | 30%                 | 30ml   |
| SDS                      | 6%                  | 6g     |
| Bromophenol blue (Sigma) | 0.3%                | 0.3g   |

Make up the volume to 85ml with distilled water. Before use, add 150 $\mu$ l of  $\beta$ -mercaptoethanol to 850 $\mu$ l of 1X buffer.

### 3.23.4. Immunofluorescence

#### 1X PBS

| Component                        | Amount |
|----------------------------------|--------|
| NaCl                             | 8g     |
| KH <sub>2</sub> PO <sub>4</sub>  | 0.2g   |
| Na <sub>2</sub> HPO <sub>4</sub> | 2.18g  |
| KCl                              | 0.2g   |
| D/W                              | 1000ml |

#### 4% paraformaldehyde in PBS

Dissolve 4gm of paraformaldehyde (Sigma) in 90ml PBS by heating at 70 $^{\circ}$ C in a water bath. Make up the volume to 100ml with PBS. Filter through a filter paper and store at 4 $^{\circ}$ C.

#### 0.3% Triton X-100 in PBS

Dissolve 0.3ml of Triton X-100 (Sigma) in 100ml of PBS and filter through a filter paper.

### 3.23.5. Soft Agar assay

#### 0.1% crystal violet solution

Dissolve 10mg of crystal violet in 90ml of water and make up the volume to 100ml.

### 3.23.6. Protein Estimation

#### CTC Solution

##### a) 20 % Sodium Carbonate

Dissolve 20g Sodium Carbonate in 50ml distilled water and make final volume to 100ml.

##### b) 0.2 % Copper Sulphate

Dissolve 0.2g Copper Sulphate in 40ml distilled water.

##### c) 0.4 % Potassium Tartarate

Dissolve 0.4g Potassium Tartarate in 40ml distilled water.

Mix solution 'b' and 'c' by constant stirring and filter the resulting solution. Then add this mixture in solution 'a' by constant stirring and filter the resulting solution. Store it in a dark bottle. Do not use for more than two months.

#### 10 % sodium Dodecyl Sulphate

Dissolve 10g SDS in 50mL distilled water and make volume to 100mn

#### 0.8 N Sodium hydroxide

Dissolve 3.2g Sodium hydroxide in 50mL distilled water and make volume to 100ML.

#### Folin Solution A

Mix equal volumes of CTC solution, 0.8N NaOH, 10% SDS and distilled water (In the ratio 1:1:1:1).

#### Folin Solution B

Dilute the commercially available Folin-Ciocalteau reagent 1:5 using D/W before using.



## **CHAPTER 4: RESULTS**



**4.1: To determine if 14-3-3 $\sigma$  loss leads to deregulation of cell-cell adhesion and to neoplastic transformation.**



Previous results from our laboratory have shown that loss of 14-3-3 $\gamma$  leads to defects in cell border localization of PG. This also leads to loss of other desmosomal proteins such as DSC2/3, DSG2, PKP2, DP and PKP3 from the cell border. However, expression of PG was not altered on loss of 14-3-3 $\gamma$  at protein as well as in mRNA level. We have observed that loss of 14-3-3 $\sigma$  leads to different observations altogether. Loss of 14-3-3 $\sigma$  leads to decrease in expression of PG at protein level with no appreciable difference in localization of PG [326]. This suggests that the regulation of cell – cell junction proteins by 14-3-3 $\gamma$  and 14-3-3 $\sigma$  are different. Therefore, we wished to determine the consequence of loss of 14-3-3 $\sigma$  in terms of cell – cell adhesion.

#### **4.1.1. Loss of 14-3-3 $\sigma$ leads to alterations in expression of multiple cell-cell junction proteins and cytoskeleton proteins**

14-3-3 $\sigma$   $-/-$  cells show a decrease in the levels of PG (JCS paper) as compared to 14-3-3 $\sigma$   $+/+$  cells. To determine if the levels of other cell-cell adhesion proteins were altered upon loss of 14-3-3 $\sigma$ , Western blots were performed to determine whether the levels of these proteins were altered in 14-3-3 $\sigma$   $-/-$  cells. It was observed that the expression of desmosomal proteins such as PG, PKP3, DPI and DPII, DSG2, DSC2/3, was decreased upon loss of 14-3-3 $\sigma$ . Expression of AJ proteins such as E cadherin and  $\beta$  catenin was also decreased on loss of 14-3-3 $\sigma$  (Fig 4.1.1.A). However, no appreciable change in expression was observed for TJ protein ZO1 (Fig 4.1.1.A). Apart from cell-cell junction proteins, we observed that expression of intermediate filament protein keratin 8 (K8) and keratin 18 (K18) was decreased in 14-3-3 $\sigma$   $-/-$  cells in comparison to 14-3-3 $\sigma$   $+/+$  cells. However, an increase in the expression of the AJ protein N cadherin and the intermediate filament protein vimentin was observed in 14-3-3 $\sigma$   $-/-$  cells as compared to the levels in 14-3-3 $\sigma$   $+/+$  cells (Fig 4.1.1.A).

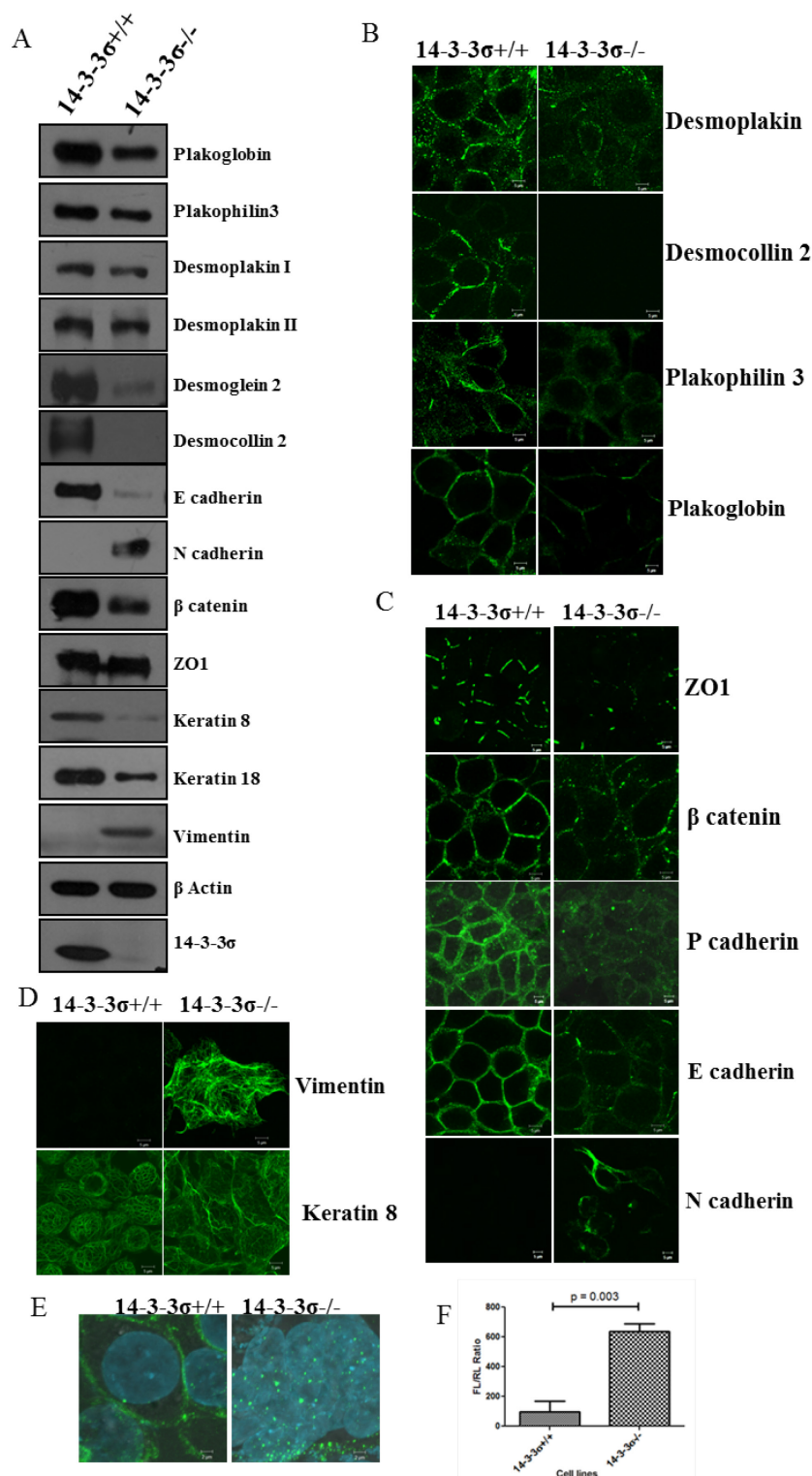


**Figure 4.1.1.** Loss of 14-3-3 $\sigma$  leads to alterations in expression of multiple cell-cell junction proteins and cytoskeleton proteins. A. Protein extracts from 14-3-3 $\sigma$ <sup>-/-</sup> cells and 14-3-3 $\sigma$ <sup>+/+</sup> cells were resolved in SDS page and Western blotting was performed with indicated antibodies.  $\beta$  actin served as loading control. B-D. 14-3-3 $\sigma$ <sup>-/-</sup> and 14-3-

*3σ<sup>+/+</sup> cells were fixed and stained with the indicated antibodies followed by confocal microscopy for desmosomal proteins (B), AJ proteins (B) and intermediate filament proteins (D) Magnification is X63 with 2X optical zoom and bars indicate 5μm. E. 14-3-3σ<sup>+/+</sup> and 14-3-3σ<sup>-/-</sup> cells were stained with antibodies against β catenin, nuclei were stained with DAPI. Magnification is X63 with 4X optical zoom and bars indicate 5μm F. Luciferase assay for β catenin responsive gene promoter. Mean and standard deviation of Firefly luciferase (FL) [is a measure of activity of promoters for β catenin responsive genes] normalized to Renilla luciferase readings (RL) were plotted on the Y axis.*

To determine if localization of various junctional proteins in 14-3-3σ<sup>-/-</sup> cells was also affected we performed immunofluorescence studies. Immunofluorescence results suggest that loss of 14-3-3σ lead to decrease in expression of desmosomal proteins such as DP, DSC2/3, PKP3 and PG; TJ and AJ proteins such as ZO1, β-catenin, E cadherin and P cadherin but there was no significant difference observed in the localization of these proteins (Fig 4.1.1.B and C), in contrast to the results we have previously obtained on loss of 14-3-3γ (JCS paper). However, an immunofluorescence analysis for β-catenin in 14-3-3σ<sup>+/+</sup> and 14-3-3σ<sup>-/-</sup> cells showed that there was increased accumulation of β catenin in the nucleus on loss of 14-3-3σ (Fig.4.1.1.E). As an increase in nuclear β-catenin levels leads to an increase in the expression of β-catenin responsive genes, luciferase reporter assays were performed in these cells to determine if the nuclear β-catenin was transcriptionally active. The luciferase based reporter assays suggest that there were increased promoter activity for β catenin responsive promoter (Fig. 4.1.1.F). Intermediate filament protein keratin 8 networks were abrogated on loss of 14-3-3σ as observed in immunofluorescence results (Fig 4.1.1.D). Quite interestingly we observed that expression intermediate filament protein vimentin and N cadherin in 14-3-3σ<sup>-/-</sup> cells whereas expression of these proteins were almost undetectable in 14-3-3σ<sup>+/+</sup> cells in

Western blot and immunofluorescence assays. Previous results from our laboratory also suggest that vimentin expression is not detectable by Western blot analysis in 14-3-3 $\sigma$ <sup>+/+</sup> cells [16]. This suggests that loss of 14-3-3 $\sigma$  promotes expression of mesenchymal intermediate filament. Such switch in expression from epithelial markers to mesenchymal markers is often encountered during an epithelial to mesenchymal transition (EMT) [348].

#### **4.1.2. Alteration in expression of cell-cell junction and cytoskeleton proteins was due to decrease in mRNA levels.**

To determine if the change in expression at protein levels of junctional and cytoskeletal proteins observed in 14-3-3 $\sigma$ <sup>-/-</sup> cells in comparison to 14-3-3 $\sigma$ <sup>+/+</sup> cells was due to change in gene expression we performed reverse transcriptase PCR (RT-PCR) assays to analyze the expression of mRNA of genes encoding various cell-cell junction proteins and cytoskeletal proteins. RT-PCR assays showed a decrease in mRNA levels of genes encoding desmosomal proteins such as PG, PKP3, DSG2 and DSC2. However there was no appreciable difference in mRNA expression of DPI/II (Fig. 4.1.2.A).

Expression of mRNA level of gene encoding of adherens junction protein E cadherin was also decreased upon loss of 14-3-3 $\sigma$ , whereas no significant difference was observed in mRNA expression of genes encoding other adherens junction proteins such as  $\beta$  catenin and P cadherin in 14-3-3 $\sigma$ <sup>+/+</sup> and 14-3-3 $\sigma$ <sup>-/-</sup> cells (Fig. 4.1.2.A). Expression of gene encoding tight junction proteins, ZO1 was also decreased at mRNA level on loss of 14-3-3 $\sigma$ . No difference was observed in mRNA expression of intermediate filament proteins such as K8 and K18, whereas vimentin mRNA expression was increased on loss of 14-3-3 $\sigma$  (Fig. 4.1.2.A). There were no change in mRNA expression of other 14-3-3 isoforms among 14-3-3 $\sigma$ <sup>-/-</sup> cells and 14-3-3 $\sigma$ <sup>+/+</sup> cells suggesting that the change in expression of various cell-cell junction proteins and cytoskeletal proteins observed in 14-3-3 $\sigma$ <sup>-/-</sup> cells

was specific for loss of 14-3-3 $\sigma$  (Fig 4.1.2.B). Expression of mRNA of GAPDH was assayed as loading control.

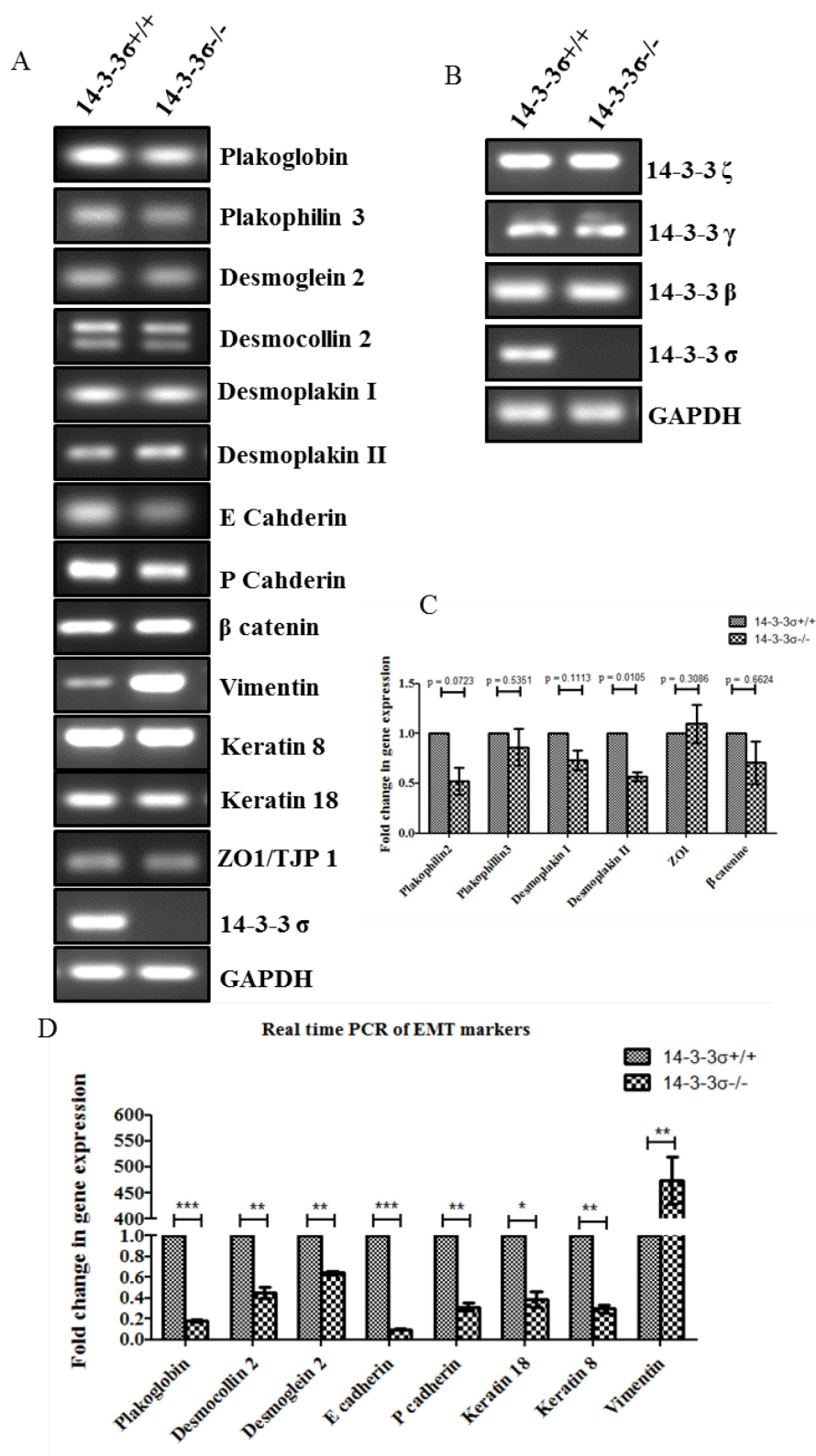


**Figure 4.1.2. Loss of 14-3-3 $\sigma$  leads to alterations in expression of multiple cell-cell junction proteins and cytoskeleton proteins at mRNA level.** A-B. Total mRNA was isolated from 14-3-3 $\sigma$ <sup>+/+</sup> cells and 14-3-3 $\sigma$ <sup>-/-</sup> cells. cDNA was synthesized and reverse-transcriptase PCR was performed with equal amount of cDNA using primers for indicated genes. GAPDH was used as loading control. Representative images of three independent experiments are shown. C. Quantitative PCR was performed using cDNA synthesized from total mRNA isolated from 14-3-3 $\sigma$ <sup>+/+</sup> cells and 14-3-3 $\sigma$ <sup>-/-</sup> cells.  $\Delta\Delta Ct$  values were calculated and normalized against GAPDH. Fold change in gene expression are plotted on Y axis for indicated genes as shown in X axis. p values were calculated using non parametric t test (\*\*\*) indicates p value > 0.001, \*\* indicates p value > 0.001 and \* indicates p value > 0.01).

To have a better quantitative measure of the change in expression of mRNA levels of the above mentioned cell-cell junction proteins and cytoskeletal proteins we performed quantitative PCR (Q-PCR). PKP2, PKP3, DPI, ZO1 and  $\beta$  catenin did not show significant difference in their mRNA expression in 14-3-3 $\sigma$ <sup>+/+</sup> and 14-3-3 $\sigma$ <sup>-/-</sup> cells; however, DPII showed significant decrease in expression of mRNA in the same assays (Fig. 4.1.2.C). We observed significant decrease at mRNA levels in expression of PG, DSC2, DSG2, E cadherin, P cadherin, K8 and K18 in 14-3-3 $\sigma$ <sup>-/-</sup> cells in comparison to 14-3-3 $\sigma$ <sup>+/+</sup> cells as indicated by the p values above the respective bars (Fig 4.1.2.D). In support of our RT PCR data and Western blot data we also observed that mRNA expression of vimentin was statistically increased on loss of 14-3-3 $\sigma$  (Fig 4.1.2.D). Results from RT-PCR and Q-PCR corroborated our Western blot data and immunofluorescence data suggesting global change observed in expression of proteins levels for various cell-cell junction proteins and cytoskeletal proteins was due to decrease in gene expression.

#### 4.1.3. 14-3-3 $\sigma$ knockout cells show EMT like phenotypic characteristics.

The results shown above suggest initiation of a possible epithelial to mesenchymal transition (EMT) program on loss of 14-3-3 $\sigma$  as indicated by increase in expression of mesenchymal markers such as N cadherin and Vimentin and decrease in expression of epithelial markers such as E cadherin, PG, and PKP3. However, EMT involves various phenotypic changes as well such as loss of cell-cell adhesion, loss of cell to ECM adhesion, increase in cell migration and increase in invasion potential (reviewed in [348]). To determine if loss of 14-3-3 $\sigma$  leads to acquisition of phenotypic characteristics associated with EMT a number of functional assays were performed.

To determine if there is loss of cell-cell adhesion on loss of 14-3-3 $\sigma$  disperse assays were performed. Disperse is a protease, which cleaves ectodomains of cell-cell junction transmembrane proteins, and thus when cell monolayers are subjected to mechanical shaking, an increase in the presence of aggregates suggests a decrease in cell-cell adhesion. Number of cell aggregates was significantly more in 14-3-3 $\sigma$ <sup>-/-</sup> cells as compared to 14-3-3 $\sigma$ <sup>+/+</sup> cells suggesting compromised cell-cell adhesion on loss of 14-3-3 $\sigma$  [388] (Fig. 4.1.3.A and B). EMT is also associated with increased production of ECM degrading enzymes (discussed in detail in the introduction chapter). To investigate if 14-3-3 $\sigma$ <sup>-/-</sup> cells also show increased production of MMPs casein zymography was performed. Data suggested an increased production of MMP3 in 14-3-3 $\sigma$ <sup>-/-</sup> cells as compared to 14-3-3 $\sigma$ <sup>+/+</sup> cells (Fig. 4.1.3.C). Therefore, Boyden chamber invasion assays were performed to investigate if loss of 14-3-3 $\sigma$  leads to increased invasion through matrigel in vitro. 14-3-3 $\sigma$ <sup>-/-</sup> cells were significantly more invasive through matrigel coated transwell membranes as compared to 14-3-3 $\sigma$ <sup>+/+</sup> cells (Fig 4.1.3.G and H).

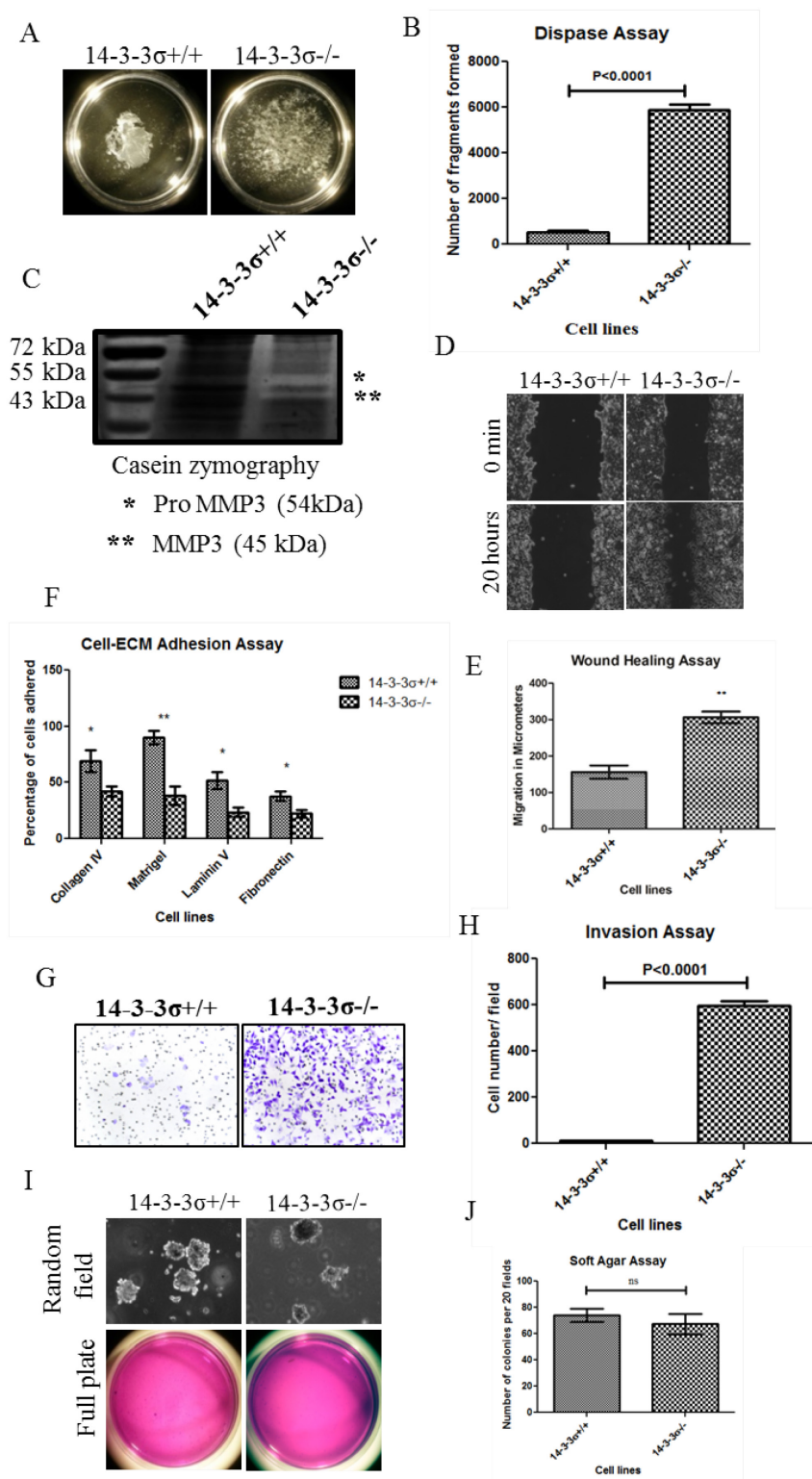


**Figure 4.1.3.** 14-3-3 $\sigma$  knockout cells show EMT like phenotypic characteristics. A-B. Representative images of dispase assays. Number of cell aggregates were measured using Image J particle counting option and are plotted on Y axis. Significance value was

calculated using non parametric t test (Reproduced from [388]). C. 14-3-3 $\sigma$ <sup>+/+</sup> and 14-3-3 $\sigma$ <sup>-/-</sup> cells were cultured in serum free media and proteins present in such media was resolved in SDS PAGE contain  $\beta$ -casein. Representative image of the zymograph is shown. D-E. Scratch wound assays were performed for 14-3-3 $\sigma$ <sup>+/+</sup> and 14-3-3 $\sigma$ <sup>-/-</sup> cells. Phase contrast images of wound closure taken at 10X as shown for 0 min at 20 hours. Cell migration was measured using Axiovision software. Mean and standard deviation were plotted. F. MTT based cell to ECM adhesion assays were performed with 14-3-3 $\sigma$ <sup>+/+</sup> and 14-3-3 $\sigma$ <sup>-/-</sup> cells. Percentage of adhered cells was calculated. Mean and standard deviation were plotted. Significance values were calculated using non parametric t test (\*\*\*) indicates p value > 0.001, \*\* indicates p value > 0.001 and \* indicates p value > 0.01) (Reproduced from [388]). G-H. Boyden chamber invasion assays were performed with 14-3-3 $\sigma$ <sup>+/+</sup> and 14-3-3 $\sigma$ <sup>-/-</sup> cells after coating the inserts with matrigel. Images of 0.1% crystal violet stained inserts were taken with Zeiss inverted microscopes at 10X objective. Number of cells was counted for 20 random fields per insert. Mean and standard deviation were plotted. p value was calculated using non parametric t test. I-J. 14-3-3 $\sigma$ <sup>+/+</sup> and 14-3-3 $\sigma$ <sup>-/-</sup> cells were plated in soft agar in 35mm tissue culture plates and number of colonies were counted for 20 random fields (10X) after 3 weeks. Images of individual colonies were taken with Zeiss inverted microscope and images of full plates after staining with 0.05% crystal violet were taken with bright field microscope. Mean and standard deviation were plotted and significance value was calculated using non parametric t test (\*\* indicates p value <0.001).

To determine if 14-3-3 $\sigma$ <sup>-/-</sup> cells also acquire increased migration potential as compared to 14-3-3 $\sigma$ <sup>+/+</sup> cells scratch wound healing assays were performed. Time lapse videos and quantitation of wound closure over 20 hours suggested that 14-3-3 $\sigma$ <sup>-/-</sup> cells migrated significantly faster than the 14-3-3 $\sigma$ <sup>+/+</sup> cells to close the wound (Fig. 4.1.3.D and E). We

also sought to determine if loss of 14-3-3 $\sigma$  leads to compromised cell to ECM adhesion. Cell to ECM adhesion with four different ECM components such as collagen IV, matrigel, laminin V and fibronectin were performed. Results from these assays suggested that cell to ECM adhesion was significantly compromised in 14-3-3 $\sigma$ <sup>-/-</sup> cells in comparison to 14-3-3 $\sigma$ <sup>+/+</sup> cells [388] (Fig. 4.1.3.F). We also wished to determine if loss of 14-3-3 $\sigma$  could lead to anchorage independent growth in soft agar, which is indicative of neoplastic transformation. No significant difference in colony formation in soft agar between 14-3-3 $\sigma$ <sup>+/+</sup> and 14-3-3 $\sigma$ <sup>-/-</sup> cells were observed, suggesting that loss of 14-3-3 $\sigma$  did not provide any additional advantage to grow in an anchorage independent manner (Fig. 4.1.3.I and J).

These in vitro functional assays described above suggested that loss of 14-3-3 $\sigma$  lead to decrease in cell-cell adhesion leading to increased cell migration. Also 14-3-3 $\sigma$ <sup>-/-</sup> cells showed more invasive potential and decreased cell to ECM adhesion as compared to 14-3-3 $\sigma$ <sup>+/+</sup> cells. However there was no appreciable difference in terms of anchorage independent growth potential in 14-3-3 $\sigma$ <sup>+/+</sup> and 14-3-3 $\sigma$ <sup>-/-</sup> cells.

#### **4.1.4. 14-3-3 $\sigma$ <sup>-/-</sup> cells did not show increased tumor formation and metastasis in immunocompromised mice.**

14-3-3 $\sigma$ <sup>-/-</sup> cells were further investigated for their ability to form primary tumor as well as distant lung metastasis in immunocompromised SCID mice in comparison to 14-3-3 $\sigma$ <sup>+/+</sup> cells. This experiment was meant to test whether the phenotypic characteristics observed in in vitro studies render any advantage to 14-3-3 $\sigma$ <sup>-/-</sup> cells in terms of tumor formation in vivo. Six mice were subcutaneously injected in the dorsal flank with either 14-3-3 $\sigma$ <sup>+/+</sup> or 14-3-3 $\sigma$ <sup>-/-</sup> cells. All the six mice injected with 14-3-3 $\sigma$ <sup>+/+</sup> cells showed tumor formation in the dorsal flank by the end of 3<sup>rd</sup> week whereas only one mouse

shown tumor formation our six mice that were injected with 14-3-3 $\sigma$ <sup>-/-</sup> cells (Fig. 4.1.4. A-C). By the end of 5<sup>th</sup> week 4 out of 6 mice showed presence of tumor in dorsal flank of mice that were injected with 14-3-3 $\sigma$ <sup>-/-</sup> cells. Mean tumor volume for mice that were injected with 14-3-3 $\sigma$ <sup>+/+</sup> cells was significantly high in comparison to mean tumor volume of mice that were injected with 14-3-3 $\sigma$ <sup>-/-</sup> cells (Fig. 4.1.4.D). Haematoxylin and eosin stained lung sections from mice injected with 14-3-3 $\sigma$ <sup>+/+</sup> cells showed presence of metastatic colonies in 2 out of 4 mice after 6 weeks whereas no metastatic colony was observed in lung sections of mice that were injected with 14-3-3 $\sigma$ <sup>-/-</sup> cells (Fig. 4.1.4.E).

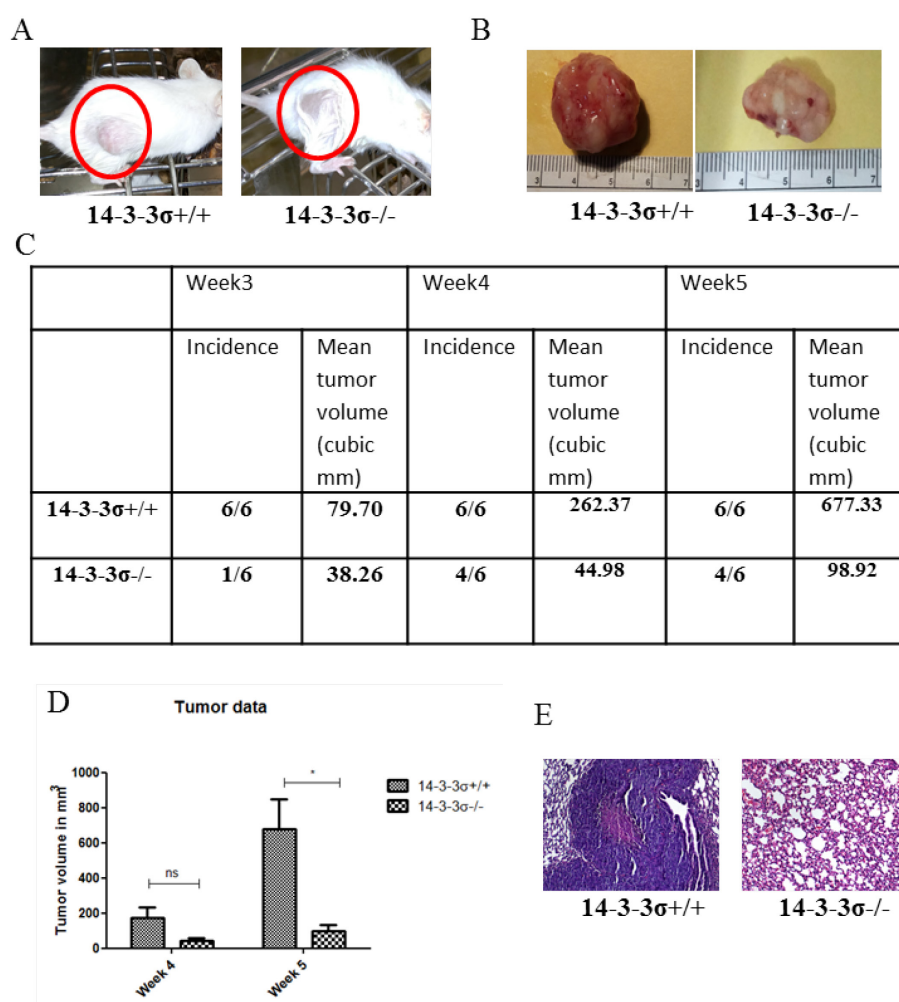


**Figure 4.1.4. 14-3-3 $\sigma$ <sup>-/-</sup> cells did not show increased tumor formation and metastasis in immunocompromised mice.** A. Six mice were injected subcutaneously at the dorsal

*flank with one million cells of either 14-3-3 $\sigma$ <sup>+/+</sup> cells or 14-3-3 $\sigma$ <sup>-/-</sup> cells each. Incidence of primary local tumor is shown in the picture. B. After 6 weeks of observation mice were sacrificed and primary local tumors were dissected out as shown in the picture. C. Tumor volumes were measured across 3rd to 5th week. Mean tumor volume is tabulated along with incidence of tumor formation in mice that were injected with 14-3-3 $\sigma$ <sup>+/+</sup> and 14-3-3 $\sigma$ <sup>-/-</sup> cells. D. Mean tumor volumes measured from mice that were injected with 14-3-3 $\sigma$ <sup>+/+</sup> and 14-3-3 $\sigma$ <sup>-/-</sup> cells were plotted for 4th and 5th week. Non parametric t test was applied for calculating p value and are indicated as \* ( $p < 0.01$ ) or ns (not significant). E. Images shown are acquired with Zeiss upright microscope at 10X objective for haematoxylin and eosin stained lung sections of mice injected with either 14-3-3 $\sigma$ <sup>+/+</sup> and 14-3-3 $\sigma$ <sup>-/-</sup> cells.*

#### **4.1.5. Ectopic expression of 14-3-3 $\sigma$ in 14-3-3 $\sigma$ <sup>-/-</sup> cells results in a reversal of the EMT phenotype.**

To determine if the phenotypic changes observed in 14-3-3 $\sigma$ <sup>-/-</sup> cells are due to loss of 14-3-3 $\sigma$  stable cell lines ectopically expressing HA tagged 14-3-3 $\sigma$  or HA pCDNA3 (vector control) were generated Two independent clones expressing 14-3-3 $\sigma$  namely SP4 and SP5 were selected for further studies along with vector control cells, VP1 and 14-3-3 $\sigma$ <sup>+/+</sup> cells (Fig. 4.1.5.A).

To determine if ectopic expression of 14-3-3 $\sigma$  can rescue expression and epithelial makers and decreased expression of mesenchymal markers in 14-3-3 $\sigma$ <sup>-/-</sup> cells, Western blot analysis and immunofluorescence analysis were performed to investigate the expression of epithelial and mesenchymal markers. In Western blot analysis both SP4 and SP5 showed increase in expression of epithelial markers such as E cadherin and PG; and decrease in mesenchymal markers such as vimentin and N cadherin in comparison to

vector control i.e. VP1. However, this rescue failed to restore the expression of epithelial markers to a level observed in 14-3-3 $\sigma$ <sup>+/+</sup> cells (Fig. 4.1.5.A).  $\beta$  actin served as loading control and 14-3-3 $\sigma$  blot showed ectopic expression of 14-3-3 $\sigma$  in 14-3-3 $\sigma$ <sup>-/-</sup> cells (Fig. 4.1.5.A).

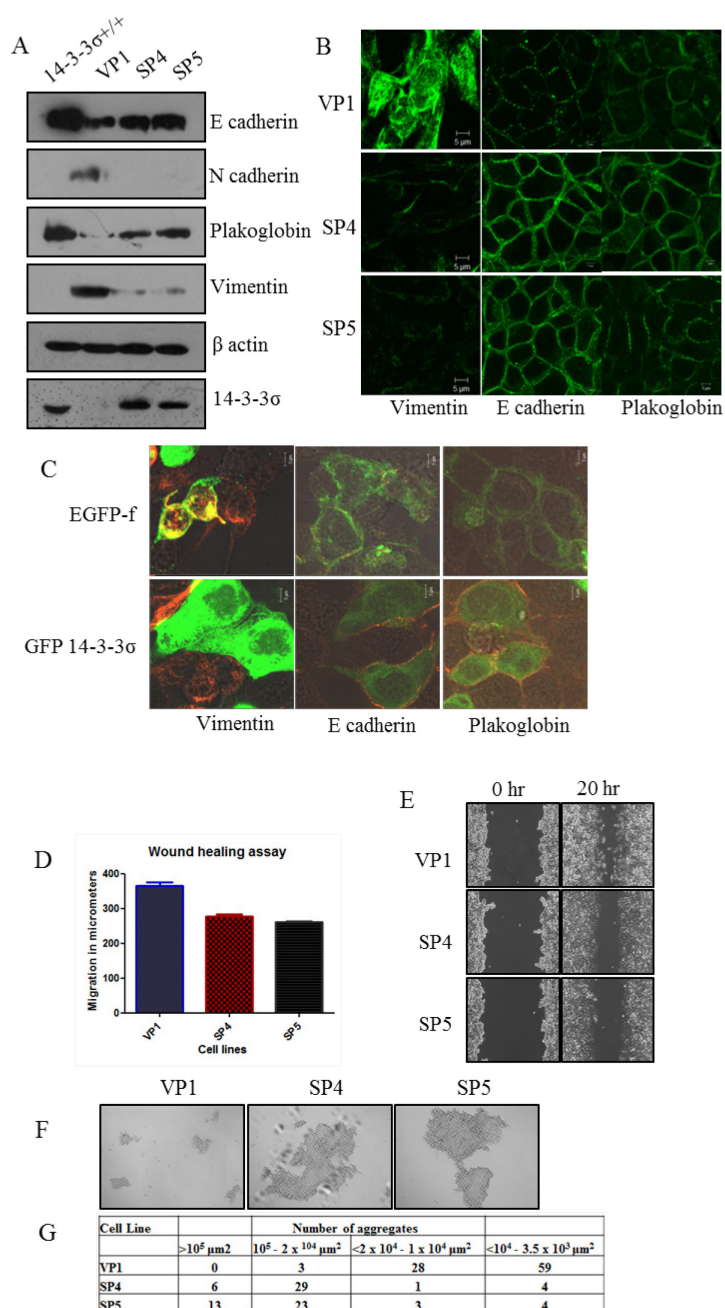


**Figure 4.1.5. Ectopic expression of 14-3-3 $\sigma$  in 14-3-3 $\sigma$ <sup>-/-</sup> cells can rescue EMT like characteristics.** A. Equivalent amount of Cell lysates from 14-3-3 $\sigma$ <sup>+/+</sup>, VP1, SP4 and

*SP5 cells were resolved in SDS page and Western blotting was performed with indicated antibodies.  $\beta$  actin served as loading control. B. VP1, SP4 and SP4 cells were fixed and stained with indicated antibodies and cells were imaged with confocal microscope. Magnification is X63 with 2X optical zoom and bars indicate 5 $\mu$ m C. 14-3-3 $\sigma$ <sup>-/-</sup> cells was transfected separately with EGFP-f and GFP 14-3-3 $\sigma$ . Cells were then fixed and stained with indicated antibodies and imaged with confocal microscope. Magnification is X63 with 3X optical zoom and bars indicate 5 $\mu$ m D-E. Scratch wound assays were performed with VP1, SP4 and SP4 cells. Cell migration in micrometers was calculated using Axiovision software. Mean and standard deviation were plotted. F-G. Hanging drop assays were performed with VP1, SP4 and SP4 cells. Images of cell aggregated were acquired with Zeiss inverted microscope and size of cell aggregates was measured using image J software.*

We also wished to investigate whether rescue of epithelial markers and decrease in mesenchymal markers can be observed in immunofluorescence analysis as well. Results show that both E cadherin and PG expression was increased in SP4 and SP4 clones in comparison to VP1. Mesenchymal marker vimentin expression was also decreased in SP4 and SP4 clones as compared to VP1 (Fig. 4.1.5.B).

Rescue experiments were also performed in transient assays to rule out any clonal effects, which can be observed in stable clones. In this assays 14-3-3 $\sigma$ <sup>-/-</sup> cells were separately transfected with GFP 14-3-3 $\sigma$  or EGFP-f vector. Immunofluorescence results suggest that 14-3-3 $\sigma$ <sup>-/-</sup> cells expressing GFP 14-3-3 $\sigma$  showed decreased expression of vimentin and increase in expression of E cadherin and PG in comparison to 14-3-3 $\sigma$ <sup>-/-</sup> cells expressing EGFP-f.

We further asked if ectopic expression of 14-3-3 $\sigma$  could also rescue the phenotypic changes observed on loss of 14-3-3 $\sigma$ . Scratch wound assays suggested that both SP4 and SP4 clones showed increase in migration in comparison to VP1 (Fig.4.1.5.D). Hanging drop assays were performed to determine the cell-cell adhesion properties of 14-3-3 $\sigma$ <sup>-/-</sup> cells on ectopic expression of 14-3-3 $\sigma$ . Both SP4 and SP4 showed increase in cell-cell adhesion in comparison to VP1 suggesting that ectopic expression of 14-3-3 $\sigma$  could rescue the defects in cell-cell adhesion observed in 14-3-3 $\sigma$ <sup>-/-</sup> cells (Fig. 4.1.5.F-G).

These results suggest that ectopic expression of 14-3-3 $\sigma$  lead to increase in expression of epithelial markers and decrease in expression of mesenchymal markers in 14-3-3 $\sigma$ <sup>-/-</sup> cells. Also phenotypic characteristic such as cell migration and cell-cell adhesion were restored close to 14-3-3 $\sigma$ <sup>+/+</sup> cells on ectopic expression of 14-3-3 $\sigma$  in 14-3-3 $\sigma$ <sup>-/-</sup> cells. So it can be concluded that EMT like characteristics observed in 14-3-3 $\sigma$ <sup>-/-</sup> cells were specifically due to loss of 14-3-3 $\sigma$ .

#### **4.1.6. 14-3-3 $\sigma$ loss leads to increase in Slug and Zeb1.**

There are four classical EMT specific transcription factors known to regulate EMT such as Snail, Slug, Zeb and Twist (described in detail in the introduction). To determine which EMT specific transcription factor is involved in regulation of EMT like characteristic observed on loss of 14-3-3 $\sigma$  we performed Western blot analyses that demonstrated that there was an increase in the protein levels of Slug and Zeb1 in 14-3-3 $\sigma$ <sup>-/-</sup> cells in comparison to 14-3-3 $\sigma$ <sup>+/+</sup> cells. However no change was observed in protein levels of Snail (Fig. 4.1.6.A). To determine if increase at protein levels of Slug and Zeb1 was due to increase in transcription, RT-PCR analysis were performed. Our RT-PCR results showed that Slug and Zeb1 mRNA levels were increased in 14-3-3 $\sigma$ <sup>-/-</sup> cells in comparison to 14-3-3 $\sigma$ <sup>+/+</sup> cells. There was no change in mRNA levels of Snail and Twist

mRNA was undetectable in both 14-3-3 $\sigma$ <sup>+/+</sup> and 14-3-3 $\sigma$ <sup>-/-</sup> cells (Fig. 4.1.6.B). To validate out RT-PCR results we performed Q-PCR analysis for the four EMT specific transcription factors. Both Slug and Zeb1 mRNA levels were increased significantly in 14-3-3 $\sigma$ <sup>-/-</sup> cells as compared to 14-3-3 $\sigma$ <sup>+/+</sup> cells. Twist mRNA levels was undetectable in Q-PCR analysis as well in both 14-3-3 $\sigma$ <sup>+/+</sup> and 14-3-3 $\sigma$ <sup>-/-</sup> cells (Fig 4.1.6.C).

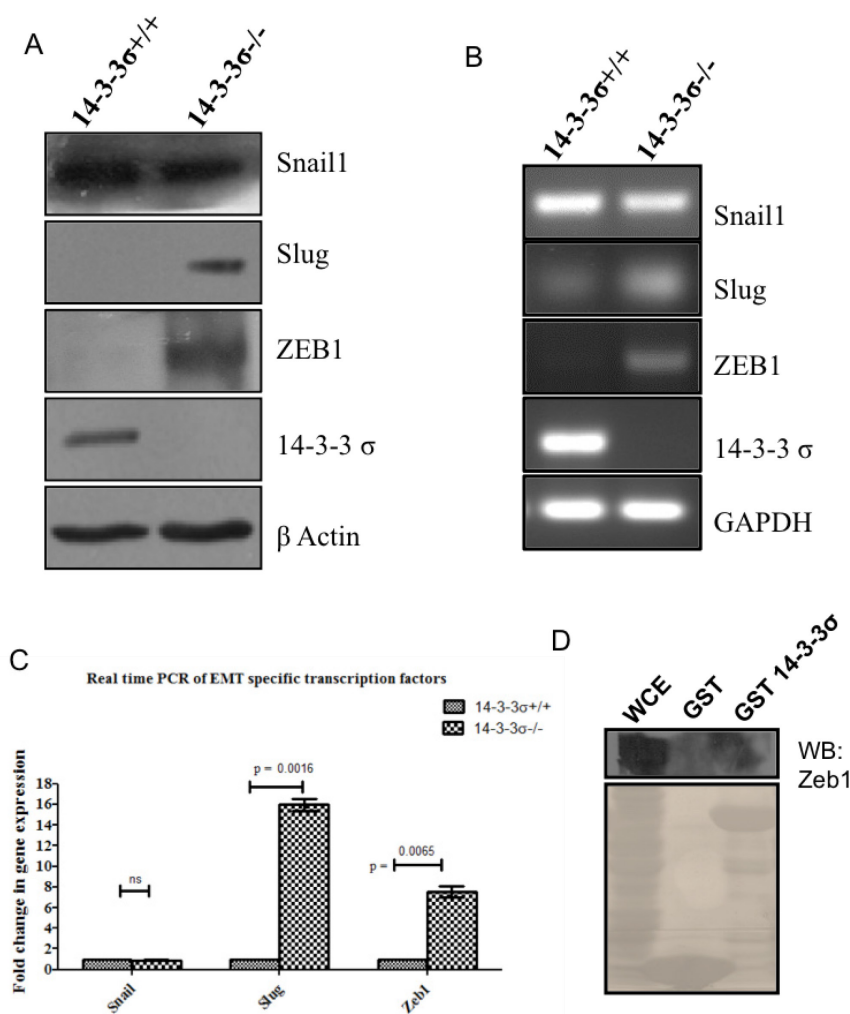


**Figure 4.1.6.** 14-3-3 $\sigma$  loss leads to increase in Slug and Zeb1. *A.* Equivalent amount of Cell lysates from 14-3-3 $\sigma$ <sup>+/+</sup> and 14-3-3 $\sigma$ <sup>-/-</sup> cells were resolved in SDS page along with 5% input for whole cell extract (WCE). Western blotting was performed with indicated antibodies.  $\beta$  actin served as loading control. *B.* Total mRNA was isolated from 14-3-3 $\sigma$ <sup>+/+</sup> cells and 14-3-3 $\sigma$ <sup>-/-</sup> cells. cDNA was synthesized and reverse-transcriptase PCR

was performed with equal amount of cDNA using primers for indicated genes. GAPDH was used as loading control. Representative images of three independent experiments are shown. C. Quantitative PCR was performed using cDNA synthesized from total mRNA isolated from 14-3-3 $\sigma$ <sup>+/+</sup> cells and 14-3-3 $\sigma$ <sup>-/-</sup> cells.  $\Delta\Delta ct$  values were calculated and normalized against GAPDH. Fold change in gene expression are plotted on Y axis for indicated genes as shown in X axis. p values were calculated using non parametric t test (\*\*\*) indicates p value > 0.001, \*\* indicates p value > 0.001 and \* indicates p value > 0.01). D. 14-3-3 $\sigma$ <sup>-/-</sup> cell lysates were incubated with bacterially purified GST or GST 14-3-3 $\sigma$ . Precipitates were resolved on SDS PAGE along with 5% input for whole cell extract (WCE). Western blotting was performed with indicated antibody. Expression of GST and GST14-3-3 $\sigma$  is shown in the ponceau stained membrane.

These results suggest that the EMT like characteristics observed on loss of 14-3-3 $\sigma$  was due to increase in Slug and Zeb1 levels. Next we wished to determine if 14-3-3 $\sigma$  can interact with Zeb1 and if this interaction is necessary for increase in Zeb1 levels. Therefore, in vitro GST pull down assays was performed where bacterially produced GST-14-3-3 $\sigma$  were incubated with cell lysates from 14-3-3 $\sigma$ <sup>-/-</sup> cells. Results showed that there was no interaction of 14-3-3 $\sigma$  and Zeb1 (Fig. 4.1.6.D).

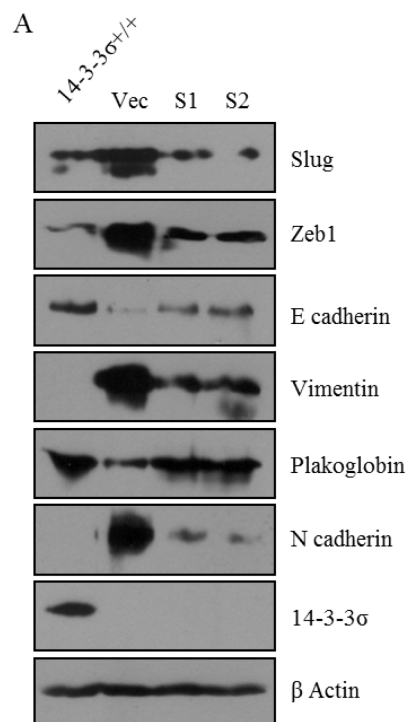
#### **4.1.7. Inhibition of Slug expression leads to a reversal of EMT like characteristics in 14-3-3 $\sigma$ <sup>-/-</sup> cells.**

To delineate whether increase in expression of Slug is necessary and sufficient for inducing EMT in 14-3-3 $\sigma$ <sup>-/-</sup> cells stable knock down clones of Slug namely S1 and S2 using published shRNA sequences and vector control cells i.e. Vec (described in materials and methods section) were generated in 14-3-3 $\sigma$ <sup>-/-</sup> cells. We wished to

determine if knock down of Slug could lead to reversal of EMT like characteristics observed on loss of 14-3-3 $\sigma$ .

Western blot analysis revealed that S1 and S2 showed increase in expression of epithelial markers such as E cadherin and PG and decrease in expression of mesenchymal markers such as vimentin and N cadherin. Down regulation of Slug also lead to decrease in Zeb1 levels suggesting that increase in Zeb1 was positively regulated by increased Slug levels (Fig. 4.1.7. A). These results suggest that the EMT like characteristics observed in 14-3-3 $\sigma$ <sup>-/-</sup> cells were due to increase in EMT specific transcription factor Slug. Increase in Slug levels in turn lead to increase in Zeb1 levels.

**Figure 4.1.7. Down-regulation of Slug leads to reversal of EMT like characteristics in 14-3-3 $\sigma$ <sup>-/-</sup> cells.** A. Equivalent amount of Cell lysates from 14-3-3 $\sigma$ <sup>+/+</sup>, Vec, S1 and S2 cells were resolved in SDS page and Western blotting was performed with indicated antibodies.  $\beta$  actin served as loading control.

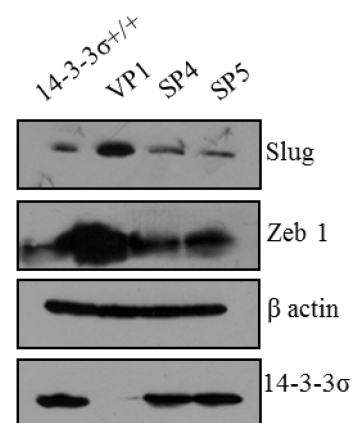


#### 4.1.8. Ectopic expression of 14-3-3 $\sigma$ in 14-3-3 $\sigma$ <sup>-/-</sup> cells leads to decrease in expression of Slug and Zeb1.

We wished to investigate whether increase in Slug protein level is a specific effect of loss of 14-3-3 $\sigma$ . To address this question expression of Slug protein levels in SP4 and SP5 clones, which express HA-14-3-3 $\sigma$ , were determined and compared with the Slug protein

expression in VP1 by Western blotting. Results show that ectopic expression of 14-3-3 $\sigma$  lead to decrease in Slug protein levels in comparison to VP1 and Slug proteins level was restored in SP4 and Sp5 close to what is observed in 14-3-3 $\sigma^{+/+}$  cells (Fig 4.1.8). Interestingly decreased Slug protein levels in SP4 and SP5 also resulted in decrease in Zeb1 protein levels suggesting that Zeb1 protein expression is regulated by Slug which is in turn negatively regulated by 14-3-3 $\sigma$  expression.

**Figure 4.1.8. Ectopic expression of 14-3-3 $\sigma$  in 14-3-3 $\sigma^{-/-}$  cells leads to decrease in expression of Slug and Zeb1.** Equivalent amount of Cell lysates from 14-3-3 $\sigma^{+/+}$ , VP1, SP4 and SP5 cells were resolved in SDS page and Western blotting was performed with indicated antibodies.  $\beta$  actin served as loading control.



These results suggest that loss of 14-3-3 $\sigma$  expression leads to increase in Slug protein levels and this in turn lead to increase in Zeb1. Increase in the EMT specific transcription factors induces EMT like characteristic in 14-3-3 $\sigma^{-/-}$  cells.

#### 4.1.9. c-Jun proteins levels are increased in 14-3-3 $\sigma^{-/-}$ cells.

Next we asked how 14-3-3 $\sigma$  regulates Slug expression. There are multiple reports of how Slug expression could be regulated (described in detail in the introduction section). We first wished to determine if Slug expression is positively regulated by MAPK pathway in 14-3-3 $\sigma^{-/-}$  cells. We performed Western blot analysis to determine activation of various kinases involved in MAPK signaling pathway such as p38, MEK, AKT and ERK. No appreciable change was observed in the level of activation specific phosphorylation of the above mentioned kinases among 14-3-3 $\sigma^{+/+}$  and 14-3-3 $\sigma^{-/-}$  cells (Fig.4.1.9.A). We did

not observe any change at the total protein level of the above-mentioned kinases as well (Fig. 4.1.9.A).

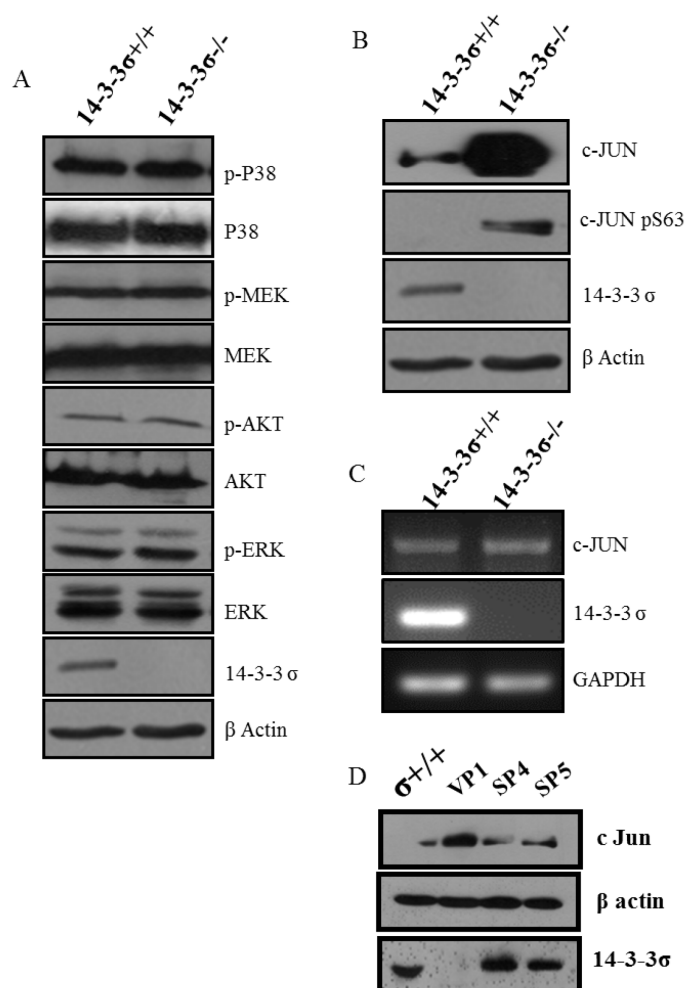


**Figure 4.1.9.** *c-Jun* proteins levels are increased in 14-3-3 $\sigma$ <sup>-/-</sup> cells. **A** and **C**. Equivalent amount of Cell lysates from 14-3-3 $\sigma$ <sup>+/+</sup> and 14-3-3 $\sigma$ <sup>-/-</sup> cells were resolved in SDS page and Western blotting was performed with indicated antibodies.  $\beta$  actin served as loading control. **B**. Total mRNA was isolated from 14-3-3 $\sigma$ <sup>+/+</sup> cells and 14-3-3 $\sigma$ <sup>-/-</sup> cells. cDNA was synthesized and reverse-transcriptase PCR was performed with equal amount of cDNA using primers for indicated genes. GAPDH was used as loading control. Representative images of three independent experiments are shown. **D**. Equivalent amount of Cell lysates from 14-3-3 $\sigma$ <sup>+/+</sup>, VP1, SP4 and SP4 cells were

*resolved in SDS page and Western blotting was performed with indicated antibodies.  $\beta$  actin served as loading control.*

Another report suggested that AP1 transcription factor c-Jun can regulate Slug protein levels (discussed in introduction) [372]. Therefore, we wished to determine if c-Jun protein levels are altered loss of 14-3-3 $\sigma$ . c-Jun protein levels were found to be increased in 14-3-3 $\sigma^{-/-}$  cells in comparison to 14-3-3 $\sigma^{+/+}$  cells. Increase in c-Jun protein level also lead to increase in active c-Jun levels. This is confirmed by the increase in phosphorylation at Serine 63 of c-Jun (Fig. 4.1.9.B). We next asked if this increase at c-Jun protein level was due to increase in transcription of c-Jun gene. RT-PCR analysis showed that total mRNA levels remained same in 14-3-3 $\sigma^{+/+}$  and 14-3-3 $\sigma^{-/-}$  cells (Fig. 4.1.9.C). This suggests that increase in c-Jun protein could be because of increased protein stability, increased translation.

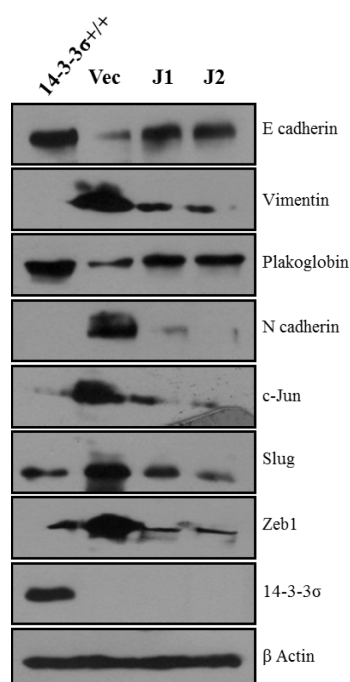
We further wanted to confirm that increase in c-Jun protein level was specifically due to loss of 14-3-3 $\sigma$ . Therefore, we asked c-Jun protein level is restored close to 14-3-3 $\sigma^{+/+}$  cells in 14-3-3 $\sigma^{-/-}$  cells ectopically expressing 14-3-3 $\sigma$ . Both SP4 and SP5 showed decreased c-Jun protein levels in comparison to VP1 and c-Jun protein level was restored close to what was observed in 14-3-3 $\sigma^{+/+}$  cells (Fig. 4.1.9.D). These results suggest that increased Slug expression in 14-3-3 $\sigma^{-/-}$  cells could be due to increase in c-Jun protein levels in 14-3-3 $\sigma^{-/-}$  cells in comparison to 14-3-3 $\sigma^{+/+}$  cells. Increased protein levels of c-Jun were not due to increased transcription of c-Jun gene. c-Jun protein levels could be restored close to what is observed in 14-3-3 $\sigma^{+/+}$  cells if 14-3-3 $\sigma$  is ectopically expressed in 14-3-3 $\sigma^{-/-}$  cells suggesting that this increase at c-Jun protein level is specifically due to loss of 14-3-3 $\sigma$ .

#### 4.1.10. Increased c-Jun proteins levels promote EMT in 14-3-3 $\sigma$ <sup>-/-</sup> cells.

To determine if increased c-Jun protein levels are sufficient to induce EMT in 14-3-3 $\sigma$ <sup>-/-</sup> cells expression of various epithelial markers, mesenchymal markers and EMT specific transcription factors in c-Jun knock down clones (J1 and J2) as compared to vector control cells (Vec) were analyzed. 14-3-3 $\sigma$ <sup>+/+</sup> cells were also included in this study to determine if downregulation of c-Jun could reverse the expression of EMT specific markers close to what is observed in 14-3-3 $\sigma$ <sup>+/+</sup> cells.

Both J1 and J2 showed increase in expression of epithelial markers such as E cadherin PG; and decrease in expression of mesenchymal markers such as vimentin and N cadherin in comparison to Vec (Fig. 4.1.10). Additionally knock down of c-Jun lead to reversal of expression of these EMT specific markers close to what is observed in 14-3-3 $\sigma$ <sup>+/+</sup> cells. Expression of EMT specific transcription factors such as Slug and Zeb1 was also decreased upon downregulation of c-Jun suggesting that c-Jun is responsible for increased expression of Slug and Zeb1 in 14-3-3 $\sigma$ <sup>-/-</sup> cells (Fig 4.1.10). These results suggests that c-Jun is involved in increased expression of Slug and Zeb1 genes which are responsible for initiating EMT in 14-3-3 $\sigma$ <sup>-/-</sup> cells.

**Figure 4.1.10. Increased c-Jun proteins levels promote EMT in 14-3-3 $\sigma$ <sup>-/-</sup> cells.** Equivalent amount of Cell lysates of 14-3-3 $\sigma$ <sup>+/+</sup>, Vec, J1 and J2 cells were resolved in SDS page and Western blotting was performed with indicated antibodies.  $\beta$  actin served as loading control.



#### 4.1.11. 14-3-3 $\sigma$ binds to c-Jun and induces the degradation of c-Jun

We first sought to determine the mechanism behind increased c-Jun protein levels in 14-3-3 $\sigma$ <sup>-/-</sup> cells in comparison to 14-3-3 $\sigma$ <sup>+/+</sup> cells. To test whether c-Jun is targeted to proteasomal degradation in 14-3-3 $\sigma$ <sup>+/+</sup> cells and loss of 14-3-3 $\sigma$  results in stabilization of c-Jun at protein level due to inhibition of proteasome mediated degradation of c-Jun, 14-3-3 $\sigma$ <sup>+/+</sup> cells were treated with MG132 to inhibit proteasome function. We hypothesized that 14-3-3 $\sigma$  could interact with c-Jun and this interaction might be required for targeting c-Jun to proteasomal degradation.

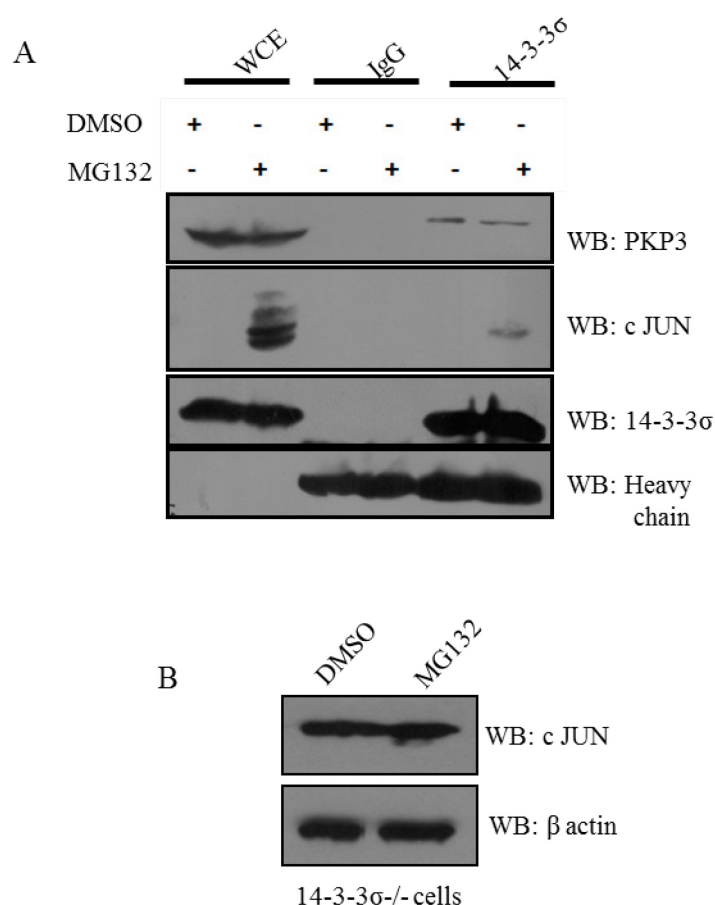


**Figure 4.1.11. 14-3-3 $\sigma$  binds to c-Jun and might target the later to proteasomal degradation.** A. 14-3-3 $\sigma$ <sup>+/+</sup> cells were treated with either MG132 or DMSO for 6 hours and cell lysates were prepared and immunoprecipitated with either 14-3-3 $\sigma$  antibody or

*isotype control (IgG). Immunocomplexes were resolved in SDS PAGE along with 5% input for whole cell extract (WCE) followed by Western blotting with indicated antibodies. Equal intensity of heavy chain across samples incubated with IgG or 14-3-3 $\sigma$  antibody suggest use of equivalent amount of antibody for IgG and 14-3-3 $\sigma$ . B. 14-3-3 $\sigma$ <sup>-/-</sup> cells was treated with DMSO or MG132. Equivalent amounts of cell lysates were loaded on SDS PAGE followed by Western blotting with indicated antibodies.  $\beta$  actin served as loading control.*

It was observed that c-Jun protein levels are stabilized in 14-3-3 $\sigma$ <sup>+/+</sup> cells when treated with MG132 and can be immunoprecipitated with 14-3-3 $\sigma$  antibody. However, c-Jun protein levels were almost undetectable when 14-3-3 $\sigma$ <sup>+/+</sup> cells were treated with DMSO and no binding was observed with 14-3-3 $\sigma$  (Fig. 4.1.11.A). On the contrary it was observed that PKP3, which forms a complex with 14-3-3 $\sigma$  (our unpublished data from our laboratory and [323]) was expressed both in DMSO and MG132 treated 14-3-3 $\sigma$ <sup>+/+</sup> cells and also formed complex with 14-3-3 $\sigma$  (Fig. 4.1.11.A). This suggests that 14-3-3 $\sigma$  interacts with c-Jun and this interaction leads to proteasomal degradation of c-Jun. To determine if treatment of MG132 itself has any effect on expression of c-Jun we treated 14-3-3 $\sigma$ <sup>-/-</sup> cells with either DMSO or MG132 and performed Western blot analysis for c-Jun protein. It was observed that there was no change in c-Jun protein levels in DMSO and MG132 treated 14-3-3 $\sigma$ <sup>-/-</sup> cells (Fig. 4.1.11.B). This suggests that c-Jun is not targeted for degradation by the proteasome in cells lacking 14-3-3 $\sigma$ .

#### **4.1.12. 14-3-3 $\sigma$ binds to c-Jun and induces its degradation by FBW7.**

To further support the hypothesis that 14-3-3 $\sigma$  target c-Jun to proteasomal degradation we wished to perform in vivo ubiquitination assays. In collaboration with Dr. Maddika Subba Reddy and Neelam Chaudari from CDFD we performed this assays. There are at least

three different E3 ligases known for mediating proteasomal degradation of c-Jun such as FBW7, COP1 and ITCH (described in detail in the introduction). We tested if FBW7 is involved in c-Jun degradation in 14-3-3 $\sigma$ <sup>+/+</sup> cells. Immunoprecipitation experiments were carried out with 14-3-3 $\sigma$ <sup>+/+</sup> and 14-3-3 $\sigma$ <sup>-/-</sup> cells after treating with MG132 to stabilize c-Jun protein levels which otherwise targeted to proteasomal degradation in 14-3-3 $\sigma$ <sup>+/+</sup> cells. Immunoprecipitation with Flag antibody followed by Western blotting with Flag antibody showed increased presence of higher molecular weight species of c-Jun in 14-3-3 $\sigma$ <sup>+/+</sup> cells that were transfected with Flag tagged c-Jun (SFB c-Jun) and Myc tagged FBW7 in comparison to 14-3-3 $\sigma$ <sup>+/+</sup> cells that were transfected with Flag tagged c-Jun (SFB c-Jun) and Myc Vector, or to experiments performed in the 14-3-3 $\sigma$ <sup>-/-</sup> cells. Western blots with the Flag and Myc antibodies confirmed that both c-Jun and FBW7 were expressed at comparable levels (Fig. 4.1.12.A). These results suggest that overexpression of FBW7 lead to increase in the ubiquitination of c-Jun in 14-3-3 $\sigma$ <sup>+/+</sup> but not in 14-3-3 $\sigma$ <sup>-/-</sup> cells (Fig. 4.1.12.A).

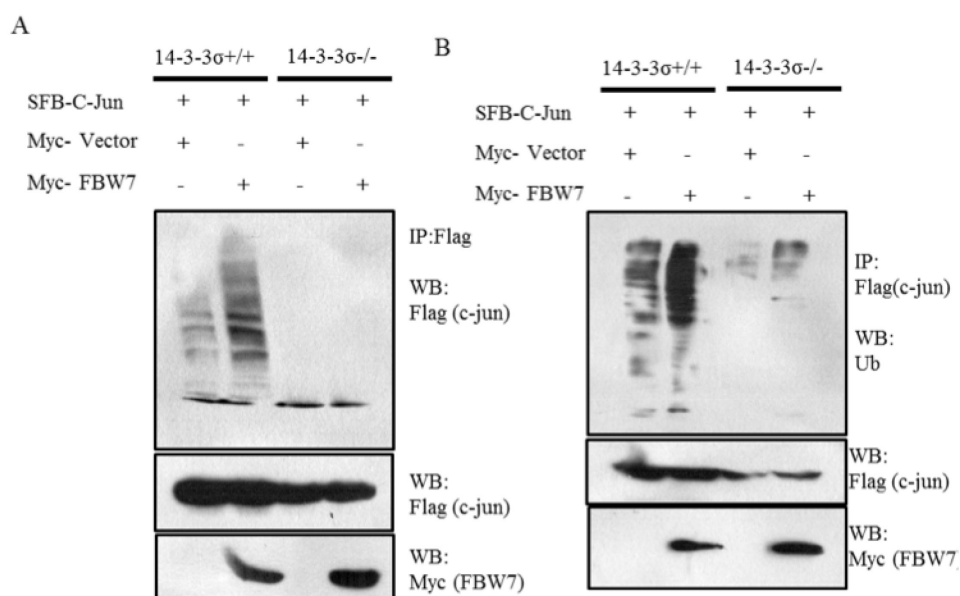


**Figure 4.1.12. 14-3-3 $\sigma$  targets to c-Jun and might to proteasomal degradation in FBW7 dependent manner.** A. 14-3-3 $\sigma$ <sup>+/+</sup> and 14-3-3 $\sigma$ <sup>-/-</sup> cells were transfected

*separately with SFB-c-Jun with Myc-vector, SFB-c-Jun with Myc-FBW7 alpha. At 24 h post transfection, cells were treated with MG132 for 6 h, and c-Jun ubiquitination was detected by immunoblotting with Flag antibody after immunoprecipitation with anti-Flag antibody. B. 14-3-3 $\sigma$ <sup>+/+</sup> and 14-3-3 $\sigma$ <sup>-/-</sup> cells were transfected separately with SFB-c-Jun with Myc-vector, SFB-c-Jun with Myc-FBW7 alpha. At 24 h post transfection, cells were treated with MG132 for 6 h, and c-Jun ubiquitination was detected by immunoblotting with ubiquitin (Ub) antibody after immunoprecipitation with anti-Flag antibody.*

To further confirm the identity of these higher molecular weight species of c-Jun similar experiment was performed followed by Western blotting with Ubiquitin (Ub) antibody after immunoprecipitation with Flag tagged c-Jun with Flag antibody. It was observed that the higher molecular weight species of c-Jun were also detected with Ub antibody suggesting that these higher molecular weight species of c-Jun are ubiquitinated in 14-3-3 $\sigma$ <sup>+/+</sup> cells. And this ubiquitination can be further induced on overexpression of FBW7. Western blot with Flag and Myc antibody confirmed that both c-Jun and FBW7 were expressed optimally (Fig. 4.1.12.B). These results suggest that 14-3-3 $\sigma$  is important for targeting c-Jun to proteasomal degradation. And FBW7 is involved in ubiquitination of c-Jun in 14-3-3 $\sigma$ <sup>+/+</sup> cells.

#### **4.1.13. Interaction of 14-3-3 $\sigma$ and c-Jun is necessary for ubiquitination of c-Jun.**

We further wished to confirm whether interaction of 14-3-3 $\sigma$  and c-Jun is necessary for ubiquitination of c-Jun. To address this question we tried to identify putative 14-3-3 protein binding motifs in c-Jun. It was found that there were two sequences in c-Jun, which could be potential 14-3-3 binding sites. One of these motifs required phosphorylation at Serine (S58) position whereas the other motif required

phosphorylation at Serine267 (S267) position. Individual mutants of S58 to Alanine (S58A) and S267 to Alanine (S267A) were generated and the ability of these mutants as well the full length wild type 14-3-3 $\sigma$  to interact with 14-3-3 $\sigma$  was tested. In vitro GST pull down assays were performed where bacterially produced GST 14-3-3 $\sigma$  was incubated with cell lysates that were separately transfected with HA tagged c-Jun wild type (HA c-Jun WT) and HA tagged Serine to Alanine mutants described above (HA c-Jun S58A and HA c-JunS267A). Western blot analysis with HA antibody showed that HA c-Jun formed a complex with bacterially expressed 14-3-3 $\sigma$  whereas, S267A mutation in c-Jun resulted in complete abrogation of interaction between 14-3-3 $\sigma$  and c-Jun. However, we did not observe any defect in interaction of HA c-JunS58A and 14-3-3 $\sigma$ . There were no nonspecific interaction either HA c-Jun WT or HA tagged mutants with GST. The ponceau stained membrane shows that equivalent amount of bacterially expressed GST alone and GST 14-3-3 $\sigma$  was used for these experiments (Fig. 4.1.13.A). These results suggest that Serine 267 residue is important for interaction of c-Jun and 14-3-3 $\sigma$ .

Next we wished to determine if S267A mutation lead to defects in ubiquitination of c-Jun. In vitro ubiquitination assays (see materials and methods for details) performed at Dr. Maddika Subba Reddy's laboratory by Neelam Chaudhary showed that GST-c-JunWT was ubiquitinated in presence of FBW7 and 14-3-3 $\sigma$  as higher molecular weight species of c-Jun was observed on Western blot with GST antibody (Fig. 4.1.13.B). This further support our hypothesis that c-Jun is ubiquitinated and targeted to proteasomal degradation by 14-3-3 $\sigma$  in FBW7 dependent manner. GST-c-JunS267A was not ubiquitinated even in presence of FBW7 and 14-3-3 $\sigma$  evident from absence of any higher molecular weight species of c-Jun on Western blotting with GST antibody (Fig. 4.1.13.B). Coomassie stained polyacrylamide gel shows that GST-C-Jun WT, GST-C-Jun S267A, MBP-14-3-3

sigma, and MBP-FBW7 alpha are expressed optimally (Fig. 4.1.13.C). These results suggest that interaction of c-Jun and 14-3-3 $\sigma$  is absolutely required for ubiquitination of c-Jun.

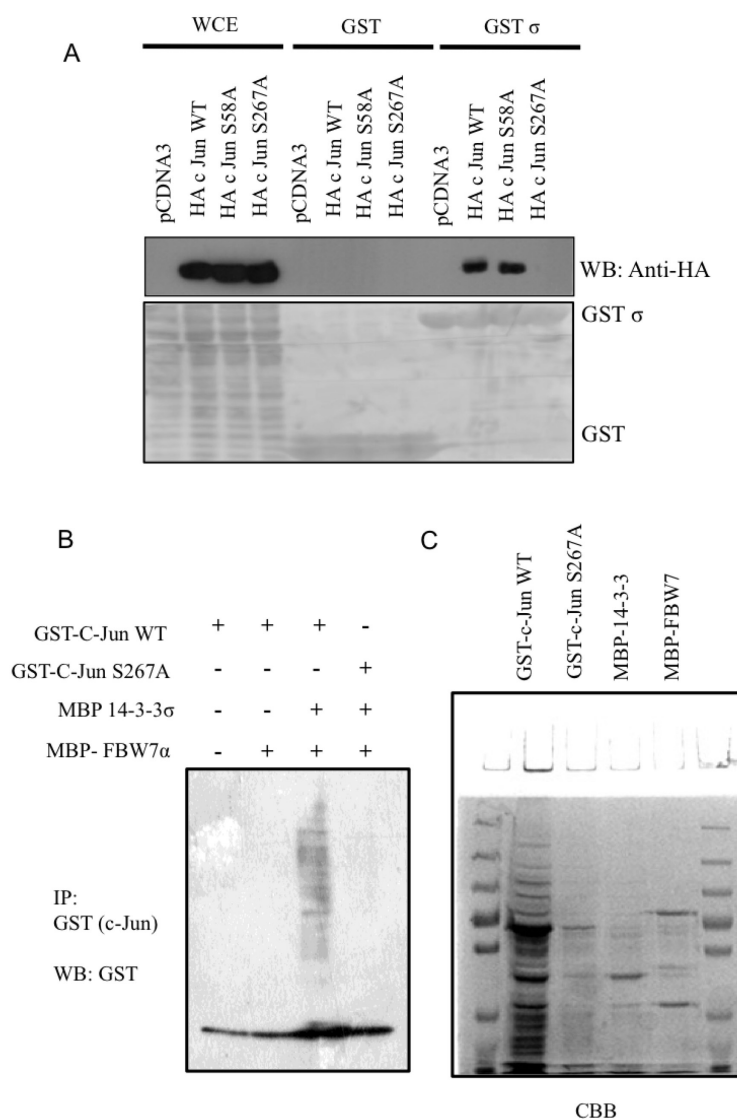


**Figure 4.1.13. Interaction of 14-3-3 $\sigma$  and c-Jun is necessary for ubiquitination of c-Jun.** *A.* HEK293 cells were transfected separately with HA c-Jun WT, HA c-Jun S58A and HA c-Jun S267A. 24 hours post transfection cell lysates were prepared and incubated with bacterially purified GST or GST 14-3-3 $\sigma$ . Precipitates were resolved on SDS PAGE along with 5% input for whole cell extract (WCE). Western blotting was performed with indicated antibody. Expression of GST and GST14-3-3 $\sigma$  is shown in the

*ponceau stained membrane. B. In vitro ubiquitination experiments were performed using bacterially purified GST-C-Jun WT and GST-C-Jun S267A as a substrate in the indicated combinations with MBP-tagged 14-3-3 sigma and MBP-tagged FBW7 alpha along with E1 (UBE1) and E2 (UbcH5B). Ubiquitinated species of GST-C-Jun WT and GST-S267A were detected by immunoblotting with anti-GST antibody. C. The expression of GST-C-Jun WT, GST-C-Jun S267A, MBP-14-3-3 sigma, and MBP-FBW7 alpha shown by Coomassie staining.*

#### **4.1.14. Interaction of 14-3-3 $\sigma$ and c-Jun is required for ubiquitination and proteasome mediated degradation of c-Jun in vivo.**

We wished to determine if interaction of c-Jun with 14-3-3 $\sigma$  is necessary for ubiquitination of c-Jun in vivo. Immunoprecipitation experiments were carried out at Dr. Reddy's laboratory with 14-3-3 $\sigma$ <sup>+/+</sup> cells transfected with Flag tagged c-Jun WT (SFB-c-Jun) and Flag tagged c-Jun S267A (SFB-c-JunS267A) with without Myc-FBW7 or with Myc Vector. MG132 was used to stabilize c-Jun protein levels which otherwise targeted to proteasomal degradation in 14-3-3 $\sigma$ <sup>+/+</sup> cells. Immunoprecipitation with Flag antibody followed by Western blotting with Flag antibody showed increased presence of higher molecular weight species of c-Jun in 14-3-3 $\sigma$ <sup>+/+</sup> cells that were transfected with Flag tagged c-Jun (SFB c-Jun) and Myc tagged FBW7 in comparison to 14-3-3 $\sigma$ <sup>+/+</sup> cells that were transfected with Flag tagged c-Jun (SFB c-Jun) and Myc Vector suggesting that overexpression of FBW7 lead to increase in the amount of higher molecular weight species of c-Jun (Fig. 4.1.14.A). However no such higher molecular weight species of c-JunS267A mutant were observed in 14-3-3 $\sigma$ <sup>+/+</sup> cells that were transfected with SFB-c-JunS267A and Myc Vector or Myc tagged FBW7 suggesting that abrogation of interaction between c-Jun and 14-3-3 $\sigma$  lead defects in ubiquitination of c-Jun. Western

blot with Flag and Myc antibody confirmed that both c-Jun and FBW7 were expressed optimally (Fig. 4.1.14.A).

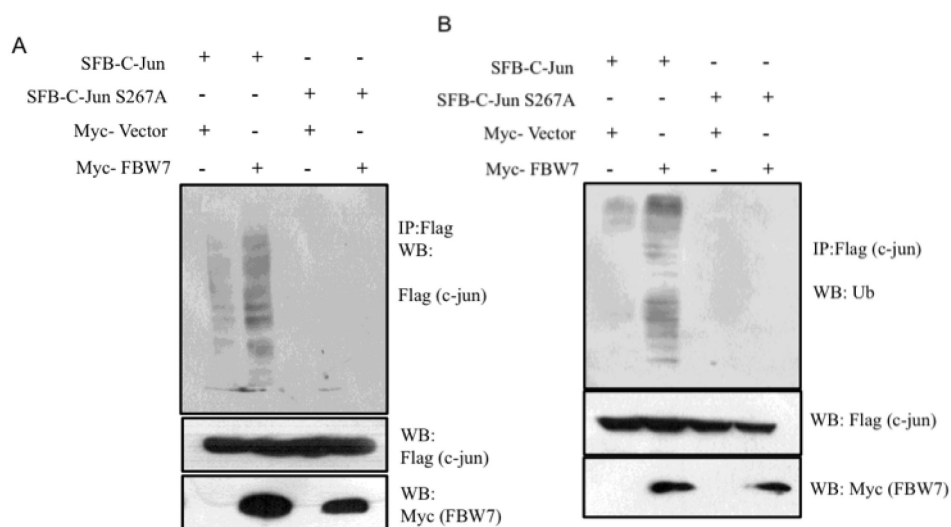


**Figure 4.1.14. Abrogation of interaction of c-Jun and 14-3-3 $\sigma$  leads to inhibition of ubiquitination and proteasomal degradation of c-Jun in vivo.** *A.* 14-3-3 $\sigma$ <sup>+/+</sup> cells were transfected with c-Jun WT and c-Jun S267A with or without Myc-FBW7 alpha. At 24 h post transfection, cells were treated with MG132 for 6 h, and c-Jun ubiquitination was detected by immunoblotting with Flag antibody after immunoprecipitation with anti-Flag antibody. *B.* 14-3-3 $\sigma$ <sup>+/+</sup> cells were transfected with c-Jun WT and c-Jun S267A with or without Myc-FBW7 alpha. At 24 h post transfection, cells were treated with MG132 for 6 h, and c-Jun ubiquitination was detected by immunoblotting with ubiquitin antibody after immunoprecipitation with anti-Flag antibody.

To further confirm the identity of these higher molecular weight species of c-Jun WT we performed same experiment followed by Western blotting with Ub antibody after immunoprecipitating c-Jun WT or S267A mutant with Flag antibody. We observed that the higher molecular weight species of c-Jun WT were also detected with Ub antibody suggesting that these higher molecular weight species of c-Jun are ubiquitinated in 14-3-

3 $\sigma$ <sup>+/+</sup> cells which are transfected with FBW7. Western blot with Flag and Myc antibody confirmed that both c-Jun and FBW7 were expressed optimally (Fig. 4.1.14.B). These results suggest that interaction of c-Jun with 14-3-3 $\sigma$  is important for targeting c-Jun to proteasomal degradation. And FBW7 is involved in ubiquitination of c-Jun in 14-3-3 $\sigma$ <sup>+/+</sup> cells.

#### **4.1.15. 14-3-3 $\sigma$ is required for the nuclear export of c-Jun.**

14-3-3 proteins are known for their function as ligand and adapter proteins and are also involved in nuclear cytoplasmic shuttling of multiple proteins (discussed in detail in the introduction section). Therefore, we wished to determine if 14-3-3 $\sigma$  is involved in sequestration of c-Jun in the cytoplasm and thereby target it to proteasomal degradation. To address leptomycin B (LMB) was used to inhibit nuclear cytoplasmic shuttling of proteins by inhibiting CRM1 protein of nuclear pore complex [389]. 14-3-3<sup>+/+</sup> cells that are transfected with either HA tagged c-Jun WT or Serine mutants (c-JunS58A and c-JunS267A) and treated with LMB showed nuclear accumulation of c-Jun as observed by immunofluorescence staining for HA antibody in DAPI stained nuclei in transfected cells identified by GFP expression. No expression was observed for either c-Jun WT or serine mutants in untransfected cells identified as GFP negative cells suggesting specificity of HA antibody. However, nuclear accumulation of c-JunS267A mutant even in LMB untreated conditions was observed suggesting that abrogation of interaction of c-Jun and 14-3-3 $\sigma$  leads to inhibition of nuclear export of c-Jun. Whereas, both c-Jun WT and c-Jun S58A mutant which can interact with 14-3-3 $\sigma$  showed no nuclear accumulation or cytoplasmic expression in cells that were not treated with LMB suggesting that when nuclear export/import was functional, 14-3-3 $\sigma$  could mediate their transport from nucleus to the cytoplasm where c-JunWT and c-JunS58A was targeted to proteasomal degradation (Fig 4.1.15.A).

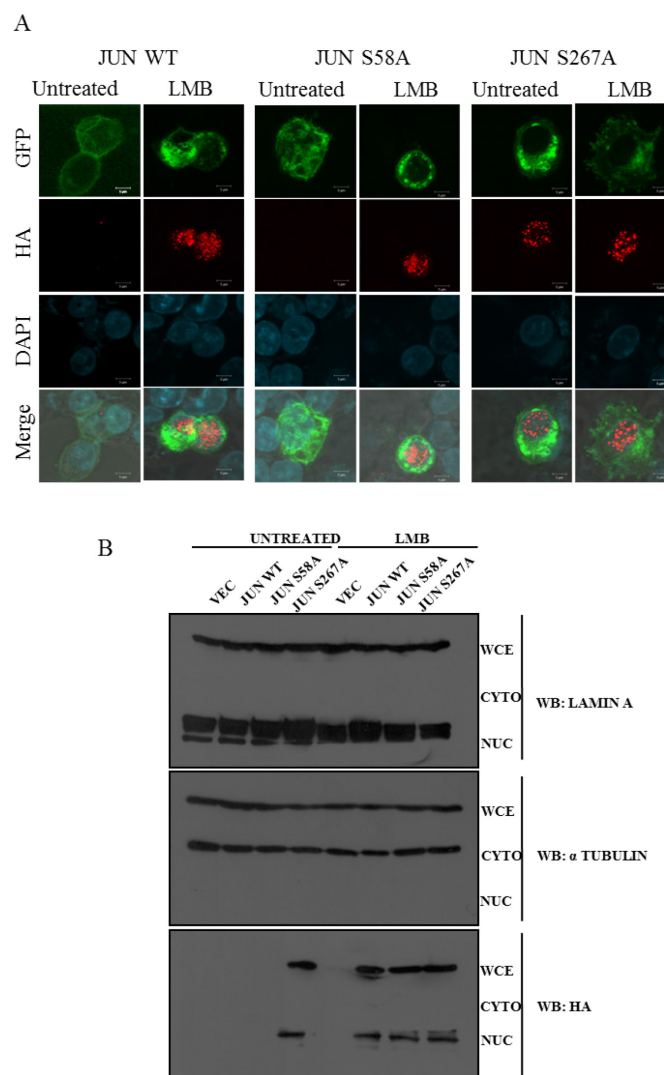


**Figure 4.1.15.** 14-3-3 $\sigma$  can induce the nuclear export of c-Jun. *A.* 14-3-3 $\sigma$ <sup>+/+</sup> cells were transfected with HA-c-JunWT, HA c-JunS58A and HA-c-JunS267A along with GFP vector. 24 hours post transfection cells were either treated or not treated with Leptomycin B (LMB) for 8 hours (see materials and methods for details). Post treatment cells were fixed and stained for indicated antibodies. Nuclei were stained with DAPI. Magnification is X63 with 4X optical zoom and bars indicate 5 $\mu$ m. *B.* 14-3-3 $\sigma$ <sup>+/+</sup> cells were transfected with HA-c-JunWT, HA c-JunS58A and HA-c-JunS267A. 24 hours post transfection cells were either treated or not treated with Leptomycin B (LMB) for 8 hours (see materials and methods for details). Post treatment cells or subjected to

*nuclear and cytoplasmic fractionation (see materials and methods for details) followed by SDG PAGE analysis and Western blotting with indicated antibodies.*

To further confirm our immunofluorescence results nuclear cytoplasmic fractionation with cells transfected with HA tagged c-Jun WT or Serine mutants (c-JunS58A and c-JunS267A) and treated or not treated with LMB were performed. Expression was observed for nuclear marker, laminin A and cytoplasmic markers,  $\alpha$ -tubulin in their respective compartments and in the whole cell lysate of both LMB treated and untreated group suggesting that nuclear cytoplasmic fractionation was clean and there were no cross contamination. In support of our immunofluorescence results it was observed that c-Jun WT and both serine mutants (c-JunS58A and c-JunS267A) showed expression in the nuclear as well as whole cell extract fractions in LMB treated group. However, only c-JunS267A mutant showed expression in both nuclear and whole cell extract fractions even in LMB untreated group suggesting that that abrogation of interaction of c-Jun and 14-3-3 $\sigma$  leads to inhibition of nuclear export of c-JunS267A mutant. Inhibition of nuclear export of c-JunS267A resulted in its unavailability to proteasomal machinery at the cytoplasm leading to its expression in the nuclear compartment (Fig. 4.1.15.B). These results suggest that interaction of 14-3-3 $\sigma$  and c-Jun is required for nuclear export of c-Jun. Once in the cytoplasm 14-3-3 $\sigma$  can target c-Jun proteasomal degradation in FBW7 dependent manner leading to low c-Jun protein levels in 14-3-3 $\sigma$ <sup>+/+</sup> cells. In 14-3-3 $\sigma$ <sup>-/-</sup> cells c-Jun is accumulated in the nuclear where it leads to increase in expression of Slug and thereby initiating EMT.

#### **4.1.16. 14-3-3 $\sigma$ regulates activation of Focal adhesion kinase (FAK).**

We have discussed in earlier sections that loss of 14-3-3 $\sigma$  leads to increase in cell migration and loss of cell to ECM adhesion. Both these processes are regulated by focal

adhesions and many other cell-cell junctions and signaling molecules (discussed in detail in introduction). To investigate if focal adhesions are differently regulated in 14-3-3 $\sigma$ <sup>+/+</sup> and 14-3-3 $\sigma$ <sup>-/-</sup> cells we wished determine activation status of FAK. FAK auto-phosphorylation at Tyrosine 397 (Y397) is a marker of its activation and known to regulate focal adhesion turnover leading to increased cell migration and compromised cell to ECM adhesion (discussed in introduction). To determine if phosphorylation at Y397 in FAK is altered on loss of 14-3-3 $\sigma$  Western blot analysis with phosphor-specific antibodies recognizing FAK when it is phosphorylated on Y397 was performed. Results showed that FAK Y397 phosphorylation was appreciably increased in 14-3-3 $\sigma$ <sup>-/-</sup> cells in comparison to 14-3-3 $\sigma$ <sup>+/+</sup> cells whereas, total protein levels of FAK remained same in both these cell lines (Fig. 4.1.16.A). This suggests that increased activation of FAK could be the upstream regulator of increased cell migration and decreased cell to ECM adhesion observed in 14-3-3 $\sigma$ <sup>-/-</sup> cells as compared to 14-3-3 $\sigma$ <sup>+/+</sup> cells.

We further wished to determine the mechanism of regulation of FAK activation by 14-3-3 $\sigma$ . It clearly appeared from the result discussed above that FAK activation was compromised in presence of 14-3-3 $\sigma$  in 14-3-3 $\sigma$ <sup>+/+</sup> cells. We hypothesized that 14-3-3 $\sigma$  could interact with FAK and this interaction might negatively regulate FAK auto-phosphorylation at Y397. To test this hypothesis, immunoprecipitation experiments were performed with 14-3-3 $\sigma$  antibody using cell lysates from 14-3-3 $\sigma$ <sup>+/+</sup> cells. It was observed FAK interacts with 14-3-3 $\sigma$  as observed by Western blot analysis using FAK antibody (Fig. 4.1.16.B). A reverse immunoprecipitation experiments were also performed where FAK was immunoprecipitated using FAK antibody. It was seen that 14-3-3 $\sigma$  could be detected in the complex immunoprecipitated with anti FAK antibody (Fig. 4.1.16.C). These results identified FAK as a novel interactor of 14-3-3 $\sigma$ .

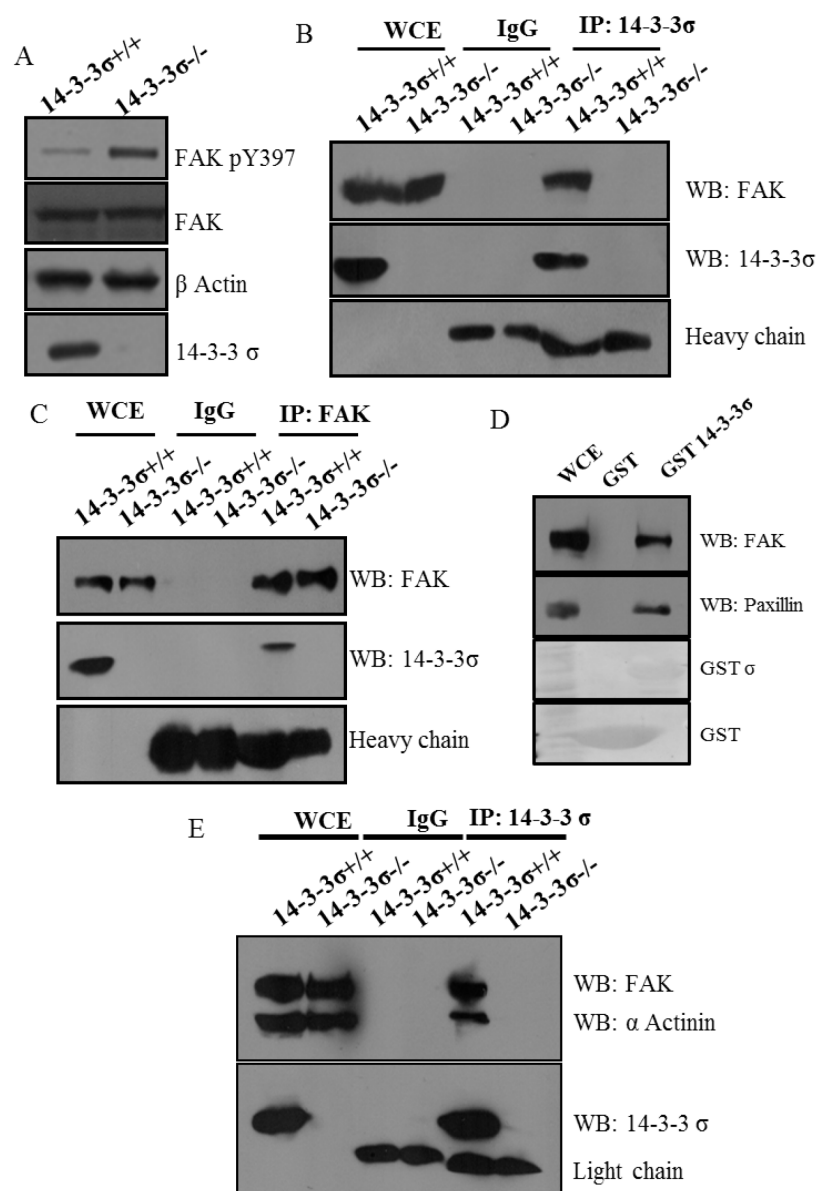


**Figure 4.1.16.** *14-3-3 $\sigma$  interacts with multiple focal adhesion proteins including Focal adhesion kinase (FAK) and regulates activation of FAK.* A. Equivalent amount of Cell lysates from 14-3-3 $\sigma$ <sup>+/+</sup> and 14-3-3 $\sigma$ <sup>-/-</sup> cells were resolved in SDS page along with 5% input was for whole cell extract (WCE). Western blotting was performed with indicated antibodies.  $\beta$  actin served as loading control. B. Equivalent amount of 14-3-3 $\sigma$ <sup>+/+</sup> and 14-3-3 $\sigma$ <sup>-/-</sup> cell lysates were immunoprecipitated with either 14-3-3 $\sigma$  antibody or isotype control (IgG). Immunocomplexes were resolved in SDS PAGE along with 5% input for whole cell extract (WCE) followed by Western blotting with indicated antibodies. Equal

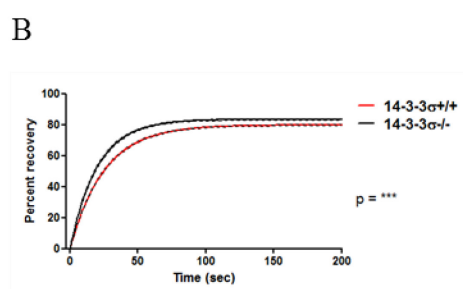
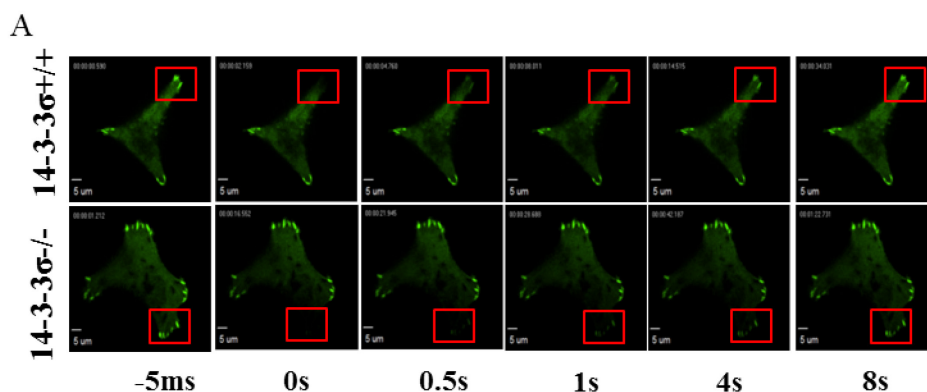
*intensity of heavy chain across samples incubated with IgG or 14-3-3 $\sigma$  antibodies suggest use of equivalent amount of antibody for IgG and 14-3-3 $\sigma$ . C. Equivalent amount of 14-3-3 $\sigma$ <sup>+/+</sup> and 14-3-3 $\sigma$ <sup>-/-</sup> cell lysates were immunoprecipitated with either FAK antibody or isotype control (IgG). Immunocomplexes were resolved in SDS PAGE along with 5% input for whole cell extract (WCE) followed by Western blotting with indicated antibodies. Equal intensity of heavy chain across samples incubated with IgG or 14-3-3 $\sigma$  antibody suggest use of equivalent amount of antibody for IgG and FAK. D. 14-3-3 $\sigma$ <sup>+/+</sup> cell lysates were incubated with bacterially purified GST or GST 14-3-3 $\sigma$ . Precipitates were resolved on SDS PAGE along with 5% input for whole cell extract (WCE). Western blotting was performed with indicated antibody. Expression of GST and GST14-3-3 $\sigma$  is shown in the ponceau stained membrane. E. Equivalent amount of 14-3-3 $\sigma$ <sup>+/+</sup> and 14-3-3 $\sigma$ <sup>-/-</sup> cell lysates were immunoprecipitated with either 14-3-3 $\sigma$  antibody or isotype control (IgG). Immunocomplexes were resolved in SDS PAGE along with 5% input for whole cell extract (WCE) followed by Western blotting with indicated antibodies. Equal intensity of heavy chain across samples incubated with IgG or 14-3-3 $\sigma$  antibody suggest use of equivalent amount of antibody for IgG and 14-3-3 $\sigma$ .*

Next we wished to determine if 14-3-3 $\sigma$  can also form complex with other focal adhesion proteins such as paxillin and  $\alpha$ -actinin. In vitro GST pull down assays with GST 14-3-3 $\sigma$  showed that paxillin could be detected by Western blot analysis in complex with 14-3-3 $\sigma$  in precipitates obtained using GST 14-3-3 $\sigma$  and not with GST alone (Fig. 4.1.16. D). Immunoprecipitation experiments carried out with 14-3-3 $\sigma$  antibody also identified  $\alpha$ -actinin in complex with 14-3-3 $\sigma$  and FAK (Fig. 4.1.16.E). These results suggest that 14-3-3 $\sigma$  can interact with FAK and also form complex with multiple focal adhesion proteins. Increased levels of auto-phosphorylation of FAK at Y397 suggest increased activation of FAK upon loss of 14-3-3 $\sigma$ . Increased activation of FAK can lead to phenotypic effects

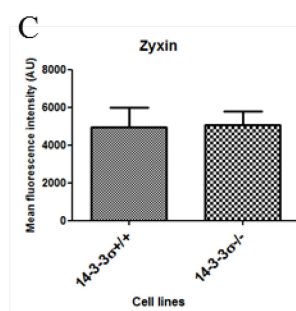
such as increased cell migration and decreased cell to ECM adhesion. There is possible that interaction of 14-3-3 $\sigma$  and FAK in 14-3-3 $\sigma$ <sup>+/+</sup> cells could inhibit activation of FAK by inhibiting auto-phosphorylation at Y397 by steric hindrance.

#### 4.1.17. 14-3-3 $\sigma$ <sup>-/-</sup> cells show increased turnover of focal adhesions.

Activation of FAK leads to multiple cellular effects as described in the introduction. Here we wished to determine if increased FAK activation can lead to increased focal adhesion turnover in 14-3-3 $\sigma$ <sup>-/-</sup> cells in comparison to 14-3-3 $\sigma$ <sup>+/+</sup> cells and thus promote cell migration as we have observed in migration assays discussed earlier.



Fluorescence recovery curve for zyxin



Mean whole cell fluorescence intensities for zyxin

D

|                 | Zyxin                          |                                |
|-----------------|--------------------------------|--------------------------------|
|                 | 14-3-3 $\sigma$ <sup>+/+</sup> | 14-3-3 $\sigma$ <sup>-/-</sup> |
| Half life       | 17.37                          | 13.85                          |
| Mobile fraction | 0.7978                         | 0.8346                         |

**Figure 4.1.17. 14-3-3 $\sigma$ <sup>-/-</sup> cells show faster recovery of mature focal adhesion protein zyxin.** A. Representative time lapse images of FRAP performed using 63x oil immersion lens and 488-Argon laser bleaching on a spinning disc confocal microscope in 14-3-3 $\sigma$ <sup>+/+</sup> or 14-3-3 $\sigma$ <sup>-/-</sup> cells separately transfected with GFP zyxin are shown (n =15). Magnification is X63 with 2X optical zoom and bars indicate 5 $\mu$ m. B. FRAP curves were plotted using GraphPad Prism software using non-linear regression curve fitting. C. Total fluorescence intensities for 14-3-3 $\sigma$ <sup>+/+</sup> or 14-3-3 $\sigma$ <sup>-/-</sup> cells separately transfected with GFP zyxin was calculated. Mean and standard deviation were plotted. D. Constants such as half-life and mobile fraction were derived from the non-linear regression curve fitting analysis are shown in the table.

To measure focal adhesion turnover we performed fluorescence recovery after photobleaching (FRAP) experiments (see materials and methods for details) using GFP tagged zyxin as marker for mature focal adhesion (discussed in detail in the introduction). GFP zyxin was expressed at a very low level to mimic physiological expression levels of zyxin in 14-3-3 $\sigma$ <sup>+/+</sup> and 14-3-3 $\sigma$ <sup>-/-</sup> cells. In addition we also quantitated total GFP intensity for GFP zyxin in 14-3-3 $\sigma$ <sup>+/+</sup> and 14-3-3 $\sigma$ <sup>-/-</sup> cells and found that there was significant difference in expression of GFP zyxin in both these cell lines (Fig. 4.1.17.C). However, fluorescence recovery over time post bleaching showed faster recovery of zyxin in 14-3-3 $\sigma$ <sup>-/-</sup> cells in comparison to 14-3-3 $\sigma$ <sup>+/+</sup> cells suggesting that mature focal adhesion which are required to provide necessary traction for during cell migration are rapidly turned over in 14-3-3 $\sigma$ <sup>-/-</sup> cells (Fig. 4.1.17.A). To analyse the kinetics of zyxin recovery in 14-3-3 $\sigma$ <sup>+/+</sup> and 14-3-3 $\sigma$ <sup>-/-</sup> cells we plotted normalized corrected fluorescence intensities for GFP zyxin at different time points post bleaching. We observed that at all the time points recovery of fluorescence intensity for zyxin was higher in 14-3-3 $\sigma$ <sup>-/-</sup> cells in comparison to 14-3-3 $\sigma$ <sup>+/+</sup> cells (Fig. 4.1.17.B). Also we observed shorter half-life and

---

greater mobile fraction for zyxin suggesting faster turnover of zyxin molecules in 14-3-3 $\sigma$ <sup>-/-</sup> cells in comparison to 14-3-3 $\sigma$ <sup>+/+</sup> cells (Fig. 4.1.17.D). These results suggest that 14-3-3 $\sigma$ <sup>-/-</sup> cells were able turnover mature focal adhesion faster than 14-3-3 $\sigma$ <sup>+/+</sup> cells. This explain why 14-3-3 $\sigma$ <sup>-/-</sup> cells are more migratory that 14-3-3 $\sigma$ <sup>+/+</sup> cells.



**4.2: To determine the role of 14-3-3 proteins in regulating transport of plakophilin3 and desmoplakin during desmosome assembly.**



Earlier results from our laboratory have shown that 14-3-3 $\gamma$  interacts with different desmosomal proteins such as PKP3, PG and DPI/II. 14-3-3 $\gamma$  has also been found to form complex with kinesin motor proteins as identified from mass spectrometry data from our laboratory. Further, a recently paper published from our laboratory suggested that 14-3-3 $\gamma$  acts as an adapter molecule between KIF5B and PG to regulate transport of PG to the cell border during desmosome formation. It was observed that loss of 14-3-3 $\gamma$  expression lead to defects in recruitment of PG to the cell border resulting in loss of desmosome function in HCT 116 cells [326]. Therefore, we wished to investigate role of 14-3-3 $\gamma$  in transport of other desmosomal proteins such as PKP3 and DP.

#### **4.2.1. PKP3 forms complex with 14-3-3 $\gamma$ and kinesin 1 family of motor proteins**

To determine if PKP3 forms a complex with 14-3-3 $\gamma$  and to identify the molecular motor proteins which could be involved in transport of PKP3 to the cell border we performed immunoprecipitation experiments and in vitro GST pull down assays. Immunoprecipitation experiments performed with anti PKP3 antibody identified KIF5B in complex with PKP3 on Western blot analysis with PKP3 antibody (Fig. 4.2.1. A). This suggests that KIF5B (heavy chain of kinesin 1 family motor proteins [discussed in detail in the introduction]) might be involved in transport of PKP3. We further wished to determine if we could identify 14-3-3 $\gamma$  as an interacting partner of KIF5B and PKP3. In vitro GST pull down assays performed with equivalent amounts of GST, GST14-3-3 $\gamma$  and GST KLC1 (light chain of kinesin 1 family motor proteins [discussed in detail in the introduction]) suggest that PKP3 can be detected in complex with 14-3-3 $\gamma$  in the precipitates obtained using GST 14-3-3 $\gamma$ . Also we identified PKP3 in complex with KLC1 in the precipitates obtained using GST KLC1 (Fig. 4. 2.1. B).

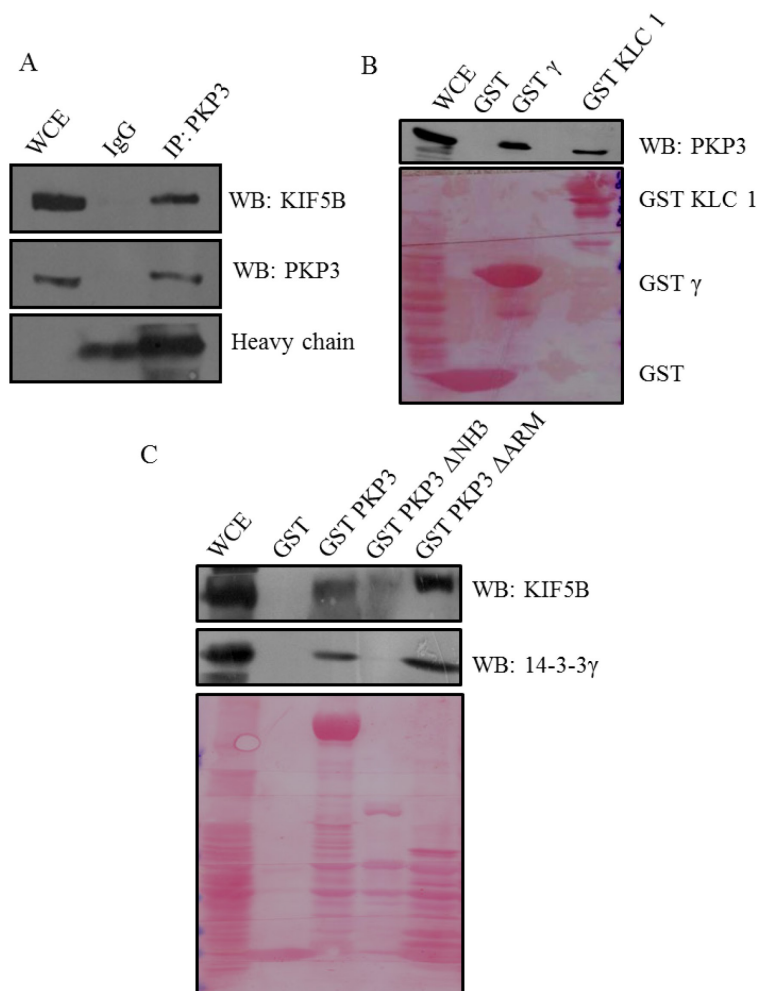


**Figure 4.2.1. PKP3 forms complex with 14-3-3 $\gamma$  and kinesin 1 family of motor proteins.** A. HCT116 Cell lysates were immunoprecipitated with either PKP3 antibody or isotype control (IgG). Immunocomplexes were resolved in SDS PAGE along with 5% input was for whole cell extract (WCE) along with 5% input for whole cell extract (WCE). Western blotting was performed with indicated antibodies. Equal intensity of heavy chain across samples incubated with IgG or PKP3 antibody suggests use of equivalent amount of antibody for IgG and PKP3. B. HCT116 cell lysates were incubated with bacterially purified GST or GST KLC1. Precipitates were resolved on SDS PAGE along with 5% input for whole cell extract (WCE). Western blotting was performed with indicated antibody. Expression of GST and GST KLC1 is shown in the ponceau stained membrane. C. HCT116 cell lysates were incubated with bacterially

*purified GST, GST PKP3, GST PKP3 $\Delta$ NH3 and GST $\Delta$ ARM proteins. Precipitates were resolved on SDS PAGE along with 5% input for whole cell extract (WCE). Western blotting was performed with indicated antibody. Expression of GST, GST PKP3, GST PKP3 $\Delta$ NH3 and GST $\Delta$ ARM proteins are shown in the ponceau stained membrane.*

To determine the domain in PKP3 which is responsible for interaction with 14-3-3 $\gamma$  and KIF5B we used in GST PKP3, GST PKP3 $\Delta$ NH3 and GST PKP3 $\Delta$ ARM which are bacterial expression constructs of full length, N-terminus deletion mutant and arm domain deletion mutant of PKP3 respectively. These constructs were previously generated in our laboratory (see material and methods for details). In vitro GST pull down assays with GST, GST PKP3, GST PKP3 $\Delta$ NH3 and GST PKP3 $\Delta$ ARM showed interaction of both KIF5B and 14-3-3 $\gamma$  with GST PKP3 $\Delta$ ARM and GST PKP3, whereas, no interaction was observed for either KIF5B or 14-3-3 $\gamma$  with GST and GST PKP3 $\Delta$ NH3 (Fig. 4. 2.1. C). These results suggest that N-terminal domain of PKP3 is important for its interaction with KIF5B and 14-3-3 $\gamma$ .

#### **4.2.2. PKP3 is necessary for interaction of 14-3-3 $\gamma$ and other desmosomal proteins.**

It was intriguing to observe that 14-3-3 $\gamma$  can interact with multiple desmosomal proteins which suggest that 14-3-3 $\gamma$  might play a role in transport of all these desmosomal proteins to the cell border. We were interested to determine if PKP3 has any role in regulating interaction of 14-3-3 $\gamma$  and other desmosomal proteins. To address this question we used PKP3 knockdown HCT116 cells (S9 and S10) and vector control cells (pTU6) previously generated in laboratory (see materials and methods for details). GST pull down assays with equivalent amount of proteins from pTU6, S9 and S10 showed that interaction of 14-3-3 $\gamma$  and DP as well as interaction of 14-3-3 $\gamma$  and PG was compromised in PKP3 knockdown cells such as S9 and S10 in comparison to vector control cells i.e. pTU6. No

nonspecific interactions with GST were seen (Fig. 4. 2.2. A). Knockdown of PKP3 can be appreciated in the Western blot analysis of whole cell extracts loaded as input.

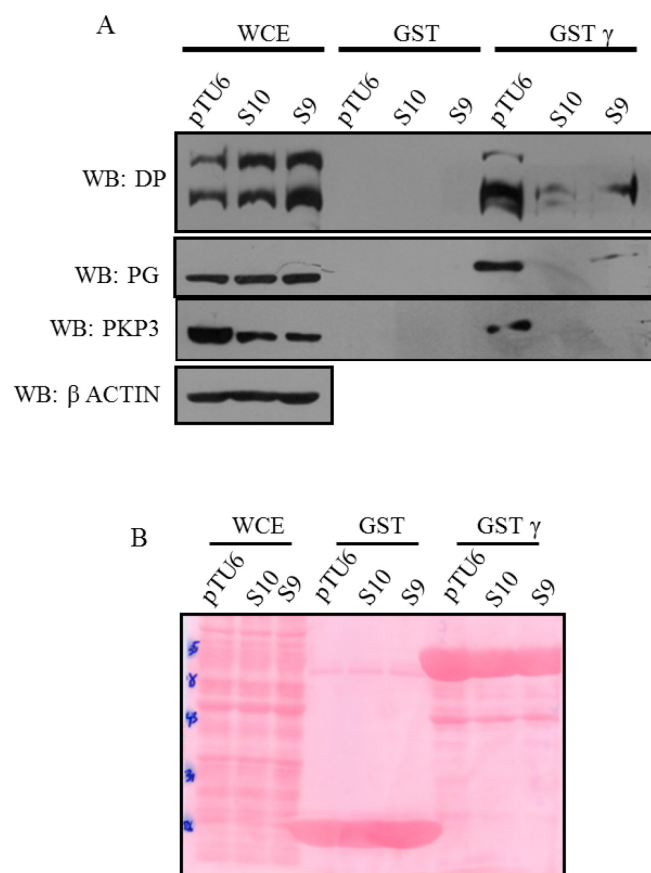


**Figure 4.2.2. Depletion of PKP3 expression leads to compromised interaction of 14-3-3 $\gamma$  and other desmosomal proteins.** A. Cell lysates of pTU6, S10 and S9 were incubated with bacterially purified GST or GST 14-3-3 $\gamma$ . Precipitates were resolved on SDS PAGE along with 5% input for whole cell extract (WCE). Western blotting was performed with indicated antibody. B. Expression of GST and GST14-3-3 $\gamma$  is shown in the ponceau stained membrane.

Equivalent amount of proteins present used for pTU6, S9 and S10 can be appreciated by  $\beta$  actin blot as well as from whole cell extracts in ponceau stained membrane. Equivalent loading for GST and GST14-3-3 $\gamma$  can also be appreciated in the ponceau stained

membrane (Fig. 4.2.2. B). These results suggest that PKP3 is necessary for interaction of 14-3-3 $\gamma$  with other desmosomal proteins such as PG and DP.

#### **4.2.3. Anterograde transport of PKP3 and PG is microtubule dependent.**

Previous results from our laboratory suggest that PG transport to the cell border requires an intact microtubule network and that PKP3 and PG are required for desmosome assembly [159, 326]. To determine if microtubules (MT) are required for the initiation of desmosome formation and transport of PKP3 to the cell border in HCT116 cells, nocodazole (NOC) was used to disrupt the microtubule network. Incubation of HCT116 cells with 10 $\mu$ M NOC for 3 hours completely disrupted the MT network (Fig. 4. 2.3. A). To determine the role of MT in anterograde transport of PKP3 during desmosome assembly, a calcium switch experiment was performed in cells treated with NOC (to disrupt MT) or DMSO (vehicle control) as described in Fig. 4.2.3. B. An immunofluorescence analysis showed that cell border localization of both PKP3 and PG was compromised upon disruption of MT post addition of calcium in comparison to DMSO treated cells (Fig. 4. 2.3. C & E).

Quantitation of the fluorescence intensity at the cell border after 30 minutes of calcium addition showed that recovery of both PKP3 and PG border staining intensity was significantly compromised in NOC treated cells compared to DMSO treated cells (Fig. 4. 2.3. D & F). However, no appreciable difference in cell border localization was observed at 0 minute post calcium switch in cell border intensity of either PKP3 or PG between NOC and DMSO treated cells (Fig. 4. 2.3. C-F). These results confirmed that the cell border recruitment of PKP3 and PG are dependent on an intact MT network and both these proteins followed a similar pattern of anterograde transport.

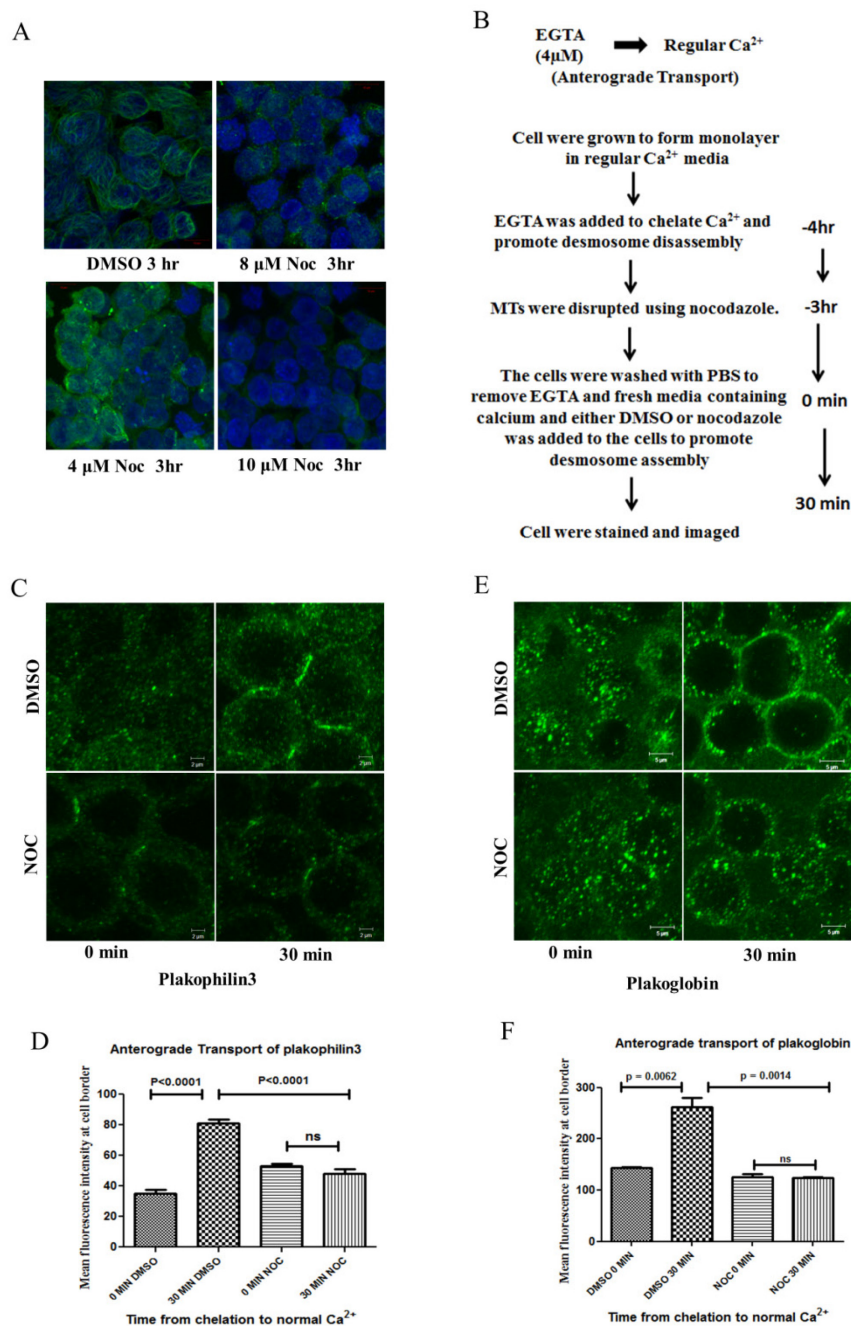


**Figure 4.2.3. Anterograde transport of PKP3 and PG is dependent on an intact microtubule network.** *A.* HCT116 cells were treated with DMSO or the indicated concentration of NOC for 3hrs. Cells were stained with antibodies to  $\alpha$ -tubulin to visualize MT and counterstained with DAPI. Magnification is X630 magnification with 2X optical zoom. *B.* Scheme of experiment to study anterograde transport of PKP3 and PG. *C-F.* HCT116 cells treated with EGTA and NOC or DMSO were fixed and stained

*with antibodies to PKP3 (C-D) or PG (E-F) followed by confocal microscopy. The intensity of border staining for both PKP3 and PG was measured for in least 30 cells in three independent experiments and the mean and standard deviation were plotted. Magnification is X630 with 4X optical zoom and bars indicate 5 $\mu$ m. p values were generated using a student's t test.*

#### **4.2.4. The retrograde transport of PKP3 and PG are differentially regulated.**

Desmosomes are dynamic and undergo continual assembly and disassembly during cell migration (described in detail in the introduction section). Therefore, we wished to determine the mechanism of transport of PKP3 and PG from the cell border to the cytoplasm during desmosome disassembly. To investigate the role of MT in the regulation of PKP3 transport during desmosome disassembly, EGTA was added to the medium to chelate calcium (described in materials and methods) either in the presence or absence of NOC (Fig. 4. 2.4. A). Three hours post addition of EGTA, PKP3 was localized at the cell border in NOC treated cells. In contrast, PKP3 levels decreased at the cell border in cells treated with DMSO upon chelation of calcium (Fig. 4. 2.4. B). No difference was observed in the localization of PKP3 in NOC and DMSO treated cells prior to addition of EGTA (Fig. 4. 2.4. B). Quantitation of fluorescence intensities at the cell border established that these differences were statistically significant (Fig. 4. 2.4. C). These results suggest that retrograde transport of PKP3 from the cell border to the cytoplasm is dependent on MT. In contrast, it was observed that NOC treatment had no effect on retrograde transport of PG upon addition of EGTA. PG localized to the cytoplasm in both NOC and DMSO treated cells 3hr post addition of EGTA (Fig. 4. 2.4. D-E). These results suggest that an intact MT network is not required for the retrograde transport of PG and different mechanisms regulate the retrograde transport of PKP3 and PG during desmosome disassembly.

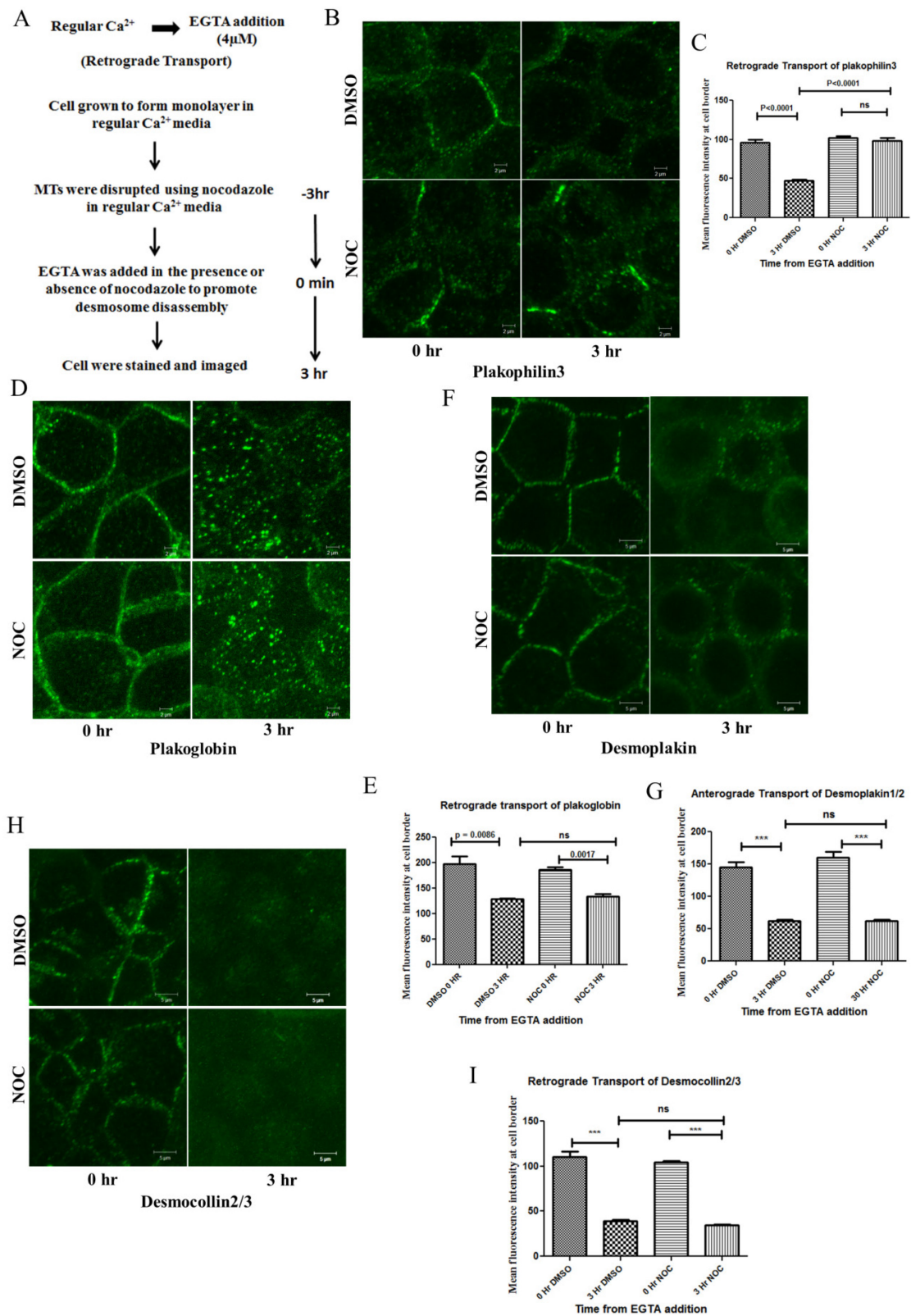


**Figure 4.2.4. Disruption of the microtubule network blocks retrograde transport of PKP3 but does not inhibit desmosome disassembly.** *A. Scheme of experiment to study retrograde transport of desmosomal proteins. B-I. HCT116 cells were treated with EGTA and NOC or DMSO and stained with antibodies to PKP3 (B-C), PG (D-E) DP (F-G) and DSC2/3 (H-I) followed by confocal microscopy. The intensity of staining at the cell border was measured for at least 30 cells in three independent experiments and mean and standard deviation were plotted. Note that disruption of the MT network results in a defect in the transport of PKP3 from the cell border to the cytoplasm in contrast to the results observed for the other desmosomal proteins. Confocal images were acquired at X630 magnification and 4X optical zoom. Bars indicate 5 $\mu$ m. *p* values were generated using a student's *t*-test.*

#### **4.2.5. Inhibition of retrograde transport of PKP3 does not inhibit desmosome disassembly.**

We have previously shown that PKP3 is required for transport of desmosomal proteins such as DSC2/3, DSG2, PKP2 and DP to the cell border and is required for initiation of desmosome assembly in HCT116 and HaCaT cells [159]. To determine whether retention of PKP3 at the cell border resulted in the retention of other desmosomal proteins at the cell border, the localization of DP and DSC2/3 in cells treated with NOC during desmosome disassembly was determined as described above.

We observed that though PKP3 is retained at the cell border 3hr post calcium chelation, both DP and DSC2/3 were not retained at the cell border (Fig. 4. 2.4. F&H). At 3hr post chelation, the levels of DP and DSC2/3 were diminished at the cell border in both NOC and DMSO treated cells, a phenotype similar to that observed for PG (Fig. 4. 2.4. G&I).

These results suggest that PKP3 retention at the cell border upon calcium chelation is not sufficient for the retention of other desmosomal proteins at the cell border.

#### **4.2.6. Desmoplakin forms complex with KLC2 and 14-3-3 $\gamma$ .**

We also wished to determine the molecular motor protein involved in transport of DP. To address this question we asked if DP interacts with kinesin motor family proteins. ). Interaction of DP with both KLC1 and KLC2 were tested by in vitro GST pull down assays. No interaction of DP with KLC1 was observed; therefore, interaction of DP with different domains of KLC1 such as TPR (Tetratricopeptide Repeat) and CC (Coiled coil) was also investigated. These constructs were previously described in published results from our laboratory [326]. In vitro GST pull down assays with GST, GST KLC1, GST TPR, GST CC, GST KLC2 and GST 14-3-3 $\gamma$  showed interaction of both 14-3-3 $\gamma$  and KLC2 with DP whereas, no interaction was observed for GST, GST KLC1, GST TPR and GST CC (Fig. 4. 2.5. A). 14-3-3 $\gamma$  was seen to form complex with both KLC1 and KLC2. Specifically TPR domain of KLC1 interacted with 14-3-3 $\gamma$  (Fig. 4. 2.5. A). This suggests that DP transport might be specifically regulated by KLC2 and not KLC1.

To determine the domain in DP, which is responsible for interaction with 14-3-3 $\gamma$  we, used DPI GFP and two deletion mutants of DP1, which contained amino acid from 1-1790 and 1-1380 respectively. These constructs were obtained from Lechler laboratory (see material and methods for details). In vitro GST pull down assays with HEK293 cell lysates which were transiently transfected with GFP vector, DPI GFP, DP 1-1790 and DP 1-1380 showed interaction of 14-3-3 $\gamma$  with DPI GFP, DP 1-1790 and DP, whereas, no interaction was observed for 14-3-3 $\gamma$  with GST (Fig. 4. 2.5. B). These results suggest that interaction 14-3-3 $\gamma$  and DP is regulated by amino acids ranging from 1-1380 of DP (Fig. 4. 2.5. B).

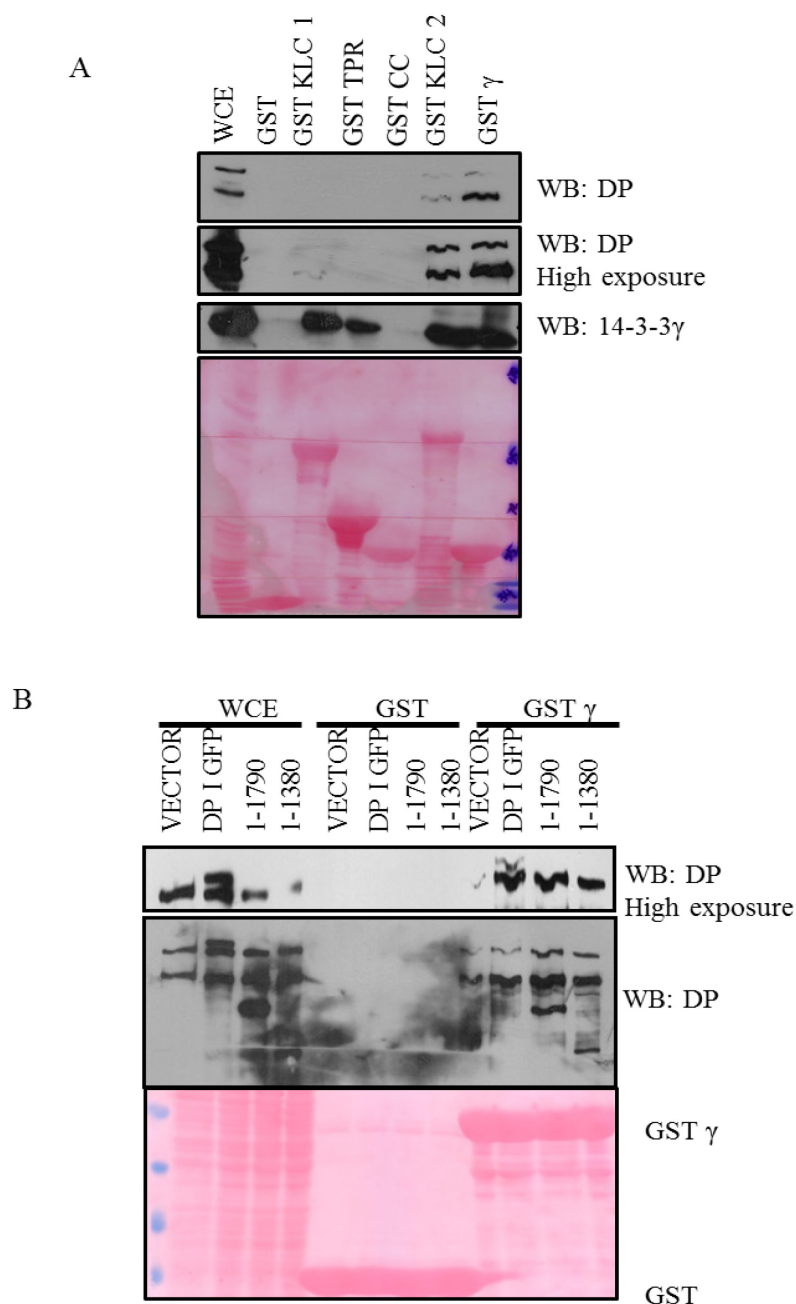


**Figure 4.2.5. Desmoplakin forms complex with 14-3-3 $\gamma$  and KLC2.** *A.* 14-3-3 $\sigma^{+/+}$  cell lysates were incubated with bacterially purified GST, GST KLC1, GST TPR, GST CC, GST KLC2 and GST 14-3-3 $\gamma$ . Precipitates were resolved on SDS PAGE along with 5% input for whole cell extract (WCE). Western blotting was performed with indicated antibody. Expression of GST, GST KLC1, GST TPR, GST CC, GST KLC2 and GST 14-3-3 $\gamma$  is shown in the ponceau stained membrane *B.* HEK293 cells were transfected

*separately with GFP vector, DPI GFP, DP 1-1790 and DP 1-1380. 24 hours post transfection cell lysates were prepared and incubated with bacterially purified GST or GST 14-3-3 $\gamma$ . Precipitates were resolved on SDS PAGE along with 5% input for whole cell extract (WCE). Western blotting was performed with indicated antibody. Expression of GST and GST14-3-3 $\gamma$  is shown in the ponceau stained membrane.*

## **CHAPTER 5: DISCUSSION**



14-3-3 proteins are known to regulate a large number of cellular processes such as cell signalling, cell polarity, cell migration, cell proliferation, apoptosis, cell cycle, protein trafficking and gene expression [288, 290-293, 326]. Aberrant regulation of expression of 14-3-3 proteins have been associated with multiple diseases including cancer progression and metastasis (reviewed in [293]). In this study we have investigated the role of 14-3-3 $\sigma$  and 14-3-3 $\gamma$  in regulation of cell-cell adhesion. We have observed that loss of 14-3-3 $\sigma$  leads to decrease in the expression of multiple cell-cell adhesion proteins. 14-3-3 $\sigma$ <sup>-/-</sup> cells showed decreased cell adhesion and increased cell migration. An elaborate study done in this thesis work showed that loss of 14-3-3 $\sigma$  lead to the initiation of an EMT program in HCT116 cells.

Earlier work from our laboratory has shown that 14-3-3 $\gamma$  is required for transport of PG to the cell border. Loss of 14-3-3 $\gamma$  leads to defects in desmosome formation and results in loss of cell-cell adhesion [326]. In continuation to these observations experiments performed towards the objectives described in this thesis showed that 14-3-3 $\gamma$  interacts with N-terminal domain of PKP3. PKP3 has been shown to interact with KIF5B and KLC1, which are heavy chain and light chain of kinesin 1 family of motor of proteins respectively. PKP3 knockdown has been shown to result in decrease in association of 14-3-3 $\gamma$  and other desmosomal proteins such as DP and PG. Though results described in this study and earlier results published from our laboratory show that both PG and PKP3 interacts with kinesin1 family of motor proteins, we have observed that anterograde and retrograde transport of PKP3 and PG are differentially regulated [384]. We have also observed that DP interacts with 14-3-3 $\gamma$  and KLC2.

### 5.1. 14-3-3 $\sigma$ loss leads to EMT

Aberrant expression of 14-3-3 proteins has been associated with multiple cancer types. Loss of expression of 14-3-3 $\sigma$  in particular has been associated with breast cancer, oral squamous cell carcinoma, urinary and bladder cancer, hepatocellular carcinoma, head and neck carcinoma, vulva squamous neoplasia and lung carcinoma [307, 309-312, 314, 315]. Previously published reports by different groups have delineated multiple mechanisms by which 14-3-3 $\sigma$  can loss promote cancer progression. These include deregulation of cell cycle checkpoint function upon DNA damage and loss of apoptotic function by regulating cyclin-CDK complex and BCL2 antiapoptotic proteins [390-393]. 14-3-3 proteins are also known to regulate raf activity [394]. Raf kinase is reported to negatively regulate cell migration through Rho signalling and Ras-MEK/Erk pathway [395, 396]. Therefore, it is possible that 14-3-3 $\sigma$  can regulate cell migration through raf. However, no such evidence exist in the literature to support this hypothesis. Reports published by other groups demonstrated a role for 14-3-3 $\sigma$  in regulation of epithelial cell polarity. Loss of cell polarity is encountered during the process of EMT as well [325]. In cancers of epithelial origin cancer progression is often accompanied with EMT [348]. However, regulation of EMT by 14-3-3 $\sigma$  during cancer progression is not well studied. But role of 14-3-3 $\sigma$  in regulation of EMT has no been investigated. Here we demonstrated for the first time that loss of 14-3-3 $\sigma$  could initiate an EMT program. This is important because it explains how loss of 14-3-3 $\sigma$  could help cells to acquire invasive and migratory phenotype to enable them to invade into local blood and lymphatic vessels. We observed that loss of 14-3-3 $\sigma$  leads to decrease in expression of proteins of multiple epithelial markers such as desmosomal proteins e.g. PKP3, PG, DSC2/3, DSG2 and DP; adherens junction proteins e.g. E cadherin and  $\beta$  catenin; tight junction protein, ZO1; intermediate filament proteins

such as K8 and K18. On the other hand expression of mesenchymal proteins such as adherens junction cadherin, N cadherin and intermediate filament protein, vimentin are increased in 14-3-3 $\sigma$ <sup>-/-</sup> cells as comparison to 14-3-3 $\sigma$ <sup>+/+</sup> cells. Thus what we observed in 14-3-3 $\sigma$ <sup>-/-</sup> cells is a distinct switch in expression from epithelial cadherin to mesenchymal cadherin and switch from epithelial intermediate filament protein expression to mesenchymal intermediate protein, vimentin. This is classical example for EMT [348]. Functional assays carried out in this study showed that 14-3-3 $\sigma$ <sup>-/-</sup> cells acquired migratory and invasive characteristics. 14-3-3 $\sigma$ <sup>-/-</sup> cells also showed decreased cell-cell adhesion and cell to ECM adhesion in comparison to 14-3-3 $\sigma$ <sup>+/+</sup> cells. A lot of matrix degrading enzymes are found to be upregulated during EMT (reviewed in [353]). We have also observed increase in the expression of MMP3 on loss of 14-3-3 $\sigma$ . We have further confirmed that these EMT like phenotypic changes and alterations in expression of epithelial or mesenchymal markers seen in 14-3-3 $\sigma$ <sup>-/-</sup> cells are specific to loss of 14-3-3 $\sigma$ . We observed reversal of these EMT like profile on ectopic expression of 14-3-3 $\sigma$  in 14-3-3 $\sigma$ <sup>-/-</sup> cells.

Change in expression of such large number of proteins during EMT is brought about by multiple EMT specific transcription factors such as Sail, Slug, ZEB and Twist. These transcription factors function in concert and exhibit mutually exclusive as well as redundant roles in regulating EMT [347-350]. We observed that 14-3-3 $\sigma$ <sup>-/-</sup> cells showed increased expression of Slug and ZEB1. Slug and ZEB1 both are known to bind to E boxes in the promoter of E cadherin and repress its expression [361, 364]. These two EMT specific transcription factors are also known to regulate expression of tight junction proteins and intermediate filament proteins [397, 398]. A positive correlation has also been observed between expression of Slug, ZEB1 and mesenchymal marker, N cadherin

[399]. Also literature suggests that Slug can promote ZEB1 expression indicating a positive feedback in regulation of these EMT specific transcription factors [400]. Our observations also confirmed existence of such positive feedback mechanism for regulation of ZEB1 by Slug. We have observed that knockdown of Slug could decrease expression of ZEB1 proteins levels. Our results also suggest that Slug is indeed implicated in regulating EMT program observed on loss of 14-3-3 $\sigma$ . We showed that knockdown of Slug in 14-3-3 $\sigma$ <sup>-/-</sup> cells lead to decreases in expression of mesenchymal markers and increase in expression of epithelial markers. Thus down-regulation of Slug in 14-3-3 $\sigma$ <sup>-/-</sup> cells could rescue epithelial characteristic in 14-3-3 $\sigma$ <sup>-/-</sup> cells. In addition we have also observed that ectopic expression of 14-3-3 $\sigma$  in 14-3-3 $\sigma$ <sup>-/-</sup> cells resulted in decreases in the protein levels of Slug suggesting that increase in Slug expression is a specific effect of loss of 14-3-3 $\sigma$ . However, we did not observed any change in expression of Sail or Twist in 14-3-3 $\sigma$ <sup>+/+</sup> and 14-3-3 $\sigma$ <sup>-/-</sup> cells. Therefore, we conclude that Slug is the master regulator of initiation of EMT program on loss of 14-3-3 $\sigma$  as observed in HCT116 cells.

There are multiple signalling and cellular mechanisms, which can regulate expression and function of Slug. TGF $\beta$  has been shown to induce expression of Sail, SNI2, ZEB and Twist family of EMT specific transcription factors [348, 370]. Slug plays an important role during the initial phase of growth factor induced EMT where it promotes desmosome dissociation, cell spreading and initiation of cell separation [371]. AP1 transcription factor c-Jun is reported to activate Slug expression [372]. There are other mechanisms and pathways, which can positively regulate expression of Slug such as MAPK signalling and transcription factors such as Myb and c-Jun [401-403]. We have tested a number of upstream regulators of Slug, which are different kinases downstream of MAPK pathway

such as ERK, p38 MAPK, AKT and MEK. We did not observe any change in expression or activation status of those upstream regulators.

We observed that in 14-3-3 $\sigma$ <sup>-/-</sup> cells Slug transcription was positively regulated by AP1 transcription factor c-Jun. We demonstrated that proteasomal degradation of c-Jun was inhibited in 14-3-3 $\sigma$ <sup>-/-</sup> cells. This resulted in accumulation of c-Jun in the nucleus of 14-3-3 $\sigma$ <sup>-/-</sup> cells, which in turn increased the Slug transcription. However, in 14-3-3 $\sigma$ <sup>+/+</sup> cells c-Jun was targeted to proteasomal degradation leading to an inhibition of Slug expression in 14-3-3 $\sigma$ <sup>+/+</sup> cells. c-Jun protein levels could be stabilized in 14-3-3 $\sigma$ <sup>+/+</sup> cells on treatment with proteasomal inhibitor MG132 and after stabilizing c-Jun protein in 14-3-3 $\sigma$ <sup>+/+</sup> cells, 14-3-3 $\sigma$  was seen to form complex with c-Jun in co-IP experiments. Our data suggest that the possible mechanism by which 14-3-3 $\sigma$  could regulate proteasomal degradation of c-Jun is by interacting with c-Jun and targeting it to the proteasomal machinery in the cytoplasm (Fig. 5.1). A similar function for 14-3-3 $\sigma$  was previously reported where 14-3-3 $\sigma$  was shown to mediate nuclear export of  $\Delta$ Np63 $\alpha$  and thereby targeting  $\Delta$ Np63 $\alpha$  to proteasomal degradation in the cytoplasm [404]. Our immunofluorescence and cytoplasmic fractionation experiments with LMB treated cells also indicated that 14-3-3 $\sigma$  is required for nuclear export of c-Jun. Results published by various other groups also suggest that 14-3-3 $\sigma$  localises to nucleus and may function as nuclear export factor for its ligands such as transcription factor FKHRL1, COP1 and  $\Delta$ Np63 $\alpha$  [404-406]. However, it has also been shown that 14-3-3 $\sigma$  can inhibit nuclear export of its ligand e.g. 14-3-3 $\sigma$  can interact with p53 and inhibit its nuclear export and mdm2 mediated targeting to proteasomal degradation [407]. A nuclear export signal (NES) has been identified in leucine rich region in the C-terminal  $\alpha$  helix of 14-3-3 $\sigma$  [405]. 14-3-3 $\sigma$  can also sequester its ligands such as Cdc25C and BAD in the cytoplasm

and thus regulate cellular events [408]. We observed that 14-3-3 $\sigma$  binding deficient mutant of c-Jun was not degraded in in vitro as well as in in vivo ubiquitination assay whereas, the wild type c-Jun as well as another serine to alanine mutant which was able to interact with c-Jun was degraded by proteasomal machinery. In addition nuclear cytoplasmic fractionation and immunofluorescence experiments with LMB also showed that 14-3-3 $\sigma$  binding deficient mutant of c-Jun failed to undergo nuclear export. It would be important to mention here that though a nuclear localization signal has been identified near the leucine zipper region of c-Jun but no NES has been reported in c-Jun protein [409]. Thus interaction of c-Jun and 14-3-3 $\sigma$  was necessary for targeting c-Jun to proteasomal degradation.

We observed in HCT116 cells 14-3-3 $\sigma$  mediated proteasomal degradation of c-Jun through FBW7. However, literature suggests presence of other E3 ligases such as COP1 and ITCH, which could also mediate degradation of c-Jun in epithelial cells [373-375]. An interesting observation that came from results published by another group suggests that loss of FBW7 also lead to EMT like profile in hepatocellular carcinoma cells [376]. This further supported our findings and showed that FBW7 could be implicated in the initiation of EMT program on loss of 14-3-3 $\sigma$ .

The in vivo tumor formation study suggests that 14-3-3 $\sigma$ <sup>-/-</sup> cells were inefficient in comparison to 14-3-3 $\sigma$ <sup>+/+</sup> cells to form primary tumor as well as distant lung metastasis. It needs to be emphasized that in vitro results suggested that loss of 14-3-3 $\sigma$  resulted in phenotypic changes associated with EMT and neoplastic progression. These contradictory results may mean that 14-3-3 $\sigma$  loss might be required at an early step during cancer progression. Indeed it has been observed that an increase in hypermethylation at 14-3-3 $\sigma$

gene is associated with transition from atypical hyperplasia to invasive breast carcinoma [308].

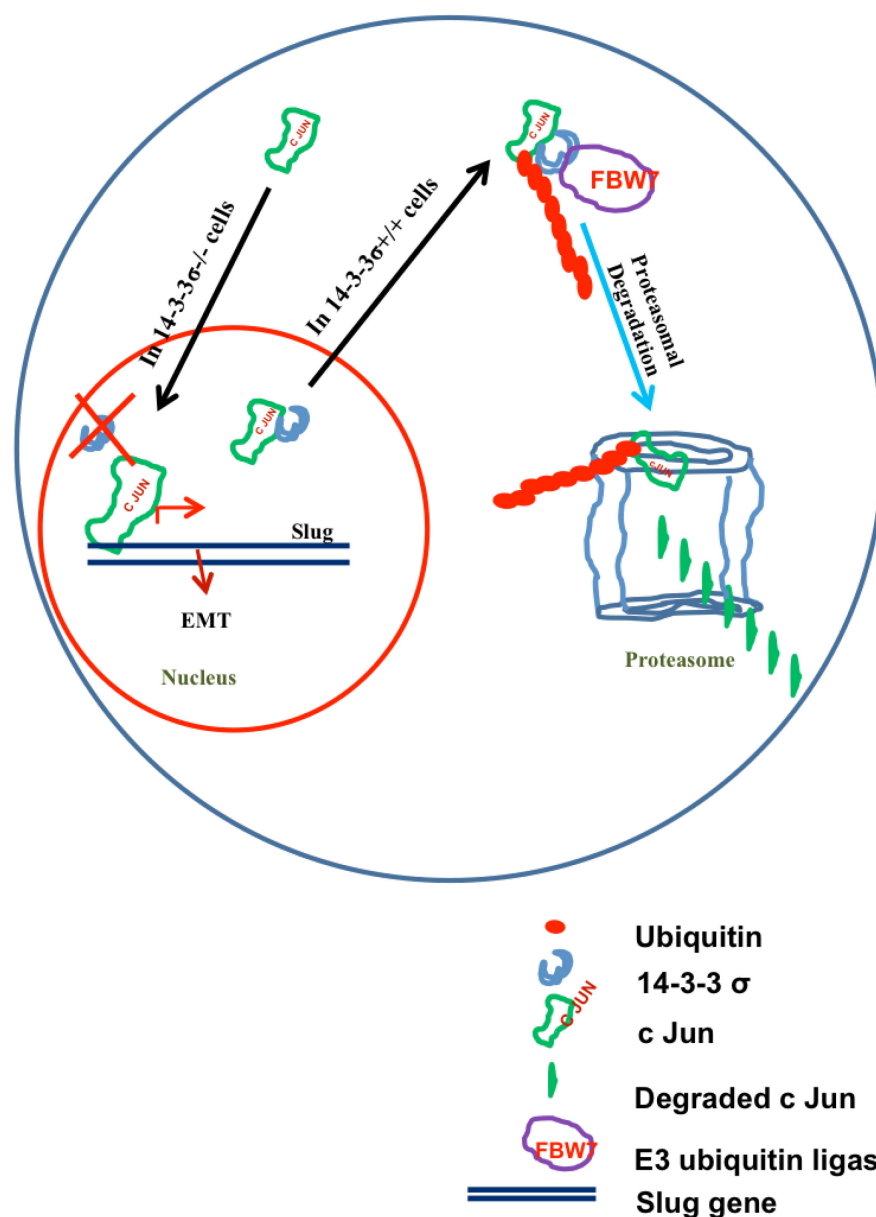


**Figure 5.1.** *14-3-3σ loss leads to epithelial to mesenchymal transition by stabilizing c-Jun protein levels. Blue circle denotes a cell and red circle denotes the nuclear compartment inside the cell. In absence on 14-3-3σ, c-Jun is not exported out from the nuclear compartment and promotes transcription of Slug gene. In 14-3-3σ<sup>+/+</sup> cells c-*

*Jun is exported out from the nucleus and targeted to proteasomal machinery in the cytoplasm in FBW7 dependent manner (see text for more details).*

Multiple reports in the literature support this hypothesis as in most of cancers expression of 14-3-3 $\sigma$  is down regulated by epigenetic modulation. SAGE analysis revealed that mRNA levels of 14-3-3 $\sigma$  were undetectable in more than 90% of primary breast carcinomas that were tested. High frequency of hypermethylation at the promoter region and CpG islands at the 14-3-3 $\sigma$  gene locus was identified as the prevalent mechanism of down-regulation of 14-3-3 $\sigma$  in breast cancer [307, 308]. Such epigenetic modulation is a reversible program. Metastasis is not only determined by the ability of the cells to undergo EMT. There is sufficient literature, which suggests that a reversal of EMT i.e. MET is required at the distant metastatic sites for successful colonisation by the cancer cells (reviewed in [353, 410, 411]). Expression of 14-3-3 $\sigma$  could be important for such reversal of EMT. Reports published by other groups and results from our work suggest that loss of 14-3-3 $\sigma$  leads to compromised cell proliferation, radio sensitivity and decrease in growth potential This could be because of increased susceptibility of 14-3-3 $\sigma$   $-/-$  cells to DNA damage and deregulation of cell cycle checkpoint function which ultimately results to apoptosis [412]. Therefore, loss of 14-3-3 $\sigma$  would inhibit the MET process [411]. This means that in cases where both alleles of 14-3-3 $\sigma$  is deleted e.g. in HCT116 14-3-3 $\sigma$   $-/-$  cells; cells undergo EMT but cannot reprogram this process and fail to initiate MET which is required for metastasis and tumor progression. However, more studies would be required to address this hypothesis. One of the approaches could be to analyse alterations in proteins that are known to contribute to tumor progression among 14-3-3 $\sigma$   $+/+$  and 14-3-3 $\sigma$   $-/-$  cells by proteomic and transcriptomic analysis.

## 5.2. 14-3-3 $\sigma$ loss leads to altered actin dynamics and focal adhesion turnover to regulate cell migration.

One of the mechanisms that play an important role in regulating cell migration is the focal adhesion turnover and associated actin dynamics [215, 413-415]. Our results suggested that 14-3-3 $\sigma$ <sup>-/-</sup> cells were more migratory and showed decreased cell to ECM adhesion in comparison to 14-3-3 $\sigma$ <sup>+/+</sup> cells. A detailed analysis for focal adhesion and actin dynamics related proteins revealed that FAK phosphorylation at tyrosine 297 (Y297) was increased in 14-3-3 $\sigma$ <sup>-/-</sup> cells in comparison to 14-3-3 $\sigma$ <sup>+/+</sup> cells. Phosphorylation of Tyrosine 397 (Y397) results in activation of FAK and this phosphorylation event is induced upon integrin engagement [231]. Further clustering of FAK at focal adhesion enhances Y397 phosphorylation generating a binding site for Src. Src phosphorylates FAK at Y576 and Y577 in the kinase domain leading to the activation of FAK kinase activity [232]. Additional phosphorylation of FAK at Y861 and Y925 by Src creates docking sites for SH2 domain containing proteins such as Grb2, which leads to activation of Ras and MAPK pathway [233, 234]. However, we have not observed any change in activation of MAPK pathway in 14-3-3 $\sigma$ <sup>+/+</sup> and 14-3-3 $\sigma$ <sup>-/-</sup> cells. FAK phosphorylation at Y397 is also known to induce focal adhesion turnover. The exact mechanism of this process has not been delineated. However, some events that occur during focal adhesion disassembly involve extension of microtubules to the focal adhesion followed by internalization of integrin by endosomes. This coincides with the recruitment of Grb2 followed by dynamin (reviewed in [215, 218]). Dynamin, which is a microtubule binding protein mediate transport of endocytic vesicles containing internalized integrin from the disassembled focal adhesion (reviewed in [215]). We have measured focal adhesion turnover using focal mature focal adhesion marker zyxin and observed that zyxin turnover was higher in 14-3-3 $\sigma$ <sup>-/-</sup> cells in comparison to 14-3-3 $\sigma$ <sup>+/+</sup> cells. Earlier results from our

laboratory showed higher turnover of nascent focal adhesion marker paxillin in 14-3-3 $\sigma$ <sup>+/+</sup> cells on comparison to 14-3-3 $\sigma$ <sup>-/-</sup> cells [387]. This is a first report where we have shown that during cell migration turnover of nascent and mature focal adhesion markers are differentially regulated. Turnover of proteins associated with nascent focal adhesions are slowed in rapidly migrating cells as nascent focal adhesions undergo maturation and doesn't go through premature turnover. However, cell, which are relatively sessile, do not show fast kinetics for focal adhesion maturation cycle. Thus nascent focal adhesions do not undergo maturation and go through premature turnover in relatively less migratory cells (Fig. 5.2). Rapidly migrating cells need continuous formation and disassembly of mature focal adhesions at the leading edge of the cell resulting in faster turnover of mature focal adhesions (Fig 5.2). We observed a faster turnover of mature focal adhesion protein, zyxin in 14-3-3 $\sigma$ <sup>-/-</sup> cells in comparison to 14-3-3 $\sigma$ <sup>+/+</sup> cells. Increased phosphorylation of FAK at Y397 also leads to decrease in focal adhesion strength. 14-3-3 $\sigma$ <sup>-/-</sup> cells, which had phosphorylation of FAK at Y397 showed, compromised focal adhesion strength in comparison to 14-3-3 $\sigma$ <sup>+/+</sup> cells [387].

We speculate that the possible mechanism through which 14-3-3 $\sigma$  could regulate phosphorylation of FAK at Y397 is by direct interaction of 14-3-3 $\sigma$  and FAK. We have observed that 14-3-3 $\sigma$  interacts with FAK and other focal adhesion proteins such as paxillin and  $\alpha$ -actinin. These results suggest that 14-3-3 $\sigma$  could either localize to focal adhesion or form complex with multiple focal adhesion proteins in the cytoplasm. However, these possibilities need to be further tested by appropriate experiments.

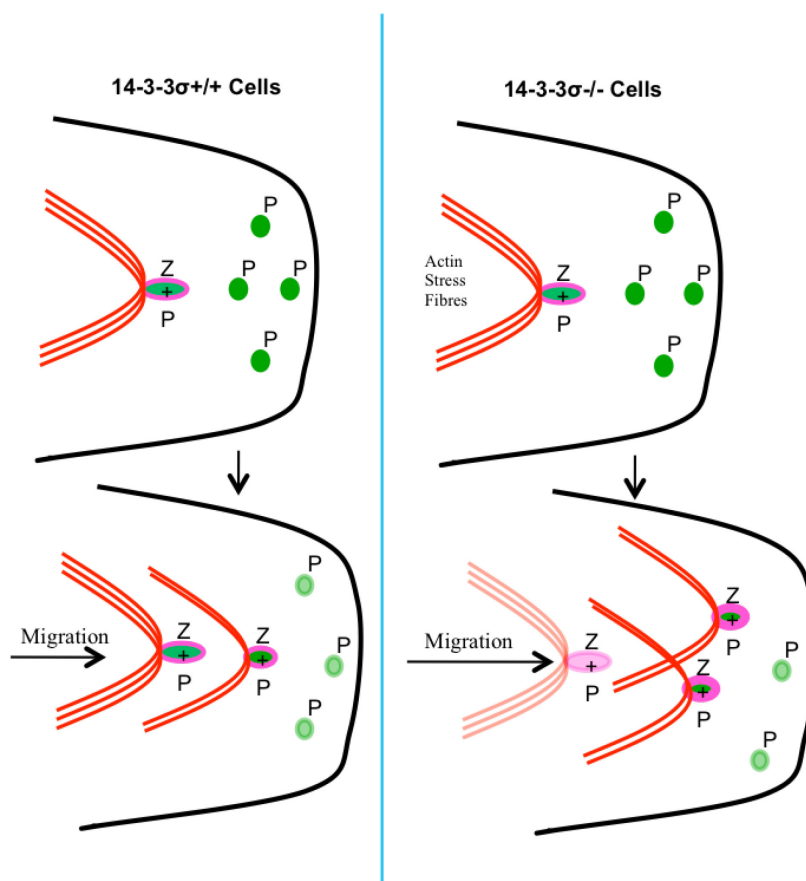


**Figure 5.2.** Turnover of nascent and mature focal adhesions are differentially regulated during rapid cell migration (reproduced from [387]). Solid green circles labelled as “P” denotes paxillin containing nascent focal adhesions. Faded green circles labelled as “P” denotes paxillin containing nascent focal adhesions that are going through disassembly. Solid pink oval structures labelled as “ZP” denotes mature focal adhesions containing both zyxin and paxillin. Faded pink oval structures labelled as “ZP” denotes mature focal adhesions containing both zyxin and paxillin that are going through disassembly. Red arcs denote dorsal actin stress fibres. Black arc indicates the migrating front of the cell.

Previous results from our laboratory (unpublished data) showed significant differences in the actin cytoskeleton and activation of actin dynamics regulating proteins in 14-3-3 $\sigma$ <sup>+/+</sup> and 14-3-3 $\sigma$ <sup>-/-</sup> cells. 14-3-3 $\sigma$ <sup>-/-</sup> cells showed more filopodia formation and decrease in

the activation of RhoA [388]. RhoGTPases such as RhoA/B/C, Rac1/2/3 and Cdc42 regulate the activity of a number of actin related proteins, kinases and phosphatases that are involved in actin filament nucleation, actin filament severing function and actin bundling.

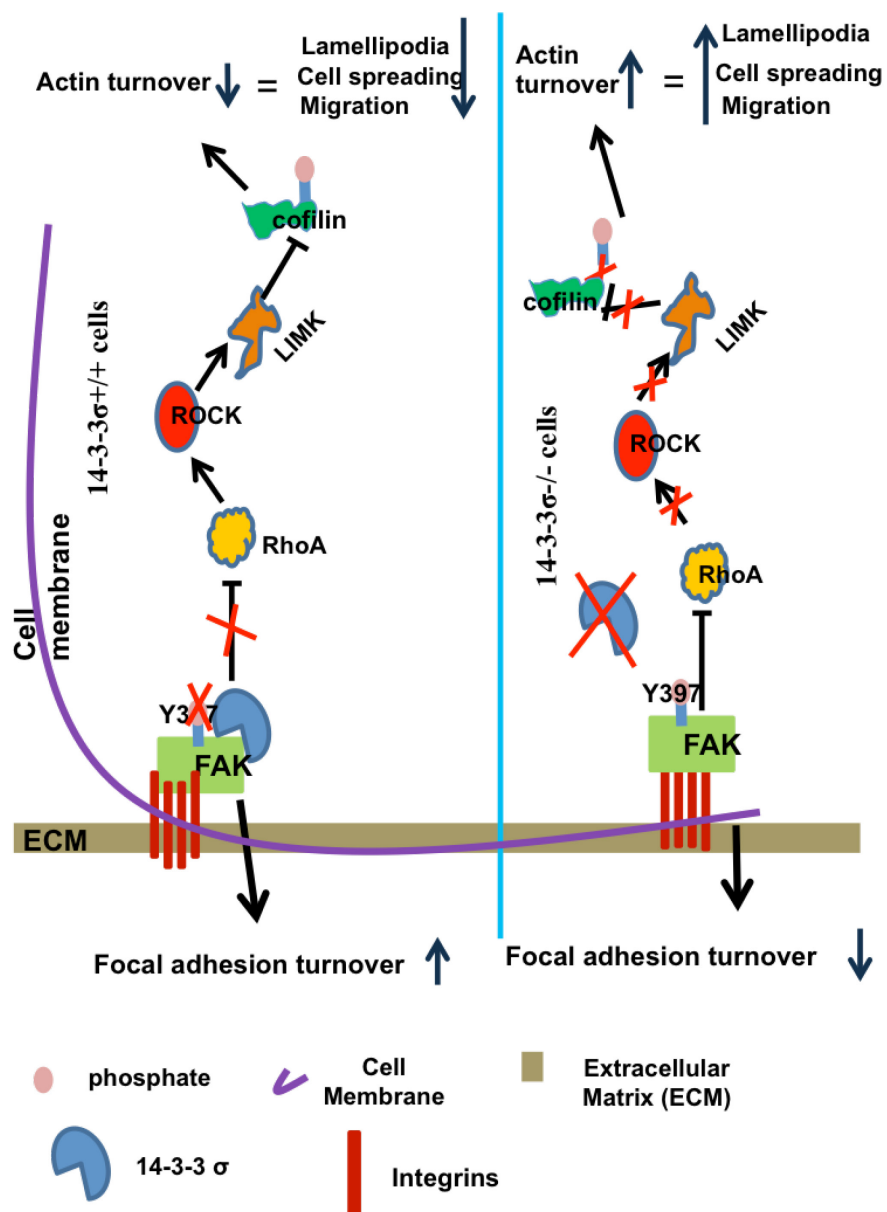


*Figure 5.3. 14-3-3 $\sigma$  regulates focal adhesion turnover and actin dynamics. See text for details.*

The activity these actin regulatory protein such as WASP, VASP, Arp2/3, Cofilin, Profilin, Myosin II, ROCK, LIMK are PAK (p21 activated kinase) are regulated by a number of activating and inhibitory phosphorylation events (reviewed in [254, 256, 257]). RhoA leads to altered actin dynamics in 14-3-3 $\sigma$ <sup>-/-</sup> cells by relieving the inhibitory phosphorylation at serine 9 (S9) position of cofilin (Fig. 5.3) [388]. Results published by other groups showed that FAK can suppress RhoA activity [416]. But the exact mechanism by which FAK regulates RhoA activity is not known. Cofilin is an actin severing protein and promotes faster actin turnover during cell migration [273, 274].

In presence of 14-3-3 $\sigma$ , activation of FAK is inhibited. In absence of activated FAK, RhoA becomes active and phosphorylates cofilin at S9 through ROCK and LIMK. This inhibitory phosphorylation of cofilin at S9 leads to loss of actin severing function of cofilin, which results in compromised actin turnover (Fig. 5.3). However, in 14-3-3 $\sigma$ <sup>-/-</sup> cells, FAK is active which inhibits activation of RhoA. In absence of activated RhoA cofilin becomes active and this could lead to faster actin turnover and promote cell migration (Fig. 5.3).

### **5.3. Role of 14-3-3 $\gamma$ in regulating transport of PKP3 and DP during desmosome assembly**

Previous results from our laboratory showed that 14-3-3 $\gamma$  could form complex with multiple desmosomal proteins such as PG, PKP3 and DP [326]. We have showed in this study that both PKP3 and DP can interact with kinesin 1 family of motor proteins. It was observed that the N-terminal domain of PKP3 is responsible and sufficient to interact with both 14-3-3 $\gamma$  and KIF5B. Also we have seen that PKP3 forms a complex with KLC1 in in vitro GST pull-down assays. This suggest that transport of PKP3 to the cell border could be regulated by kinesin 1 family of motor proteins and 14-3-3 $\gamma$  could play a role of

adaptor proteins between PKP3 and motor proteins. Results published from our laboratory have already suggested similar role for 14-3-3 $\gamma$  during transport of PG to the cell border during desmosome assembly [326]. Interestingly, we observed that knockdown of PKP3 compromised the interaction of 14-3-3 $\gamma$  and other desmosomal proteins such as PG and DP. This suggest that role of PKP3 and PG during desmosome assembly could be differentially regulated by 14-3-3 $\gamma$ .

The process of desmosome assembly and disassembly is not completely understood, especially the process of desmosome disassembly. The results presented in this report demonstrate that the transport of PG and PKP3 from the cell border to the cytoplasm upon desmosome disassembly is differentially regulated, with an intact MT network being an absolute requirement for the retrograde transport of PKP3. These results suggest that the different ARM proteins are transported to the cytoplasm by different pathways upon desmosome disassembly.

It is also interesting to note that border retention of PKP3 on treatment with NOC at 3hr post calcium chelation was not sufficient to retain DP and DSC2/3 at the cell border. While PKP3 plays a crucial role in recruiting DP, PKP2, DSG2 and DSC2/3 proteins to the cell border [10,11,15,20], the results reported here suggest that PKP3 might not play a similar role during desmosome disassembly. It is possible that loss of PKP3 from the cell border is not required for desmosome disassembly and that the PKP3 present at the cell border under conditions of calcium chelation might have desmosome independent functions or serve as a marker for the formation of new desmosomes upon the restoration of calcium to the medium. Further, Kowalczyk et.al. have shown that PV IgG antibodies against DSG3 that are produced during the autoimmune disease PV cause dissolution of desmosomes, retraction of keratin filaments and internalization of DSG3 in a complex

with PG and DP in a membrane raft dependent manner [23,24,25]. It is possible that upon addition of EGTA, PKP3 is localized to a portion of the membrane not associated with membrane rafts; thereby preventing its internalization along with the other desmosomal proteins.

Both PG and PKP3 required an intact MT network to be transported to the cell border and transport of PG to the cell border is dependent on KIF5B and KLC1 [9]. However, unlike PKP3, transport of PG from the cell border to the cytoplasm upon calcium chelation did not require an intact MT network. These results indicate that some other yet unidentified transport process is responsible for retrograde transport of PG and other desmosomal proteins such as DP and DSC2/3 that is independent of an intact MT network. Other reports suggest that both MT and actin filaments are required for the transport of DSC2 to the cell border [15,17]. Therefore, an actin-based mechanism might regulate the retrograde transport of PG, DP and DSC2/3 in HCT116 cells. We have also observed that DP doesn't interact with KLC1 motor proteins, which has been identified as a common binding partner for PKP3 and PG. This indicates that transport of DP is differently regulated than armadillo proteins. Reports published by other laboratories supports this assumption. It has been shown that DP transport is regulated by actin filaments whereas; desmosomal cadherins utilize microtubule based kinesin motor proteins for their transport to the cell membrane [342, 417].

#### **5.4. Conclusion and Future directions.**

We have shown identified a novel mechanism through which 14-3-3 $\sigma$  could regulate and maintain epithelial characteristics. We show that loss of 14-3-3 $\sigma$  leads to EMT through c-Jun-Slug axis. We have also identified FBW7 as the E3 ligase involved in proteasome mediated degradation of c-Jun. In further studies role of other E3 ligases such as ITCH

and COP1 in 14-3-3 $\sigma$  mediated degradation of c-Jun could be investigated. However, we have observed that an EMT doesn't lead to increased tumor formation in vivo on loss of 14-3-3 $\sigma$  and in fact compromised the potential for tumor formation of 14-3-3 $\sigma$ <sup>+/+</sup> cells. This suggests that loss of 14-3-3 $\sigma$  could be an early event during cancer progression and 14-3-3 $\sigma$  is required at a later stage, perhaps during MET. This hypothesis remains to be tested by further studies. We have also shown that 14-3-3 $\sigma$  could directly regulate cell migration and actin cytoskeleton dynamics by regulating activation of FAK. We have identified a downstream signaling cascade downstream of FAK, which involves RhoA, ROCK, LIMK and cofilin through which 14-3-3 $\sigma$  regulate actin dynamics. However, we do not have a clear mechanism to explain how 14-3-3 $\sigma$  regulates phosphorylation of FAK at Y397. We hypothesize that 14-3-3 $\sigma$  binding to FAK leads to steric hindrances which inhibits autophosphorylation of FAK at Y397. It would be interesting to test this hypothesis by further biochemical experiments.

We have also identified PKP3 as a novel interacting partner for KIF5B. Our studies show that both 14-3-3 $\gamma$  and KIF5B interact at the N-terminal domain of PKP3. Loss of PKP3 leads to compromised interaction of 14-3-3 $\gamma$  and other desmosomal proteins. We have determined that an intact MT network is required for the retrograde transport of PKP3 during desmosome disassembly and suggest that PKP3 and PG might have different roles to play during desmosome disassembly. However, additional studies are required to address the significance of the MT network in regulating desmosome disassembly and in regulation of PKP3 transport.

## **CHAPTER 6: BIBLIOGRAPHY**



1. Nam, H.J., Kim, I., Bowie, J.U., and Kim, S. (2015). Metazoans evolved by taking domains from soluble proteins to expand intercellular communication network. *Sci Rep* 5, 9576.
2. King, N., Westbrook, M.J., Young, S.L., Kuo, A., Abedin, M., Chapman, J., Fairclough, S., Hellsten, U., Isogai, Y., Letunic, I., et al. (2008). The genome of the choanoflagellate *Monosiga brevicollis* and the origin of metazoans. *Nature* 451, 783-788.
3. Abedin, M., and King, N. (2010). Diverse evolutionary paths to cell adhesion. *Trends Cell Biol* 20, 734-742.
4. Gumbiner, B.M. (1996). Cell adhesion: the molecular basis of tissue architecture and morphogenesis. *Cell* 84, 345-357.
5. Kowalczyk, A.P., and Nanes, B.A. (2012). Adherens junction turnover: regulating adhesion through cadherin endocytosis, degradation, and recycling. *Subcell Biochem* 60, 197-222.
6. Ogata, S., Morokuma, J., Hayata, T., Kolle, G., Niehrs, C., Ueno, N., and Cho, K.W. (2007). TGF-beta signaling-mediated morphogenesis: modulation of cell adhesion via cadherin endocytosis. *Genes Dev* 21, 1817-1831.
7. Steinberg, M.S., and Takeichi, M. (1994). Experimental specification of cell sorting, tissue spreading, and specific spatial patterning by quantitative differences in cadherin expression. *Proc Natl Acad Sci U S A* 91, 206-209.
8. Ohsugi, M., Larue, L., Schwarz, H., and Kemler, R. (1997). Cell-junctional and cytoskeletal organization in mouse blastocysts lacking E-cadherin. *Dev Biol* 185, 261-271.

9. Larue, L., Ohsugi, M., Hirchenhain, J., and Kemler, R. (1994). E-cadherin null mutant embryos fail to form a trophectoderm epithelium. *Proc Natl Acad Sci U S A* *91*, 8263-8267.
10. Gallicano, G.I., Kouklis, P., Bauer, C., Yin, M., Vasioukhin, V., Degenstein, L., and Fuchs, E. (1998). Desmoplakin is required early in development for assembly of desmosomes and cytoskeletal linkage. *J Cell Biol* *143*, 2009-2022.
11. Den, Z., Cheng, X., Merched-Sauvage, M., and Koch, P.J. (2006). Desmocollin 3 is required for pre-implantation development of the mouse embryo. *J Cell Sci* *119*, 482-489.
12. Chidgey, M., Brakebusch, C., Gustafsson, E., Cruchley, A., Hail, C., Kirk, S., Merritt, A., North, A., Tselepis, C., Hewitt, J., et al. (2001). Mice lacking desmocollin 1 show epidermal fragility accompanied by barrier defects and abnormal differentiation. *J Cell Biol* *155*, 821-832.
13. Bierkamp, C., McLaughlin, K.J., Schwarz, H., Huber, O., and Kemler, R. (1996). Embryonic heart and skin defects in mice lacking plakoglobin. *Dev Biol* *180*, 780-785.
14. Grossmann, K.S., Grund, C., Huelsken, J., Behrend, M., Erdmann, B., Franke, W.W., and Birchmeier, W. (2004). Requirement of plakophilin 2 for heart morphogenesis and cardiac junction formation. *J Cell Biol* *167*, 149-160.
15. Haegel, H., Larue, L., Ohsugi, M., Fedorov, L., Herrenknecht, K., and Kemler, R. (1995). Lack of beta-catenin affects mouse development at gastrulation. *Development* *121*, 3529-3537.
16. Khapare, N., Kundu, S.T., Sehgal, L., Sawant, M., Priya, R., Gosavi, P., Gupta, N., Alam, H., Karkhanis, M., Naik, N., et al. (2012). Plakophilin3 loss leads to an

- increase in PRL3 levels promoting K8 dephosphorylation, which is required for transformation and metastasis. *PLoS One* 7, e38561.
17. Kundu, S.T., Gosavi, P., Khapare, N., Patel, R., Hosing, A.S., Maru, G.B., Ingle, A., Decaprio, J.A., and Dalal, S.N. (2008). Plakophilin3 downregulation leads to a decrease in cell adhesion and promotes metastasis. *Int J Cancer* 123, 2303-2314.
  18. Tsukita, S., Furuse, M., and Itoh, M. (2001). Multifunctional strands in tight junctions. *Nat Rev Mol Cell Biol* 2, 285-293.
  19. Roignot, J., Peng, X., and Mostov, K. (2013). Polarity in mammalian epithelial morphogenesis. *Cold Spring Harb Perspect Biol* 5.
  20. Farquhar, M.G., and Palade, G.E. (1963). Junctional complexes in various epithelia. *J Cell Biol* 17, 375-412.
  21. Furuse, M. (2010). Molecular basis of the core structure of tight junctions. *Cold Spring Harb Perspect Biol* 2, a002907.
  22. Dermietzel, R. (1974). Junctions in the central nervous system of the cat. I. Membrane fusion in central myelin. *Cell Tissue Res* 148, 565-576.
  23. Tetzlaff, W. (1978). The development of a zonula occludens in peripheral myelin of the chick embryo. A freeze-fracture study. *Cell Tissue Res* 189, 187-201.
  24. Mruk, D.D., and Cheng, C.Y. (2010). Tight junctions in the testis: new perspectives. *Philos Trans R Soc Lond B Biol Sci* 365, 1621-1635.
  25. Abbott, N.J., Patabendige, A.A., Dolman, D.E., Yusof, S.R., and Begley, D.J. (2010). Structure and function of the blood-brain barrier. *Neurobiol Dis* 37, 13-25.
  26. Guillemot, L., Paschoud, S., Pulimeno, P., Foglia, A., and Citi, S. (2008). The cytoplasmic plaque of tight junctions: a scaffolding and signalling center. *Biochim Biophys Acta* 1778, 601-613.

27. Krause, G., Winkler, L., Mueller, S.L., Haseloff, R.F., Piontek, J., and Blasig, I.E. (2008). Structure and function of claudins. *Biochim Biophys Acta* 1778, 631-645.
28. Blasig, I.E., Winkler, L., Lassowski, B., Mueller, S.L., Zuleger, N., Krause, E., Krause, G., Gast, K., Kolbe, M., and Piontek, J. (2006). On the self-association potential of transmembrane tight junction proteins. *Cell Mol Life Sci* 63, 505-514.
29. Piontek, J., Winkler, L., Wolburg, H., Muller, S.L., Zuleger, N., Piehl, C., Wiesner, B., Krause, G., and Blasig, I.E. (2008). Formation of tight junction: determinants of homophilic interaction between classic claudins. *Faseb J* 22, 146-158.
30. Anderson, J.M., and Van Itallie, C.M. (2009). Physiology and function of the tight junction. *Cold Spring Harb Perspect Biol* 1, a002584.
31. Wen, H., Watry, D.D., Marcondes, M.C., and Fox, H.S. (2004). Selective decrease in paracellular conductance of tight junctions: role of the first extracellular domain of claudin-5. *Mol Cell Biol* 24, 8408-8417.
32. Itoh, M., Furuse, M., Morita, K., Kubota, K., Saitou, M., and Tsukita, S. (1999). Direct binding of three tight junction-associated MAGUKs, ZO-1, ZO-2, and ZO-3, with the COOH termini of claudins. *J Cell Biol* 147, 1351-1363.
33. Jeansonne, B., Lu, Q., Goodenough, D.A., and Chen, Y.H. (2003). Claudin-8 interacts with multi-PDZ domain protein 1 (MUPP1) and reduces paracellular conductance in epithelial cells. *Cell Mol Biol (Noisy-le-grand)* 49, 13-21.
34. Roh, M.H., Liu, C.J., Laurinec, S., and Margolis, B. (2002). The carboxyl terminus of zona occludens-3 binds and recruits a mammalian homologue of discs lost to tight junctions. *J Biol Chem* 277, 27501-27509.
35. Sakakibara, A., Furuse, M., Saitou, M., Ando-Akatsuka, Y., and Tsukita, S. (1997). Possible involvement of phosphorylation of occludin in tight junction formation. *J Cell Biol* 137, 1393-1401.

36. Basuroy, S., Sheth, P., Kuppaswamy, D., Balasubramanian, S., Ray, R.M., and Rao, R.K. (2003). Expression of kinase-inactive c-Src delays oxidative stress-induced disassembly and accelerates calcium-mediated reassembly of tight junctions in the Caco-2 cell monolayer. *J Biol Chem* 278, 11916-11924.
37. Chen, Y.H., Lu, Q., Goodenough, D.A., and Jeansonne, B. (2002). Nonreceptor tyrosine kinase c-Yes interacts with occludin during tight junction formation in canine kidney epithelial cells. *Mol Biol Cell* 13, 1227-1237.
38. Siu, E.R., Wong, E.W., Mruk, D.D., Porto, C.S., and Cheng, C.Y. (2009). Focal adhesion kinase is a blood-testis barrier regulator. *Proc Natl Acad Sci U S A* 106, 9298-9303.
39. Seth, A., Sheth, P., Elias, B.C., and Rao, R. (2007). Protein phosphatases 2A and 1 interact with occludin and negatively regulate the assembly of tight junctions in the CACO-2 cell monolayer. *J Biol Chem* 282, 11487-11498.
40. Ikenouchi, J., Sasaki, H., Tsukita, S., and Furuse, M. (2008). Loss of occludin affects tricellular localization of tricellulin. *Mol Biol Cell* 19, 4687-4693.
41. Ikenouchi, J., Furuse, M., Furuse, K., Sasaki, H., and Tsukita, S. (2005). Tricellulin constitutes a novel barrier at tricellular contacts of epithelial cells. *J Cell Biol* 171, 939-945.
42. Mandell, K.J., Babbin, B.A., Nusrat, A., and Parkos, C.A. (2005). Junctional adhesion molecule 1 regulates epithelial cell morphology through effects on beta1 integrins and Rap1 activity. *J Biol Chem* 280, 11665-11674.
43. Cera, M.R., Fabbri, M., Molendini, C., Corada, M., Orsenigo, F., Rehberg, M., Reichel, C.A., Krombach, F., Pardi, R., and Dejana, E. (2009). JAM-A promotes neutrophil chemotaxis by controlling integrin internalization and recycling. *J Cell Sci* 122, 268-277.

44. Konopka, G., Tekiela, J., Iverson, M., Wells, C., and Duncan, S.A. (2007). Junctional adhesion molecule-A is critical for the formation of pseudocanaliculi and modulates E-cadherin expression in hepatic cells. *J Biol Chem* 282, 28137-28148.
45. Gonzalez-Mariscal, L., Dominguez-Calderon, A., Raya-Sandino, A., Ortega-Olvera, J.M., Vargas-Sierra, O., and Martinez-Revollar, G. (2014). Tight junctions and the regulation of gene expression. *Semin Cell Dev Biol* 36, 213-223.
46. Forster, C. (2008). Tight junctions and the modulation of barrier function in disease. *Histochem Cell Biol* 130, 55-70.
47. Matter, K., Aijaz, S., Tsapara, A., and Balda, M.S. (2005). Mammalian tight junctions in the regulation of epithelial differentiation and proliferation. *Curr Opin Cell Biol* 17, 453-458.
48. Steed, E., Balda, M.S., and Matter, K. (2010). Dynamics and functions of tight junctions. *Trends Cell Biol* 20, 142-149.
49. Goodenough, D.A., and Paul, D.L. (2009). Gap junctions. *Cold Spring Harb Perspect Biol* 1, a002576.
50. Gilula, N.B., Reeves, O.R., and Steinbach, A. (1972). Metabolic coupling, ionic coupling and cell contacts. *Nature* 235, 262-265.
51. Bennett, M.V., and Zukin, R.S. (2004). Electrical coupling and neuronal synchronization in the Mammalian brain. *Neuron* 41, 495-511.
52. Goldberg, G.S., Lampe, P.D., and Nicholson, B.J. (1999). Selective transfer of endogenous metabolites through gap junctions composed of different connexins. *Nat Cell Biol* 1, 457-459.
53. Paul, D.L. (1995). New functions for gap junctions. *Curr Opin Cell Biol* 7, 665-672.
54. Phelan, P., and Starich, T.A. (2001). Innexins get into the gap. *Bioessays* 23, 388-396.

- 
55. Panchin, Y., Kelmanson, I., Matz, M., Lukyanov, K., Usman, N., and Lukyanov, S. (2000). A ubiquitous family of putative gap junction molecules. *Curr Biol* 10, R473-474.
56. Cruciani, V., and Mikalsen, S.O. (2007). Evolutionary selection pressure and family relationships among connexin genes. *Biological chemistry* 388, 253-264.
57. Wiszniewski, L., Limat, A., Saurat, J.H., Meda, P., and Salomon, D. (2000). Differential expression of connexins during stratification of human keratinocytes. *J Invest Dermatol* 115, 278-285.
58. Wagner, C. (2008). Function of connexins in the renal circulation. *Kidney Int* 73, 547-555.
59. Unger, V.M., Kumar, N.M., Gilula, N.B., and Yeager, M. (1999). Three-dimensional structure of a recombinant gap junction membrane channel. *Science* 283, 1176-1180.
60. Unwin, N. (1986). Is there a common design for cell membrane channels? *Nature* 323, 12-13.
61. Bruzzone, R., White, T.W., and Paul, D.L. (1994). Expression of chimeric connexins reveals new properties of the formation and gating behavior of gap junction channels. *J Cell Sci* 107 (Pt 4), 955-967.
62. Falk, M.M., Buehler, L.K., Kumar, N.M., and Gilula, N.B. (1997). Cell-free synthesis and assembly of connexins into functional gap junction membrane channels. *Embo J* 16, 2703-2716.
63. Segretain, D., and Falk, M.M. (2004). Regulation of connexin biosynthesis, assembly, gap junction formation, and removal. *Biochim Biophys Acta* 1662, 3-21.
64. Patel, P.I., and Lupski, J.R. (1994). Charcot-Marie-Tooth disease: a new paradigm for the mechanism of inherited disease. *Trends Genet* 10, 128-133.

65. Richard, G., Smith, L.E., Bailey, R.A., Itin, P., Hohl, D., Epstein, E.H., Jr., DiGiovanna, J.J., Compton, J.G., and Bale, S.J. (1998). Mutations in the human connexin gene GJB3 cause erythrokeratoderma variabilis. *Nat Genet* *20*, 366-369.
66. Mackay, D., Ionides, A., Kibar, Z., Rouleau, G., Berry, V., Moore, A., Shiels, A., and Bhattacharya, S. (1999). Connexin46 mutations in autosomal dominant congenital cataract. *Am J Hum Genet* *64*, 1357-1364.
67. Paznekas, W.A., Boyadjiev, S.A., Shapiro, R.E., Daniels, O., Wollnik, B., Keegan, C.E., Innis, J.W., Dinulos, M.B., Christian, C., Hannibal, M.C., et al. (2003). Connexin 43 (GJA1) mutations cause the pleiotropic phenotype of oculodentodigital dysplasia. *Am J Hum Genet* *72*, 408-418.
68. Borradori, L., and Sonnenberg, A. (1999). Structure and function of hemidesmosomes: more than simple adhesion complexes. *The Journal of investigative dermatology* *112*, 411-418.
69. Litjens, S.H., de Pereda, J.M., and Sonnenberg, A. (2006). Current insights into the formation and breakdown of hemidesmosomes. *Trends Cell Biol* *16*, 376-383.
70. Wilhelmsen, K., Litjens, S.H., and Sonnenberg, A. (2006). Multiple functions of the integrin  $\alpha 6\beta 4$  in epidermal homeostasis and tumorigenesis. *Mol Cell Biol* *26*, 2877-2886.
71. Margadant, C., Frijns, E., Wilhelmsen, K., and Sonnenberg, A. (2008). Regulation of hemidesmosome disassembly by growth factor receptors. *Curr Opin Cell Biol* *20*, 589-596.
72. Tasanen, K., Tunggal, L., Chometon, G., Bruckner-Tuderman, L., and Aumailley, M. (2004). Keratinocytes from patients lacking collagen XVII display a migratory phenotype. *Am J Pathol* *164*, 2027-2038.

73. Juliano, R.L., and Varner, J.A. (1993). Adhesion molecules in cancer: the role of integrins. *Current opinion in cell biology* 5, 812-818.
74. Rabinovitz, I., and Mercurio, A.M. (1996). The integrin alpha 6 beta 4 and the biology of carcinoma. *Biochem Cell Biol* 74, 811-821.
75. Guo, L., Degenstein, L., Dowling, J., Yu, Q.C., Wollmann, R., Perman, B., and Fuchs, E. (1995). Gene targeting of BPAG1: abnormalities in mechanical strength and cell migration in stratified epithelia and neurologic degeneration. *Cell* 81, 233-243.
76. Andra, K., Lassmann, H., Bittner, R., Shorny, S., Fassler, R., Propst, F., and Wiche, G. (1997). Targeted inactivation of plectin reveals essential function in maintaining the integrity of skin, muscle, and heart cytoarchitecture. *Genes Dev* 11, 3143-3156.
77. Takeichi, M. (1991). Cadherin cell adhesion receptors as a morphogenetic regulator. *Science* 251, 1451-1455.
78. Meng, W., and Takeichi, M. (2009). Adherens junction: molecular architecture and regulation. *Cold Spring Harb Perspect Biol* 1, a002899.
79. Takeichi, M. (2014). Dynamic contacts: rearranging adherens junctions to drive epithelial remodelling. *Nature reviews. Molecular cell biology* 15, 397-410.
80. Gottardi, C.J., and Peifer, M. (2008). Terminal regions of beta-catenin come into view. *Structure* 16, 336-338.
81. Takeichi, M., Hatta, K., Nose, A., and Nagafuchi, A. (1988). Identification of a gene family of cadherin cell adhesion molecules. *Cell Differ Dev* 25 *Suppl*, 91-94.
82. Overduin, M., Harvey, T.S., Bagby, S., Tong, K.I., Yau, P., Takeichi, M., and Ikura, M. (1995). Solution structure of the epithelial cadherin domain responsible for selective cell adhesion. *Science* 267, 386-389.
83. Takeichi, M. (1988). The cadherins: cell-cell adhesion molecules controlling animal morphogenesis. *Development* 102, 639-655.

84. Reynolds, A.B., Herbert, L., Cleveland, J.L., Berg, S.T., and Gaut, J.R. (1992). p120, a novel substrate of protein tyrosine kinase receptors and of p60v-src, is related to cadherin-binding factors beta-catenin, plakoglobin and armadillo. *Oncogene* 7, 2439-2445.
85. Shibamoto, S., Hayakawa, M., Takeuchi, K., Hori, T., Miyazawa, K., Kitamura, N., Johnson, K.R., Wheelock, M.J., Matsuyoshi, N., Takeichi, M., et al. (1995). Association of p120, a tyrosine kinase substrate, with E-cadherin/catenin complexes. *J Cell Biol* 128, 949-957.
86. Hatzfeld, M. (2005). The p120 family of cell adhesion molecules. *Eur J Cell Biol* 84, 205-214.
87. Knudsen, K.A., and Wheelock, M.J. (1992). Plakoglobin, or an 83-kD homologue distinct from beta-catenin, interacts with E-cadherin and N-cadherin. *J Cell Biol* 118, 671-679.
88. Ozawa, M., and Kemler, R. (1992). Molecular organization of the uvomorulin-catenin complex. *J Cell Biol* 116, 989-996.
89. Knudsen, K.A., Soler, A.P., Johnson, K.R., and Wheelock, M.J. (1995). Interaction of alpha-actinin with the cadherin/catenin cell-cell adhesion complex via alpha-catenin. *J Cell Biol* 130, 67-77.
90. Hatzfeld, M. (2005). The p120 family of cell adhesion molecules. *Eur J Cell Biol* 84, 205-214.
91. Watabe-Uchida, M., Uchida, N., Imamura, Y., Nagafuchi, A., Fujimoto, K., Uemura, T., Vermeulen, S., van Roy, F., Adamson, E.D., and Takeichi, M. (1998). alpha-Catenin-vinculin interaction functions to organize the apical junctional complex in epithelial cells. *J Cell Biol* 142, 847-857.

92. Abe, K., and Takeichi, M. (2008). EPLIN mediates linkage of the cadherin catenin complex to F-actin and stabilizes the circumferential actin belt. *Proc Natl Acad Sci U S A* *105*, 13-19.
93. Taguchi, K., Ishiuchi, T., and Takeichi, M. (2011). Mechanosensitive EPLIN-dependent remodeling of adherens junctions regulates epithelial reshaping. *J Cell Biol* *194*, 643-656.
94. Abe, K., and Takeichi, M. (2008). EPLIN mediates linkage of the cadherin catenin complex to F-actin and stabilizes the circumferential actin belt. *Proc Natl Acad Sci U S A* *105*, 13-19.
95. Pulimeno, P., Paschoud, S., and Citi, S. (2011). A role for ZO-1 and PLEKHA7 in recruiting paracingulin to tight and adherens junctions of epithelial cells. *J Biol Chem* *286*, 16743-16750.
96. Harris, T.J., and Tepass, U. (2010). Adherens junctions: from molecules to morphogenesis. *Nat Rev Mol Cell Biol* *11*, 502-514.
97. Laprise, P., and Tepass, U. (2011). Novel insights into epithelial polarity proteins in *Drosophila*. *Trends Cell Biol* *21*, 401-408.
98. Sen, A., Nagy-Zsver-Vadas, Z., and Krahn, M.P. (2012). *Drosophila* PATJ supports adherens junction stability by modulating Myosin light chain activity. *J Cell Biol* *199*, 685-698.
99. Nakanishi, H., and Takai, Y. (2004). Roles of nectins in cell adhesion, migration and polarization. *Biol Chem* *385*, 885-892.
100. Rikitake, Y., Mandai, K., and Takai, Y. (2012). The role of nectins in different types of cell-cell adhesion. *J Cell Sci* *125*, 3713-3722.
101. Irie, K., Shimizu, K., Sakisaka, T., Ikeda, W., and Takai, Y. (2004). Roles and modes of action of nectins in cell-cell adhesion. *Semin Cell Dev Biol* *15*, 643-656.

102. Takai, Y., Irie, K., Shimizu, K., Sakisaka, T., and Ikeda, W. (2003). Nectins and nectin-like molecules: roles in cell adhesion, migration, and polarization. *Cancer Sci* *94*, 655-667.
103. Miyahara, M., Nakanishi, H., Takahashi, K., Satoh-Horikawa, K., Tachibana, K., and Takai, Y. (2000). Interaction of nectin with afadin is necessary for its clustering at cell-cell contact sites but not for its cis dimerization or trans interaction. *J Biol Chem* *275*, 613-618.
104. Yokoyama, S., Tachibana, K., Nakanishi, H., Yamamoto, Y., Irie, K., Mandai, K., Nagafuchi, A., Monden, M., and Takai, Y. (2001). alpha-catenin-independent recruitment of ZO-1 to nectin-based cell-cell adhesion sites through afadin. *Mol Biol Cell* *12*, 1595-1609.
105. Yang, C.C., Graves, H.K., Moya, I.M., Tao, C., Hamaratoglu, F., Gladden, A.B., and Halder, G. (2015). Differential regulation of the Hippo pathway by adherens junctions and apical-basal cell polarity modules. *Proc Natl Acad Sci U S A* *112*, 1785-1790.
106. Hartsock, A., and Nelson, W.J. (2008). Adherens and tight junctions: structure, function and connections to the actin cytoskeleton. *Biochim Biophys Acta* *1778*, 660-669.
107. Lewis, J.E., Wahl, J.K., 3rd, Sass, K.M., Jensen, P.J., Johnson, K.R., and Wheelock, M.J. (1997). Cross-talk between adherens junctions and desmosomes depends on plakoglobin. *J Cell Biol* *136*, 919-934.
108. Berx, G., Cleton-Jansen, A.M., Nollet, F., de Leeuw, W.J., van de Vijver, M., Cornelisse, C., and van Roy, F. (1995). E-cadherin is a tumour/invasion suppressor gene mutated in human lobular breast cancers. *Embo J* *14*, 6107-6115.

109. Berx, G., Cleton-Jansen, A.M., Strumane, K., de Leeuw, W.J., Nollet, F., van Roy, F., and Cornelisse, C. (1996). E-cadherin is inactivated in a majority of invasive human lobular breast cancers by truncation mutations throughout its extracellular domain. *Oncogene* *13*, 1919-1925.
110. Nelson, W.J., and Nusse, R. (2004). Convergence of Wnt, beta-catenin, and cadherin pathways. *Science* *303*, 1483-1487.
111. Delva, E., Tucker, D.K., and Kowalczyk, A.P. (2009). The desmosome. *Cold Spring Harb Perspect Biol* *1*, a002543.
112. Garrod, D., and Chidgey, M. (2008). Desmosome structure, composition and function. *Biochim Biophys Acta* *1778*, 572-587.
113. Al-Amoudi, A., Castano-Diez, D., Devos, D.P., Russell, R.B., Johnson, G.T., and Frangakis, A.S. (2011). The three-dimensional molecular structure of the desmosomal plaque. *Proc Natl Acad Sci U S A* *108*, 6480-6485.
114. Watt, F.M., Matthey, D.L., and Garrod, D.R. (1984). Calcium-induced reorganization of desmosomal components in cultured human keratinocytes. *J Cell Biol* *99*, 2211-2215.
115. Al-Amoudi, A., Norlen, L.P., and Dubochet, J. (2004). Cryo-electron microscopy of vitreous sections of native biological cells and tissues. *J Struct Biol* *148*, 131-135.
116. Witcher, L.L., Collins, R., Puttagunta, S., Mechanic, S.E., Munson, M., Gumbiner, B., and Cowin, P. (1996). Desmosomal cadherin binding domains of plakoglobin. *J Biol Chem* *271*, 10904-10909.
117. Schmidt, A., and Koch, P.J. (2007). Desmosomes: just cell adhesion or is there more? *Cell Adh Migr* *1*, 28-32.
118. Hatsell, S., and Cowin, P. (2001). Deconstructing desmoplakin. *Nat Cell Biol* *3*, E270-272.

119. Desai, B.V., Harmon, R.M., and Green, K.J. (2009). Desmosomes at a glance. *J Cell Sci* *122*, 4401-4407.
120. Wallis, S., Lloyd, S., Wise, I., Ireland, G., Fleming, T.P., and Garrod, D. (2000). The alpha isoform of protein kinase C is involved in signaling the response of desmosomes to wounding in cultured epithelial cells. *Mol Biol Cell* *11*, 1077-1092.
121. Hunt, D.M., Sahota, V.K., Taylor, K., Simrak, D., Hornigold, N., Arnemann, J., Wolfe, J., and Buxton, R.S. (1999). Clustered cadherin genes: a sequence-ready contig for the desmosomal cadherin locus on human chromosome 18. *Genomics* *62*, 445-455.
122. Koch, P.J., Goldschmidt, M.D., Zimbelmann, R., Troyanovsky, R., and Franke, W.W. (1992). Complexity and expression patterns of the desmosomal cadherins. *Proc Natl Acad Sci U S A* *89*, 353-357.
123. Arnemann, J., Sullivan, K.H., Magee, A.I., King, I.A., and Buxton, R.S. (1993). Stratification-related expression of isoforms of the desmosomal cadherins in human epidermis. *J Cell Sci* *104 (Pt 3)*, 741-750.
124. Kottke, M.D., Delva, E., and Kowalczyk, A.P. (2006). The desmosome: cell science lessons from human diseases. *J Cell Sci* *119*, 797-806.
125. Getsios, S., Amargo, E.V., Dusek, R.L., Ishii, K., Sheu, L., Godsel, L.M., and Green, K.J. (2004). Coordinated expression of desmoglein 1 and desmocollin 1 regulates intercellular adhesion. *Differentiation* *72*, 419-433.
126. Chitaev, N.A., and Troyanovsky, S.M. (1997). Direct Ca<sup>2+</sup>-dependent heterophilic interaction between desmosomal cadherins, desmoglein and desmocollin, contributes to cell-cell adhesion. *J Cell Biol* *138*, 193-201.

127. Syed, S.E., Trinnaman, B., Martin, S., Major, S., Hutchinson, J., and Magee, A.I. (2002). Molecular interactions between desmosomal cadherins. *Biochem J* 362, 317-327.
128. Pertz, O., Bozic, D., Koch, A.W., Fauser, C., Brancaccio, A., and Engel, J. (1999). A new crystal structure, Ca<sup>2+</sup> dependence and mutational analysis reveal molecular details of E-cadherin homoassociation. *Embo J* 18, 1738-1747.
129. Getsios, S., Huen, A.C., and Green, K.J. (2004). Working out the strength and flexibility of desmosomes. *Nat Rev Mol Cell Biol* 5, 271-281.
130. Holthofer, B., Windoffer, R., Troyanovsky, S., and Leube, R.E. (2007). Structure and function of desmosomes. *Int Rev Cytol* 264, 65-163.
131. Merritt, A.J., Berika, M.Y., Zhai, W., Kirk, S.E., Ji, B., Hardman, M.J., and Garrod, D.R. (2002). Suprabasal desmoglein 3 expression in the epidermis of transgenic mice results in hyperproliferation and abnormal differentiation. *Mol Cell Biol* 22, 5846-5858.
132. Brennan, D., Hu, Y., Joubeh, S., Choi, Y.W., Whitaker-Menezes, D., O'Brien, T., Uitto, J., Rodeck, U., and Mahoney, M.G. (2007). Suprabasal Dsg2 expression in transgenic mouse skin confers a hyperproliferative and apoptosis-resistant phenotype to keratinocytes. *J Cell Sci* 120, 758-771.
133. Koch, P.J., Mahoney, M.G., Ishikawa, H., Pulkkinen, L., Uitto, J., Shultz, L., Murphy, G.F., Whitaker-Menezes, D., and Stanley, J.R. (1997). Targeted disruption of the pemphigus vulgaris antigen (desmoglein 3) gene in mice causes loss of keratinocyte cell adhesion with a phenotype similar to pemphigus vulgaris. *J Cell Biol* 137, 1091-1102.

134. Eshkind, L., Tian, Q., Schmidt, A., Franke, W.W., Windoffer, R., and Leube, R.E. (2002). Loss of desmoglein 2 suggests essential functions for early embryonic development and proliferation of embryonal stem cells. *Eur J Cell Biol* *81*, 592-598.
135. Chen, J., Den, Z., and Koch, P.J. (2008). Loss of desmocollin 3 in mice leads to epidermal blistering. *J Cell Sci* *121*, 2844-2849.
136. Riggelman, B., Wieschaus, E., and Schedl, P. (1989). Molecular analysis of the armadillo locus: uniformly distributed transcripts and a protein with novel internal repeats are associated with a *Drosophila* segment polarity gene. *Genes Dev* *3*, 96-113.
137. Green, K.J., and Gaudry, C.A. (2000). Are desmosomes more than tethers for intermediate filaments? *Nat Rev Mol Cell Biol* *1*, 208-216.
138. Hatzfeld, M. (2007). Plakophilins: Multifunctional proteins or just regulators of desmosomal adhesion? *Biochim Biophys Acta* *1773*, 69-77.
139. Hatzfeld, M., Kristjansson, G.I., Plessmann, U., and Weber, K. (1994). Band 6 protein, a major constituent of desmosomes from stratified epithelia, is a novel member of the armadillo multigene family. *J Cell Sci* *107 (Pt 8)*, 2259-2270.
140. Schmidt, A., Langbein, L., Rode, M., Pratzel, S., Zimbelmann, R., and Franke, W.W. (1997). Plakophilins 1a and 1b: widespread nuclear proteins recruited in specific epithelial cells as desmosomal plaque components. *Cell Tissue Res* *290*, 481-499.
141. Bonne, S., van Hengel, J., Nollet, F., Kools, P., and van Roy, F. (1999). Plakophilin-3, a novel armadillo-like protein present in nuclei and desmosomes of epithelial cells. *J Cell Sci* *112 (Pt 14)*, 2265-2276.
142. Kapprell, H.P., Owaribe, K., and Franke, W.W. (1988). Identification of a basic protein of Mr 75,000 as an accessory desmosomal plaque protein in stratified and complex epithelia. *J Cell Biol* *106*, 1679-1691.

143. Sobolik-Delmaire, T., Katafiasz, D., and Wahl, J.K., 3rd (2006). Carboxyl terminus of Plakophilin-1 recruits it to plasma membrane, whereas amino terminus recruits desmoplakin and promotes desmosome assembly. *J Biol Chem* *281*, 16962-16970.
144. Hatzfeld, M., Haffner, C., Schulze, K., and Vinzens, U. (2000). The function of plakophilin 1 in desmosome assembly and actin filament organization. *J Cell Biol* *149*, 209-222.
145. Hofmann, I., Mertens, C., Brettel, M., Nimmrich, V., Schnolzer, M., and Herrmann, H. (2000). Interaction of plakophilins with desmoplakin and intermediate filament proteins: an in vitro analysis. *J Cell Sci* *113 (Pt 13)*, 2471-2483.
146. Tucker, D.K., Stahley, S.N., and Kowalczyk, A.P. (2014). Plakophilin-1 protects keratinocytes from pemphigus vulgaris IgG by forming calcium-independent desmosomes. *The Journal of investigative dermatology* *134*, 1033-1043.
147. McGrath, J.A., McMillan, J.R., Shemanko, C.S., Runswick, S.K., Leigh, I.M., Lane, E.B., Garrod, D.R., and Eady, R.A. (1997). Mutations in the plakophilin 1 gene result in ectodermal dysplasia/skin fragility syndrome. *Nat Genet* *17*, 240-244.
148. Fischer-Keso, R., Breuninger, S., Hofmann, S., Henn, M., Rohrig, T., Strobel, P., Stoecklin, G., and Hofmann, I. (2014). Plakophilins 1 and 3 bind to FXR1 and thereby influence the mRNA stability of desmosomal proteins. *Mol Cell Biol* *34*, 4244-4256.
149. Bonne, S., van Hengel, J., and van Roy, F. (1998). Chromosomal mapping of human armadillo genes belonging to the p120(ctn)/plakophilin subfamily. *Genomics* *51*, 452-454.
150. Mertens, C., Kuhn, C., and Franke, W.W. (1996). Plakophilins 2a and 2b: constitutive proteins of dual location in the karyoplasm and the desmosomal plaque. *J Cell Biol* *135*, 1009-1025.

151. Muller, J., Ritt, D.A., Copeland, T.D., and Morrison, D.K. (2003). Functional analysis of C-TAK1 substrate binding and identification of PKP2 as a new C-TAK1 substrate. *Embo J* 22, 4431-4442.
152. Mertens, C., Hofmann, I., Wang, Z., Teichmann, M., Sepehri Chong, S., Schnolzer, M., and Franke, W.W. (2001). Nuclear particles containing RNA polymerase III complexes associated with the junctional plaque protein plakophilin 2. *Proc Natl Acad Sci U S A* 98, 7795-7800.
153. Chen, X., Bonne, S., Hatzfeld, M., van Roy, F., and Green, K.J. (2002). Protein binding and functional characterization of plakophilin 2. Evidence for its diverse roles in desmosomes and beta -catenin signaling. *J Biol Chem* 277, 10512-10522.
154. Bonne, S., Gilbert, B., Hatzfeld, M., Chen, X., Green, K.J., and van Roy, F. (2003). Defining desmosomal plakophilin-3 interactions. *J Cell Biol* 161, 403-416.
155. Munoz, W.A., Lee, M., Miller, R.K., Ahmed, Z., Ji, H., Link, T.M., Lee, G.R., Kloc, M., Ladbury, J.E., and McCrea, P.D. (2014). Plakophilin-3 catenin associates with the ETV1/ER81 transcription factor to positively modulate gene activity. *PLoS One* 9, e86784.
156. Hofmann, I., Casella, M., Schnolzer, M., Schlechter, T., Spring, H., and Franke, W.W. (2006). Identification of the junctional plaque protein plakophilin 3 in cytoplasmic particles containing RNA-binding proteins and the recruitment of plakophilins 1 and 3 to stress granules. *Mol Biol Cell* 17, 1388-1398.
157. Kedersha, N., Chen, S., Gilks, N., Li, W., Miller, I.J., Stahl, J., and Anderson, P. (2002). Evidence that ternary complex (eIF2-GTP-tRNA(i)(Met))-deficient preinitiation complexes are core constituents of mammalian stress granules. *Mol Biol Cell* 13, 195-210.

158. Sklyarova, T., Bonne, S., D'Hooge, P., Denecker, G., Goossens, S., De Rycke, R., Borgonie, G., Bosl, M., van Roy, F., and van Hengel, J. (2008). Plakophilin-3-deficient mice develop hair coat abnormalities and are prone to cutaneous inflammation. *J Invest Dermatol* *128*, 1375-1385.
159. Gosavi, P., Kundu, S.T., Khapare, N., Sehgal, L., Karkhanis, M.S., and Dalal, S.N. (2011). E-cadherin and plakoglobin recruit plakophilin3 to the cell border to initiate desmosome assembly. *Cell Mol Life Sci* *68*, 1439-1454.
160. Keirsebilck, A., Bonne, S., Staes, K., van Hengel, J., Nollet, F., Reynolds, A., and van Roy, F. (1998). Molecular cloning of the human p120ctn catenin gene (CTNND1): expression of multiple alternatively spliced isoforms. *Genomics* *50*, 129-146.
161. Hatzfeld, M., and Nachtshiem, C. (1996). Cloning and characterization of a new armadillo family member, p0071, associated with the junctional plaque: evidence for a subfamily of closely related proteins. *J Cell Sci* *109 (Pt 11)*, 2767-2778.
162. Setzer, S.V., Calkins, C.C., Garner, J., Summers, S., Green, K.J., and Kowalczyk, A.P. (2004). Comparative analysis of armadillo family proteins in the regulation of a431 epithelial cell junction assembly, adhesion and migration. *J Invest Dermatol* *123*, 426-433.
163. Cowin, P., Kapprell, H.P., Franke, W.W., Tamkun, J., and Hynes, R.O. (1986). Plakoglobin: a protein common to different kinds of intercellular adhering junctions. *Cell* *46*, 1063-1073.
164. Kowalczyk, A.P., Bornslaeger, E.A., Borgwardt, J.E., Palka, H.L., Dhaliwal, A.S., Corcoran, C.M., Denning, M.F., and Green, K.J. (1997). The amino-terminal domain of desmoplakin binds to plakoglobin and clusters desmosomal cadherin-plakoglobin complexes. *J Cell Biol* *139*, 773-784.

165. Palka, H.L., and Green, K.J. (1997). Roles of plakoglobin end domains in desmosome assembly. *J Cell Sci 110 (Pt 19)*, 2359-2371.
166. Kowalczyk, A.P., Stappenbeck, T.S., Parry, D.A., Palka, H.L., Virata, M.L., Bornslaeger, E.A., Nilles, L.A., and Green, K.J. (1994). Structure and function of desmosomal transmembrane core and plaque molecules. *Biophys Chem 50*, 97-112.
167. Miravet, S., Piedra, J., Castano, J., Raurell, I., Franci, C., Dunach, M., and Garcia de Herreros, A. (2003). Tyrosine phosphorylation of plakoglobin causes contrary effects on its association with desmosomes and adherens junction components and modulates beta-catenin-mediated transcription. *Mol Cell Biol 23*, 7391-7402.
168. Ruiz, P., Brinkmann, V., Ledermann, B., Behrend, M., Grund, C., Thalhammer, C., Vogel, F., Birchmeier, C., Gunthert, U., Franke, W.W., et al. (1996). Targeted mutation of plakoglobin in mice reveals essential functions of desmosomes in the embryonic heart. *J Cell Biol 135*, 215-225.
169. McKoy, G., Protonotarios, N., Crosby, A., Tsatsopoulou, A., Anastasakis, A., Coonar, A., Norman, M., Baboonian, C., Jeffery, S., and McKenna, W.J. (2000). Identification of a deletion in plakoglobin in arrhythmogenic right ventricular cardiomyopathy with palmoplantar keratoderma and woolly hair (Naxos disease). *Lancet 355*, 2119-2124.
170. Bierkamp, C., McLaughlin, K.J., Schwarz, H., Huber, O., and Kemler, R. (1996). Embryonic heart and skin defects in mice lacking plakoglobin. *Developmental biology 180*, 780-785.
171. Salomon, D., Sacco, P.A., Roy, S.G., Simcha, I., Johnson, K.R., Wheelock, M.J., and Ben-Ze'ev, A. (1997). Regulation of beta-catenin levels and localization by overexpression of plakoglobin and inhibition of the ubiquitin-proteasome system. *J Cell Biol 139*, 1325-1335.

172. Simcha, I., Shtutman, M., Salomon, D., Zhurinsky, J., Sadot, E., Geiger, B., and Ben-Ze'ev, A. (1998). Differential nuclear translocation and transactivation potential of beta-catenin and plakoglobin. *J Cell Biol* *141*, 1433-1448.
173. Green, K.J., Parry, D.A., Steinert, P.M., Virata, M.L., Wagner, R.M., Angst, B.D., and Nilles, L.A. (1990). Structure of the human desmoplakins. Implications for function in the desmosomal plaque. *J Biol Chem* *265*, 11406-11407.
174. Sumigray, K.D., Chen, H., and Lechler, T. (2011). Lis1 is essential for cortical microtubule organization and desmosome stability in the epidermis. *J Cell Biol* *194*, 631-642.
175. Whittock, N.V., Wan, H., Morley, S.M., Garzon, M.C., Kristal, L., Hyde, P., McLean, W.H., Pulkkinen, L., Uitto, J., Christiano, A.M., et al. (2002). Compound heterozygosity for non-sense and mis-sense mutations in desmoplakin underlies skin fragility/woolly hair syndrome. *J Invest Dermatol* *118*, 232-238.
176. Jonkman, M.F., Pasmooij, A.M., Pasmans, S.G., van den Berg, M.P., Ter Horst, H.J., Timmer, A., and Pas, H.H. (2005). Loss of desmoplakin tail causes lethal acantholytic epidermolysis bullosa. *Am J Hum Genet* *77*, 653-660.
177. Armstrong, D.K., McKenna, K.E., Purkis, P.E., Green, K.J., Eady, R.A., Leigh, I.M., and Hughes, A.E. (1999). Haploinsufficiency of desmoplakin causes a striate subtype of palmoplantar keratoderma. *Human molecular genetics* *8*, 143-148.
178. Gallicano, G.I., Kouklis, P., Bauer, C., Yin, M., Vasioukhin, V., Degenstein, L., and Fuchs, E. (1998). Desmoplakin is required early in development for assembly of desmosomes and cytoskeletal linkage. *J Cell Biol* *143*, 2009-2022.
179. Yang, L., Chen, Y., Cui, T., Knosel, T., Zhang, Q., Albring, K.F., Huber, O., and Petersen, I. (2012). Desmoplakin acts as a tumor suppressor by inhibition of the

- Wnt/beta-catenin signaling pathway in human lung cancer. *Carcinogenesis* 33, 1863-1870.
180. Tsang, S.M., Brown, L., Lin, K., Liu, L., Piper, K., O'Toole, E.A., Grose, R., Hart, I.R., Garrod, D.R., Fortune, F., et al. (2012). Non-junctional human desmoglein 3 acts as an upstream regulator of Src in E-cadherin adhesion, a pathway possibly involved in the pathogenesis of pemphigus vulgaris. *The Journal of pathology* 227, 81-93.
181. Chidgey, M. (2002). Desmosomes and disease: an update. *Histology and histopathology* 17, 1179-1192.
182. Fukuoka, J., Dracheva, T., Shih, J.H., Hewitt, S.M., Fujii, T., Kishor, A., Mann, F., Shilo, K., Franks, T.J., Travis, W.D., et al. (2007). Desmoglein 3 as a prognostic factor in lung cancer. *Human pathology* 38, 276-283.
183. Chen, Y.J., Chang, J.T., Lee, L., Wang, H.M., Liao, C.T., Chiu, C.C., Chen, P.J., and Cheng, A.J. (2007). DSG3 is overexpressed in head neck cancer and is a potential molecular target for inhibition of oncogenesis. *Oncogene* 26, 467-476.
184. Chidgey, M., and Dawson, C. (2007). Desmosomes: a role in cancer? *Br J Cancer* 96, 1783-1787.
185. Teh, M.T., Parkinson, E.K., Thurlow, J.K., Liu, F., Fortune, F., and Wan, H. (2011). A molecular study of desmosomes identifies a desmoglein isoform switch in head and neck squamous cell carcinoma. *Journal of oral pathology & medicine : official publication of the International Association of Oral Pathologists and the American Academy of Oral Pathology* 40, 67-76.
186. Hiraki, A., Shinohara, M., Ikebe, T., Nakamura, S., Kurahara, S., and Garrod, D.R. (1996). Immunohistochemical staining of desmosomal components in oral squamous cell carcinomas and its association with tumour behaviour. *Br J Cancer* 73, 1491-1497.

187. Davies, E.L., Gee, J.M., Cochrane, R.A., Jiang, W.G., Sharma, A.K., Nicholson, R.I., and Mansel, R.E. (1999). The immunohistochemical expression of desmoplakin and its role in vivo in the progression and metastasis of breast cancer. *European journal of cancer* 35, 902-907.
188. Canes, D., Chiang, G.J., Billmeyer, B.R., Austin, C.A., Kosakowski, M., Rieger-Christ, K.M., Libertino, J.A., and Summerhayes, I.C. (2005). Histone deacetylase inhibitors upregulate plakoglobin expression in bladder carcinoma cells and display antineoplastic activity in vitro and in vivo. *Int J Cancer* 113, 841-848.
189. Shiina, H., Breault, J.E., Basset, W.W., Enokida, H., Urakami, S., Li, L.C., Okino, S.T., Deguchi, M., Kaneuchi, M., Terashima, M., et al. (2005). Functional Loss of the gamma-catenin gene through epigenetic and genetic pathways in human prostate cancer. *Cancer research* 65, 2130-2138.
190. Winn, R.A., Bremnes, R.M., Bemis, L., Franklin, W.A., Miller, Y.E., Cool, C., and Heasley, L.E. (2002). gamma-Catenin expression is reduced or absent in a subset of human lung cancers and re-expression inhibits transformed cell growth. *Oncogene* 21, 7497-7506.
191. Breault, J.E., Shiina, H., Igawa, M., Ribeiro-Filho, L.A., Deguchi, M., Enokida, H., Urakami, S., Terashima, M., Nakagawa, M., Kane, C.J., et al. (2005). Methylation of the gamma-catenin gene is associated with poor prognosis of renal cell carcinoma. *Clinical cancer research : an official journal of the American Association for Cancer Research* 11, 557-564.
192. Aberle, H., Bierkamp, C., Torchard, D., Serova, O., Wagner, T., Natt, E., Wirsching, J., Heidkamper, C., Montagna, M., Lynch, H.T., et al. (1995). The human plakoglobin gene localizes on chromosome 17q21 and is subjected to loss of

- heterozygosity in breast and ovarian cancers. *Proc Natl Acad Sci U S A* 92, 6384-6388.
193. Amitay, R., Nass, D., Meitar, D., Goldberg, I., Davidson, B., Trakhtenbrot, L., Brok-Simoni, F., Ben-Ze'ev, A., Rechavi, G., and Kaufmann, Y. (2001). Reduced expression of plakoglobin correlates with adverse outcome in patients with neuroblastoma. *Am J Pathol* 159, 43-49.
194. Rieger-Christ, K.M., Ng, L., Hanley, R.S., Durrani, O., Ma, H., Yee, A.S., Libertino, J.A., and Summerhayes, I.C. (2005). Restoration of plakoglobin expression in bladder carcinoma cell lines suppresses cell migration and tumorigenic potential. *Br J Cancer* 92, 2153-2159.
195. Holen, I., Whitworth, J., Nutter, F., Evans, A., Brown, H.K., Lefley, D.V., Barbaric, I., Jones, M., and Ottewill, P.D. (2012). Loss of plakoglobin promotes decreased cell-cell contact, increased invasion, and breast cancer cell dissemination in vivo. *Breast cancer research : BCR* 14, R86.
196. Bailey, C.K., Mittal, M.K., Misra, S., and Chaudhuri, G. (2012). High motility of triple-negative breast cancer cells is due to repression of plakoglobin gene by metastasis modulator protein SLUG. *J Biol Chem* 287, 19472-19486.
197. Franzen, C.A., Todorovic, V., Desai, B.V., Mirzoeva, S., Yang, X.J., Green, K.J., and Pelling, J.C. (2012). The desmosomal armadillo protein plakoglobin regulates prostate cancer cell adhesion and motility through vitronectin-dependent Src signaling. *PLoS One* 7, e42132.
198. Schwarz, J., Ayim, A., Schmidt, A., Jager, S., Koch, S., Baumann, R., Dunne, A.A., and Moll, R. (2006). Differential expression of desmosomal plakophilins in various types of carcinomas: correlation with cell type and differentiation. *Human pathology* 37, 613-622.

199. Furukawa, C., Daigo, Y., Ishikawa, N., Kato, T., Ito, T., Tsuchiya, E., Sone, S., and Nakamura, Y. (2005). Plakophilin 3 oncogene as prognostic marker and therapeutic target for lung cancer. *Cancer research* *65*, 7102-7110.
200. Mege, R.M., Gavard, J., and Lambert, M. (2006). Regulation of cell-cell junctions by the cytoskeleton. *Curr Opin Cell Biol* *18*, 541-548.
201. Koestler, S.A., Rottner, K., Lai, F., Block, J., Vinzenz, M., and Small, J.V. (2009). F- and G-actin concentrations in lamellipodia of moving cells. *PLoS One* *4*, e4810.
202. Kovacs, E.M., Goodwin, M., Ali, R.G., Paterson, A.D., and Yap, A.S. (2002). Cadherin-directed actin assembly: E-cadherin physically associates with the Arp2/3 complex to direct actin assembly in nascent adhesive contacts. *Curr Biol* *12*, 379-382.
203. Verma, S., Shewan, A.M., Scott, J.A., Helwani, F.M., den Elzen, N.R., Miki, H., Takenawa, T., and Yap, A.S. (2004). Arp2/3 activity is necessary for efficient formation of E-cadherin adhesive contacts. *J Biol Chem* *279*, 34062-34070.
204. Pokutta, S., Drees, F., Takai, Y., Nelson, W.J., and Weis, W.I. (2002). Biochemical and structural definition of the I-afadin- and actin-binding sites of alpha-catenin. *J Biol Chem* *277*, 18868-18874.
205. Yamazaki, Y., Umeda, K., Wada, M., Nada, S., Okada, M., and Tsukita, S. (2008). ZO-1- and ZO-2-dependent integration of myosin-2 to epithelial zonula adherens. *Mol Biol Cell* *19*, 3801-3811.
206. Goldman, R.D., Cleland, M.M., Murthy, S.N., Mahammad, S., and Kuczmarski, E.R. (2012). Inroads into the structure and function of intermediate filament networks. *J Struct Biol* *177*, 14-23.
207. Kowalczyk, A.P., and Kottke, M.D. (2007). Making connections: desmoplakin as an intermediate filament-binding protein. *J Invest Dermatol* *127*, E8-9.

208. Conde, C., and Caceres, A. (2009). Microtubule assembly, organization and dynamics in axons and dendrites. *Nat Rev Neurosci* *10*, 319-332.
209. Kollman, J.M., Merdes, A., Mourey, L., and Agard, D.A. (2011). Microtubule nucleation by gamma-tubulin complexes. *Nat Rev Mol Cell Biol* *12*, 709-721.
210. Avila, J. (1990). Microtubule dynamics. *Faseb J* *4*, 3284-3290.
211. Karpova, A., Bar, J., and Kreutz, M.R. (2012). Long-distance signaling from synapse to nucleus via protein messengers. *Adv Exp Med Biol* *970*, 355-376.
212. Verhey, K.J., Kaul, N., and Soppina, V. (2011). Kinesin assembly and movement in cells. *Annu Rev Biophys* *40*, 267-288.
213. Eschbach, J., and Dupuis, L. (2011). Cytoplasmic dynein in neurodegeneration. *Pharmacol Ther* *130*, 348-363.
214. Stehbens, S., and Wittmann, T. (2012). Targeting and transport: how microtubules control focal adhesion dynamics. *J Cell Biol* *198*, 481-489.
215. Nagano, M., Hoshino, D., Koshikawa, N., Akizawa, T., and Seiki, M. (2012). Turnover of focal adhesions and cancer cell migration. *Int J Cell Biol* *2012*, 310616.
216. van der Flier, A., and Sonnenberg, A. (2001). Function and interactions of integrins. *Cell and tissue research* *305*, 285-298.
217. Hynes, R.O. (2002). Integrins: bidirectional, allosteric signaling machines. *Cell* *110*, 673-687.
218. Wozniak, M.A., Modzelewska, K., Kwong, L., and Keely, P.J. (2004). Focal adhesion regulation of cell behavior. *Biochim Biophys Acta* *1692*, 103-119.
219. Izzard, C.S., and Lochner, L.R. (1980). Formation of cell-to-substrate contacts during fibroblast motility: an interference-reflexion study. *J Cell Sci* *42*, 81-116.
220. Regen, C.M., and Horwitz, A.F. (1992). Dynamics of beta 1 integrin-mediated adhesive contacts in motile fibroblasts. *J Cell Biol* *119*, 1347-1359.

- 
221. Lauffenburger, D.A., and Horwitz, A.F. (1996). Cell migration: a physically integrated molecular process. *Cell* 84, 359-369.
222. Guan, J.L. (1997). Role of focal adhesion kinase in integrin signaling. *Int J Biochem Cell Biol* 29, 1085-1096.
223. Small, J.V., Stradal, T., Vignat, E., and Rottner, K. (2002). The lamellipodium: where motility begins. *Trends Cell Biol* 12, 112-120.
224. Laukaitis, C.M., Webb, D.J., Donais, K., and Horwitz, A.F. (2001). Differential dynamics of alpha 5 integrin, paxillin, and alpha-actinin during formation and disassembly of adhesions in migrating cells. *J Cell Biol* 153, 1427-1440.
225. Edlund, M., Lotano, M.A., and Otey, C.A. (2001). Dynamics of alpha-actinin in focal adhesions and stress fibers visualized with alpha-actinin-green fluorescent protein. *Cell motility and the cytoskeleton* 48, 190-200.
226. Schaller, M.D., Borgman, C.A., Cobb, B.S., Vines, R.R., Reynolds, A.B., and Parsons, J.T. (1992). pp125FAK a structurally distinctive protein-tyrosine kinase associated with focal adhesions. *Proc Natl Acad Sci U S A* 89, 5192-5196.
227. Cooper, L.A., Shen, T.L., and Guan, J.L. (2003). Regulation of focal adhesion kinase by its amino-terminal domain through an autoinhibitory interaction. *Mol Cell Biol* 23, 8030-8041.
228. Polte, T.R., and Hanks, S.K. (1995). Interaction between focal adhesion kinase and Crk-associated tyrosine kinase substrate p130Cas. *Proc Natl Acad Sci U S A* 92, 10678-10682.
229. Yano, Y., Geibel, J., and Sumpio, B.E. (1996). Tyrosine phosphorylation of pp125FAK and paxillin in aortic endothelial cells induced by mechanical strain. *Am J Physiol* 271, C635-649.

230. Zhao, J.H., Reiske, H., and Guan, J.L. (1998). Regulation of the cell cycle by focal adhesion kinase. *J Cell Biol* *143*, 1997-2008.
231. Schaller, M.D., Hildebrand, J.D., Shannon, J.D., Fox, J.W., Vines, R.R., and Parsons, J.T. (1994). Autophosphorylation of the focal adhesion kinase, pp125FAK, directs SH2-dependent binding of pp60src. *Mol Cell Biol* *14*, 1680-1688.
232. Calalb, M.B., Polte, T.R., and Hanks, S.K. (1995). Tyrosine phosphorylation of focal adhesion kinase at sites in the catalytic domain regulates kinase activity: a role for Src family kinases. *Mol Cell Biol* *15*, 954-963.
233. Schlaepfer, D.D., Jones, K.C., and Hunter, T. (1998). Multiple Grb2-mediated integrin-stimulated signaling pathways to ERK2/mitogen-activated protein kinase: summation of both c-Src- and focal adhesion kinase-initiated tyrosine phosphorylation events. *Mol Cell Biol* *18*, 2571-2585.
234. Schlaepfer, D.D., Hanks, S.K., Hunter, T., and van der Geer, P. (1994). Integrin-mediated signal transduction linked to Ras pathway by GRB2 binding to focal adhesion kinase. *Nature* *372*, 786-791.
235. Mitra, S.K., and Schlaepfer, D.D. (2006). Integrin-regulated FAK-Src signaling in normal and cancer cells. *Current opinion in cell biology* *18*, 516-523.
236. Katz, B.Z., Romer, L., Miyamoto, S., Volberg, T., Matsumoto, K., Cukierman, E., Geiger, B., and Yamada, K.M. (2003). Targeting membrane-localized focal adhesion kinase to focal adhesions: roles of tyrosine phosphorylation and SRC family kinases. *J Biol Chem* *278*, 29115-29120.
237. Liu, S., Kiosses, W.B., Rose, D.M., Slepak, M., Salgia, R., Griffin, J.D., Turner, C.E., Schwartz, M.A., and Ginsberg, M.H. (2002). A fragment of paxillin binds the alpha 4 integrin cytoplasmic domain (tail) and selectively inhibits alpha 4-mediated cell migration. *J Biol Chem* *277*, 20887-20894.

238. Choi, C.K., Zareno, J., Digman, M.A., Gratton, E., and Horwitz, A.R. (2011). Cross-correlated fluctuation analysis reveals phosphorylation-regulated paxillin-FAK complexes in nascent adhesions. *Biophys J* *100*, 583-592.
239. Petit, V., Boyer, B., Lentz, D., Turner, C.E., Thiery, J.P., and Valles, A.M. (2000). Phosphorylation of tyrosine residues 31 and 118 on paxillin regulates cell migration through an association with CRK in NBT-II cells. *J Cell Biol* *148*, 957-970.
240. Koetsier, J.L., Amargo, E.V., Todorovic, V., Green, K.J., and Godsel, L.M. (2014). Plakophilin 2 affects cell migration by modulating focal adhesion dynamics and integrin protein expression. *The Journal of investigative dermatology* *134*, 112-122.
241. Lamorte, L., Rodrigues, S., Sangwan, V., Turner, C.E., and Park, M. (2003). Crk associates with a multimolecular Paxillin/GIT2/beta-PIX complex and promotes Rac-dependent relocalization of Paxillin to focal contacts. *Mol Biol Cell* *14*, 2818-2831.
242. Wang, Y., and Gilmore, T.D. (2003). Zyxin and paxillin proteins: focal adhesion plaque LIM domain proteins go nuclear. *Biochim Biophys Acta* *1593*, 115-120.
243. Zaidel-Bar, R., Ballestrem, C., Kam, Z., and Geiger, B. (2003). Early molecular events in the assembly of matrix adhesions at the leading edge of migrating cells. *J Cell Sci* *116*, 4605-4613.
244. Yi, J., Kloeker, S., Jensen, C.C., Bockholt, S., Honda, H., Hirai, H., and Beckerle, M.C. (2002). Members of the Zyxin family of LIM proteins interact with members of the p130Cas family of signal transducers. *J Biol Chem* *277*, 9580-9589.
245. Yoshigi, M., Hoffman, L.M., Jensen, C.C., Yost, H.J., and Beckerle, M.C. (2005). Mechanical force mobilizes zyxin from focal adhesions to actin filaments and regulates cytoskeletal reinforcement. *J Cell Biol* *171*, 209-215.

246. Hirata, H., Tatsumi, H., and Sokabe, M. (2008). Mechanical forces facilitate actin polymerization at focal adhesions in a zyxin-dependent manner. *J Cell Sci* *121*, 2795-2804.
247. Mori, M., Nakagami, H., Koibuchi, N., Miura, K., Takami, Y., Koriyama, H., Hayashi, H., Sabe, H., Mochizuki, N., Morishita, R., et al. (2009). Zyxin mediates actin fiber reorganization in epithelial-mesenchymal transition and contributes to endocardial morphogenesis. *Mol Biol Cell* *20*, 3115-3124.
248. Li, B., and Trueb, B. (2001). Analysis of the alpha-actinin/zyxin interaction. *J Biol Chem* *276*, 33328-33335.
249. Drees, B., Friederich, E., Fradelizi, J., Louvard, D., Beckerle, M.C., and Golsteyn, R.M. (2000). Characterization of the interaction between zyxin and members of the Ena/vasodilator-stimulated phosphoprotein family of proteins. *J Biol Chem* *275*, 22503-22511.
250. Schneider, L., Cammer, M., Lehman, J., Nielsen, S.K., Guerra, C.F., Veland, I.R., Stock, C., Hoffmann, E.K., Yoder, B.K., Schwab, A., et al. (2010). Directional cell migration and chemotaxis in wound healing response to PDGF-AA are coordinated by the primary cilium in fibroblasts. *Cell Physiol Biochem* *25*, 279-292.
251. Aman, A., and Piotrowski, T. (2010). Cell migration during morphogenesis. *Dev Biol* *341*, 20-33.
252. Weijer, C.J. (2009). Collective cell migration in development. *J Cell Sci* *122*, 3215-3223.
253. Tracey A. Martin, L.Y., Andrew J. Sanders, Jane Lane, and Wen G. Jiang (2000). *Cancer Invasion and Metastasis: Molecular and Cellular Perspective*. Madame Curie Bioscience Database [Internet]. Austin (TX): Landes Bioscience.

- 
254. Yamaguchi, H., and Condeelis, J. (2007). Regulation of the actin cytoskeleton in cancer cell migration and invasion. *Biochim Biophys Acta* 1773, 642-652.
255. Fournier, M.F., Sauser, R., Ambrosi, D., Meister, J.J., and Verkhovsky, A.B. (2010). Force transmission in migrating cells. *J Cell Biol* 188, 287-297.
256. Spiering, D., and Hodgson, L. (2011). Dynamics of the Rho-family small GTPases in actin regulation and motility. *Cell adhesion & migration* 5, 170-180.
257. Ridley, A.J. (2006). Rho GTPases and actin dynamics in membrane protrusions and vesicle trafficking. *Trends Cell Biol* 16, 522-529.
258. Ridley, A.J., and Hall, A. (1992). The small GTP-binding protein rho regulates the assembly of focal adhesions and actin stress fibers in response to growth factors. *Cell* 70, 389-399.
259. Bourne, H.R., Sanders, D.A., and McCormick, F. (1990). The GTPase superfamily: a conserved switch for diverse cell functions. *Nature* 348, 125-132.
260. O'Connor, K., and Chen, M. (2013). Dynamic functions of RhoA in tumor cell migration and invasion. *Small GTPases* 4, 141-147.
261. Gibbs, J.B., Marshall, M.S., Scolnick, E.M., Dixon, R.A., and Vogel, U.S. (1990). Modulation of guanine nucleotides bound to Ras in NIH3T3 cells by oncogenes, growth factors, and the GTPase activating protein (GAP). *J Biol Chem* 265, 20437-20442.
262. Snyder, J.T., Worthylake, D.K., Rossman, K.L., Betts, L., Pruitt, W.M., Siderovski, D.P., Der, C.J., and Sondek, J. (2002). Structural basis for the selective activation of Rho GTPases by Dbl exchange factors. *Nat Struct Biol* 9, 468-475.
263. Dovas, A., and Couchman, J.R. (2005). RhoGDI: multiple functions in the regulation of Rho family GTPase activities. *Biochem J* 390, 1-9.

264. Lin, Q., Fuji, R.N., Yang, W., and Cerione, R.A. (2003). RhoGDI is required for Cdc42-mediated cellular transformation. *Current biology : CB* *13*, 1469-1479.
265. Nobes, C.D., and Hall, A. (1995). Rho, rac, and cdc42 GTPases regulate the assembly of multimolecular focal complexes associated with actin stress fibers, lamellipodia, and filopodia. *Cell* *81*, 53-62.
266. Sit, S.T., and Manser, E. (2011). Rho GTPases and their role in organizing the actin cytoskeleton. *J Cell Sci* *124*, 679-683.
267. Vega, F.M., and Ridley, A.J. (2008). Rho GTPases in cancer cell biology. *FEBS Lett* *582*, 2093-2101.
268. Machacek, M., Hodgson, L., Welch, C., Elliott, H., Pertz, O., Nalbant, P., Abell, A., Johnson, G.L., Hahn, K.M., and Danuser, G. (2009). Coordination of Rho GTPase activities during cell protrusion. *Nature* *461*, 99-103.
269. O'Connor, K.L., Shaw, L.M., and Mercurio, A.M. (1998). Release of cAMP gating by the alpha6beta4 integrin stimulates lamellae formation and the chemotactic migration of invasive carcinoma cells. *J Cell Biol* *143*, 1749-1760.
270. Chrzanowska-Wodnicka, M., and Burridge, K. (1996). Rho-stimulated contractility drives the formation of stress fibers and focal adhesions. *J Cell Biol* *133*, 1403-1415.
271. Arber, S., Barbayannis, F.A., Hanser, H., Schneider, C., Stanyon, C.A., Bernard, O., and Caroni, P. (1998). Regulation of actin dynamics through phosphorylation of cofilin by LIM-kinase. *Nature* *393*, 805-809.
272. DesMarais, V., Ghosh, M., Eddy, R., and Condeelis, J. (2005). Cofilin takes the lead. *J Cell Sci* *118*, 19-26.
273. Mouneimne, G., Soon, L., DesMarais, V., Sidani, M., Song, X., Yip, S.C., Ghosh, M., Eddy, R., Backer, J.M., and Condeelis, J. (2004). Phospholipase C and cofilin are

- required for carcinoma cell directionality in response to EGF stimulation. *J Cell Biol* *166*, 697-708.
274. Huang, T.Y., DerMardirossian, C., and Bokoch, G.M. (2006). Cofilin phosphatases and regulation of actin dynamics. *Current opinion in cell biology* *18*, 26-31.
275. Ghosh, M., Song, X., Mouneimne, G., Sidani, M., Lawrence, D.S., and Condeelis, J.S. (2004). Cofilin promotes actin polymerization and defines the direction of cell motility. *Science* *304*, 743-746.
276. Agnew, B.J., Minamide, L.S., and Bamburg, J.R. (1995). Reactivation of phosphorylated actin depolymerizing factor and identification of the regulatory site. *J Biol Chem* *270*, 17582-17587.
277. Hotulainen, P., Paunola, E., Vartiainen, M.K., and Lappalainen, P. (2005). Actin-depolymerizing factor and cofilin-1 play overlapping roles in promoting rapid F-actin depolymerization in mammalian nonmuscle cells. *Mol Biol Cell* *16*, 649-664.
278. Zebda, N., Bernard, O., Bailly, M., Welti, S., Lawrence, D.S., and Condeelis, J.S. (2000). Phosphorylation of ADF/cofilin abolishes EGF-induced actin nucleation at the leading edge and subsequent lamellipod extension. *J Cell Biol* *151*, 1119-1128.
279. Hagedorn, E.J., Kelley, L.C., Naegeli, K.M., Wang, Z., Chi, Q., and Sherwood, D.R. (2014). ADF/cofilin promotes invadopodial membrane recycling during cell invasion in vivo. *J Cell Biol* *204*, 1209-1218.
280. Collazo, J., Zhu, B., Larkin, S., Martin, S.K., Pu, H., Horbinski, C., Koochekpour, S., and Kyprianou, N. (2014). Cofilin drives cell-invasive and metastatic responses to TGF-beta in prostate cancer. *Cancer research* *74*, 2362-2373.
281. Wang, W., and Shakes, D.C. (1996). Molecular evolution of the 14-3-3 protein family. *J Mol Evol* *43*, 384-398.

282. Wilker, E., and Yaffe, M.B. (2004). 14-3-3 Proteins--a focus on cancer and human disease. *J Mol Cell Cardiol* 37, 633-642.
283. Yaffe, M.B., Rittinger, K., Volinia, S., Caron, P.R., Aitken, A., Leffers, H., Gamblin, S.J., Smerdon, S.J., and Cantley, L.C. (1997). The structural basis for 14-3-3:phosphopeptide binding specificity. *Cell* 91, 961-971.
284. Yaffe, M.B., and Elia, A.E. (2001). Phosphoserine/threonine-binding domains. *Curr Opin Cell Biol* 13, 131-138.
285. Pozuelo Rubio, M., Geraghty, K.M., Wong, B.H., Wood, N.T., Campbell, D.G., Morrice, N., and Mackintosh, C. (2004). 14-3-3-affinity purification of over 200 human phosphoproteins reveals new links to regulation of cellular metabolism, proliferation and trafficking. *Biochem J* 379, 395-408.
286. Wang, W., and Shakes, D.C. (1996). Molecular evolution of the 14-3-3 protein family. *J Mol Evol* 43, 384-398.
287. Mackintosh, C. (2004). Dynamic interactions between 14-3-3 proteins and phosphoproteins regulate diverse cellular processes. *Biochem J* 381, 329-342.
288. Bridges, D., and Moorhead, G.B. (2005). 14-3-3 proteins: a number of functions for a numbered protein. *Sci STKE* 2005, re10.
289. Bridges, D., and Moorhead, G.B. (2004). 14-3-3 proteins: a number of functions for a numbered protein. *Sci STKE* 2004, re10.
290. Darling, D.L., Yingling, J., and Wynshaw-Boris, A. (2005). Role of 14-3-3 proteins in eukaryotic signaling and development. *Curr Top Dev Biol* 68, 281-315.
291. Hermeking, H., and Benzinger, A. (2006). 14-3-3 proteins in cell cycle regulation. *Semin Cancer Biol* 16, 183-192.
292. Pozuelo Rubio, M., Geraghty, K.M., Wong, B.H., Wood, N.T., Campbell, D.G., Morrice, N., and Mackintosh, C. (2004). 14-3-3-affinity purification of over 200

- human phosphoproteins reveals new links to regulation of cellular metabolism, proliferation and trafficking. *Biochem J* 379, 395-408.
293. Tzivion, G., Gupta, V.S., Kaplun, L., and Balan, V. (2006). 14-3-3 proteins as potential oncogenes. *Semin Cancer Biol* 16, 203-213.
294. Yang, X., Lee, W.H., Sobott, F., Papagrigoriou, E., Robinson, C.V., Grossmann, J.G., Sundstrom, M., Doyle, D.A., and Elkins, J.M. (2006). Structural basis for protein-protein interactions in the 14-3-3 protein family. *Proc Natl Acad Sci U S A* 103, 17237-17242.
295. Chaudhri, M., Scarabel, M., and Aitken, A. (2003). Mammalian and yeast 14-3-3 isoforms form distinct patterns of dimers in vivo. *Biochem Biophys Res Commun* 300, 679-685.
296. Dintenfass, L. (1977). Blood viscosity factors in nondiabetic and diabetic retinopathy. *Bibl Anat*, 422-424.
297. Xiao, B., Smerdon, S.J., Jones, D.H., Dodson, G.G., Soneji, Y., Aitken, A., and Gamblin, S.J. (1995). Structure of a 14-3-3 protein and implications for coordination of multiple signalling pathways. *Nature* 376, 188-191.
298. Aitken, A. (2002). Functional specificity in 14-3-3 isoform interactions through dimer formation and phosphorylation. Chromosome location of mammalian isoforms and variants. *Plant Mol Biol* 50, 993-1010.
299. Benzinger, A., Popowicz, G.M., Joy, J.K., Majumdar, S., Holak, T.A., and Hermeking, H. (2005). The crystal structure of the non-liganded 14-3-3sigma protein: insights into determinants of isoform specific ligand binding and dimerization. *Cell Res* 15, 219-227.

300. Liu, D., Bienkowska, J., Petosa, C., Collier, R.J., Fu, H., and Liddington, R. (1995). Crystal structure of the zeta isoform of the 14-3-3 protein. *Nature* 376, 191-194.
301. Dubois, T., Rommel, C., Howell, S., Steinhussen, U., Soneji, Y., Morrice, N., Moelling, K., and Aitken, A. (1997). 14-3-3 is phosphorylated by casein kinase I on residue 233. Phosphorylation at this site in vivo regulates Raf/14-3-3 interaction. *J Biol Chem* 272, 28882-28888.
302. Powell, D.W., Rane, M.J., Joughin, B.A., Kalmukova, R., Hong, J.H., Tidor, B., Dean, W.L., Pierce, W.M., Klein, J.B., Yaffe, M.B., et al. (2003). Proteomic identification of 14-3-3zeta as a mitogen-activated protein kinase-activated protein kinase 2 substrate: role in dimer formation and ligand binding. *Mol Cell Biol* 23, 5376-5387.
303. Aitken, A., Howell, S., Jones, D., Madrazo, J., and Patel, Y. (1995). 14-3-3 alpha and delta are the phosphorylated forms of raf-activating 14-3-3 beta and zeta. In vivo stoichiometric phosphorylation in brain at a Ser-Pro-Glu-Lys MOTIF. *J Biol Chem* 270, 5706-5709.
304. Obsilova, V., Herman, P., Vecer, J., Sulc, M., Teisinger, J., and Obsil, T. (2004). 14-3-3zeta C-terminal stretch changes its conformation upon ligand binding and phosphorylation at Thr232. *J Biol Chem* 279, 4531-4540.
305. Leffers, H., Madsen, P., Rasmussen, H.H., Honore, B., Andersen, A.H., Walbum, E., Vandekerckhove, J., and Celis, J.E. (1993). Molecular cloning and expression of the transformation sensitive epithelial marker stratifin. A member of a protein family that has been involved in the protein kinase C signalling pathway. *J Mol Biol* 231, 982-998.
306. Taylor, J.W. (1975). Depression in thyrotoxicosis. *Am J Psychiatry* 132, 552-553.

307. Ferguson, A.T., Evron, E., Umbricht, C.B., Pandita, T.K., Chan, T.A., Hermeking, H., Marks, J.R., Lambers, A.R., Futreal, P.A., Stampfer, M.R., et al. (2000). High frequency of hypermethylation at the 14-3-3 sigma locus leads to gene silencing in breast cancer. *Proc Natl Acad Sci U S A* 97, 6049-6054.
308. Umbricht, C.B., Evron, E., Gabrielson, E., Ferguson, A., Marks, J., and Sukumar, S. (2001). Hypermethylation of 14-3-3 sigma (stratifin) is an early event in breast cancer. *Oncogene* 20, 3348-3353.
309. Bhawal, U.K., Sugiyama, M., Nomura, Y., Kuniyasu, H., and Tsukinoki, K. (2008). Loss of 14-3-3 sigma protein expression and presence of human papillomavirus type 16 E6 in oral squamous cell carcinoma. *Arch Otolaryngol Head Neck Surg* 134, 1055-1059.
310. Kunze, E., Wendt, M., and Schlott, T. (2006). Promoter hypermethylation of the 14-3-3 sigma, SYK and CAGE-1 genes is related to the various phenotypes of urinary bladder carcinomas and associated with progression of transitional cell carcinomas. *Int J Mol Med* 18, 547-557.
311. Moreira, J.M., Gromov, P., and Celis, J.E. (2004). Expression of the tumor suppressor protein 14-3-3 sigma is down-regulated in invasive transitional cell carcinomas of the urinary bladder undergoing epithelial-to-mesenchymal transition. *Mol Cell Proteomics* 3, 410-419.
312. Iwata, N., Yamamoto, H., Sasaki, S., Itoh, F., Suzuki, H., Kikuchi, T., Kaneto, H., Iku, S., Ozeki, I., Karino, Y., et al. (2000). Frequent hypermethylation of CpG islands and loss of expression of the 14-3-3 sigma gene in human hepatocellular carcinoma. *Oncogene* 19, 5298-5302.

313. Suzuki, H., Itoh, F., Toyota, M., Kikuchi, T., Kakiuchi, H., and Imai, K. (2000). Inactivation of the 14-3-3 sigma gene is associated with 5' CpG island hypermethylation in human cancers. *Cancer research* *60*, 4353-4357.
314. Villaret, D.B., Wang, T., Dillon, D., Xu, J., Sivam, D., Cheever, M.A., and Reed, S.G. (2000). Identification of genes overexpressed in head and neck squamous cell carcinoma using a combination of complementary DNA subtraction and microarray analysis. *Laryngoscope* *110*, 374-381.
315. Gasco, M., Sullivan, A., Repellin, C., Brooks, L., Farrell, P.J., Tidy, J.A., Dunne, B., Gusterson, B., Evans, D.J., and Crook, T. (2002). Coincident inactivation of 14-3-3sigma and p16INK4a is an early event in vulval squamous neoplasia. *Oncogene* *21*, 1876-1881.
316. Urano, T., Saito, T., Tsukui, T., Fujita, M., Hosoi, T., Muramatsu, M., Ouchi, Y., and Inoue, S. (2002). Efp targets 14-3-3 sigma for proteolysis and promotes breast tumour growth. *Nature* *417*, 871-875.
317. Ravi, D., Chen, Y., Karia, B., Brown, A., Gu, T.T., Li, J., Carey, M.S., Hennessy, B.T., and Bishop, A.J. (2011). 14-3-3 sigma expression effects G2/M response to oxygen and correlates with ovarian cancer metastasis. *PLoS One* *6*, e15864.
318. Kuramitsu, Y., Baron, B., Yoshino, S., Zhang, X., Tanaka, T., Yashiro, M., Hirakawa, K., Oka, M., and Nakamura, K. (2010). Proteomic differential display analysis shows up-regulation of 14-3-3 sigma protein in human scirrhous-type gastric carcinoma cells. *Anticancer Res* *30*, 4459-4465.
319. Hayashi, E., Kuramitsu, Y., Fujimoto, M., Zhang, X., Tanaka, T., Uchida, K., Fukuda, T., Furumoto, H., Ueyama, Y., and Nakamura, K. (2009). Proteomic profiling of differential display analysis for human oral squamous cell carcinoma: 14-

- 3-3 sigma Protein is upregulated in human oral squamous cell carcinoma and dependent on the differentiation level. *Proteomics Clin Appl* 3, 1338-1347.
320. Nakayama, H., Sano, T., Motegi, A., Oyama, T., and Nakajima, T. (2005). Increasing 14-3-3 sigma expression with declining estrogen receptor alpha and estrogen-responsive finger protein expression defines malignant progression of endometrial carcinoma. *Pathol Int* 55, 707-715.
321. Chan, T.A., Hermeking, H., Lengauer, C., Kinzler, K.W., and Vogelstein, B. (1999). 14-3-3Sigma is required to prevent mitotic catastrophe after DNA damage. *Nature* 401, 616-620.
322. Stavridi, E.S., Chehab, N.H., Malikzay, A., and Halazonetis, T.D. (2001). Substitutions that compromise the ionizing radiation-induced association of p53 with 14-3-3 proteins also compromise the ability of p53 to induce cell cycle arrest. *Cancer research* 61, 7030-7033.
323. Roberts, B.J., Reddy, R., and Wahl, J.K., 3rd (2013). Stratifin (14-3-3 sigma) limits plakophilin-3 exchange with the desmosomal plaque. *PLoS One* 8, e77012.
324. Boudreau, A., Tanner, K., Wang, D., Geyer, F.C., Reis-Filho, J.S., and Bissell, M.J. (2013). 14-3-3sigma stabilizes a complex of soluble actin and intermediate filament to enable breast tumor invasion. *Proc Natl Acad Sci U S A* 110, E3937-3944.
325. Ling, C., Zuo, D., Xue, B., Muthuswamy, S., and Muller, W.J. (2010). A novel role for 14-3-3sigma in regulating epithelial cell polarity. *Genes Dev* 24, 947-956.
326. Sehgal, L., Mukhopadhyay, A., Rajan, A., Khapare, N., Sawant, M., Vishal, S.S., Bhatt, K., Ambatipudi, S., Antao, N., Alam, H., et al. (2014). 14-3-3gamma-Mediated transport of plakoglobin to the cell border is required for the initiation of desmosome assembly in vitro and in vivo. *J Cell Sci* 127, 2174-2188.

327. Sehgal, L. (2012). Generation of knockdown mice that lack 14-3-3 $\epsilon$  and 14-3-3 $\gamma$  using RNA interference. Ph.D. Thesis HOMI BHABHA NATIONAL INSTITUTE.
328. Hosing, A.S., Kundu, S.T., and Dalal, S.N. (2008). 14-3-3 Gamma is required to enforce both the incomplete S phase and G2 DNA damage checkpoints. *Cell Cycle* 7, 3171-3179.
329. Dalal, S.N., Schweitzer, C.M., Gan, J., and DeCaprio, J.A. (1999). Cytoplasmic localization of human cdc25C during interphase requires an intact 14-3-3 binding site. *Mol Cell Biol* 19, 4465-4479.
330. MUKHOPADHYAY, A. (2012). REGULATION OF CELL CYCLE CHECKPOINT PATHWAYS BY 14-3-3 $\epsilon$  AND 14-3-3 $\gamma$ . Ph.D. Thesis.
331. Qi, W., Liu, X., Chen, W., Li, Q., and Martinez, J.D. (2007). Overexpression of 14-3-3 $\gamma$  causes polyploidization in H322 lung cancer cells. *Mol Carcinog* 46, 847-856.
332. Jin, Y.H., Kim, Y.J., Kim, D.W., Baek, K.H., Kang, B.Y., Yeo, C.Y., and Lee, K.Y. (2008). Sirt2 interacts with 14-3-3 beta/gamma and down-regulates the activity of p53. *Biochem Biophys Res Commun* 368, 690-695.
333. Hirokawa, N., and Noda, Y. (2008). Intracellular transport and kinesin superfamily proteins, KIFs: structure, function, and dynamics. *Physiol Rev* 88, 1089-1118.
334. Miki, H., Setou, M., Kaneshiro, K., and Hirokawa, N. (2001). All kinesin superfamily protein, KIF, genes in mouse and human. *Proc Natl Acad Sci U S A* 98, 7004-7011.
335. Hirokawa, N. (1998). Kinesin and dynein superfamily proteins and the mechanism of organelle transport. *Science* 279, 519-526.

336. Miki, H., Okada, Y., and Hirokawa, N. (2005). Analysis of the kinesin superfamily: insights into structure and function. *Trends Cell Biol* *15*, 467-476.
337. Hirokawa, N., Pfister, K.K., Yorifuji, H., Wagner, M.C., Brady, S.T., and Bloom, G.S. (1989). Submolecular domains of bovine brain kinesin identified by electron microscopy and monoclonal antibody decoration. *Cell* *56*, 867-878.
338. Marx, A., Hoenger, A., and Mandelkow, E. (2009). Structures of kinesin motor proteins. *Cell Motil Cytoskeleton* *66*, 958-966.
339. Meng, W., Mushika, Y., Ichii, T., and Takeichi, M. (2008). Anchorage of microtubule minus ends to adherens junctions regulates epithelial cell-cell contacts. *Cell* *135*, 948-959.
340. Mary, S., Charrasse, S., Meriane, M., Comunale, F., Travo, P., Blangy, A., and Gauthier-Rouviere, C. (2002). Biogenesis of N-cadherin-dependent cell-cell contacts in living fibroblasts is a microtubule-dependent kinesin-driven mechanism. *Mol Biol Cell* *13*, 285-301.
341. Chen, X., Kojima, S., Borisy, G.G., and Green, K.J. (2003). p120 catenin associates with kinesin and facilitates the transport of cadherin-catenin complexes to intercellular junctions. *J Cell Biol* *163*, 547-557.
342. Nekrasova, O.E., Amargo, E.V., Smith, W.O., Chen, J., Kreitzer, G.E., and Green, K.J. (2011). Desmosomal cadherins utilize distinct kinesins for assembly into desmosomes. *J Cell Biol* *195*, 1185-1203.
343. Ichimura, T., Wakamiya-Tsuruta, A., Itagaki, C., Taoka, M., Hayano, T., Natsume, T., and Isobe, T. (2002). Phosphorylation-dependent interaction of kinesin light chain 2 and the 14-3-3 protein. *Biochemistry* *41*, 5566-5572.

344. Dorner, C., Ullrich, A., Haring, H.U., and Lammers, R. (1999). The kinesin-like motor protein KIF1C occurs in intact cells as a dimer and associates with proteins of the 14-3-3 family. *J Biol Chem* 274, 33654-33660.
345. Fan, S., Hurd, T.W., Liu, C.J., Straight, S.W., Weimbs, T., Hurd, E.A., Domino, S.E., and Margolis, B. (2004). Polarity proteins control ciliogenesis via kinesin motor interactions. *Curr Biol* 14, 1451-1461.
346. Gindhart, J.G. (2006). Towards an understanding of kinesin-1 dependent transport pathways through the study of protein-protein interactions. *Brief Funct Genomic Proteomic* 5, 74-86.
347. Lim, J., and Thiery, J.P. (2012). Epithelial-mesenchymal transitions: insights from development. *Development* 139, 3471-3486.
348. Thiery, J.P., Acloque, H., Huang, R.Y., and Nieto, M.A. (2009). Epithelial-mesenchymal transitions in development and disease. *Cell* 139, 871-890.
349. Larue, L., and Bellacosa, A. (2005). Epithelial-mesenchymal transition in development and cancer: role of phosphatidylinositol 3' kinase/AKT pathways. *Oncogene* 24, 7443-7454.
350. Nistico, P., Bissell, M.J., and Radisky, D.C. (2012). Epithelial-mesenchymal transition: general principles and pathological relevance with special emphasis on the role of matrix metalloproteinases. *Cold Spring Harb Perspect Biol* 4.
351. Radisky, D.C. (2005). Epithelial-mesenchymal transition. *J Cell Sci* 118, 4325-4326.
352. Kalluri, R., and Weinberg, R.A. (2009). The basics of epithelial-mesenchymal transition. *J Clin Invest* 119, 1420-1428.
353. Tsai, J.H., and Yang, J. (2013). Epithelial-mesenchymal plasticity in carcinoma metastasis. *Genes Dev* 27, 2192-2206.

354. Davis, F.M., Stewart, T.A., Thompson, E.W., and Monteith, G.R. (2014). Targeting EMT in cancer: opportunities for pharmacological intervention. *Trends Pharmacol Sci* 35, 479-488.
355. Creighton, C.J., Chang, J.C., and Rosen, J.M. (2010). Epithelial-mesenchymal transition (EMT) in tumor-initiating cells and its clinical implications in breast cancer. *J Mammary Gland Biol Neoplasia* 15, 253-260.
356. Trimboli, A.J., Fukino, K., de Bruin, A., Wei, G., Shen, L., Tanner, S.M., Creasap, N., Rosol, T.J., Robinson, M.L., Eng, C., et al. (2008). Direct evidence for epithelial-mesenchymal transitions in breast cancer. *Cancer research* 68, 937-945.
357. Bonnomet, A., Syne, L., Brysse, A., Feyereisen, E., Thompson, E.W., Noel, A., Foidart, J.M., Birembaut, P., Polette, M., and Gilles, C. (2012). A dynamic in vivo model of epithelial-to-mesenchymal transitions in circulating tumor cells and metastases of breast cancer. *Oncogene* 31, 3741-3753.
358. M. Gurjar, K.R., S. N. Dalal, (January 2015). Loss of the desmosomal plaque protein plakophilin 3 does not induce the epithelial mesenchymal transition. *J Biosci Tech* 6, 647
359. Tarin, D., Thompson, E.W., and Newgreen, D.F. (2005). The fallacy of epithelial mesenchymal transition in neoplasia. *Cancer research* 65, 5996-6000; discussion 6000-5991.
360. Battle, E., Sancho, E., Franci, C., Dominguez, D., Monfar, M., Baulida, J., and Garcia De Herreros, A. (2000). The transcription factor snail is a repressor of E-cadherin gene expression in epithelial tumour cells. *Nature cell biology* 2, 84-89.
361. Hajra, K.M., Chen, D.Y., and Fearon, E.R. (2002). The SLUG zinc-finger protein represses E-cadherin in breast cancer. *Cancer research* 62, 1613-1618.

362. Cano, A., Perez-Moreno, M.A., Rodrigo, I., Locascio, A., Blanco, M.J., del Barrio, M.G., Portillo, F., and Nieto, M.A. (2000). The transcription factor snail controls epithelial-mesenchymal transitions by repressing E-cadherin expression. *Nature cell biology* 2, 76-83.
363. Medici, D., Hay, E.D., and Olsen, B.R. (2008). Snail and Slug promote epithelial-mesenchymal transition through beta-catenin-T-cell factor-4-dependent expression of transforming growth factor-beta3. *Mol Biol Cell* 19, 4875-4887.
364. Comijn, J., Berx, G., Vermassen, P., Verschueren, K., van Grunsven, L., Bruyneel, E., Mareel, M., Huylebroeck, D., and van Roy, F. (2001). The two-handed E box binding zinc finger protein SIP1 downregulates E-cadherin and induces invasion. *Mol Cell* 7, 1267-1278.
365. Korpala, M., Lee, E.S., Hu, G., and Kang, Y. (2008). The miR-200 family inhibits epithelial-mesenchymal transition and cancer cell migration by direct targeting of E-cadherin transcriptional repressors ZEB1 and ZEB2. *J Biol Chem* 283, 14910-14914.
366. Ohkubo, T., and Ozawa, M. (2004). The transcription factor Snail downregulates the tight junction components independently of E-cadherin downregulation. *J Cell Sci* 117, 1675-1685.
367. Vandewalle, C., Comijn, J., De Craene, B., Vermassen, P., Bruyneel, E., Andersen, H., Tulchinsky, E., Van Roy, F., and Berx, G. (2005). SIP1/ZEB2 induces EMT by repressing genes of different epithelial cell-cell junctions. *Nucleic Acids Res* 33, 6566-6578.
368. Chen, Y., and Gridley, T. (2013). The SNAI1 and SNAI2 proteins occupy their own and each other's promoter during chondrogenesis. *Biochem Biophys Res Commun* 435, 356-360.

369. Wels, C., Joshi, S., Koefinger, P., Bergler, H., and Schaidler, H. (2011). Transcriptional activation of ZEB1 by Slug leads to cooperative regulation of the epithelial-mesenchymal transition-like phenotype in melanoma. *The Journal of investigative dermatology* *131*, 1877-1885.
370. Eckert, M.A., Lwin, T.M., Chang, A.T., Kim, J., Danis, E., Ohno-Machado, L., and Yang, J. (2011). Twist1-induced invadopodia formation promotes tumor metastasis. *Cancer Cell* *19*, 372-386.
371. Savagner, P., Yamada, K.M., and Thiery, J.P. (1997). The zinc-finger protein slug causes desmosome dissociation, an initial and necessary step for growth factor-induced epithelial-mesenchymal transition. *J Cell Biol* *137*, 1403-1419.
372. Chen, H., Zhu, G., Li, Y., Padia, R.N., Dong, Z., Pan, Z.K., Liu, K., and Huang, S. (2009). Extracellular signal-regulated kinase signaling pathway regulates breast cancer cell migration by maintaining slug expression. *Cancer research* *69*, 9228-9235.
373. Wertz, I.E., O'Rourke, K.M., Zhang, Z., Dornan, D., Arnott, D., Deshaies, R.J., and Dixit, V.M. (2004). Human De-etiolated-1 regulates c-Jun by assembling a CUL4A ubiquitin ligase. *Science* *303*, 1371-1374.
374. Gao, M., Labuda, T., Xia, Y., Gallagher, E., Fang, D., Liu, Y.C., and Karin, M. (2004). Jun turnover is controlled through JNK-dependent phosphorylation of the E3 ligase Itch. *Science* *306*, 271-275.
375. Nateri, A.S., Riera-Sans, L., Da Costa, C., and Behrens, A. (2004). The ubiquitin ligase SCFFbw7 antagonizes apoptotic JNK signaling. *Science* *303*, 1374-1378.
376. Yu, J., Zhang, W., Gao, F., Liu, Y.X., Chen, Z.Y., Cheng, L.Y., Xie, S.F., and Zheng, S.S. (2014). FBW7 increases chemosensitivity in hepatocellular carcinoma cells through suppression of epithelial-mesenchymal transition. *Hepatobiliary Pancreat Dis Int* *13*, 184-191.

377. Mei, Y., Yuan, Z., Song, B., Li, D., Ma, C., Hu, C., Ching, Y.P., and Li, M. (2008). Activating transcription factor 3 up-regulated by c-Jun NH(2)-terminal kinase/c-Jun contributes to apoptosis induced by potassium deprivation in cerebellar granule neurons. *Neuroscience* *151*, 771-779.
378. Niessen, K., Fu, Y., Chang, L., Hoodless, P.A., McFadden, D., and Karsan, A. (2008). Slug is a direct Notch target required for initiation of cardiac cushion cellularization. *J Cell Biol* *182*, 315-325.
379. D'souza, R. (2014). Role of 14-3-3  $\sigma$  in regulating Epithelial Mesenchymal Transition. M.Sc. Thesis Mumbai University
380. Spector DL, G.R., Leinwand LA, eds. (1998). *Cells: a laboratory manual*. Cold Spring Harbor, NY: Cold Spring Harbor Laboratory, *vol. 2*.
381. Chaudhary, N., and Maddika, S. (2014). WWP2-WWP1 ubiquitin ligase complex coordinated by PPM1G maintains the balance between cellular p73 and DeltaNp73 levels. *Mol Cell Biol* *34*, 3754-3764.
382. Hosing, A.S. (2009). Regulation Of The G2/M Dna Damage Checkpoint By 14-3-3 Proteins In Human Cells. Ph.D. Thesis University of Mumbai.
383. Subhra, K.S.T. (2009). Regulation Of The G2 / M Dna Damage Checkpoint And Neoplastic Progression By 14-3-3 Sigma And Plakophilin 3. Ph.D. Thesis University of Mumbai.
384. K. Raychaudhuri, M.G.a.S.N.D. (2015). Plakophilin3 and Plakoglobin recycling are differentially regulated during the disassembly of desmosomes. *Journal of Bioscience And Technology* *6*, 634-642.
385. Mansa Gurjar, K.R., Sorab N. Dalal (2015). Loss of the desmosomal plaque protein plakophilin 3 does not induce the epithelial mesenchymal transition. *Journal of Bioscience And Technology* *Vol 6*, 647-652.

386. Alam, H., Kundu, S.T., Dalal, S.N., and Vaidya, M.M. (2011). Loss of keratins 8 and 18 leads to alterations in alpha6beta4-integrin-mediated signalling and decreased neoplastic progression in an oral-tumour-derived cell line. *J Cell Sci* *124*, 2096-2106.
387. Shah, P.P. (2014). ROLE OF 14-3-3 $\sigma$  AND PLAKOPHILIN3 IN REGULATION OF FOCAL ADHESION STRENGTH AND TURNOVER. Master of science desertation thesis of Sardar Patel University
388. Limzerwala, J.F. (2014). Role of 14-3-3 $\sigma$  In Regulating Focal Adhesion Turnover. Dissertation thesis University Of Mumbai.
389. Kudo, N., Matsumori, N., Taoka, H., Fujiwara, D., Schreiner, E.P., Wolff, B., Yoshida, M., and Horinouchi, S. (1999). Leptomycin B inactivates CRM1/exportin 1 by covalent modification at a cysteine residue in the central conserved region. *Proc Natl Acad Sci U S A* *96*, 9112-9117.
390. Lodygin, D., and Hermeking, H. (2005). The role of epigenetic inactivation of 14-3-3sigma in human cancer. *Cell Res* *15*, 237-246.
391. Hermeking, H. (2003). Serial analysis of gene expression and cancer. *Current opinion in oncology* *15*, 44-49.
392. Hermeking, H., Lengauer, C., Polyak, K., He, T.C., Zhang, L., Thiagalingam, S., Kinzler, K.W., and Vogelstein, B. (1997). 14-3-3 sigma is a p53-regulated inhibitor of G2/M progression. *Mol Cell* *1*, 3-11.
393. Datta, S.R., Katsov, A., Hu, L., Petros, A., Fesik, S.W., Yaffe, M.B., and Greenberg, M.E. (2000). 14-3-3 proteins and survival kinases cooperate to inactivate BAD by BH3 domain phosphorylation. *Mol Cell* *6*, 41-51.
394. Fischer, A., Baljuls, A., Reinders, J., Nekhoroshkova, E., Sibilski, C., Metz, R., Albert, S., Rajalingam, K., Hekman, M., and Rapp, U.R. (2009). Regulation of RAF

- activity by 14-3-3 proteins: RAF kinases associate functionally with both homo- and heterodimeric forms of 14-3-3 proteins. *J Biol Chem* 284, 3183-3194.
395. Ehrenreiter, K., Piazzolla, D., Velamoor, V., Sobczak, I., Small, J.V., Takeda, J., Leung, T., and Baccarini, M. (2005). Raf-1 regulates Rho signaling and cell migration. *J Cell Biol* 168, 955-964.
396. Slack, J.K., Catling, A.D., Eblen, S.T., Weber, M.J., and Parsons, J.T. (1999). c-Raf-mediated inhibition of epidermal growth factor-stimulated cell migration. *J Biol Chem* 274, 27177-27184.
397. Aigner, K., Dampier, B., Descovich, L., Mikula, M., Sultan, A., Schreiber, M., Mikulits, W., Brabletz, T., Strand, D., Obrist, P., et al. (2007). The transcription factor ZEB1 (deltaEF1) promotes tumour cell dedifferentiation by repressing master regulators of epithelial polarity. *Oncogene* 26, 6979-6988.
398. Masuda, R., Semba, S., Mizuuchi, E., Yanagihara, K., and Yokozaki, H. (2010). Negative regulation of the tight junction protein tricellulin by snail-induced epithelial-mesenchymal transition in gastric carcinoma cells. *Pathobiology : journal of immunopathology, molecular and cellular biology* 77, 106-113.
399. Qian, X., Anzovino, A., Kim, S., Suyama, K., Yao, J., Hult, J., Agiostratidou, G., Chandiramani, N., McDaid, H.M., Nagi, C., et al. (2014). N-cadherin/FGFR promotes metastasis through epithelial-to-mesenchymal transition and stem/progenitor cell-like properties. *Oncogene* 33, 3411-3421.
400. Wels, C., Joshi, S., Koefinger, P., Bergler, H., and Schaidt, H. (2011). Transcriptional activation of ZEB1 by Slug leads to cooperative regulation of the epithelial-mesenchymal transition-like phenotype in melanoma. *J Invest Dermatol* 131, 1877-1885.

401. Tanahashi, T., Osada, S., Yamada, A., Kato, J., Yawata, K., Mori, R., Imai, H., Sasaki, Y., Saito, S., Tanaka, Y., et al. (2013). Extracellular signal-regulated kinase and Akt activation play a critical role in the process of hepatocyte growth factor-induced epithelial-mesenchymal transition. *International journal of oncology* 42, 556-564.
402. Gui, T., Sun, Y., Shimokado, A., and Muragaki, Y. (2012). The Roles of Mitogen-Activated Protein Kinase Pathways in TGF-beta-Induced Epithelial-Mesenchymal Transition. *Journal of signal transduction* 2012, 289243.
403. Tanno, B., Sesti, F., Cesi, V., Bossi, G., Ferrari-Amorotti, G., Bussolari, R., Tirindelli, D., Calabretta, B., and Raschella, G. (2010). Expression of Slug is regulated by c-Myb and is required for invasion and bone marrow homing of cancer cells of different origin. *J Biol Chem* 285, 29434-29445.
404. Fomenkov, A., Zangen, R., Huang, Y.P., Osada, M., Guo, Z., Fomenkov, T., Trink, B., Sidransky, D., and Ratovitski, E.A. (2004). RACK1 and stratifin target DeltaNp63alpha for a proteasome degradation in head and neck squamous cell carcinoma cells upon DNA damage. *Cell Cycle* 3, 1285-1295.
405. Brunet, A., Kanai, F., Stehn, J., Xu, J., Sarbassova, D., Frangioni, J.V., Dalal, S.N., DeCaprio, J.A., Greenberg, M.E., and Yaffe, M.B. (2002). 14-3-3 transits to the nucleus and participates in dynamic nucleocytoplasmic transport. *J Cell Biol* 156, 817-828.
406. Su, C.H., Zhao, R., Velazquez-Torres, G., Chen, J., Gully, C., Yeung, S.C., and Lee, M.H. (2010). Nuclear export regulation of COP1 by 14-3-3sigma in response to DNA damage. *Molecular cancer* 9, 243.

407. Yang, H.Y., Wen, Y.Y., Chen, C.H., Lozano, G., and Lee, M.H. (2003). 14-3-3 sigma positively regulates p53 and suppresses tumor growth. *Mol Cell Biol* 23, 7096-7107.
408. Zha, J., Harada, H., Yang, E., Jockel, J., and Korsmeyer, S.J. (1996). Serine phosphorylation of death agonist BAD in response to survival factor results in binding to 14-3-3 not BCL-X(L). *Cell* 87, 619-628.
409. Waldmann, I., Walde, S., and Kehlenbach, R.H. (2007). Nuclear import of c-Jun is mediated by multiple transport receptors. *J Biol Chem* 282, 27685-27692.
410. Alderton, G.K. (2013). Metastasis: Epithelial to mesenchymal and back again. *Nature reviews. Cancer* 13, 3.
411. Brabletz, T. (2012). EMT and MET in metastasis: where are the cancer stem cells? *Cancer Cell* 22, 699-701.
412. Meng, S., Arbit, T., Veeriah, S., Mellinghoff, I.K., Fang, F., Vivanco, I., Rohle, D., and Chan, T.A. (2009). 14-3-3sigma and p21 synergize to determine DNA damage response following Chk2 inhibition. *Cell Cycle* 8, 2238-2246.
413. Burridge, K., Fath, K., Kelly, T., Nuckolls, G., and Turner, C. (1988). Focal adhesions: transmembrane junctions between the extracellular matrix and the cytoskeleton. *Annu Rev Cell Biol* 4, 487-525.
414. Hao, H., Naomoto, Y., Bao, X., Watanabe, N., Sakurama, K., Noma, K., Motoki, T., Tomono, Y., Fukazawa, T., Shirakawa, Y., et al. (2009). Focal adhesion kinase as potential target for cancer therapy (Review). *Oncol Rep* 22, 973-979.
415. Wehrle-Haller, B. (2012). Assembly and disassembly of cell matrix adhesions. *Current opinion in cell biology* 24, 569-581.

- 
416. Ren, X.D., Kiosses, W.B., Sieg, D.J., Otey, C.A., Schlaepfer, D.D., and Schwartz, M.A. (2000). Focal adhesion kinase suppresses Rho activity to promote focal adhesion turnover. *J Cell Sci 113 (Pt 20)*, 3673-3678.
417. Godsel, L.M., Hsieh, S.N., Amargo, E.V., Bass, A.E., Pascoe-McGillicuddy, L.T., Huen, A.C., Thorne, M.E., Gaudry, C.A., Park, J.K., Myung, K., et al. (2005). Desmoplakin assembly dynamics in four dimensions: multiple phases differentially regulated by intermediate filaments and actin. *J Cell Biol 171*, 1045-1059.



---

**REPRINTS OF PUBLISHED ARTICLES FROM  
THE THESIS**

## Plakophilin3 and Plakoglobin recycling are differentially regulated during the disassembly of desmosomes.

K. Raychaudhuri, M. Gurjar and S. N. Dalal\*.

KS230, Advanced Centre for Treatment, Research and Education in Cancer (ACTREC), Tata Memorial Centre, Sector 22, Kharghar, Navi Mumbai, 410210, India.

\*For Correspondence: [sdalal@actrec.gov.in](mailto:sdalal@actrec.gov.in)

### ABSTRACT:

During cell migration, wound healing and tissue remodeling the desmosome goes through cycles of assembly and disassembly. Desmosome assembly requires the localization of two armadillo (ARM) repeat containing proteins, plakophilin3 (PKP3) and plakoglobin (PG), at the cell border. **Aims:** The goal of this study was to determine the regulation of transport of PKP3 and PG during desmosome assembly and disassembly. We particularly investigated the contribution of microtubules (MT) in the transport of these proteins to and from the cell border during desmosome assembly and disassembly. **Methods:** Nocodazole was used to disrupt microtubules in HCT116 cells and anterograde and retrograde transport of desmosomal proteins were investigated by calcium switch and calcium chelation experiments respectively followed by confocal microscopy. **Results:** The results in this paper demonstrate that microtubule dependent anterograde transport is required for the localization of PKP3 and PG to the cell border. However, during desmosome disassembly, retrograde transport of PKP3 but not PG, was dependent on an intact microtubule network. PKP3 is retained at the cell border, unlike other desmosomal proteins, when microtubule organization was disrupted. **Conclusion:** These results suggest that PKP3 transport from the cell border to the cytoplasm occurs via a mechanism that is distinct from other desmosomal proteins and might reflect functions of PKP3 that are independent of its role in desmosome formation and maintenance.

**Key words:**  
Desmosome;  
Plakophilin3;  
Plakoglobin;  
Microtubule;  
Anterograde transport;  
Retrograde transport.

### 1. INTRODUCTION

Desmosomes are calcium dependent cell-cell junctions that anchor intermediate filaments (IF) to the cell membrane resulting in the formation of a tissue wide IF network and provide mechanical strength and rigidity to tissues [1,2,3]. Desmosomes are composed of the plasma membrane spanning cadherins (desmogleins [DSGs] and desmocollins [DSCs]), the ARM family proteins (plakoglobin [PG] and plakophilins [PKPs]) and a Plakin family member such as desmoplakin (DP), which connects the desmosome to the IF network [2,4]. Desmosomes are very dynamic structures [5], especially when cells migrate in a specific direction during wound healing [6,7]. The rate of cell migration is determined by the assembly and disassembly of desmosomes. Deregulation of the desmosome assembly-disassembly cycle can lead to abnormal

development, tumor progression or to diseases such as Pemphigus Vulgaris (PV) [8,9,10,11,12,13,14].

During desmosome assembly, the desmosomal proteins are transported from the cytoplasm to the cell border and during desmosome disassembly; the desmosomal proteins are transported from the cell border to the cytoplasm. Multiple reports have demonstrated that both actin filaments and microtubules are required for the transport of desmosomal proteins during desmosome assembly e.g. transport of DP is dependent on an actin filament network, whereas an intact microtubule network is required for the transport of desmosomal cadherins and PG to the cell border. [9,15,16,17,18]. However, the mechanisms underlying the retrograde transport of desmosomal proteins i.e. from the cell border to the cytoplasm remain unclear [11,15,16,17,19].

The regulation of transport of PKP3 and PG to and from the cell border is important as our previous results suggest that depletion of either PG or PKP3 led to defects in desmosome assembly as the other desmosomal proteins fail to localize to the cell border [11,12,20]. PG transport to the desmosome is microtubule dependent and is mediated by 14-3-3 $\gamma$  and the KIF5B motor protein and is required for desmosome formation [9]. Therefore, we wished to determine whether the transport of PG and PKP3 are regulated by the same mechanisms during desmosome assembly and disassembly. To our surprise we observed that while both proteins required an intact microtubule network for transport to the cell border, only PKP3 required an intact microtubule network for transport from the cell border to the cytoplasm during desmosome disassembly.

## 2. MATERIALS AND METHODS

### 2.1 Tissue culture.

The HCT116 (ATCC) cell line was cultured in Dulbecco's modified Eagles medium (DMEM) (GIBCO) supplemented with 10% Fetal bovine Serum (JRH), 100 U of penicillin (Nicholas Piramal), 100  $\mu$ g/ml of streptomycin (Nicholas Piramal) and 2  $\mu$ g/ml of amphotericin B (HiMedia).

### 2.2 Immunofluorescence.

HCT116 cells were fixed in absolute methanol for 10 minutes at -20°C to detect  $\alpha$ -tubulin, PKP3 and DP or in 4% paraformaldehyde for 20 minutes at room temperature to detect DSC2/3. After fixation, cells were permeabilized with Triton X-100 as described previously [11]. PKP3, DP DSC2/3 and  $\alpha$ -tubulin antibodies were used for immunofluorescence analysis as described previously [9,10,11,12]. DAPI was used to stain the nucleus as previously described [9]. Confocal images were obtained by using a

LSM 510 Meta Carl Zeiss confocal system with argon 488-nm laser. All images were obtained by using LSM meta software at a magnification of X630 (X63 objective and X10 eyepiece) with 1X, 2X or 4X optical zoom. The fluorescence intensity of staining at the cell border was measured for the different proteins in a minimum of 30 cells using the Image J software (NIH). Mean and standard deviation were plotted and p values determined using a student's t test.

## 3. RESULTS

### 3.1. Anterograde transport of PKP3 and PG is microtubule dependent.

Our previous results suggest that PG transport to the cell border requires an intact microtubule network and that PKP3 and PG are required for desmosome assembly [9,11]. To address whether microtubules (MT) are required for the initiation of desmosome formation and transport of PKP3 to the cell border in HCT116 cells, nocodazole (NOC) was used to disrupt the microtubule network. Incubation of HCT116 cells with 10 $\mu$ M NOC for 3 hours completely disrupted the MT network (Fig 1A). To determine the role of MT in anterograde transport of PKP3 during desmosome assembly, a calcium switch experiment was performed in cells treated with NOC (to disrupt MT) or DMSO (vehicle control) as described in Fig 1B. An immunofluorescence analysis showed that cell border localization of both PKP3 and PG was compromised upon disruption of MT post addition of calcium in comparison to DMSO treated cells (Fig 1C & E). Quantitation of the fluorescence intensity at the cell border after 30 minutes of calcium addition showed that recovery of both PKP3 and PG border staining intensity was significantly compromised in NOC treated cells compared to DMSO treated cells (Fig 1D & F). However, no appreciable difference in cell border localization was observed at 0 minute post calcium switch in

cell border intensity of either PKP3 or PG between NOC and DMSO treated cells (Fig 1C-F). Line scans drawn across the cell showed that at 0 minute post calcium switch both PKP3 and PG did not localize at the cell border and remained cytoplasmic and at 30 minutes post calcium switch localized to the cell border in DMSO treated cells but not in NOC treated cells (Fig 2). These results confirmed that the cell border recruitment of PKP3 and PG are dependent on an intact MT network and both these proteins followed a similar pattern of anterograde transport.

### **3.2. The retrograde transport of PKP3 and PG are differentially regulated.**

Since desmosomes are dynamic and undergo continual assembly and disassembly during cell migration [6], we wished to determine the mechanism of transport of PKP3 and PG from the cell border to the cytoplasm during desmosome disassembly. To investigate the role of MT in the regulation of PKP3 transport during desmosome disassembly, EGTA was added to the medium to chelate calcium as described [21,22], either in the presence or absence of NOC (Fig 3A). Three hours post addition of EGTA, PKP3 was localized at the cell border in NOC treated cells. In contrast, PKP3 levels decreased at the cell border in cells treated with DMSO upon chelation of calcium (Fig 3B). No difference was observed in the localization of PKP3 in NOC and DMSO treated cells prior to addition of EGTA (Fig 3B). Quantitation of fluorescence intensities at the cell border established that these differences were statistically significant (Fig 3C). Consistent with these observations, line scans drawn across the cell showed a peak of fluorescence intensity for PKP3 staining at the cell border on NOC treatment, which was not observed in DMSO treated cells (Fig 4). These results suggest that retrograde transport of PKP3 from the cell border to the cytoplasm is dependent on MT. In contrast, it was

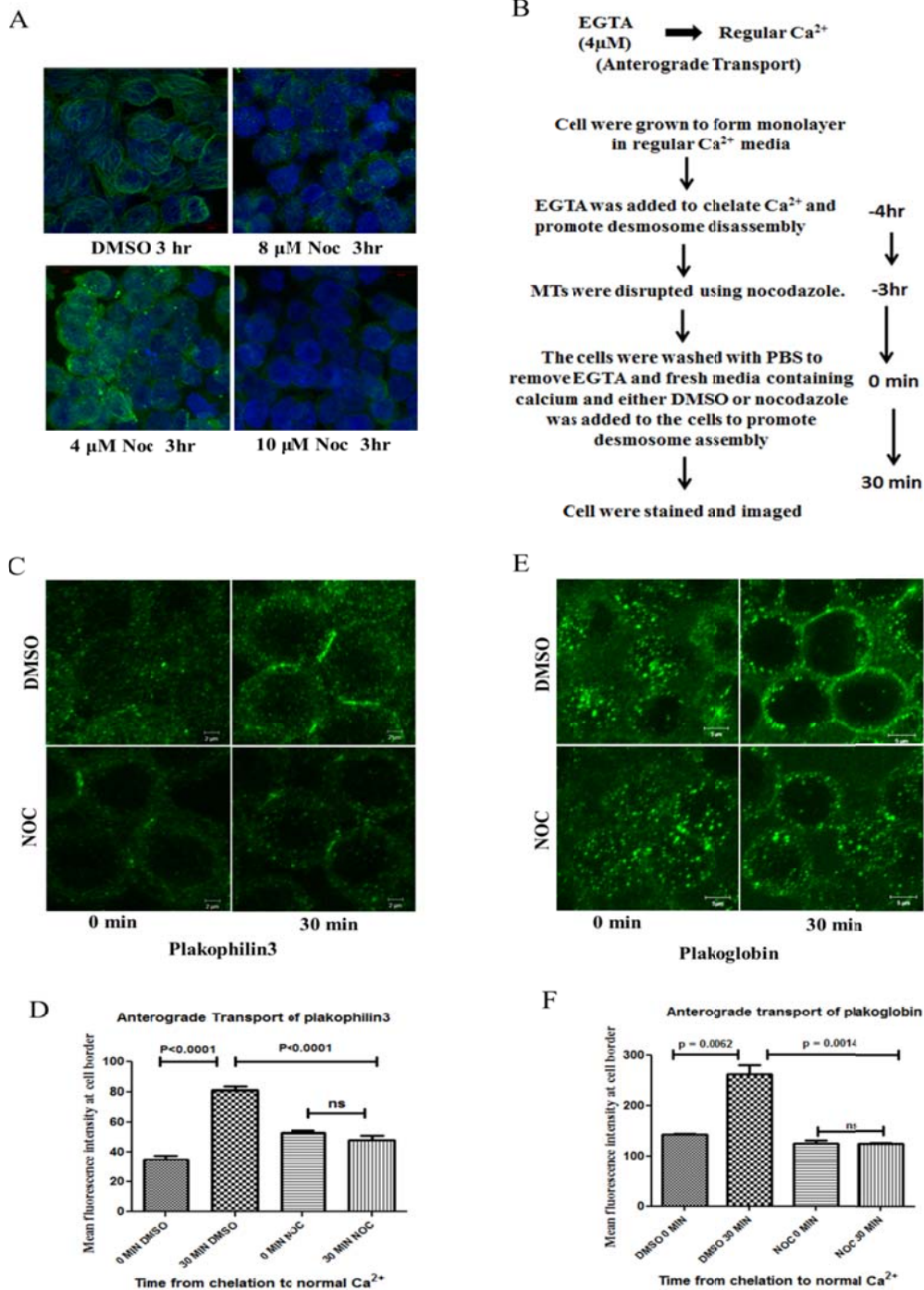
observed that NOC treatment had no effect on retrograde transport of PG upon addition of EGTA. PG localized to the cytoplasm in both NOC and DMSO treated cells 3hr post addition of EGTA (Fig 3D-E). Line scans drawn across the cell showed extensive cytoplasmic accumulation of PG at 3hr post EGTA addition in both NOC and DMSO treated cells (Fig 4). These results suggest that an intact MT network is not required for the retrograde transport of PG and different mechanisms regulate the retrograde transport of PKP3 and PG during desmosome disassembly.

### **3.3. Inhibition of retrograde transport of PKP3 does not inhibit desmosome disassembly.**

We have previously shown that PKP3 is required for transport of desmosomal proteins such as DSC2/3, DSG2, PKP2 and DP to the cell border and is required for initiation of desmosome assembly in HCT116 and HaCaT cells [11]. Similarly, other groups have demonstrated that loss of PKP3 leads to diffused cytoplasmic localization of DP in HaCaT and SCC9 cells [20]. To determine whether retention of PKP3 at the cell border resulted in the retention of other desmosomal proteins at the cell border, the localization of DP and DSC2/3 in cells treated with NOC during desmosome disassembly was determined as described above. Though PKP3 is retained at the cell border 3hr post calcium chelation, both DP and DSC2/3 were not retained at the cell border (Fig 3F&H). At 3hr post chelation, the levels of DP and DSC2/3 were diminished at the cell border in both NOC and DMSO treated cells, a phenotype similar to that observed for PG (Fig 3G&I). These results suggest that PKP3 retention at the cell border upon calcium chelation is not sufficient for the retention of other desmosomal proteins at the cell border.

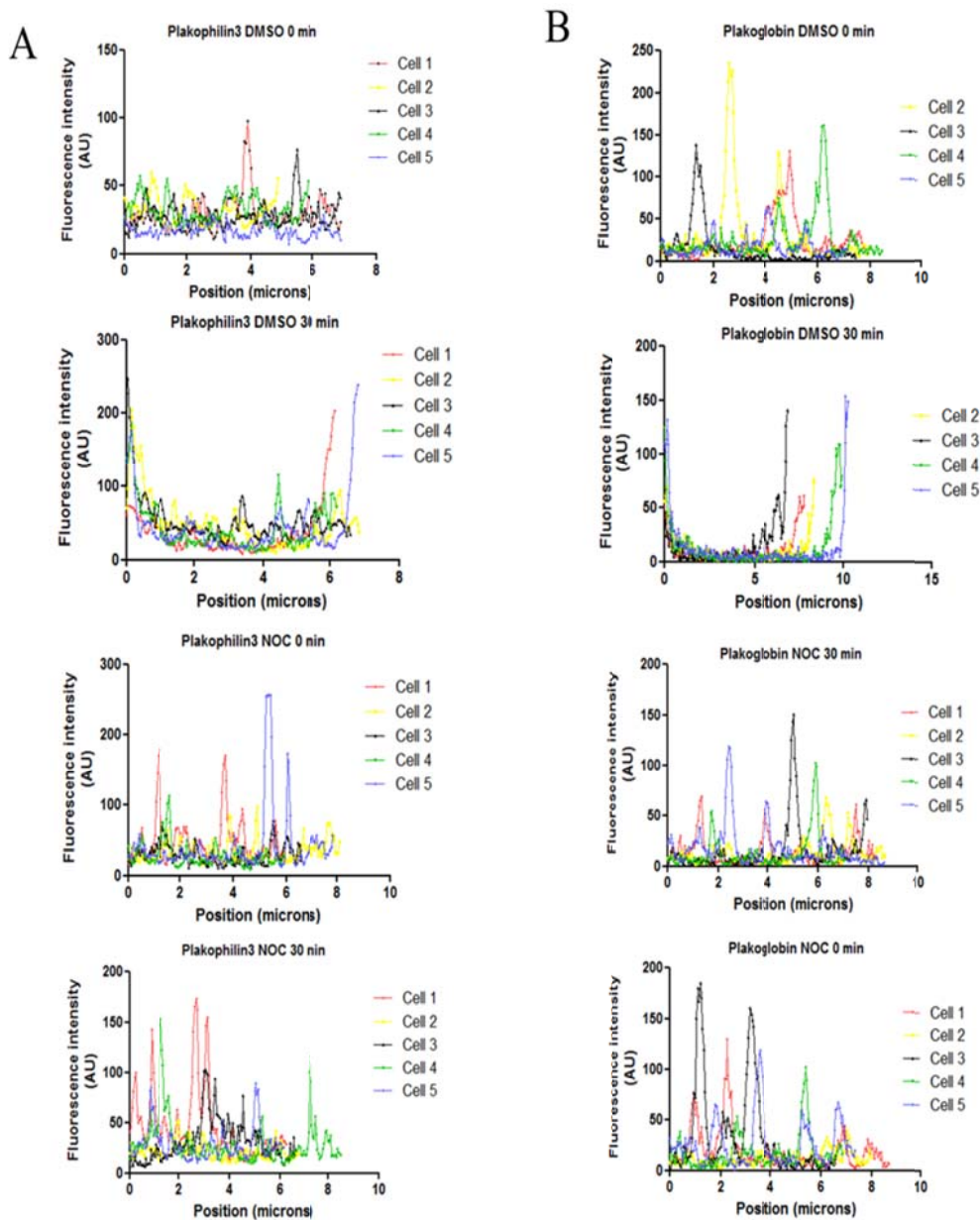
**Figure 1.**

**Anterograde transport of PKP3 and PG is dependent on an intact microtubule network.**



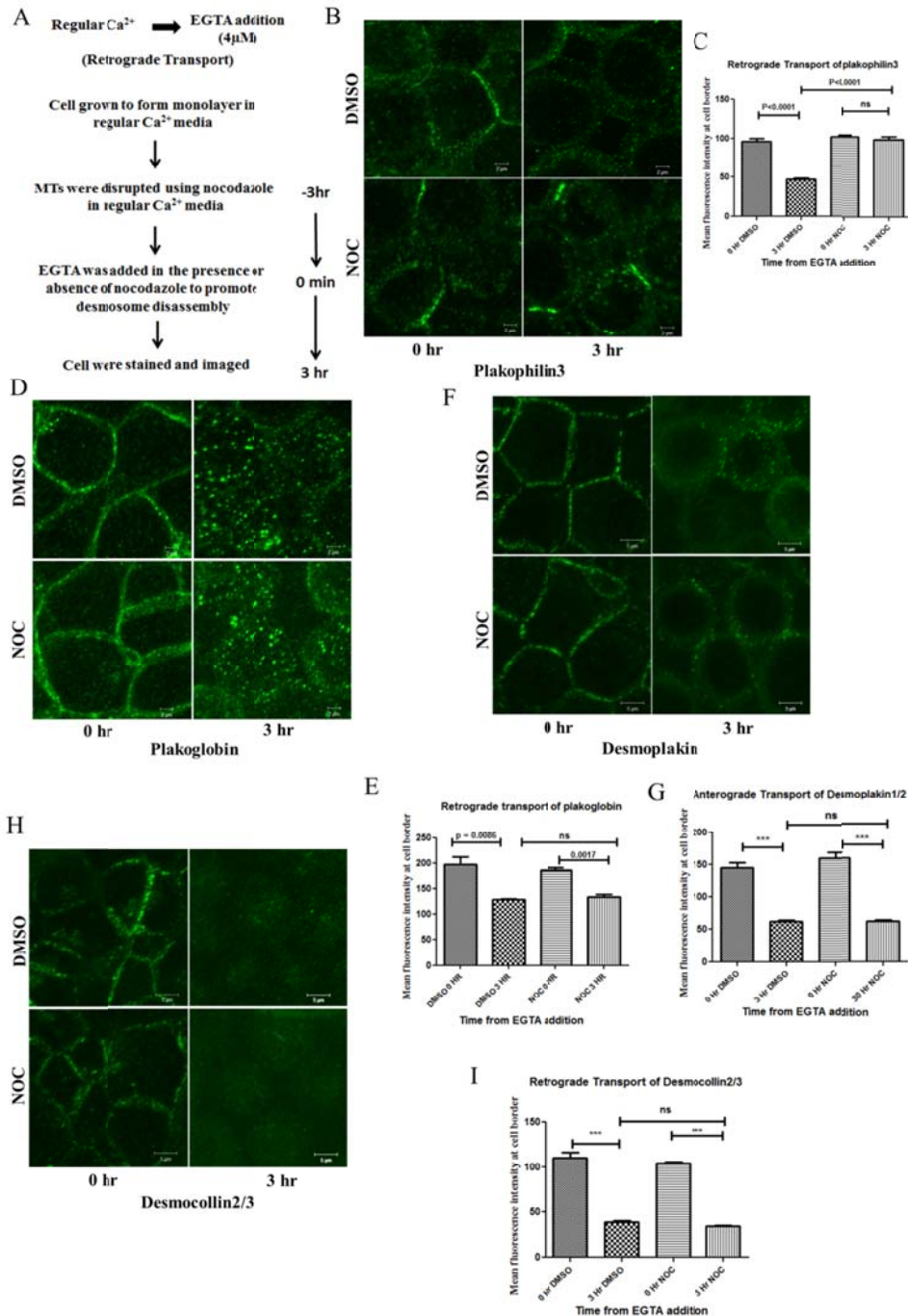
(A) HCT116 cells were treated with DMSO or the indicated concentration of NOC for 3hrs. Cells were stained with antibodies to  $\alpha$ -tubulin to visualize MT and counterstained with DAPI. Magnification is X630 magnification with 2X optical zoom. (B) Scheme of experiment to study anterograde transport of PKP3 and PG. (C-F) HCT116 cells treated with EGTA and NOC or DMSO were fixed and stained with antibodies to PKP3 (C-D) or PG (E-F) followed by confocal microscopy. The intensity of border staining for both PKP3 and PG was measured for in least 30 cells in three independent experiments and the mean and standard deviation were plotted. Magnification is X630 with 4X optical zoom and bars indicate 5 $\mu$ m. p values were generated using a student's t test.

**Figure. 2**  
**Effect of nocodazole on anterograde transport of plakophilin3 and plakoglobin.**



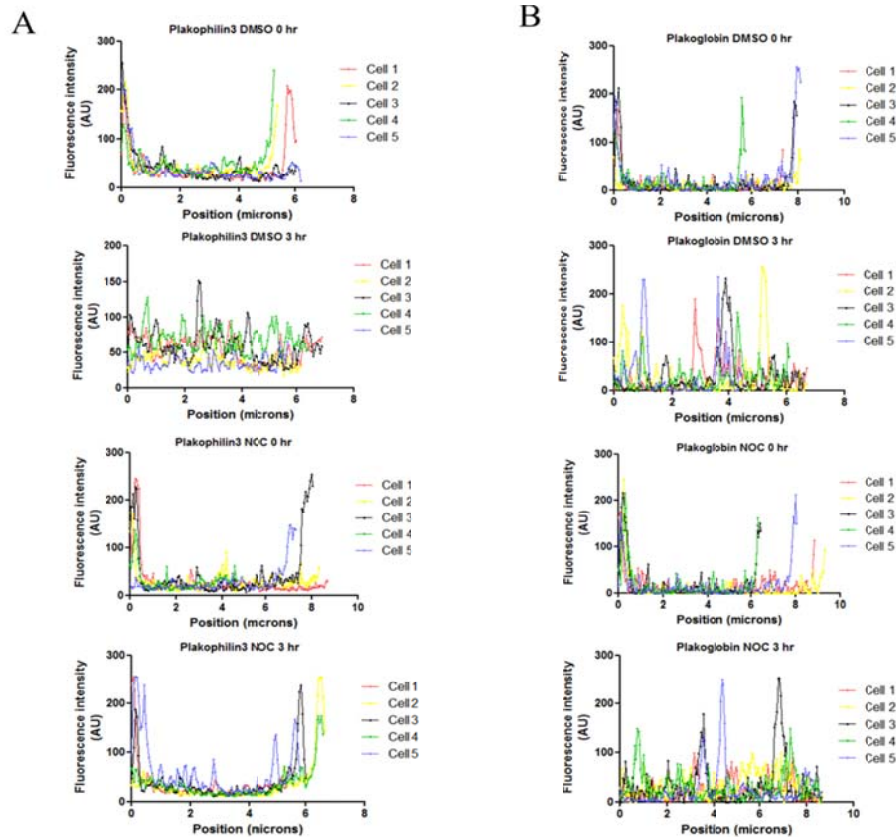
(A-B) Line scans were drawn across 5 random cells that were immunostained for PKP3 (A) or PG (B) 30 minutes post calcium addition. Fluorescence intensities were measured across the line using Image J and were plotted on the Y-axis. X axis represents position along the line that was drawn across the diameter of the cell.

**Figure 3.**  
**Disruption of the microtubule network blocks retrograde transport of PKP3**  
**but does not inhibit desmosome disassembly.**



(A) Scheme of experiment to study retrograde transport of desmosomal proteins. (B-I) HCT116 cells were treated with EGTA and NOC or DMSO and stained with antibodies to PKP3 (B-C), PG (D-E) DP (F-G) and DSC2/3 (H-I) followed by confocal microscopy. The intensity of staining at the cell border was measured for at least 30 cells in three independent experiments and mean and standard deviation were plotted. Note that disruption of the MT network results in a defect in the transport of PKP3 from the cell border to the cytoplasm in contrast to the results observed for the other desmosomal proteins. Confocal images were acquired at X630 magnification and 4X optical zoom. Bars indicate 5 $\mu$ m. p values were generated using a student's t-test.

**Figure 4.**  
**Effect of nocodazole on retrograde transport of plakophilin3 and plakoglobin.**



(A-B) Line scans were drawn across 5 random cells that were immunostained for PKP3 (A) or PG (B) three hours post addition of EGTA. Fluorescence intensities were measured across the line using Image J and were plotted on the Y-axis. X axis represents position along the line that was drawn across the diameter of the cell.

#### 4. DISCUSSION

The process of desmosome assembly and disassembly is not completely understood, especially the process of desmosome disassembly. As the process of desmosome assembly and disassembly is essential for cell migration during wound healing and other developmental processes, this report focused on the identifying the requirements for the transport PG and PKP3, which are both required for desmosome formation, during desmosome assembly. The results presented in this report demonstrate that the transport of PG and PKP3 from the cell border to the cytoplasm upon desmosome disassembly is differentially regulated, with an intact MT

network being an absolute requirement for the retrograde transport of PKP3. These results suggest that the different ARM proteins are transported to the cytoplasm by different pathways upon desmosome disassembly.

It is also interesting to note that border retention of PKP3 on treatment with NOC at 3hr post calcium chelation was not sufficient to retain DP and DSC2/3 at the cell border. While PKP3 plays a crucial role in recruiting DP, PKP2, DSG2 and DSC2/3 proteins to the cell border [10,11,15,20], the results reported here suggest that PKP3 might not play a similar role during desmosome disassembly. It is possible that loss of PKP3 from the cell border is not required for desmosome

disassembly and that the PKP3 present at the cell border under conditions of calcium chelation might have desmosome independent functions or serve as a marker for the formation of new desmosomes upon the restoration of calcium to the medium. Further, Kowalczyk *et.al.* have shown that PV IgG antibodies against DSG3 that are produced during the autoimmune disease PV cause dissolution of desmosomes, retraction of keratin filaments and internalization of DSG3 in a complex with PG and DP in a membrane raft dependent manner [23,24,25]. It is possible that upon addition of EGTA, PKP3 is localized to a portion of the membrane not associated with membrane rafts; thereby preventing its internalization along with the other desmosomal proteins.

Both PG and PKP3 required an intact MT network to be transported to the cell border and transport of PG to the cell border is dependent on KIF5B and KLC1 [9]. However, unlike PKP3, transport of PG from the cell border to the cytoplasm upon calcium chelation did not require an intact MT network. These results indicate that some other yet unidentified transport process is responsible for retrograde transport of PG and other desmosomal proteins such as DP and DSC2/3 that is independent of an intact MT network. Other reports suggest that both MT and actin filaments are required for the transport of DSC2 to the cell border [15,17]. Therefore, an actin based mechanism might regulate the retrograde transport of PG, DP and DSC2/3 in HCT116 cells.

## 5. CONCLUSION

In conclusion, our studies have determined that an intact MT network is required for the retrograde transport of PKP3 during desmosome disassembly and suggest that PKP3 and PG might have different roles to play during desmosome disassembly. However, additional studies are required to

address the significance of the MT network in regulating desmosome disassembly and in regulation of PKP3 transport.

## Conflict of Interest

The authors have no conflict of interest.

## Acknowledgements

We thank Dr. Rita Mulherkar for critically reading the manuscript. KK and MG were supported by a fellowship from Council of Scientific and Industrial Research, Ministry of Human Resource and Development. This work was supported by grants from the Department of Biotechnology, Government of India and ACTREC.

## 6. REFERENCES

- [1]. B.V. Desai, R.M. Harmon, K.J. Green, Desmosomes at a glance, *Journal of cell science* 122 (2009) 4401-4407.
- [2]. E. Delva, D.K. Tucker, A.P. Kowalczyk, The desmosome, *Cold Spring Harbor perspectives in biology* 1 (2009) a002543.
- [3]. K.J. Green, C.L. Simpson, Desmosomes: new perspectives on a classic, *The Journal of investigative dermatology* 127 (2007) 2499-2515.
- [4]. B. Holthofer, R. Windoffer, S. Troyanovsky, R.E. Leube, Structure and function of desmosomes, *International review of cytology* 264 (2007) 65-163.
- [5]. R. Windoffer, M. Borchert-Stuhltrager, R.E. Leube, Desmosomes: interconnected calcium-dependent structures of remarkable stability with significant integral membrane protein turnover, *Journal of cell science* 115 (2002) 1717-1732.
- [6]. K.J. Green, S. Getsios, S. Troyanovsky, L.M. Godsel, Intercellular junction assembly, dynamics, and homeostasis, *Cold Spring Harbor perspectives in biology* 2 (2010) a000125.
- [7]. O. Ilina, P. Friedl, Mechanisms of collective cell migration at a glance, *Journal of cell science* 122 (2009) 3203-3208.
- [8]. Y. Kitajima, New insights into desmosome regulation and pemphigus blistering as a desmosome-remodeling disease, *The Kaohsiung journal of medical sciences* 29 (2013) 1-13.
- [9]. L. Sehgal, A. Mukhopadhyay, A. Rajan, N. Khapare, M. Sawant, S.S. Vishal, K. Bhatt, S. Ambatipudi, N. Antao, H. Alam, M. Gurjar, S. Basu, R. Mathur, L. Borde, A.S. Hosing, M.M.

- Vaidya, R. Thorat, F. Samaniego, U. Kolthur-Seetharam, S.N. Dalal, 14-3-3gamma-Mediated transport of plakoglobin to the cell border is required for the initiation of desmosome assembly in vitro and in vivo, *Journal of cell science* 127 (2014) 2174-2188.
- [10]. N. Khapare, S.T. Kundu, L. Sehgal, M. Sawant, R. Priya, P. Gosavi, N. Gupta, H. Alam, M. Karkhanis, N. Naik, M.M. Vaidya, S.N. Dalal, Plakophilin3 loss leads to an increase in PRL3 levels promoting K8 dephosphorylation, which is required for transformation and metastasis, *PloS one* 7 (2012) e38561.
- [11]. P. Gosavi, S.T. Kundu, N. Khapare, L. Sehgal, M.S. Karkhanis, S.N. Dalal, E-cadherin and plakoglobin recruit plakophilin3 to the cell border to initiate desmosome assembly, *Cellular and molecular life sciences : CMLS* 68 (2011) 1439-1454.
- [12]. S.T. Kundu, P. Gosavi, N. Khapare, R. Patel, A.S. Hosing, G.B. Maru, A. Ingle, J.A. Decaprio, S.N. Dalal, Plakophilin3 downregulation leads to a decrease in cell adhesion and promotes metastasis, *International journal of cancer. Journal international du cancer* 123 (2008) 2303-2314.
- [13]. J.P. Dou, B. Jiao, J.J. Sheng, Z.B. Yu, [Dynamic assembly of intercalated disc during postnatal development in the rat myocardium], *Sheng li xue bao : [Acta physiologica Sinica]* 66 (2014) 569-574.
- [14]. A. Vreeker, L. van Stuijvenberg, T.J. Hund, P.J. Mohler, P.G. Nikkels, T.A. van Veen, Assembly of the cardiac intercalated disk during pre- and postnatal development of the human heart, *PloS one* 9 (2014) e94722.
- [15]. B.J. Roberts, A. Pashaj, K.R. Johnson, J.K. Wahl, 3rd, Desmosome dynamics in migrating epithelial cells requires the actin cytoskeleton, *Experimental cell research* 317 (2011) 2814-2822.
- [16]. L.M. Godsel, S.N. Hsieh, E.V. Amargo, A.E. Bass, L.T. Pascoe-McGillicuddy, A.C. Huen, M.E. Thorne, C.A. Gaudry, J.K. Park, K. Myung, R.D. Goldman, T.L. Chew, K.J. Green, Desmoplakin assembly dynamics in four dimensions: multiple phases differentially regulated by intermediate filaments and actin, *The Journal of cell biology* 171 (2005) 1045-1059.
- [17]. O.E. Nekrasova, E.V. Amargo, W.O. Smith, J. Chen, G.E. Kreitzer, K.J. Green, Desmosomal cadherins utilize distinct kinesins for assembly into desmosomes, *The Journal of cell biology* 195 (2011) 1185-1203.
- [18]. S. McHarg, G. Hopkins, L. Lim, D. Garrod, Down-regulation of desmosomes in cultured cells: the roles of PKC, microtubules and lysosomal/proteasomal degradation, *PloS one* 9 (2014) e108570.
- [19]. I.D. Burdett, K.H. Sullivan, Desmosome assembly in MDCK cells: transport of precursors to the cell surface occurs by two phases of vesicular traffic and involves major changes in centrosome and Golgi location during a Ca(2+) shift, *Experimental cell research* 276 (2002) 296-309.
- [20]. V. Todorovic, J.L. Koetsier, L.M. Godsel, K.J. Green, Plakophilin 3 mediates Rap1-dependent desmosome assembly and adherens junction maturation, *Molecular biology of the cell* 25 (2014) 3749-3764.
- [21]. C. Ramachandran, S.P. Srinivas, Formation and disassembly of adherens and tight junctions in the corneal endothelium: regulation by actomyosin contraction, *Investigative ophthalmology & visual science* 51 (2010) 2139-2148.
- [22]. B. Rothen-Rutishauser, F.K. Riesen, A. Braun, M. Gunthert, H. Wunderli-Allenspach, Dynamics of tight and adherens junctions under EGTA treatment, *The Journal of membrane biology* 188 (2002) 151-162.
- [23]. J.M. Jennings, D.K. Tucker, M.D. Kottke, M. Saito, E. Delva, Y. Hanakawa, M. Amagai, A.P. Kowalczyk, Desmosome disassembly in response to pemphigus vulgaris IgG occurs in distinct phases and can be reversed by expression of exogenous Dsg3, *The Journal of investigative dermatology* 131 (2011) 706-718.
- [24]. S.N. Stahley, M. Saito, V. Faundez, M. Koval, A.L. Mattheyses, A.P. Kowalczyk, Desmosome assembly and disassembly are membrane raft-dependent, *PloS one* 9 (2014) e87809.
- [25]. C.C. Calkins, S.V. Setzer, J.M. Jennings, S. Summers, K. Tsunoda, M. Amagai, A.P. Kowalczyk, Desmoglein endocytosis and desmosome disassembly are coordinated responses to pemphigus autoantibodies, *The Journal of biological chemistry* 281 (2006) 7623-7634.

## Loss of the desmosomal plaque protein plakophilin 3 does not induce the epithelial mesenchymal transition.

Mansa Gurjar, Kumarkrishna Raychaudhuri, Sorab N. Dalal\*.

KS215, Advanced Centre for Treatment Research and Education in Cancer (ACTREC),  
Tata Memorial Centre, Kharghar Node, Navi Mumbai - 410210, Maharashtra, India.

Email: [sdalal@actrec.gov.in](mailto:sdalal@actrec.gov.in)

### Abstract:

**Aims:**We investigated whether the increased neoplastic progression promoted by PKP3 loss is accompanied by induction of EMT. **Methods:**Quantitative real time PCR, Cell-ECM adhesion assay and Immunohistochemistry. **Results:**There was no significant difference in the levels of EMT regulating transcription factors and cell-ECM adhesion between vector control and PKP3 knockdown HCT116 derived cells or EMT markers in primary tumour and lung metastasis samples. **Conclusion:** PKP3 knockdown does not lead to induction of EMT both *in vitro* and *in vivo*.

### Keywords:

Desmosomes, Epithelial Mesenchymal Transition, Plakophilin 3, Snail, Vimentin.

### 1. INTRODUCTION:

The Epithelial Mesenchymal Transition (EMT) is a developmental process by which epithelial cells get reprogrammed to a mesenchymal phenotype during gastrulation and neural crest formation. EMT leads to the dissolution of cell-cell adhesion junctions like desmosomes and an increase in cell migration and invasion, which leads to the acquisition of metastatic properties in primary tumour cells. The loss of desmosomal cell-cell adhesion is considered to be a hallmark for EMT (reviewed in [13]). Desmosomes are cell-cell adhesion junctions that are found in all epithelial tissues and cardiac muscle. The primary role of desmosomal junctions is to maintain tissue integrity and structure by providing mechanical strength.

The adhesion is mediated by calcium dependent homophilic and heterophilic interactions between transmembrane desmosomal cadherins, namely desmocollins and desmogleins. On the intracellular side, the desmosomal cadherins interact with armadillo family proteins like plakophilins and plakoglobin, which in turn interact with the plakin family protein desmoplakin. Desmoplakin anchors intermediate filaments of the cell that leads to an appearance of an electron dense region when imaged with an

electron microscope ([4] and reviewed in [57]).

Desmosome composition varies depending on tissue type with different tissues expressing different desmosomal cadherins and different plakophilin family members (reviewed in [57]). However, in contrast to other plakophilin family members, plakophilin 3 (PKP3) is ubiquitously expressed in all epithelial tissues with the exception of hepatocytes [8; 9]. PKP3 has been shown to interact with almost all other desmosomal proteins like desmoglein 1, desmoglein 2, desmoglein 3, desmocollin 3a, desmocollin 3b, plakoglobin, desmoplakin, and keratin 18 [10]. Our laboratory has previously demonstrated that PKP3 is essential for desmosome assembly and loss of PKP3 is accompanied by a decrease in desmosome size and cell-cell adhesion, and an increase in cell migration, anchorage independent growth and, tumour formation and lung metastasis in immunocompromised mice [11; 12]. As metastasis is often accompanied by the induction of EMT, the levels of molecular markers of EMT (reviewed in [13-15]) were studied in the PKP3 knockdown cells in comparison to the vector control, to determine whether the increased metastasis observed on PKP3 loss is due to an increase in EMT.

## 2. MATERIALS AND METHODS:

### 2.2. Cell lines

The HCT-116 based PKP3 knockdown clones used in this study were previously described [11]. Cells were cultured in Dulbecco's modified Eagles medium (DMEM) (GIBCO) supplemented with 10% Fetal bovine Serum (GIBCO), 100 U of penicillin (Nicholas Piramal), 100 µg/ml of streptomycin (Nicholas Piramal) and 2 µg/ml of amphotericin B (HiMedia) as well as 5 µg/ml of blasticidin (Invitrogen) for selection.

### 2.3. Real time PCR

RNA was prepared using RNeasy Plus kit (Qiagen). 2µg of RNA was converted to cDNA using High-Capacity cDNA Reverse Transcription Kit (Applied Biosystems). Quantitative real time PCR was performed using SYBR® Green PCR Master Mix (Applied Biosystems) using GAPDH as a control. Fold change was determined by relative quantitation method by determining  $2^{-\Delta\Delta C_t}$  values or quantitation was done by determining the  $2^{-\Delta C_t}$  values. The significance was determined using the Student's t-test. The primer sequences used are listed in table 1.

### 2.4. Cell-extracellular matrix adhesion assay

The extracellular matrix (ECM) substrates – Matrigel (BD Biosciences), laminin 5 (Sigma), collagen IV (Sigma) and fibronectin (BD Biosciences) were coated at the concentration of 10 µg/mL in a 96-well plate and incubated overnight at 4°C. After a wash with PBS, the ECM substrates were incubated with 2% BSA for 2 hours at 37°C. 40,000 cells in 100 µL of DMEM with 0.1% BSA were seeded and incubated at 37°C with 5% CO<sub>2</sub> for 30-60 minutes. Non adherent cells were washed gently twice with PBS and the adherent cells were quantitated using MTT (Sigma).

### 2.5. Immunohistochemistry

The tissue blocks used for immunohistochemistry have been described earlier [11]. Five micron sections of paraffin-embedded formalin fixed tissues were prepared and immunohistochemistry was performed by standard methods [11]. Antigen retrieval was performed by microwaving the tissue for 10 minutes in 3M sodium citrate buffer. Vimentin antibody was used at 1:50 dilution (Sigma M 0725) and staining was performed using M.O.M. staining kit (Vector Laboratories) according to manufacturer's instructions. MMP9 antibody was used at 1:100 dilution (Abcam ab38898) and staining was performed using ABC staining kit (Vector Laboratories) according to manufacturer's instructions. Images were captured using a 10x objective on a Zeiss Axiovert upright microscope.

## 3. RESULTS AND DISCUSSION:

### 3.1. PKP3 knockdown does not increase expression of mesenchymal transcription factors *in vitro*

Our lab had previously reported that PKP3 knockdown led to an increase in cell migration, decreased cell-cell adhesion, increased anchorage independent growth and an increase in tumour formation and lung metastasis in immunocompromised mice in HCT116 cells [11]. These phenotypes are characteristic of the changes observed upon induction of EMT (reviewed in [13]). The established “master” regulators of EMT are the transcription factors Snail, Slug, Twist 1 and Zeb 1. Snail, Slug, Twist 1 and Zeb 1 are all known to directly or indirectly repress E-cadherin expression and induce vimentin expression while Slug and Zeb1 are also known to promote dissolution of desmosomes (reviewed in [13,15]). Real time PCR demonstrated that Snail was the only EMT regulating transcription factor that was expressed in both the HCT116 derived vector

control and PKP3 knockdown cells shpkp3-1 and shpkp3-2 (Figure 1A and 1B). However, no significant difference was observed in the Snail expression between the vector control and the PKP3 knockdown cells (Figure 1A). The EMT regulating transcription factors Slug, Twist 1 and Zeb1 were absent in both the vector control and the PKP3 knockdown cells, AW13516 [16; 17] cells were used as a positive control to validate the primers used (Figure 1B). Thus PKP3 knockdown does not lead to any change in the expression of EMT regulating transcription factors with Snail being the only tested EMT regulating transcription factor that is expressed with no significant difference between the HCT116 derived vector control and the PKP3 knockdown cells.

Repression of E-cadherin expression, an adherens cell-cell junction cadherin or change in E-cadherin localization from cell membrane to cytoplasm and induction of vimentin expression, a type III intermediate filament protein, are classical markers of EMT (reviewed in [1315]). Previous results from our lab have demonstrated that vimentin is not expressed in the vector control or the PKP3 knockdown cells [16]. We have also observed that PKP3 knockdown does not change E-cadherin localization to the membrane [12]. Thus PKP3 knockdown does not lead to change in any of the tested molecular markers of EMT *in vitro*.

### 3.2. PKP3 knockdown does not change cell-ECM substrate adhesion

Cells interact with their microenvironment through integrin based focal adhesions or hemidesmosomes. The physical interaction of integrin with the proteins in the extracellular matrix (ECM) leads to activation of integrin based signal transduction cascades through activation of integrin associated kinases like Src or FAK (reviewed in [13; 18; 19]). The activation of these signalling cascades is

promoted by an increase in focal adhesion turnover and reduced focal adhesion strength that aides cell migration and decreases cell-ECM adhesion [18; 19]. An increase in cell migration accompanied by a decrease in cell-ECM adhesion is thus an important functional change observed in EMT. As our previous results showed that PKP3 knockdown leads to an increase in cell migration [11], we hence investigated whether PKP3 loss also leads to a decrease in cell-ECM adhesion. Cell-ECM substrate adhesion assays showed that PKP3 knockdown does not change the cell adhesion to any of the substrates tested like Matrigel, fibronectin, laminin 5 and collagen IV (Figure 1C). This shows that Pkp3 knockdown does not show the EMT phenotype of decrease in cell-ECM substrate adhesion.

### 3.3. PKP3 knockdown does not increase expression of mesenchymal factors *in vivo*

Although PKP3 knockdown did not show expression of EMT markers *in vitro*, the increased primary tumour growth and lung metastasis observed in immunocompromised mice lead to the question whether an EMT is observed in when these cells grow as tumours in immunocompromised mice.

Immunohistochemistry studies with markers of mesenchymal cells such as vimentin and MMP9, a matrix metalloprotease that is known to promote invasion and aide metastasis (reviewed in [1315]), showed the presence of both mesenchymal markers vimentin and MMP9, in the tumour as well as the lung metastasis, in both the vector control as well as the PKP3 knockdown shpkp3-2 samples (Figure 1D and 1E). The presence of these mesenchymal markers shows that EMT does indeed take place *in vivo*, but it is not induced or enhanced by PKP3 knockdown. Thus PKP3 knockdown does not induce or enhance EMT *in vivo*.

**Table: 1****List of primers used for real time PCR.**

| S. No. | Name of primer | Sequence              |
|--------|----------------|-----------------------|
| 1      | Slug fwd       | AGACCCCATGCCATTGAAG   |
| 2      | Slug rev       | GGCCAGCCAGAAAAAGTTG   |
| 3      | Snail fwd      | TAGCGAGTGGTTCTTCTGCG  |
| 4      | Snail rev      | AGGGCTGCTGGAAGGTAAC   |
| 5      | Twist 1 fwd    | AGCTGAGCAAGATTCAGACCC |
| 6      | Twist 1 rev    | GCAGCTTGCCATCTTGGAGT  |
| 7      | Zeb 1 fwd      | AGGATGACCTGCCAACAGAC  |
| 8      | Zeb 1 rev      | CTTCAGGCCCCAGGATTCTT  |

**4. CONCLUSION:**

Multiple reports in the literature suggest that the induction of EMT is required for tumour progression and metastasis (reviewed in [13]). Our lab had previously shown that PKP3 knockdown promotes neoplastic progression and metastasis [11]. Some of the effects of PKP3 knockdown like an increase in cell migration, decrease in cell-cell adhesion as well as increase in tumour formation and lung metastasis are synonymous with characteristics of EMT [11]. However, in the present study, we show that PKP3 knockdown does not induce or enhance expression of any of the tested mesenchymal markers nor does it change cell-ECM adhesion. We conclude that PKP3 knockdown does not promote neoplastic progression through the process of EMT.

**List of abbreviations used:**

EMT = epithelial mesenchymal transition  
 PKP3 = plakophilin 3  
 ECM = extracellular matrix  
 FAK = focal adhesion kinase  
 Src = sarcoma  
 MMP9 = matrix metalloprotease 9  
 PCR = polymerase chain reaction

**Competing interests:**

The authors declare that they have no competing interests.

**Acknowledgements:**

We would like to thank Mr. Mohd Yasser and Dr. Tanuja Teni for providing AW13516 mRNA samples. We thank the ACTREC histology and microscope facilities. M.G. and K.R. were supported by fellowships from CSIR. This work was supported in part by grants from the Department of Biotechnology (DBT) and ACTREC.

**Figure 1**

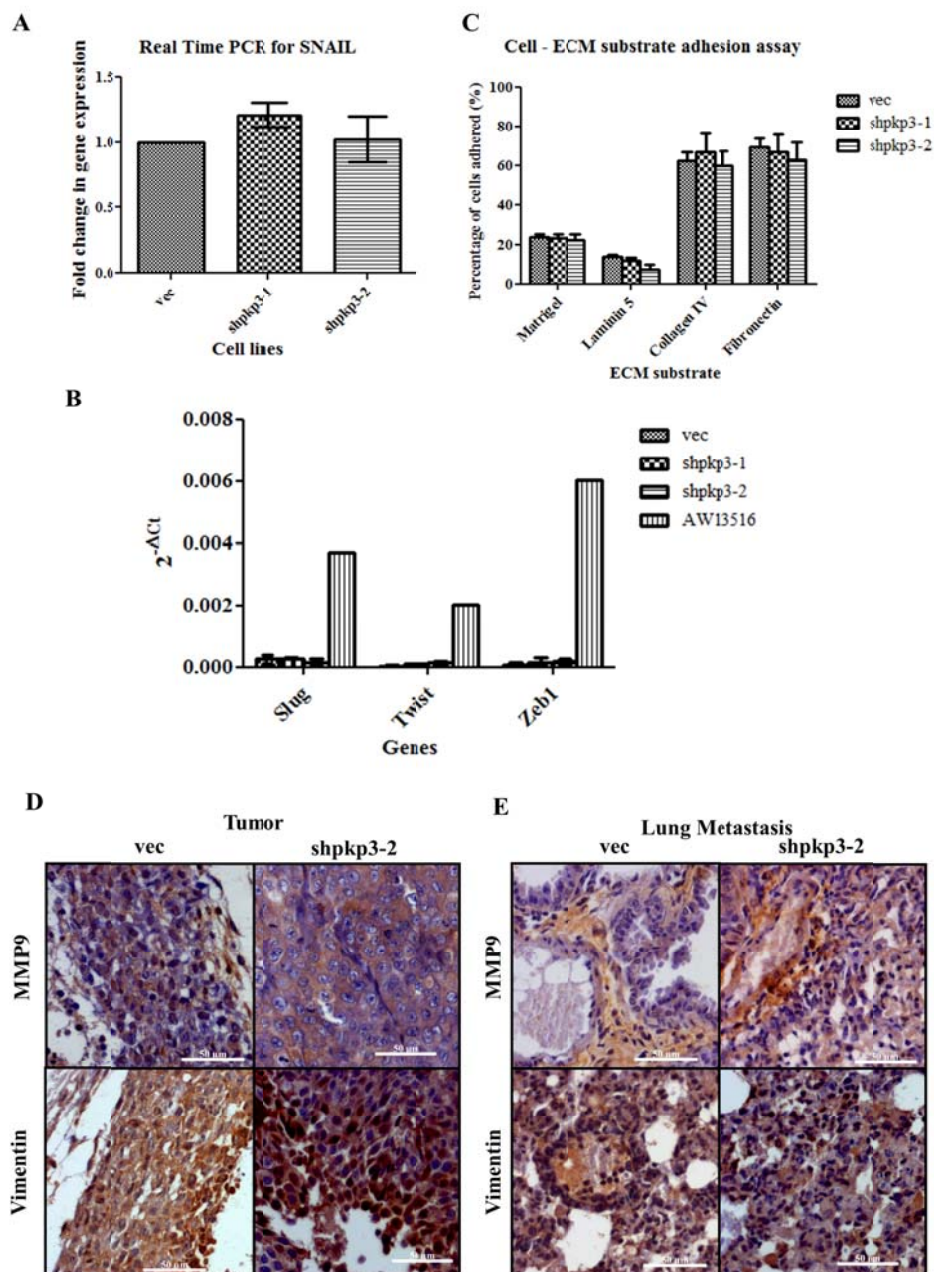


**Figure 1. Plakophilin 3 knockdown does not lead to EMT both *in vitro* and *in vivo*.** A. RNA was isolated from the HCT116 derived vector control (vec) and PKP3 knockdown clones (shpkp3-1 and shpkp3-2) and quantitative real time PCR was performed to detect the levels of Snail. GAPDH was used as a control. The fold change in expression is plotted on the Y-axis. B. RNA was isolated from the indicated cell types and quantitative real time PCR was performed to detect the levels of Slug, Twist and Zeb1. GAPDH was used as a control.  $2^{-\Delta Ct}$  values are plotted on the Y-axis. Note that the HCT116 derived cells do not express these transcription factors in contrast to the AW13516 cells. C. Cell – ECM substrate adhesion assays were performed with the indicated ECM substrates and the percentage of adhered cells determined and the mean and standard deviation from three independent experiments was plotted on the Y-axis. D-E. Cells were injected subcutaneously in immunocompromised mice and immunohistochemical staining was performed on paraffin embedded sections of the primary tumour and lung metastases with the indicated antibodies. Images were captured on a Zeiss Axiovert upright microscope with a 40x objective. Representative images are shown. (A-C. p values were determined using a Student’s t-test.)

## 5. REFERENCES:

- [1]. Baum, B., J. Settleman, and M. P. Quinlan (2008) Transitions between epithelial and mesenchymal states in development and disease. *Semin Cell Dev Biol.* 19: 294-308.
- [2]. Kalluri, R., and R. A. Weinberg (2009) The basics of epithelial-mesenchymal transition. *J Clin Invest.* 119: 1420-1428.
- [3]. Thiery, J. P., and J. P. Sleeman (2006) Complex networks orchestrate epithelial-mesenchymal transitions. *Nat Rev Mol Cell Biol.* 7: 131-142.
- [4]. North, A. J., W. G. Bardsley, J. Hyam, E. A. Bornslaeger, H. C. Cordingley, B. Trinnaman, M. Hatzfeld, K. J. Green, A. I. Magee, and D. R. Garrod (1999) Molecular map of the desmosomal plaque. *J Cell Sci.* 112 ( Pt 23): 4325-4336.
- [5]. Harmon, R. M., and K. J. Green (2013) Structural and functional diversity of desmosomes. *Cell Commun Adhes.* 20: 171-187.
- [6]. Garrod, D. (2010) Desmosomes in vivo. *Dermatol Res Pract.* 2010: 212439.
- [7]. Desai, B. V., R. M. Harmon, and K. J. Green (2009) Desmosomes at a glance. *J Cell Sci.* 122: 4401-4407.
- [8]. Bonne, S., J. van Hengel, F. Nollet, P. Kools, and F. van Roy (1999) Plakophilin-3, a novel armadillo-like protein present in nuclei and desmosomes of epithelial cells. *J Cell Sci.* 112 ( Pt 14): 2265-2276.
- [9]. Schmidt, A., L. Langbein, S. Pratzel, M. Rode, H. R. Rackwitz, and W. W. Franke (1999) Plakophilin 3--a novel cell-type-specific desmosomal plaque protein. *Differentiation.* 64: 291-306.
- [10]. Bonne, S., B. Gilbert, M. Hatzfeld, X. Chen, K. J. Green, and F. van Roy (2003) Defining desmosomal plakophilin-3 interactions. *J Cell Biol.* 161: 403-416.
- [11]. Kundu, S. T., P. Gosavi, N. Khapare, R. Patel, A. S. Hosing, G. B. Maru, A. Ingle, J. A. Decaprio, and S. N. Dalal (2008) Plakophilin3 downregulation leads to a decrease in cell adhesion and promotes metastasis. *Int J Cancer.* 123: 2303-2314.
- [12]. Gosavi, P., S. T. Kundu, N. Khapare, L. Sehgal, M. S. Karkhanis, and S. N. Dalal (2011) E-cadherin and plakoglobin recruit plakophilin3 to the cell border to initiate desmosome assembly. *Cell Mol Life Sci.* 68: 1439-1454.
- [13]. Lee, J. M., S. Dedhar, R. Kalluri, and E. W. Thompson (2006) The epithelial-mesenchymal transition: new insights in signaling, development, and disease. *J Cell Biol.* 172: 973-981.
- [14]. Zeisberg, M., and E. G. Neilson (2009) Biomarkers for epithelial-mesenchymal transitions. *J Clin Invest.* 119: 1429-1437.
- [15]. Moreno-Bueno, G., H. Peinado, P. Molina, D. Olmeda, E. Cubillo, V. Santos, J. Palacios, F. Portillo, and A. Cano (2009) The morphological and molecular features of the epithelial-to-mesenchymal transition. *Nat Protoc.* 4: 1591-1613.
- [16]. Khapare, N., S. T. Kundu, L. Sehgal, M. Sawant, R. Priya, P. Gosavi, N. Gupta, H. Alam, M. Karkhanis, N. Naik, M. M. Vaidya, and S. N. Dalal (2012) Plakophilin3 loss leads to an increase in PRL3 levels promoting K8 dephosphorylation, which is required for transformation and metastasis. *PLoS One.* 7: e38561.
- [17]. Alam, H., S. T. Kundu, S. N. Dalal, and M. M. Vaidya (2011) Loss of keratins 8 and 18 leads to alterations in alpha6beta4-integrin-mediated signalling and decreased neoplastic progression in an oral-tumour-derived cell line. *J Cell Sci.* 124: 2096-2106.
- [18]. Gardel, M. L., I. C. Schneider, Y. Aratyn-Schaus, and C. M. Waterman (2010) Mechanical integration of actin and adhesion dynamics in cell migration. *Annu Rev Cell Dev Biol.* 26: 315-333.
- [19]. Nagano, M., D. Hoshino, N. Koshikawa, T. Akizawa, and M. Seiki (2012) Turnover of focal adhesions and cancer cell migration. *Int J Cell Biol.* 2012: 310616.